THE USE OF FLUORINATED MALEIMIDES AS PROTEIN SULFHYDRYL REAGENTS FOR ^{19}F-NMR STUDIES

BY

FRANK VICTOR PUZZUOLI, B.Sc.

A THESIS

Submitted to the School of Graduate Studies
in Partial Fulfillment of the Requirements
for the Degree

Doctor of Philosophy
(Chemistry)

McMaster University

FLUORINATED MALEIMIDES FOR PROTEIN ^{19}F-NMR STUDIES

DOCTOR OF PHILOSOPHY (1985)
(Chemistry)

McMaster University
Hamilton, Ontario

TITLE: The Use of Fluorinated Maleimides as Protein Sulfhydryl Reagents for ^{19}F-nmr Studies

AUTHOR: Frank V. Puzzuoli, B.Sc., (McMaster University)

SUPERVISOR: Doctor B.E. McCarry

NUMBER OF PAGES: xviii, 240

ABSTRACT

The overall objectives of this work were the development of a) fluorinated maleimides for the specific modification of protein sulfhydryl groups and subsequent ^{19}F-nmr studies and b) fluorinated phospholipids for the study of protein-lipid interactions by ^{19}F-nmr. Two fluorinated analogues of N-ethylmaleimide, N-2,2,2-trifluoroethylmaleimide (FEM) and a deuterated analogue N-2,2,2-trifluoro-1,1-dideuteroethyl-maleimide (FEM-d_2) were synthesized from trifluoroacetamide in three steps. A detailed kinetic study showed that FEM reacted at least 10 times faster with thiols than with either other amino acid side chains namely imidazoles, amines, alcohols or water. The rates of reaction between FEM and thiols increased ten-fold for each unit increase in pH, in addition, apparent activation parameters were determined for these reactions at pH 6.65. The FEM-thiol adducts were also isolated and fully characterized.

Bovine serum albumin (BSA) on exposure to FEM-d_2 reacted rapidly at the single sulfhydryl residue exclusively. On the other hand, 3-bromo-1,1,1-trifluoropropanone reacted with BSA at the sulfhydryl group and at other sites on the protein to the extent of 20%. The neutral to fast (N-F) transition of BSA was examined by ^{19}F-NMR following modification of the protein with FEM-d_2 (BSA-FEM-d_2) or Br-TFP (BSA-TFP) . Over the pH range 3.0-6.0 at least three distinct ^{19}F-NMR resonances were

observed for both modified proteins; the linewidths, chemical shifts and peak areas of these resonances changed as a function of pH. Circular dichroism and fluorescence spectra of modified and unmodified BSA proteins in the pH 3.0-6.0 range were indistinguishable indicating that the sulfhydryl labels caused little structural perturbation to the protein. At pHs above 8.0, BSA-FEM-d_2 underwent an irreversible chemical reaction; likely opening of the succinimide ring by an amino group of the protein. Chemical shift anisotropy contributions to the ^{19}F-nmr linewidths for both BSA-FEM-d_2 and BSA-TFP increased linearly on going from 84.66 to 235.36 MHz.

Two phospholipids fluorinated in the acyl chains were synthesized for the purpose of incorporating them into vesicles with lipophilin, an integral membrane protein; bis-8-fluoro, 8-deutero- and bis-12-fluoro, 12-deuterodimyristoylphosphatidylcholine were synthesized and characterized by ^{2}H-nmr and calorimetric studies. However, ^{19}F-nmr studies of lipophilin/fluorolipid mixtures showed no evidence for the presence of any immobilized or "boundary lipid" around the protein. In addition, lipophilin was modified with FEM-d_2 but ^{19}F-nmr experiments provided no information about the environment of the FEM-d_2 labelled cysteine residues of the protein.

ACKNOWLEDGEMENTS

I wish to express my gratitude to Dr. Brian E. McCarry for his guidance and encouragement throughout the duration of this work.

I also wish to thank Drs. R.A. Bell and R.M. Epand for many helpful suggestions and discussions. A special acknowledgement is due to Dr. James H. Davis (Dept. of Physics, University of Guelph) for finding the time to run ^{2}H-nmr spectra. For excellent technical assistance, I wish to thank the following people: Maelly Lew and Fadjar Ramelan for running mass spectra, Ian Thompson and Claus Schönfeld for their technical expertise, Van Tzannidakis and Alan Sandercock for their assistance in operating the stopped flow kinetics apparatus, Leslie R. Berry and Mark Hatton (Dept. of Pathology) for the use of their protein ultrafiltration apparatus, Dr. G.J. Schrobilgen for his assistance in setting up fluorination reactions, Dr. J.J. McCullough for the use of his fluorimeter, Emmanuel Osei-Twum for his aid in gas chromatographic analysis and special thanks to Brian G. Sayer for his patience in teaching me to operate the nmr instruments. For their friendship and good humour I wish to thank John Varadarajan,

Bill Mills, Charles Elkhouri and Adrian "Shecky" Schwan. Joyce Ridgewell, Sharon Piedimonte and especially Linda Horridge-Palmer are thanked for typing this manuscript and their patience to put up with many changes.

Finally, my love and deepest gratitude to my parents for their love and support.

TO MY PARENTS

TABLE OF CONTENTS

	PAGE
CHAPTER ONE: INTRODUCTION	1
1.1 Proteins - general introduction	1
1.2 Methods for the study of proteins	5
1.2.1 Chemical Methods	5
1.2.2 Physical Methods	6
1.3 Membranes	8
1.3.1 Physical Methods for Studying Lipids	11
1.4 Nuclear Magnetic Resonance	13
1.4.1 General Use in Biological Studies	13
1.4.2 Protein nmr Studies	16
1.4.3 NMR Studies of Lipids	17
1.5 ^{19}F-NMR	19
1.5.1 Protein and Lipid Studies by ^{19}F-NMR	20
1.6 Summary	22
1.7 Thesis Proposal	22
CHAPTER TWO: BACKGROUND	25
2.1 General	25
2.2 Kinetic Studies	28
2.3 Bovine Serum Albumin	36
2.4 Lipophilin	40
CHAPTER THREE: RESULTS AND DISCUSSION	52
3.1 Synthesis of FEM and FEM-d_2	52
3.2 Kinetic Studies of the reaction of FEM with Thiols, Oxygen and Nitrogen Nucleophiles	52
3.2.1 Preliminary kinetic studies with Bovine Serum Albumin	63
3.3 Examination of the N-F transition of BSA	64
3.3.1 Specificity of the FEM-d_2 and Bromotrifluoro-propanone labels	64
3.3.2 Circular Dichroism (CD) and fluorescence profiles of BSA, BSA-FEM-d_2 and BSA-TFP	66
3.3.3 ^{19}F-nmr studies of BSA-FEM-d_2	73
3.3.3.1 pH 3.0 - 6.0	73
3.3.3.2 pH 7.0 - 10.0	

PAGE

3.3.4 ^{19}F-nmr Studies of BSA-TFP 90

3.3.5 A comparison of FEM-d_2 and Br-TFP Sulfhydryl Labels 100

3.4 Synthesis of bis-8-fluoro, 8-deutero and 12-fluoro, 12-deutero dimyrisotoylphosphalidylcholines 107

3.5 Calorimetric and ^{2}H-nmr studies of F-8, D-8 and F-12, D-12 DMPC 108

3.6 Modification of Lipophilin cysteine residues 121

3.7 ^{19}F-nmr studies of lipophilin and lip-FEM-d_2 incorporated into F-8, D-8 and F-12, D-12 DMPC 122

3.8 Summary and Conclusions 131

CHAPTER FOUR: EXPERIMENTAL 134

4.1 General - Instruments and Standards 134

4.2 Synthesis of FEM and FEM-d_2 140

4.2.1 N-2,2,2-trifluoromaleiamic acid 21a 140

4.2.2 N-2,2,2-trifluoromaleimide 22a 145

4.2.3 FEM-d_2 22b 146

4.3 Kinetics of the Reaction of Low Molecular Weight Thiols with FEM 147

4.3.1 pH dependance of kobs at 30.0°C 147

4.3.2 Determination of kapp at pH 6.65 148

4.3.3 Determination of Apparent Activation Parameters for the Reaction of FEM and thiols at pH 6.65 149

4.3.4 Kinetic Study of FEM hydrolysis at 30°C 149

4.3.5 Kinetic Study of the Reaction of FEM with L-lysine, L-Histidine and L-serine 150

4.4 Characterization of FEM-thiol adducts 151

4.5 Purification of Defatted Mercaptalbumin Monomer 158

4.5.1 Preparation of BSA-FEM-d_2 161

4.5.2 Preparation of Acetamide-BSA 162

PAGE

4.5.3 Preparation of BSA-TFP 163
4.5.4 Treatment of BSA-FEM-d_2 with trifluoropropanone 164
4.5.5 Fluorescence measurements 164
4.5.6 Circular Dichroism Spectra 165
4.5.7 84.66 and 235.36 MHz ^{19}F-nmr Spectra 166
4.6 Synthesis of Monofluoro, monodeutero DMPC's 167
4.6.1 Monoethyl acid esters (10a-c) 167
4.6.2 Monoethylester acid chlorides (11a-c) 170
4.6.3 Preparation of Alkyl Grignards (12a-c) 172
4.6.4 Ethyl oxo-myristates (14a-c) 173
4.6.5 Attempted synthesis of gem difluoro-myristates 19a-c 174
4.6.6 Ethyl-hydroxy, deuteromyristates (27a,b) 179
4.6.7 Ethyl fluorodeuteromyristates (28a,b) 182
4.6.8 Gas Chromatographic Analysis of (28a,b) 184
4.6.9 Fluoro, deuteromyristic acids (29a,b) 184
4.6.10 Fluorodeuteromyristic anhydrides (30a,b) 186
4.6.11 Cadmium Chloride Complex of 1-α Glycero-phosphorylcholine 18 189
4.6.12 Synthesis of DMPC 31, F-8, D-8, and F-12, D-12 DMPC (32a and b) 191
4.7 Preparation of lipophilin-FEM-d_2 193
4.8 Preparation of protein/fluorophospholipid mixtures 199
4.8.1 ^{19}F-nmr Studies 200
CHAPTER FIVE: APPENDICES 201
Appendix I 201
5.1 Plane vs. Circularily Polarized Light 201
5.2 Fluorescence Spectroscopy 204
5.3 Differential Scanning Calorimetry 207

PAGE

5.4	NMR	208
5.4.1	Dipolar Interactions	217
5.4.2	Chemical Shift Anisotropy	219
5.4.3	^{19}F-dipolar NMR Spectra	220
5.4.4	^{2}H-quadrupole echo spectra	221
5.4.5	2-Dimensional NMR	223
Appendix II	Bartlett Procedure for Phosphate Analysis	225
REFERENCES		227

LIST OF FIGURES

		PAGE
Figure 1a:	General Structure of Proteins	3
b:	α-helix	
c:	β-pleated sheet	
d:	Planar amide linkage in proteins	
Figure 2	Cell membrane	8
Figure 3	Variation of T_1 and T_2 with τ_c	14
Figure 4	Phosphatidylcholine (1) backbone conformation	18
Figure 5	1-palmitoyl-2-8, 8-difluoropalmitoyl sn-glycerophosphoryl-choline 2	21
Figure 6	1,4 addition of thiols to maleimides	22
Figure 7	FEM and FEM-d_2	23
Figure 8	Reaction of thiols with 3-bromo-1,1,1-trifluoropropanone	25
Figure 9	Possible reactions of FEM	29
Figure 10	Scheme for the reaction of carboxythiols with maleimides	30
Figure 11	Maleimides spin labels used to study BSA	38
Figure 12	Specifically chain deuterated phosphatidylcholines (8a-c)	44
Figure 13	12-doxyl and 8-doxyl stearic acid (9a and b)	46
Figure 14	Proposed Scheme for the synthesis of gem-difluroo DMPCs 19a-c	49
Figure 15	Composite plot of log kobs vs pH for the reaction of thiols and other nucleophiles with FEM	57
Figure 16	kobs vs [Thiol] at pH 6.65	59
Figure 17	log kapp vs pKa SH at pH 6.65	61
Figure 18	Arrhenius Plots for the reaction of thiols with FEM	62

		PAGE
Figure 19	84.66 MHz ^{19}F-nmr spectra of BSA	67
Figure 20	235.36 MHz ^{19}F-nmr spectrum of BSA-FEM-d_2 treated with Br-TFP	68
Figure 21	CD spectrum of BSA, BSA-FEM-d_2 or BSA-TFP	69
Figure 22	$[\theta]_{262}$ vs pH plots for BSA, BSA-FEM-d_2 and BSA-TFP	70
Figure 23 a/	Dependance of λ emission with pH and	72
b/	Relative fluorescence at 343nm for BSA, BSA-FEM-d_2 and BSA-TFP	
Figure 24	84.66 MHz ^{19}F-nmr spectra of BSA-FEM-d_2	74
Figure 25	235.66 MHz ^{19}F-nmr spectra of BSA-FEM-d_2	75
Figure 26	Comparison of 84.66 and 235.36 MHz ^{19}F-nmr spectra of BSA-FEM-d_2 at pH 4.25	76
Figure 27	Percentage area vs. pH plots for curve resolved 235.36 MHz ^{19}F-nmr resonances of BSA-FEM-d_2	77
Figure 28.1-.4	Percentage area, chemical shift and line-width correlations for the curve resolved ^{19}F- resonances of BSA-FEM-d_2	79
Figure 29	235.36 MHz ^{19}F-nmr spectra of BSA-FEM-d2 (A) in the absence of urea and (B) in the presence of urea.	84
Figure 30	Intramolecular cyclization of BSA-FEM-d_2 above pH 7.0	85
Figure 31	Hydrolysis of the BSA-FEM-d_2 succinimide label	86
Figure 32	Intramolecular cyclization by an aminothiol maleimide adduct	87
Figure 33	^{19}F-nmr spectra of L-cysteine (23) and N-acetyl-L-cysteine-FEM adducts (25) pH 7.0	88
Figure 34	Lactam products from an intramolecular cyclization of the L-cysteine-FEM adduct 23	89
Figure 35	235.36 MHz ^{19}F-nmr spectra of BSA-TFP	91

		PAGE
Figure 36	Percentage area vs. pH for the curve resolved ^{19}F-nmr resonances of BSA-TFP	92
Figure 37 .1-.4	Percentage Area, chemical shift and line-width vs pH correlations for the ^{19}F-nmr resonances of BSA-TFP	94-97
Figure 38	^{19}F-nmr spectra of BSA-TFP showing a small amount (~3%) of non-sulfhydryl labelling	98
Figure 39	Percentage area vs. pH plots for the curve resolved 235.36 MHz ^{19}F-nmr resonances of BSA-TFP above pH 6.0	99
Figure 40.1-.3	Percentage area, chemical shift and line-width correlations for the curve resolved ^{19}F resonances of BSA-TFP	101-103
Figure 41	A comparison of FEM and trifluoropropanone BSA labels	104
Figure 42	Geminal diol of the trifluoropropanone BSA label	105
Figure 43	Scheme I; Lactonization of Ethyl 4-oxo-myristate, Scheme II; Synthesis of fluoro, deutero DMPCs	109,110
Figure 44	DSC traces of DMPC 31, F-8, D-8 (32a) and F-12, D-12, DMPC (32b)	111
Figure 45	DSC traces of F-12, D-12 DMPC (32b) and a 1/1 F-12, D-12 DMPC (32b)/DMPC (31) molar mixture	112
Figure 46	DSC traces of F-8, D-8 DMPC(32a)/DMPC (31), mixtures of varying mole ratio	114
Figure 47	Percentage total enthalpy for the higher temperature transitions of F-8, D-8 DMPC (32a) for various DMPC/F-8, D-8 DMPC molar ratios	115
Figure 48	^{2}H-quadrupole echo spectra of F-8, D-8 (32a) and F-12, D-12 DMPC (32b)	117

		PAGE
Figure 49	S_{CD} vs temperature for 32a, 32b and their gem dideutero analogues.	118
Figure 50	A sample 235.36MHz ^{19}F-nmr spectrum of a lip-FEM-d_2/F-8,D-8 DMPC (32a) mixture at 35°.	123
Figure 51A,B	Linewidth vs temperature plots for lipophilin and lip-FEM-d_2/fluorophospholipid mixtures	126,127
Figure 52A,B	Linewidth vs percentage total weight protein for lip-FEM-d_2 and lipophilin/ fluorophospholipid complexes	128,129
Figure 53	Scheme for the synthesis of FEM(d_2)	141
Figure 54	Chromatogram for the purification of BSA by DEAE-Sephadex chromatography	160
Figure 55	Plane polarized radiation	201
Figure 56	Circularily polarized radiation	202
Figure 57	Vector picture of plane polarized radiation	202
Figure 58	Vector picture of circularily polarized radiation	203
Figure 59	Rotation of plane polarized light by an optically active substance	203
Figure 60	CD curves for α, β and random coil conformations of polylysine	204
Figure 61	Decay mechanisms for electronically excited states	205
Figure 62	A typical DSC thermogram	207
Figure 63	Orientation of a nuclear magnetic moment, $\hat{\mu}$ relative to the direction of an applied field	208
Figure 64	Possible orientations of $\hat{\mu}$ for an I=½ nucleus	209

PAGE

Figure 65	Orientations of an ensemble of nuclear magnetic moments in a magnetic field	210
Figure 66	Zeeman diagrams for $I=\frac{1}{2}$, 1 and 3/2 nuclei	211
Figure 67	Application of an H_1 field to induce transitions from low to high energy states for an $I=\frac{1}{2}$ nucleus	211
Figure 68	^{1}H-nmr spectrum of ethyl chloride	212
Figure 69	Orientation of magnetic moments in a rotating frame of reference	213
Figure 70	Pulsed FT-NMR experiment	214
Figure 71	FT-NMR experiment as viewed from the x'y' plane	214
Figure 72	Fourier transformation to an FID to give a desired nmr spectrum	215
Figure 73	Dipolar interactions	217
Figure 74	Spin States for an AX spin system	218
Figure 75	Origins of deuterium quadrupolar spectra	222
Figure 76	Scheme for a 2-D correlated spectrum (COSY)	224

LIST OF TABLES

		PAGE
Table 1	Common amino acids found in nature	2
2	Physical techniques for studying proteins	7
3	Lipids commonly found in nature	9
4	Physical Methods for studying lipids	12
5	A comparison of nuclei used in biological nmr studies	13
6	Structures of the thiols L-cysteine 3, N-acetyl-L-cysteine 4, glutathione 5 and β-mercaptoethanol 6	31
7	pKas of thiols 3, 4, 5 and 6	33
8	Lipid and protein components of myelin	41
9a/b	kobs and $t_{\frac{1}{2}}$ values for the reaction of FEM with a/ thiols (3-6) and b/ other nucleophiles	54
10	kapp values for the reaction of FEM with thiols (3-6) at pH 6.65	59
11	Activation parameters for the reaction of FEM with thiols (3-6)	62
12	Correlation of CD, Fluorescence and ^{19}F-nmr. data for BSA-FEM-d_2 and BSA-TFP	106
13	Transition temperatures and enthalpies for DMPC 31, F-8, D-8 (32a) and F-12, D-12 DMPC (32b)	111
14	ΔV_Q and S_{CD} values for fluorophosphatidylcholines 32a and b and gem dideutero analogues	117
15	DTNB analysis of lipophilin and lip-FEM-d_2	122
16	Linewidths for various lipophilin and lip-FEM-d_2/fluorophospholipid (32a and b) mixtures at 84.66 and 235.36 MHz at various temperatures	125
17	Data for FEM 22a FEM-d_2 and their precursors (20 and 21 a, b)	142,143

PAGE

Table 18	^{1}H-nmr data for FEM-thiol adducts (23-26)	153-155
19	Data for FEM-thiol Adducts (23-26)	156, 157
20	Data for monoethylacid esters 10a-c	168
21	Data for monoethylester acid chlorides	171
22	Data for ethyl oxo-myristates 14a-c	176
23	Data for ethyl 8-hydroxy, 8-deutero(27a) and 12-hydroxy, 12-deutero myristates(27b)	181
24	Data for ethyl 8-fluoro, 8-deutero(28a) and 12-fluoro, 12-deuteromyristates(28b)	185
25	Data for 8-fluoro, 12-deutero(29a) and 12-fluoro, 12-deuteromyristic acid (29b)	187
26	Data for 8-fluoro, 8-deutero(30a) and 12-fluoro, 12-deuteromyristic anhydride(30b)	189
27	Description of fractions collected from the isolation of phosphatidylcholines from egg yolk lecithin	190
28	Data for DMPC (31) and bis 8-fluoro,8-deutero (32a) and 12-fluoro, 12-deutero-dimyristoylphosphatidylcholine (32b)	193,194
29	CD and ORD data for random coil, α-helix and β-conformations.	205

CHAPTER ONE

INTRODUCTION

The study of proteins and other biological molecules by nuclear magnetic resonance has become increasingly popular over the past twenty years. This increased popularity is reflected by an approximate ten-fold increase in the nmr literature (~50-500 papers/year) over this peiod. The work presented in this thesis deals primarily with ^{19}F-nmr studies of two proteins: the first, bovine serum albumium (BSA), a protein soluble in aqueous solution and the other lipophilin a myelin intrinsic membrane protein in a reconstituted fluorophospholipid matrix. Prior to a review of nmr methods which have been used in soluble protein and membrane lipid protein studies, a general overview of proteins and lipids will be given. This overview will deal first with general aspects of the structures of proteins and lipids and secondly with the physical and chemical methods for the study of these systems. Subsequently, a general review of nmr methods and studies including a discussion of ^{19}F-nmr will be presented.

1.1 Proteins - General Introduction

Proteins are biologically important polymers whose monomer units consist of any of the 20 naturally occurring amino acids (Table 1) that in turn are linked by peptide (amide) linkages (Figure 1a).[1,2] The molecular weights of proteins range from 5,000 Daltons (or atomic mass units, amu)

Table 1: Amino Acids $HN_3^+-C(R)(H)-COO^-$ Found in Proteins

Table 1

Amino Acid	R	Amino Acid	R
Alanine (Ala)	CH_3-	Threonine (Thr)	$CH_3C(OH)H-$
Valine (Val)	$(CH_3)_2CH-$	Cysteine (Cys)	$HSCH_2-$
Leucine (Leu)	$(CH_3)_2CH-CH_2-$	Tyrosine (Tyr)	$HO-C_6H_4-CH_2-$
Isoleucine (Ile)	$CH_3CH_2CH(CH_3)-$	Asparagine (Asn)	$H_2NC(=O)CH_2-$
Proline (Pro)	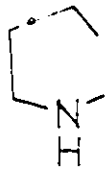	Glutamine (Gln)	$H_2NC(=O)CH_2CH_2-$
Phenylalanine (Phe)	$C_6H_5-CH_2-$	Aspartic Acid (Asp)	$HOC(=O)CH_2-$
Tryptophan (Trp)	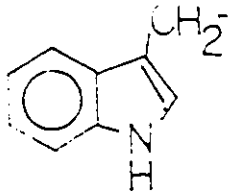	Glutamic Acid (Glu)	$HOC(=O)CH_2CH_2-$
Methionine (Met)	$CH_3SCH_2CH_2-$	Lysine (lys)	$H_2N(CH_2)_4-$
Glycine (Gly)	$H-$	Arginine (Arg)	$H_2NC(=NH)NH(CH_2)_3-$
Serine (Ser)	$HOCH_2-$	Histidine (His)	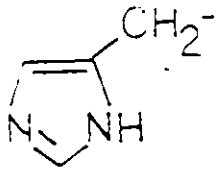

FIGURE 1a

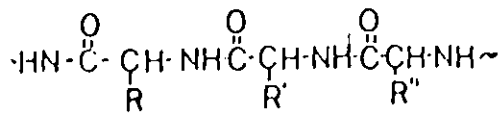

FIGURE 1b

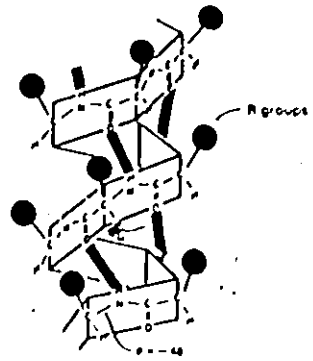

FIGURE 1c

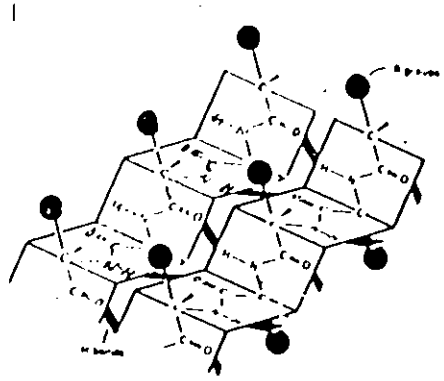

FIGURE 1d

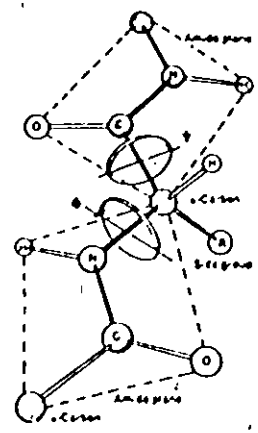

Figure 1a: Polypeptide or polyamide sequence common to all proteins.
Figure 1b: α-helix conformation.
Figure 1c: β-pleated sheet.
Figure 1d: The angles ϕ and ψ are the angles of rotation about the C_α-N and C_α-C bonds respectively.
Figures 1b-d were taken from reference 5.

to 1 million or more Daltons. Similar polymers with molecular weights less than 5,000 are referred to as polypeptides.

Protein structure can be described by several terms. "Primary structure" describes the covalently bonded sequence of amino acid residues while "secondary structure" refers to a regular, recurring arrangement of the polypeptide in one dimension namely α-helix, β-pleated sheet (Figure 1b and c) and random coil conformations. These repetitive arrays can be ascribed to the planar amide linkage and the angle of rotation about the C_α-N bond ϕ, and ψ the angle of rotation about the C_α-C bond (Figure 1d). By virtue of the steric bulk of the side chains (R), α, β or random coil arrays will be preferred.[3,4] "Tertiary structure" refers to 3 dimensional folding or bending of the protein chain while the term "quaternary structure" applies to proteins with more than one subunit and describes non-covalent interactions between these subunits. The overall term, conformation, applies to the combined secondary, tertiary and quaternary structure. Protein conformational changes are of great importance since they are often associated with a protein's function for example, conformational changes associated with an enzyme upon substrate binding.

1.2 Methods for Studying Proteins

1.2.1 Chemical Modification

The chemical modification of proteins is based on the wide range of amino acid R groups present[5-10] (Table 1) and has served several aims: i) alteration or removal of biological activity, ii) a change in physical properties or iii) introduction of "reporter" groups which are usually spectroscopic labels.[6] The choice of a modifying reagent is governed by several criteria. Of primary importance is the reagent's solubility in aqueous media; in some cases the organic reagent must first be dissolved in an inert solvent such as dioxane or acetonitrile. The reagent of choice must also be stable at pHs and temperatures at which the protein is biologically active if the effects of modification are to be interpreted relative to the biological activity of the protein. Above all, the reagent must be quantitative and specific for the target R group.

A great deal of effort has been devoted to the development of reagents for irreversible enzymatic inhibition. These reagents are catagorized as either affinity labels or active site reagents better known as "suicide substrates.[7]" The former class of compounds are structural analogues of enzyme substrates which upon binding to the enzyme react with a nucleophilic R group and renders the enzyme inactive. The

limitation of this approach is non-specific modification because of the wide variety of components present in cells. The latter category, suicide substrates, differ from the first since the enzyme itself unmasks the latent functional gruop resulting in less of catalytic activity. Many examples of suicide substrates are dealt with in a review by Walsh.[7]

1.2.2 Physical Methods

A wide variety of physical methods have been applied to the study and characterization of proteins.[10] Included in these methods are: i) X-ray crystallography, ii) optical methods such as circular dichroism (CD), optical rotary dispersion (ORD), light scattering and fluorescence spectroscopy iii) magnetic resonance methods such as electron spin resonance (esr) and nuclear magnetic resonance (nmr) and iv) chromatogrphic methods such as molecular exclusion chromatography and ultracentrifugation. Since each method provides a specific piece of data about a protein, a combination of two or more methods is required to provide a complete overall picture of a complex macromolecule such as a protein. The information attainable by each method is summarized in Table 2. A discussion of nmr studies is presented separately in Sect. 1.4 and 1.5.

Table 2: Summary of Physical Techniques used for Studying Proteins and the Information Obtained from Them.

Method	Information	Ref.	Method	Information	Ref.
X-Ray	Location of amino acid residues in space.	11	b) depolarizaiton	Lifetimes of fluorophores which relate to viscosity, temperature and protein shape	27
	Conformational changes of enzymes upon binding to substrates.		c) quenching	Degree of exposure of intrinsic or extrinsic fluorophores.	27
Optical Methods i) CD and ORD	α,β and random coil content (Sect. 5.1)	16-18	Size Exclusion Chromatography	Molecular weight.	12-15
ii) Light scattering	R_G, radius of gyration which is shape dependent Molecular weight.	19,20	Ultracentrifugation	f, the frictional coefficient or s, the sedimentation coefficient both related to protein shape.	28
iii) Infrared spectroscopy	C=O & NH stretching frequencies distinct for α and β conformations.	21,22	Viscosity	ν_0, the specific volume which is maximal for random coils.	29,30
iv) Fluorescence a) Emission-spectra	λ shifts showing changes in the environments of tryptophan, phenylalamine or tyrosine residues (Sect. 5.2).	23-26	ESR	g value-identity of paramagnetic species generated τ_c, rotational correlation time which is related to to the proteins motion in solution. Line broadening of ^{1}H-nmr resonances which is $1/r^6$ dependant where r is the distance between ^{1}H and the paramagnetic site.	31-33

1.3 Membranes - General Overview

Cellular membranes act as both barriers separating aqueous compartments and a base to which enzymatic systems are bound. Typically, membranes are ~ 8 nm wide and comprised of approximately 60% protein and 40% lipid with considerable variation in this composition. Lipids commonly found in membranes are shown in Table 3. The most widely accepted model for the structure of the cell membrane is the "fluid mosaic" model[34] in which the lipids are arranged in a bilayer to form a liquid crystalline martix as depicted in Figure 2.

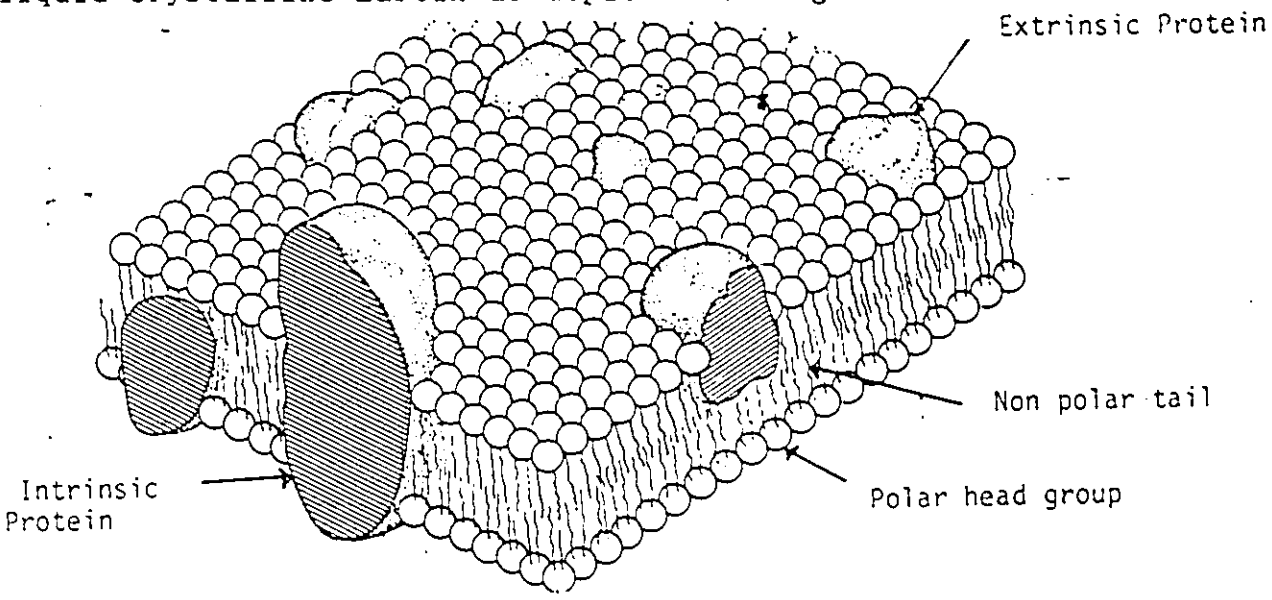

Figure 2 (Taken from Ref. 1)

Two types of membrane protein mey be distinguished: extrinsic (peripheral) proteins which are loosely attached to the membrane surface and intrinsic (integral) proteins which are buried in the lipid bilayer and make up to 70% of membrane proteins.

Table 3: - Common Lipids Found in Nature, Lipids 1/-6/ and 9/ are Common Constituents of Cell Membranes.

Lipid	Structure
1/ Fatty Acids	$HOC(=O)(CH_2)_N CH_3$ N = 3 - 24 (Saturated or unsaturated)
2/ Triglycerides	$CH_2(OR)\,CH(OR')\,CH_2(OR'')$ R = fatty acyl chain R' = " " " R'' = " " "
3/ Alkyl ether glycerols	R = $(CH_2)_N CH_3$, H R' = " " R'' = " " N = 3-24
4/ Glycosylacyl glcerols	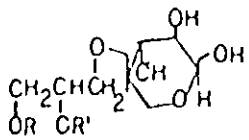 R,R' = fatty acyl chain
5/ Phosphoglycerides	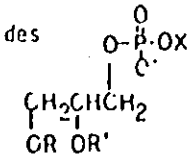 R,R' = fatty acyl chain or H X = $CH_2CH_2\overset{+}{N}H_3$ - phosphatidylethanolamines $CH_2CH_2\overset{+}{N}(CH_3)_3$ - phosphatidylcholines $H_3\overset{+}{N}-CH(COO^-)-CH_2$ - phosphatidylserines 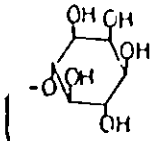 - phosphatidylinistidols $-CH_2CH(OH)CH_2OC(=O)CH(NH_3^+)(CH_2)_4NH_3$ -3'-O-lysylphosphatidylcholines 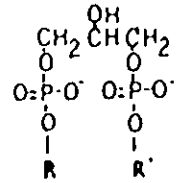 -cardiolipins R,R' = $CH_2CH(OR)CH_2$ (see, triglycerides, 2/)

Table 3 - Continued

Lipid	Structure
6/ Sphingolipids	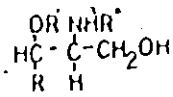
	R' = H R'' = H - sphingosine R = $CH{=}CH(CH_2)_{12}CH_3$
	R' = R'' = H , R = $CH_2(CH_2)_{13}CH_3$ - dihydrosphingosine
	R = $CH{=}CH(CH_2)_{12}CH_3$ - ceramides R' = H , R'' = fatty acyl chain
	R = $CH{=}CH(CH_2)_{13}CH_3$ R' = $C{-}\overset{O}{\overset{\|}{P}}{-}O(CH_2)_2\overset{+}{N}(CH_3)_3$ - sphingomyleins R'' = fatty acyl chain
	R = $CH{=}CH(CH_2)_{12}CH_3$ R' = 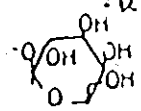 - glactocerebrocides R'' = fatty acyl chain
7/ Waxes	$CH_3(CH_2)_N\overset{O}{\overset{\|}{C}}OR'$ N = 3-24 R' is a long chain alcohol (C_6 - C_{24}) or steroid

Lipid	Structure
8/ Terpenes	Constructed multiples of isopyrene 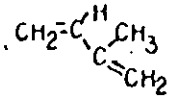 e.g., Vitamine A_1, retinol 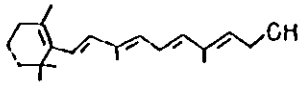
9/ Steroids	derivatives of perhydrocyclopentanoanthrene 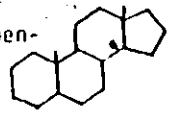 e.g., testosterone 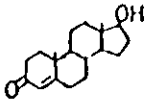
10/ Prostoglandins	derivatives of prostanoic acid 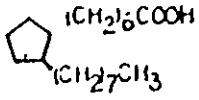 e.g., prostoglandin E_1 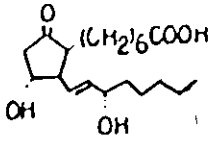

Both protein-lipid and lipid-lipid interactions are important in overall membrane organization. These interactions when ionic in nature depend on the pH and ionic strength of the aqueous medium.[35] Hydrophobic interactions between non-polar amino acid residues and the non-polar segments of lipids as well as those between the non-polar segments of lipids themselves are also of importance. The net effect is a reduction in lipid fluidity. A more detailed discussion is presented by Boggs.[36]

1.3.1 Physical Methods for Studying Lipids

As it is the case with proteins, a wide variety of physical methods are available to study lipids as either pure, mixed or protein/lipid mixtures. Included in these techniques are X-ray and neutron scattering, electron microscopy, optical methods such as Raman and fluorescence spectroscopy, photobleaching and magnetic resonance methods such as esr and nmr. Again, a combination of two or more of these methods is often required for a complete overall picture. The type of information available by each technique is summarized in Table 4. The reader is again reminded that a discussion of nmr studies is presented in later sections (1.4 and 1.5).

Table 4: A Summary of Physical Methods for Studying Lipids and Information Attained from them.

Method	Information	Ref.	Method	Information	Ref.
X-ray and neutron diffraction Electron microscopy	Calculation of membrane thickness.	37,38	ii) Raman light scattering	C-C bands which are distinct for the trans and gauche conformers in the gel and liquid crystalline states respectively.	43,44
Differential Scanning Calorimetry (DSC)	Temperatures, enthalpies and cooperativity of gel to liquid crystalline phase transition(Sect. 5.3)	39,40	ESR	τ_c, rotational cor-time of the spin label which depends on bilayer fluidity.	45
Optical Methods a) Depolarization	i) Fluorescence Motional properties of fluorescent probes which depends on bilayer viscosity.	41,42		S, order parameter which depends on the motion and orientation of the spin label with respect to magnetic field.	
b) Photobleaching Recovery	Lateral diffusion rates across the membrane.				

1.4 Nuclear Magnetic Resonance (Sect. 5.4)

1.4.1 General Applications in Biological Chemistry

Nuclear magnetic resonance has proven to be a good method for studying biological molecules in solution. The most commonly studied nuclei in biological nmr are ^{1}H, ^{13}C, ^{19}F, ^{2}H, ^{31}P and ^{15}N [46,47] From their nmr spectra it is posible to device information regarding molecular conformation from the measurement of chemical shifts (δ), coupling constants (J), and the relaxation times T_1 and T_2. This is summarized in Table 5.[51,52]

Table 5 A Comparison of Various Nuclei Used in Biological NMR Studies

Isotope	I	Relative Sensitivity (%)	Resonant Frequency(MHz) Relative to ^{1}H	Chemical Shift Range(ppm)	Parameter and Information
^{1}H	1/2	100	100.0	10	δ: position of anisotropic groups, H-bonds charged groups J: Dihedral angles, conformer population. T_1: Internal motions, paramagnetic sites. Line Shapes: Conformational dynamics.
^{2}H	1	0.1	15.36	10	$\Delta\nu_Q$: order parameter & C-D bond orientation T_1: Conformational dynamics
^{13}C	1/2	1.7	25.14	340	δ: Electronic environment. T_1: Conformational Flexibility. J: dihedral angles.
^{15}N	1/2	0.1	10.13	620	δ: molecular environment. J : dihedral angles.
^{31}P	1/2	6.6	40.46	700	δ: phosphate group conformation. Line Shape: anisotropic motion J: dihedral angles.
^{19}F	1/2	83	94.06	960	δ: Environment of labelled positions S_{FF} & S_{CF}: Conformational dynamics. T_1: Conformational flexibility

These parameters may be studied as a function of any desired perturbation. Of particular importance is the variation of T_1, the spin-lattice and T_2 the spin-spin relaxation times with the rotational correlation time τ_c, the average time a molecule takes to rotate through one radian[48,49] (Figure 3). Both T_1 and T_2 vary with the applied field frequency ν_o.

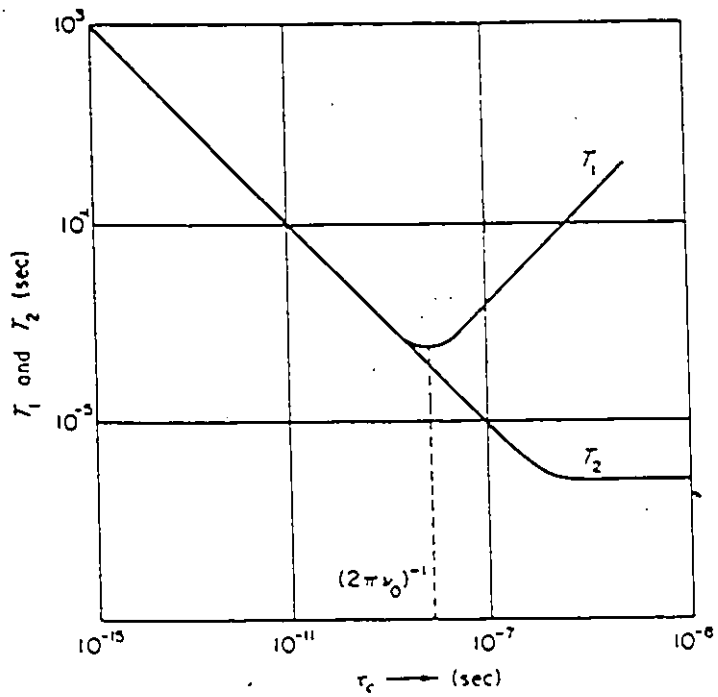

Figure 3 (Taken from Ref. 48)

For molecules with molecular weights of les than 1,000 T_1, or $T_2 \simeq 0.1 - 10$ sec. in non-viscous media. However, at smaller τ_c values, dipolar relaxation mechanisms became more efficient resulting in broadened nmr lines.

Although a great deal of information can be obtained from nmr studies, there are inherent difficulties and disadvantages in the use of nmr to study proteins and other biological molecules. Since many biomolecules have limited solubilities, many hours of spectral accumulation are required to obtain spectra with reasonable signal to noise ratios. Chemical shift anisotropy (CSA) (Sect. 5.4.2) may contribute to line broadening for some nuclei such as ^{19}F particlarily at higher field strengths.[50].

The advent of two dimensional or 2D-nmr has been of paramount importance in biological nmr studies[53-55] (Sect. 5.4.5). 2D experiments can be used to determine whether nuclei interact via spin coupling, mutual relaxation, chemical exchange or shielding. As a result, conformational information can be obtained. Correlated spectroscopy (COSY), Spin-Echo Correlated Spectroscopy (SECSY) and Nuclear Overhauser Enhancement Spectroscopy (NOESY) are widely used 2D-nmr methods. Polarization transfer nmr experiments such as DEPT (Distortionless Enhancement by Polarization Transfer) or INEPT (Insensitive Nuclei Enhanced by Polarization Transter)[56,57] have been valuable particularly in ^{13}C-nmr studie_ where it is possible to selectively examine methyl, methylene or methine carbons by spectral editing.

In general, ^{1}H and ^{13}C nmr studies of macromolecules are often difficult because of the large number of overlapping resonance. A common practice is to examine resonances which are well removed from crowded regions of the spectrum. Deuterium (as well as ^{19}F or ^{15}N) labelled biomolecules can be prepared chemical or biosynthetic methods. The quadrupolar moment of deuterium is of primary importance when looking at ordered systems (such as proteins and membranes) where the observed quadrupolar splitting, $\Delta\nu_Q$, provides information with regards to degree of motion about the C-D bond (Sect. 5.4.4)[58,59] Because of the inherently low natural abundance and sensitivity of ^{15}N, chemical enrichment of biological samples is necessary to observe nmr signals at reasonable sample concentration. ^{31}P on the other hand is present in relatively few biomolecules and has the advantage of having fewer resonances to assign. Both ^{31}P-nmr lineshapes and chemical shifts are sensitive to molecular conformations.

1.4.2 Protein nmr Studies - General

^{13}C and ^{1}H are the most popular nuclei in protein nmr studies. Chemical shift analysis of specific side chains (R groups) have been useful in studying conformationally dependent intermolecular interactions. ^{13}C chemical shifts of hydrogen bonded carbonyl groups can be used in the evaluation of protein secondary structure.[31] The angular dependence of two and three

bond $^{1}H-^{13}C$ coupling constants complimented by other data has lead to three dimensional pictures of peptides. 2D and NOE difference nmr experiments have aided in the interpretation of complex protein ^{13}C and ^{1}H-nmr spectra since nuclei interacting in only the manner selective for these experiments are observed.[60]

^{15}N-nmr chemical shifts vary with both the primary and secondary structure of polypeptides. The amide chemical shifts cover a range of 250-280 ppm and depend on the sequence of amino acid residues.[62] Three bond $^{15}N-^{1}H$ coupling constant measurements have aided also in conformational studies.

Protein ^{31}P-nmr studies has been limited to the examination of phosphoryl transfer enzymes and in particular the perturbations caused by the substitution of ^{18}O and ^{17}O for ^{18}O in the phosphate group.[61]

^{2}H-nmr has involved the incorporation into proteins of specifically deuterated amino acid side chains,[63,64] and looking at the dynamics and the degree of order about these side chains from the measurement of the quadrupolar splitting $\Delta\nu_Q$.

1.4.3 NMR Studies of Lipids

The structure and organization of lipids in biomembranes have been studied by ^{1}H, ^{2}H, ^{13}C, ^{31}P and to lesser extent ^{19}F-nmr. The calculation of three bond proton coupling constants have been used to show that the staggered conformation of the glycerol beckbone of phosphatidylcholines was preferred (Figure 4).[65]

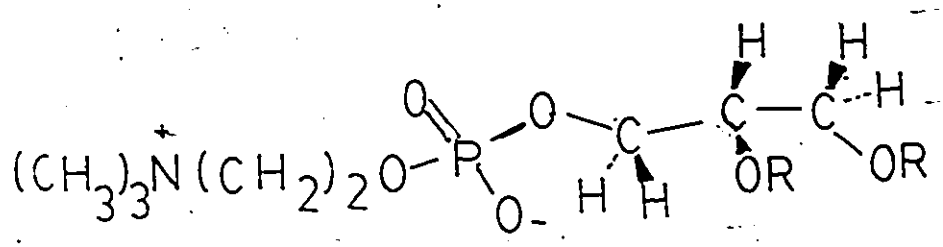

1

Figure 4

Likewise, $^{13}C-^{1}H$, $^{1}H-^{13}C$, and $^{13}C-^{31}P$ coupling constants were used in the assessment of the conformation of the acyl chain and choline moieties of phosphatidyl cholines.[66,67]

Both the rotational motions about single bonds and the lateral motions across the membrane surfaces have been examined by nmr. $^{13}C-T_1$ measurements for ^{13}C nuclei at varying positions along the acyl chains showed that the rotational motion abut C-C bonds increases with increasing distance from the lipid head group.[68] Similarily, $^{31}P-T_2$ measurements have been interpreted in terms of anisotropic motions in the head group.[69] $^{31}P-^{1}H$ NOE measurements by Yeagle[70,71] have shown that the T_1 relaxation mechanism is predominantly dipolar and resulted from the irradiation of the $-\overset{+}{N}(CH_3)_3$ protons thereby showing the proximity of the phosphate and trimethylammonium moieties. The measurement of ^{2}H quadrupolar splitting for lipids wiht $-CD_2-$ units along the acyl chain by Seelig[72,73] complimented previous $^{13}C-T_1$ measurements[74] by showing the degree of randomness, (as reflected in ΔV_Q) increased with increasing distance from the head group moiety.[81] In some cases, the two hydrocarbon chains of the lipid are non-equivalent and show two sets of lines in the NMR

spectrum.[82-90] The order parameter S_{CD} (claculated from $\Delta\nu_Q$, Sect. 5.4.4) decreased with increasing temperature and difficult to obtain at temperatures below the phase transition temperature of the lipid due to line broadening from the inherently smaller ^2H-T_2 values in the gel state. ^{31}P chemcial shift anisotropy (CSA) measurements have demonstrated that motions of the phosphate group are restricted in phosphatidylcholine bilayers.[94,78-80]

Lateral motions across the surface of membranes have been reflected in spin-spin interactions between neighbouring lipid molecules. Metcalf et. al.[75-79] showed an increase ^1H-T_1 for dipalmitoyl lecithins (DPLs) where increasing amounts of DPLs deuterated the alkyl chain were added to the protio species. ^1H-T_2 values were also shown to be dependent on lateral diffusion rates.

1.5 ^{19}F-NMR - General

The use of ^{19}F-nmr to study biopolymers has become increasingly popular.[91] The ^{19}F nucleus has several inherent advantages when compared to the other nuclei listed in Table 5.[92] which include; 1) The relative sensitivity is comparable to ^1H and far greater than the other nuclei, 2) ^{19}F is 100% abundant with spin of 1/2 and therefore no quadrupole moment 3) the chemical shift range of fluorine is large and sensitive to local environmental affects and 4) ^{19}F is not a natural component of proteins or other biopolymers. As a conseqnence

of the first two advantages, the only fluorines observed spectroscopically are those introduced into the protein and changes about the ^{19}F nucleus will likely be reflected in changes in the chemical shift or linewidth. A thorough review with many examples of the use of ^{19}F nmr in the study of biological molecules has been given by Gehrig.[91]

1.5.1 Protein and Lipid Studies by ^{19}F-nmr

The biosynthetic incorporation of fluorinated amino acid analogues into proteins has been usd to study the environment about specific amino acid residues by ^{19}F-nmr. For example, after the incorporation of monofluorotyrosine into *E. Coli* alkaline phosphatase,[93] all eleven tyrosine residues were monitored from their well resolved ^{19}F nmr signals. Chemical modification of specific amino acid side chains with fluorinated reagents as well as the use of fluorinated analogues of protein substrates have been used to study proteins by ^{19}F nmr.[94-100]

^{19}F nmr has also been used to study lipid bilayers. Birdsall et. al.[101,102] have examined the fluorine spectra of monofluorooleic acids in lecithin vesicles. Linewidths of the ^{19}F signals were monitored as a function of the position of -CHF- along the fatty acid backbone, were found to decrease toward the methyl terminus. This result was interpreted in terms of increasing rates of molecular motion toward the center of the bilayer which agreed with previous ^{13}C-T_1 measurements,

^2H order parameters and spin-labelling experiments. Gent et. al.[103,104] have synthesized 1-palmitoyl-2-8,8-difluoropalmitoyl sn-glycero-3-phosphorylcholine 2 (Figure 5) and prepared micelles and bilayers.

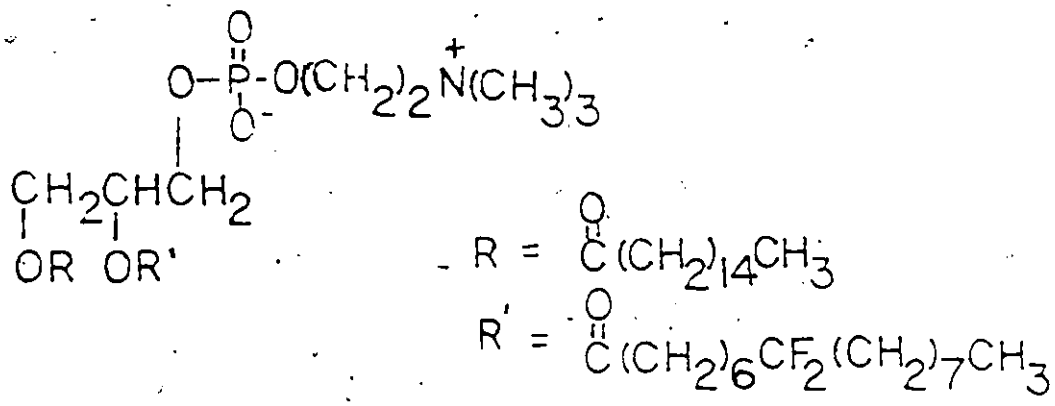

2

Figure 5

By dilution with fully deuterated dipalmitoyl phosphatidyl cholines (DPPCs) relaxation via F-C-F and C-F--H-C dipolar interactions could be separated. Chemical shift anisotropy contributions were also found to be dominant. ^{19}F-dipolar spectra have been obtained from dimyristoylphosphatidyl cholines (DMPCs) substituted with $-CF_2-$ groups[105-107] as well as DPPCs with -CHF- units at various positions along the acyl chain.[108-110] Both studies have led to the calculation of C-F order parameters which agree to within approximately 10% with C-D order parameters reported for CD_2 analogues (Sect. 5.4.3, 5.4.4).

1.6 Summary

There are a variety of chemical and physical methods abailable for the study of proteins and lipids. No one method can provide a complete picture of the structure and function of these biological molecules. NMR spectroscopy can provide a great deal of information about these systems particularly in conjunction with other physical methods.

1.7 Thesis Proposal

Maleimides are known sulfhydryl reagnets which react with thiol groups in a 1,4 addition process and have been used to label the cysteine sulfhydryl residues of proteins[5,6] (Figure 6).

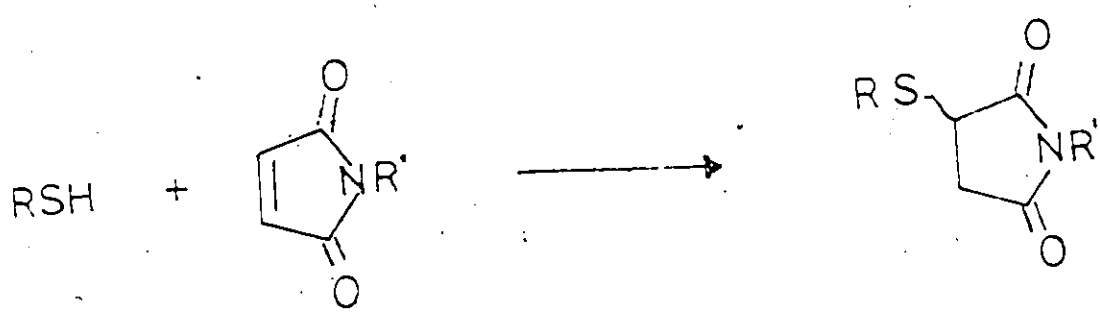

Figure 6

Reaction with non-thiol nucleophiles such as water, amines, and imidazoles have been observed,[111,112] but the relative rates of these reactions have not been investigated, in particular, relative to the rates of reaction with thiols.

Recognizing the advantages of ^{19}F over other nuclei in nmr studies of biomolecules (Sect. 1.5), it was proposed to synthesize a fluorine-containing maleimide for protein sulfhydryl labelling and subsequent ^{19}F-NMR studies. The maleimide was N-2,2,2-trifluoroethylmaleimide (FEM) and its dideuterated analogue N-2,2,2-trifluoro-1,1,-dideuteroethyl-maleimide (FEM-d_2) shown in Figure 7.

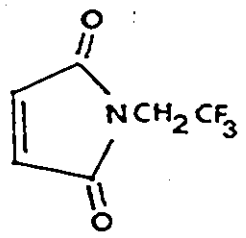

N-2,2,2,-trifluoroethylmaleimide (FEM)

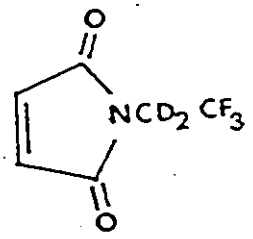

N-2,2,2,-trifluoro-1,1-dideuteroethylmaleimide (FEM D_2)

Figure 7

An investigation of the relative rates of reaction between FEM and low molecular weight thiols as well as other nucleophiles would be undertaken. In order to evaluate this reagent the protein bovine serum albumin (BSA) with one sulfhydryl group per mole of protein was selected for examination of its pH dependant conformational change by ^{19}F-NMR.

A second protein chosen for modification was the myelin intrinsic membrane protein lipophilin. In the study of lipid-protein interactions, the physical techniques employed examine either the protein or lipid. It was proposed to examine both the protein and lipid environment simultaneously after the incorporation an FEM-d_2 labelled lipophilin, into phospholipids whose hydrocarbon chains had been labelled with fluorine at various positions. In order to carry out this study, the synthesis and characterization of the fluorophospholipids was required.

CHAPTER TWO

BACKGROUND

2.1 GENERAL

An important criterion for the selection of a reagent for the introduction of a spectroscopic "reporter group" in order to probe the microenvironment of a protein, is the quantitative and specific reaction of this reagent with the target protein functional group. A great deal of information concerning the protein mechanism has been obtained by studying proteins after chemical modifications (Section 1.3). It should not be assumed *a priori* that a given reagent will react specifically at a given protein site because of the large of reactive (R) groups on a protein (Table 1) present and possible side reactions. For example, it was assumed by Heustis and Raftery that when hemoglobin was treated with 3-bromo-1,1,1-trifluoropropanone (Br-TFP), only exclusive alkylation of the sulfhydryl group of the cysteine residue at 3.97[113-118] occurred (Figure 8).

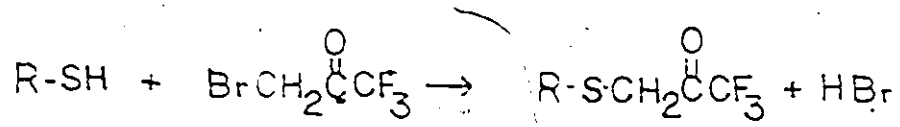

Figure 8

Subsequent investigations with (^{14}C)-Tabelled Br-TFP[119] showed that in addition to cysteine modifications, alkylation

of an amino group of a lysine residue had also occurred.

Since it was intended to develop FEM(d_2) for the purpose of modifying thiol groups in proteins for ^{19}F-nmr studies, it was felt a kinetic study to determine the rates of reaction of FEM with thiols and other potential protein nucleophilic R groups such as amines, alcohols or imidazoles was important in order to assess the specificity of the FEM label.

Bovine serum albumin (BSA) was selected as a model protein ^{19}F nmr studies for several reasons: the protein is abundant, relatively inexpensive, easily purified and has a single sulfhydryl group per mole. BSA is known to undergo conformational changes in the pH 3.0 - 6.0 region; the fast-neutral or F-N transition and in the pH 3.0 - 6.0 region the neutral-basic or N-B transition. In particular, the F-N transition has been well characterized by esr, fluorescence and circular dichroism studies. However, prior to any ^{19}F-nmr studies of the F-N transition of the modified protein, the specificity of the reaction of FEM-d_2 for the cysteine residue of BSA and the perturbing nature of the fluorine label had to be investigated.

Comparative ^{19}F-nmr studies using 3-bromo-1,1,1-trifluoropropanone (Br-TFP) to label BSA were felt to be of interest since i) Zurawaki[120] used this label to modify the sulfhydryl group of BSA in order to study the N-B conformational change of the modified protein, and ii) the likelihood of

non-sulfhydryl modification made the interpretation of these results questionable. Consequently, the investigation of the N-F transition of the Br-TFP as well as the FEM-d_2 modified proteins by ^{19}F-nmr were undertaken.

Investigations of the interactions of integral membrane proteins with membrane lipids have focused on either the protein or the lipid separately. Many of these studies have been carried out by the reconstitution of protein/lipid mixtures and the use of one or more physical methods (Section 1.2.2) to study either component. By incorporating a FEM-d_2 modified protein into a fluorophospholipid matrix, it was thought possible to monitor both the protein and lipid environments simultaneously by ^{19}F-nmr. Lipophilin, an integral protein of the myelin sheath surrounding nerve axons, was selected for this study since it has been reported to have five sulfhydryls per mole, two of which become oxidized during the course of isolation of the protein. It has also been postulated on the basis of esr and calorimetric studies of lipophilin incorporated into phospholipid bilayers that immobile or "boundary" lipid is present around the protein. This boundary lipid is distinct from the bulk lipid which behaves normally. It was proposed to incorporate lipophilin and FEM-d_2 modified lipophilin into synthetic fluorophosphatidylcholines and examine the lipid and protein ^{19}F-nmr resonances as a function of both temperature

and protein/lipid mole ratio.

The next three sections of this chapter will cover in detail the background for the studies undertaken in this thesis including kinetic studies, ^{19}F-nmr investigation of the N-F transition of FEM-d_2 and Br-TFP modified BSA and FEM-d_2 modified lipophilin incorporated into fluorophosphatidycholines as well as the experimental objectives in each of these studies.

2.2 Kinetic Studies

Maleimides, such as N-ethylmaleimide for example, have been used extensively as protein thiol modification reagents. From numerous kinetic studies of the reaction between prtein cysteine residues and maleimides,[121-128] it was evident that the thiol groups were readily modified. However, the relative rates of reaction of maleimides with water or with other protein nucleophiles such as amines, imidazoles and alcohols have never been studied. In order to evaluate the specificity of FEM as a thiol reagent, it was important that kinetic parameters be determined for a series of thiols in addition to a range of other nucleophiles which may compete with thiols under the conditions that a protein is modified.

The reactions with FEM of interest are shown in Figure 9.

Figure 9

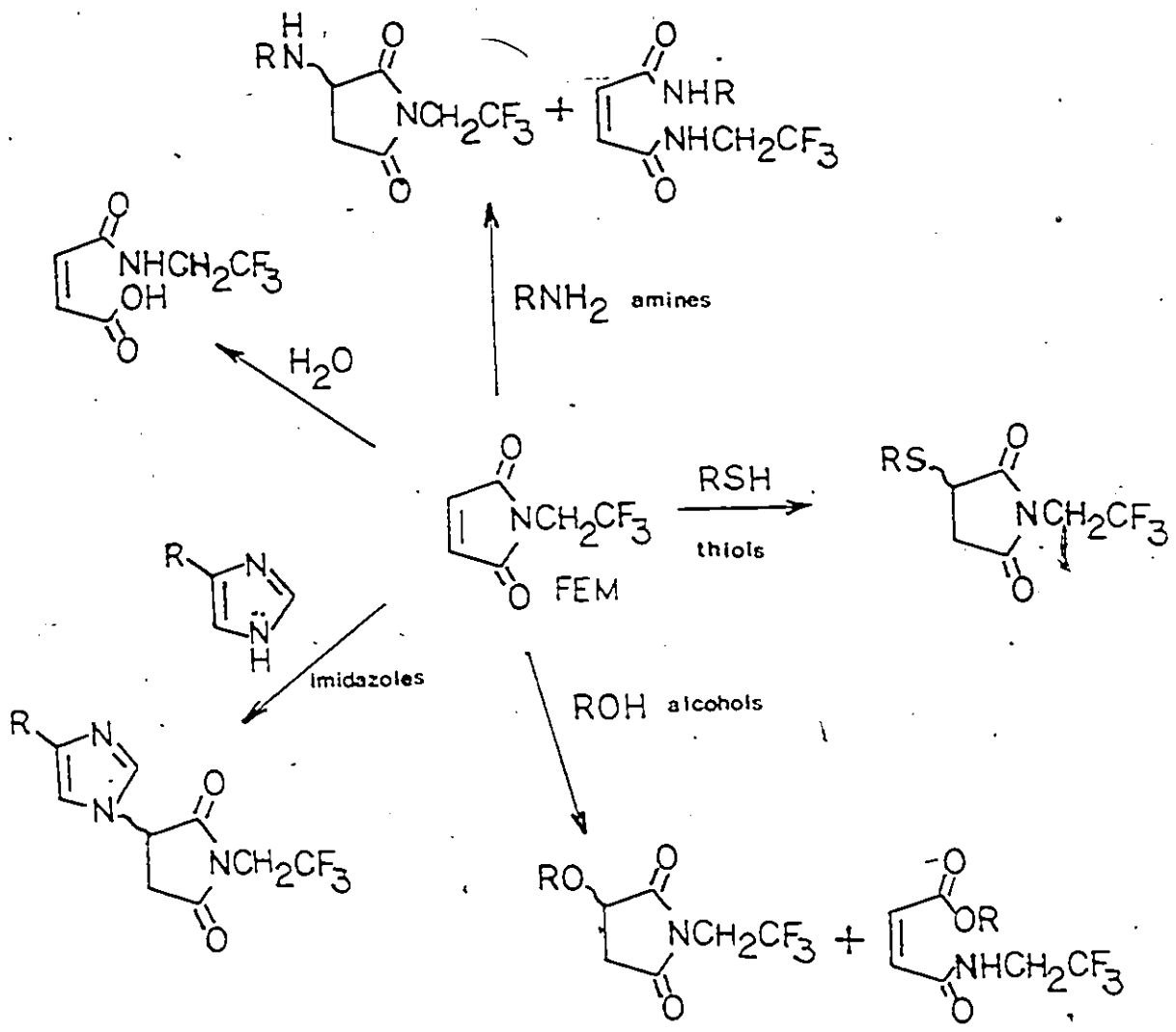

Possible Reactions of FEM

The thiols chosen for this study were L-cysteine 5, N-acetyl-L-cysteine 4, glutathione 5, and β-mercaptoethanol 6. (Table 6). The amino acids histidine, serine and lysine(Table 1) contai imidazole, alcohol and amine nucleophiles respectively.

In the investigation of the reaction between FEM and thiols, it was necessary to consider two types of sulfur nucleophiles which may react, the thiol (RSH) and the thiolate anion (RS^-) The equilibrium concentrations of these two nucleophiles will depend upon the pH of the medium relative to the pKa of the thiol. It is expected that the rate of reaction of FEM with the more nucleophilic thiolate anion will be substantially greater than with the thiol. Sekine et al[129-130] have investigated the pH dependence of the second order rate constant for the reaction of various carboxy thiols with fluorescent maleimides. A scheme of the following type was assumed (Figure 10).

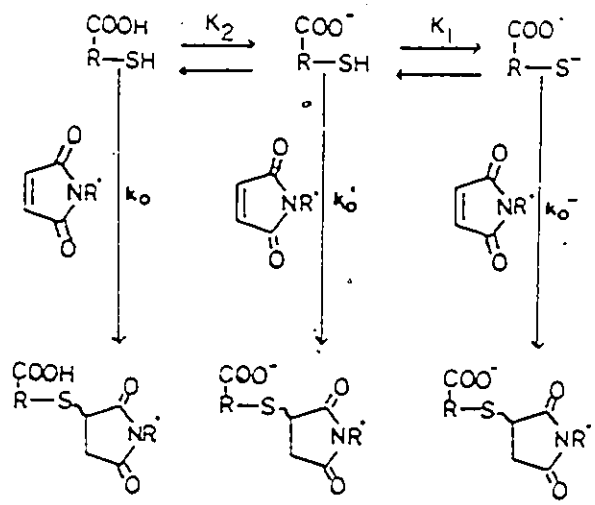

Figure 10

Table 6: Thiols Reacted with FEM.

Thiol	Structure
L-cysteine	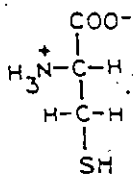 3
N-acetyl-L-cysteine	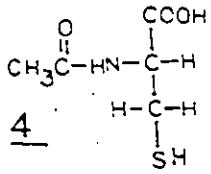 4
Glutathione	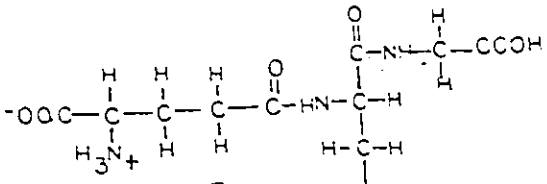 5
β mercaptoethanol	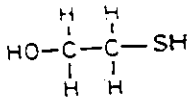 6

K_1 and K_2 are the dissociation constants of the thiol and carboxyl group respectively and k_o', k_o, and k_o^-, the true 2nd order rate constants for each ionized form of the carboxy thiol. The observed rate of reaction was assumed to be:

Eq: 1 $$[k_o^- . a + k_o . b + k_o' . c]\ [X] = k_{app}\ [a+b+c][X]$$

Where a, b. and c represent the concentration of $R(COO^-)(S^-)$ $R(COO^-)(S^-)$, $R(COO^-)(S^-)$ and $R(COOH)(SH)$ respectively, (X) the concentration of maleimide and k_{app} the observed second-order rare constant. k_{app} may be expressed in three ways depending on the pH of the system:[130]

Eqn.2 i) When $K_1 << K_2 << [H_3O^+]$

$$k_{app} = \frac{k_o . K_2}{(H_3O^+)} + k_o^1$$

Eqn.3 ii) Where $K_1 << [H_3O^+] << K_2$

$$k_{app} = \frac{k_o^- . K_1}{[H_3O^+]} + k_o \text{ and}$$

Eqn.4 iii) $[H_3O^+] << K_1 << K_2$

$$\frac{1}{k_{app}} = \frac{1}{k_o . K_1}\ [H_3O^+] + \frac{1}{k_o^-}$$

Three of the four thiols reacted with FEM were carboxyl thiols: L-cysteine 3, N-acetyl-L-cysteine 4 and glutathione 5: only β-mercaptoethanol 6 was not (Table 6), pKa values for each thiol

are given in Table 7 .

Table 7

Thiol	pKa SH
L-cysteine	8.3
Glutathione	9.1
β-mercaptoethanol	9.6
N-acetyl-L-cysteine	10.0

It is expected that in the pH 5.0-7.5 region, ionizations such as

$$HO.CH_2CH_2S^- + {}^-OH \rightleftharpoons {}^-OCH_2CH_2S^- + H_2O$$

for β-ME and

$$CH_3\text{-}N\text{-}\overset{\overset{O}{\|}}{C}\text{-}R + {}^-OH \rightleftharpoons CH_3N^{\ominus}\overset{\overset{O}{\|}}{C}\text{-}R + H_2O$$

for N-acetyl-L-cysteine can be ignored. For a thiol such as β-ME where only an ionization of the type

$$RSH + H_2O \overset{Ka}{\rightleftharpoons} RS^- + H_3O^+$$

is considered the observed rate of reaction may be written as:

Eqn. 5 $$\frac{-d[mal]}{dt} = (k_1[RSH] + k_2[RS^{\ominus}])\ [mal]$$

where [mal] = concentration of maleimide k_1 and k_2 are the true second-order rate constants for the reaction of RSH and $RS^{\ominus}$ with maleimide respectively. By assuming the following relationship,

Eqn. 6 $$\frac{-d[mal]}{dt} = k_{app}([RSH] + [RS^-])\ [mal]$$

and substituting (RSH) and ($RS^{\ominus}$) in terms of K_a, the dissociation constant of the thiol, expression for k_{app} becomes:

Eqn. 7 $$k_{app} = ([H_3O^+] + Ka)^{-1}\ (k_1[H_3O^+] + k_2.K_a[RSH])$$

when $[H_3O^+] >> Ka$,

Eqn. 8 $$k_{app} = \frac{k_2.K_a}{[H_3O^+]} + k_1$$

which is of the same form as Eq. 3.

The kinetic studies of the reaction between FEM and thiols or other nucleophiles were carried out under pseudo-first order conditions where the reactants were at least ten-fold or greater in excess of FEM.

For a pseudo-first order reactions of the type

$$A + B \underset{k_2}{\overset{k_1}{\rightleftharpoons}} C \quad \text{where} \quad [A] >> [B]$$

where (A) remains essentially unchanged over the course of the reaction, the observed pseudo-first order rate constant

k_{obs} is $k_1[A] + k_2$. In the case where $k_2 << k_1$ (i.e. the reaction is essentially irreversible), $k_{obs} = k_1[A]$. For the reaction of excess thiol with FEM, $k_{obs} = k_{app}$ [Thiol] where k_{app} can be expressed as Eqn. 2, 3, 4, or 7 (for β-ME) depending on the pH of the solution. Neither k_{app} nor k_{obs} are true rate constants since their expressions are pH dependent (Eqn. 2 to 7). The true second order rate constants k_o, k_o^1, k_o^- and k_1 and k_2 were not determined since the object of the kinetic studies was to compare the relative rates of reaction between FEM and thiols with FEM and other nucleophiles namely water, alcohol amino and imidazole groups. The pH dependance of k_{obs} for the reaction of FEM with thiols in the pH 5.0-7.5 region and other nucleophilic groups were examined. k_{app} values for each thiol were determined for comparison at pH 6.55. In addition, the apparent activation parameters ($\Delta H^{\ddagger}_{app}$, $\Delta G^{\ddagger}_{app}$, $\Delta S^{\ddagger}_{app}$, & $\Delta E^{\ddagger}_{app}$) for the reaction of each thiol with FEM were determined at pH 6.55. In the determination of these parameters, thermodynamic relationships of the following type were assumed;[131-134]

Eqn. 9 $$k_{app} = \frac{kT}{h} \exp(\Delta S^{\ddagger}_{app}/R)\exp(-\Delta H^{\ddagger}_{app}/RT)$$

and since $k_{obs} = k_{app}$(Thiol)

Eqn. 10 $$k_{obs} = \frac{kT}{h} \exp(\Delta S^{\ddagger}_{app}/R)\exp(-\Delta H^{\ddagger}_{app}/RT)$$

A plot of ln k_{obs} vs. 1/T (or Arrhenius plot) would have a slope of $-\Delta H^{\ddagger}_{app}/R$ and intercept of $\ln(KT/h) + \Delta S^{\ddagger}_{app}/R + \ln(\text{Thiol})$ allowing the calculation of both $\Delta H^{\ddagger}_{app}$ and $\Delta G^{\ddagger}_{app}$. Similarily, E_{app} and ΔG_{app} may be determined since $E^{\ddagger}_{app} = \Delta H_{app} + RT$ and

Eqn. 11 $$\Delta G^{\ddagger}_{app} = \Delta H^{\ddagger}_{app} - T\Delta S^{\ddagger}_{app}$$

Note, that since k_{app} is not a true rate constant, the activation parameters are labelled as "apparent".

In addition to the determination of the activation parameters for each thiol, the products of the thiol reaction with FEM were characterized

2.3 Bovine Serum Albumin

Bovine serum albumin (BSA) was chosen as a novel protein for initial modification for subsequent ^{19}F-NMR studies for the reasons stated previously in Section 2.1. Before discussing the experimental objectives involving BSA, some background information about this protein should be provided.

BSA is a protein with a molecular weight of 67,000 with a single reactive cysteine (Cys -34)[135-137] residue located near the amino end of the polypeptide. A principle biological role of this protein is the binding and transport of a host of non-polar compounds throughout the body via the bloodstream. Molecules such as fatty acids, and thyroid hormones

bind to BSA by strong non-covalent interactions.[135,138-140]

The protein is known to undergo two pH dependant conformational changes; one in the pH 3.0-6.0 known as the N-F transition and one in the pH 6.0-8.0 region known as the N-B transition. Studies of the N-F transition have shown that on lowering the pH of a BSA solution from 6.0 (N state) to 3.0 (F state) an expansion of the protein occurs exposing a hydrophobic crevice.[135,141] This transition is reversible and has been studied by circular dichroism, fluorescence and electron spin resonance spectroscopy.

Circular dichroism (CD) studies have shown that the ellipticity[Θ] at 262 nm (or [Θ] at 269 nm) increases 20% on going from the N (pH 6.0) to F form (pH 3.0).[142,143] The transitions at 262 nm or 269 nm are mainly due to the proteins internal disulfide linkages (17 in total) since when the protein disulfide groups are reduced under denaturing conditions these transitions disappear. The increase in $[\Theta]_{262nm}$ at higher pH's have been attributed to an overall increase in the number of rigidly oriented disulfide linkages.

Fluorescence studies of this transition have shown a shift of the wavelength of the emission maximum for the single tryptophan residue toward longer wavelengths (327-343 nm, λ_{ex} = 280nm) as the pH of the solution is increased.[144] This so called "red shift" is also accompanied by an

approximately 1.3-fold increase in fluorescence intensity at 343nm which has lead to the interpretation that tryptophan enters a hydrophobic crevice of the protein at the higher pHs of the transition.

Maleimide spin labels (Figure 11) have been used to modify the sulfhydryl residue of BSA and study the rotational correlation time (τ_c) of the spin label as a function of both methylene chain length and pH.[145-147] While τ_c increased as

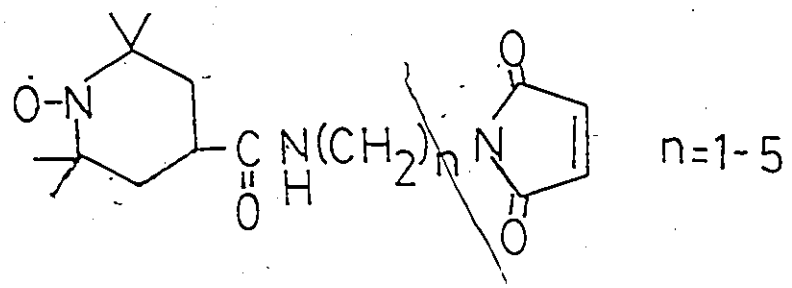

Figure 11

the pH increased, the overall greatest increase in τ_c was observed with n=3. This led to the interpretation that the hydrophobic crevice of BSA is approximately 10A° deep.

With an abundance of information about the N-F transition of BSA, the following studies were proposed:

1) A preliminary kinetic study of the reaction of FEM and BSA in order to assess whether or not a reaction between the sulfhydryl residue of the protein and FEM occurred. In addition, the sulfhydryl content of the protein would be

quantitated before and after modification. In order to assess the specificity of the reaction of FEM with the sulfhydryl residue of BSA, the protein would first be reacted with iodoacetamide under conditions where it is known that the sulfhydryl group is exclusively and quantitatively modified and then treated with FEM. The presence or absence of ^{19}F-nmr resonance in the "sulfhydryl blocked" protein would be used to assess non-sulfhydryl labelling.

2) A similar study to (1) would be performed using 3-bromo-1,1,1-trifluoropropanone to modify the BSA sulfhydryl residue. As mentioned in Section 2.1 of this chapter, non-SH labelling was observed in attempts to modify the β-97 cysteine residue of hemoglobin. Since this reagent was used to modify the cysteine residue of BSA and subsequently study the N-B transition, the question arose as to whether or not the observed ^{19}F-signals were due to sulfhydryl labelling alone. It was proposed to observe the modification of BSA by Br-TFP at two pH's as well as BSA whose sulfhydryl group had been "blocked" by any differences present in the ^{19}F-nmr spectra of each protein.

3) The perturbing nature of either FEM-d_2 or TFP labels had to be assessed by examining CD and fluorescence spectra of modified as well as unmodified proteins at pH's within the N-F transition.

4) Examine ^{19}F-nmr spectra of both BSA-FEM-d_2 as well as BSA-TFP at pH's in the N-F transition and observe either changes in the nmr linewidths or chemical shifts or the observed

5) Chemical Shift Anisotropy contributions to the ^{19}F-nmr linewidths would be assessed by comparing spectra obtained at 84.66 and 235.36 MHz. Since CSA contributions in the worst case can increase as the square of the applied magnetic field, (see Appendix I, Sect. 5.4.2) obtaining spectra at the highest possible field strength may be inappropriate.

2.4 Lipophilin

Myelin, a membrane found in the nervous system of vertebrates, is organized in segments along selected nerve fibres and functions as an insulator increasing the velocity of the stimuli transmitted along a nerve axon. Structurally, myelin is a lipid bimolecular leaflet, sandwiched between two layers of protein.[148-150] The myelin sheath is wrapped in a spiral fashion around segments of the axon resulting in a sheath up to 40 lipoprotein lamellae deep. Myelin is approximately 70% lipid and 30% protein by weight, the major lipid and protein components of human myelin are summarized in Table 8.

Table 8: Lipids and Proteins found in Human Myelin (taken from ref. 150).

Lipid Composition (μmoles/mg lipid)	
Cholesterol	.85
Galactolipids	
Cerobrosides	.248
Sulfatides	.051
Gangliosides	
Phospholipids	
Phosphatidylinisitols	.009
phosphatidylethanol amines	.250
phosphatidyl serines	.108
phosphatidyl cholines	.111
Sphinyomyelin	.089
Phosphatidic acid	
Cardiolipin	.042
Plasmalogens	.236

Protein Composition (mg/100mg protein)	
Low molecular weight protein (MW approx. 14,000)	3.23
Myelin Basic Protein	14.25
Lipophilin	12.20
Myelin Wolfgram Protein	
W_1	3.70
W_2	3.05

Multiple sclerosis (MS) is a disease affecting the central nervous system in which demyelination and destruction of nerve axons take place.[151-159] Although the disease is wide-spread throughout the central nervous system, there are preferred sites for the characteristic plaques of demyelinated nerve tract. Notably, many of these sites are found in the brain.[160] Presently the cause for this disease is unknown. Postmortem examination of MS patients has shown increased levels of lipophilin in their brains which lead to the proposal that this intrinsic myelin protein may be linked to the course of the disease.[161-170] Although the protein has no known enzymatic or dynamic function it is a major constitutent of the myelin membrane. (Table 8).

Approximately two thirds of lipophilin's amino acids have non-polar side chains; consequently, the isolated protein prefers to partition into non-polar solvents rather than water.[171-172] The protein has been shown to contain 2 moles of covalently bound fatty acids per mole of protein which enhances its solubility in non-polar environments.[169,173-175] Lipophilin contains five sulfhydryl residues, two of which are readily oxidized during the course of isolation. Of the remaining sulfhydryl residues, 1.5-2.0 residues react with sulfhydryl reagents such as DTNB even in denaturing media.[176]

Typically, the protein is isolated from the brain white

matter and purified by Sephadex LH-20 chromatography. A water soluble form of the protein may be prepared by dialysis of the protein from a 2-chloroethanol solution. CD as well as ORD measurements have shown that the protein has ~ 70% α-helical content in H_2O compared to 100% in 2-chloroethanol. α and β conformations of the protein were confirmed by infrared analysis.[175]

The interaction of intrinsic membrane proteins with phospholipids has been an area of considerable interest in recent years. A controversy has arisen as to whether or not an annulus of immobilized lipid or "boundary" lipid surrounds a protein embedded in a phospholipid bilayer. Before returning to a discussion of lipophilin, some experimental evidence which has lead to the aforementioned controversy will be presented.

Among those membrane proteins studied in detail are cytochrome C oxidase, sarcoplasmic and Ca^{2+} ATPase and rhodopsin.[177-185] Electron spin resonance studies of dilute fatty acid spin labels in protein recombinants have indicated that there is more than one environment for the esr probe. These results have been interpreted in terms of a two-state model, one state which is relatively mobile and identical to the bulk lipid before protein addition and the other, a relatively immobile state. The broader immobile component of the esr

spectra has been associated with spin probes in contact with the protein embedded in the bilayer which has led to the interpretation that the lipid in contact with the protein is motionally restricted to some degree. This latter lipid has been termed "boundary lipid".

In general, ^{31}P and ^{2}H-nmr studies of these same protein/lipid recombinants have shown little or no evidence for two lipid environments; this constitutes the basis for the controversy regarding the existance of boundary lipid. ^{2}H-nmr studies using phospholipids containing fatty acid chains which had been labelled with deuterium at specific positions (Figure 12) has shown little (1-2 KHz) or no change in the observed quadrupolar splitting (ΔV_Q) in the presence of protein although the nmr linewidths increase.

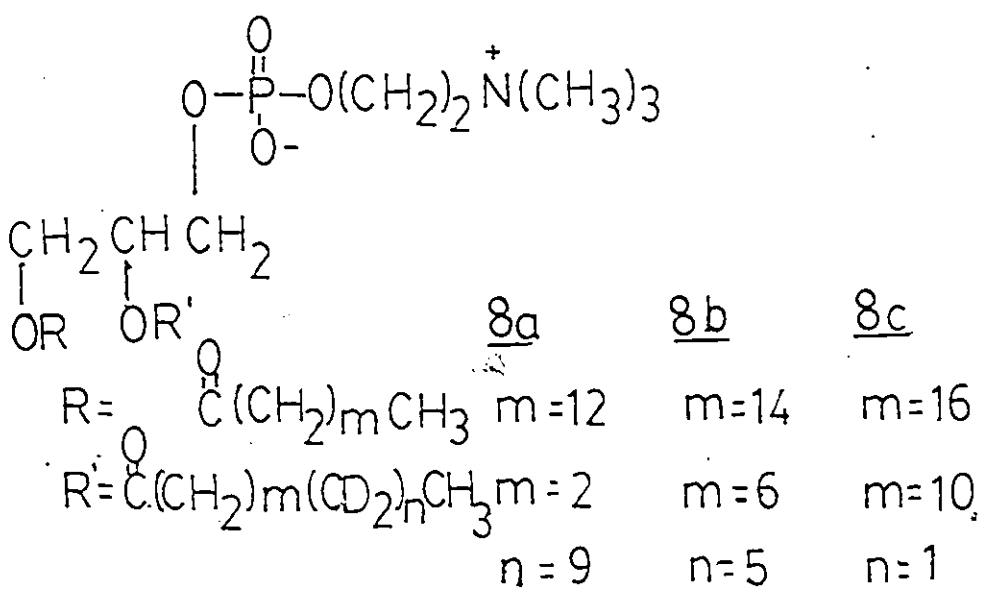

Figure 12

T_1 measurements obtained from ^2H and ^{31}P nmr studies of sarcoplasmic reticulum ATPase were unchanged in the presence of protein which showed a lack of orientational dependance if the lipids sampled a range of orientations over a smaller time compared to T_1.[186,187]

^{31}P-NMR studies by Yeagle[188] of glycophorin/phospholipid reconstituted systems have shown two overlapping ^{31}P-nmr signals - a major narrow signal atop a minor broad signal. The relative percentage of the broad component increased with increasing protein and is interpreted as evidence in support of a boundary lipid. It is important however to note that lipid head-group/protein interactions examined by ^{31}P-nmr and hydrocarbon chain/ protein interactions examined by ^2H-nmr may be totally different, accounting for the lack of evidence of "boundary" lipid by ^2H-nmr Two differing conclusions reached on the basis of esr and ^2H or ^{31}P-nmr experiments can be accounted for on the basis of different time scales: 10^{-6}-10^{-8}s for esr and $\sim 10^{-3}$ for nmr. Consequently, if boundary lipids exchange with bulk lipids at a rate faster than the nmr time scale but slower than the esr time scale, nmr data will show only an "average" picture.

At first it was believed that esr probes could hydrogen bond to the protein via the nitroxyl moiety but in the light of fluorescence anisotropy measurements,[189-193] this view has

been abandoned. Fluorescence depolarization studies using parinaric acid (9,11,13,15 octatetraenoic acid) or 1,6-diphenylhexatriene probes have quantitatively agreed with data obtained from esr experiments. The fluorescent probes were shown to be in two different lipid environments as was the case with the esr probes. Recent esr and fluorescent anisotropy measurements on Ca^{2+} -ATPase/DPPC mixtures agree with a model in which there is no stoichiometric ratio of protein to boundary lipid.[194]

Both esr and differential scanning calorimetric studies of lipophilin incorporated into phospholipid bilayers have indicated the presence of boundary lipid. Esr evidence has been obtained from the use of 12- and 8-doxyl stearic acids, 9a,b (Figure 13) as well as other niroxide spin labels.[195-198]

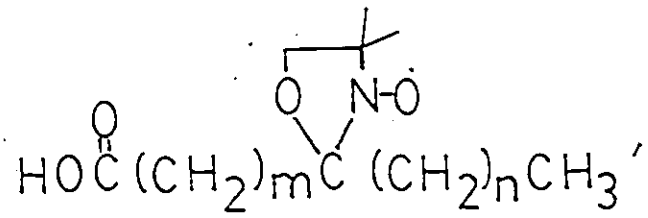

9a m=10 n=5

b m=6 n=9

Figure 13

In increasing the relative amount of protein, the corresponding amount of an immobilized component of the esr spectrum increased. Also, a small increase in the order parameter of the spin label (.49 to .55) was also evident on increasing the protein content from 10 to 30% by weight. DSC studies have shown that although the enthalpy of the phase transition of the lipid in the protein/lipid mixtures decreased on increasing amounts of protein, the temperature of the transition was unchanged.[199-201] This suggested that less lipid participated in the phase transition with increasing amounts of protein present. A linear extrapolation of enthalpy (ΔH) vs protein lipid mole ratio plot to where $\Delta H=0$, it was shown that 16-23 lipid molecules per molecule of protein didn't participate in the bulk lipid phase transition.

In contrast to these observations, an ^{2}H-NMR investigation of lipophilin incorporated into phospholipids deuterated at various methylene segments of the acyl chain, 8a-c produced no evidence for boundary lipid.[202] Increasing amount of protein had no observable effect on lipid order parameters which led to the conclusion that bulk and boundary lipid may exchange faster than the nmr time scale but slower than the time scale of the esr experiment.

^{19}F-dipolar spectra in contrast to ^{2}H-NMR studies of lipophilin incorporated into 4,4-difluorodimyristoylphosphat-

idylcholines 19a (Figure 14) showed a slight decrease in order parameter S_{FF} (.29 to .26 at 25°C) (Sect.5.4.3) on increasing protein from 23 to 70% by weight.[203]

Since the ultimate objective of this study was to attempt to simultaneously observe the protein and lipid environments using ^{19}F-nmr by incorporation of FEM-d_2 modified lipophilin into fluorophospholipids it was necessary to perform the following experiments.

1) Investigate conditions for the modification of lipophilin with FEM-d_2. Since the protein is very insoluble in water, various solvents in which lipophilin was soluble would be investigated using N-acetyl-L-cysteine as a model thiol compound.

2) Synthesize a series of fluorine-containing dimyristoylphosphatidylcholines, with CF_2 groups at varying positions of the acyl chains. The proposed synthetic scheme is outlined in Figure 14. Since each mole of phospholipid contains 4 fluorine atoms, relatively few nmr pulses would be required for good signal to noise ratios. The differences in the DSC traces of DMPC and the fluorinated DMPCs could also be used to assess the effect of introducing the ^{19}F label.

3) Finally, both lipophilin and lipophilin which was modified with FEM-d_2 would be incorporated into gemdifluoro DMPC mixtures and their ^{19}F-nmr chemical shifts and line-

Figure 14

Proposed Synthesis for Gem difluorophosphatidylcholines
(DAST - diethylamino sulfurtrifluoride)

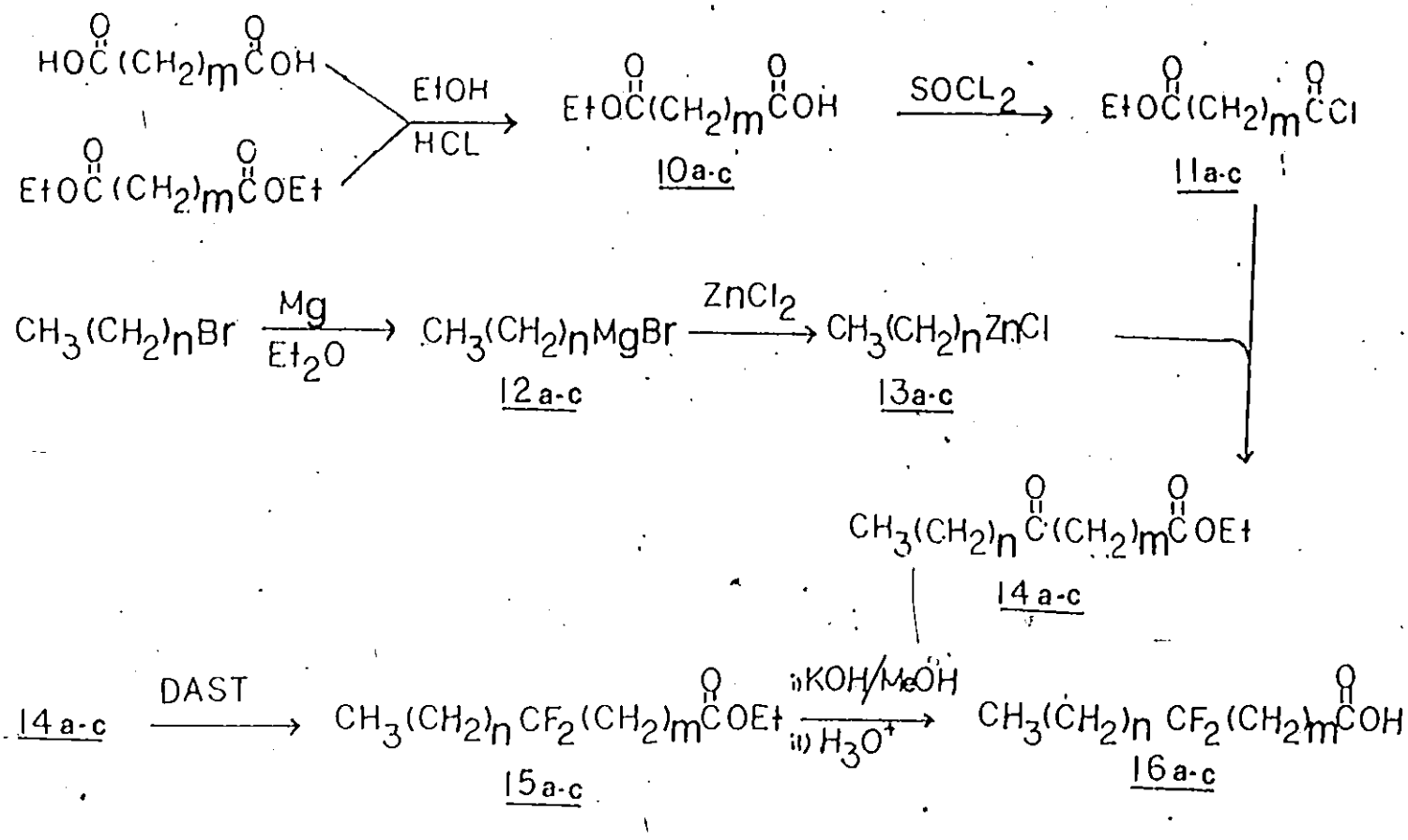

(DAST - diethylamino sulfurtrifluoride)

For compounds 10 & 11
- a m=2
- b m=6
- c m=10

12 & 13
- a n=9
- b n=5
- c n=1

For compounds 14-16
- a n=9, m=2
- b n=5, m=6
- c n=1, m=10

Figure 14 (CONT)

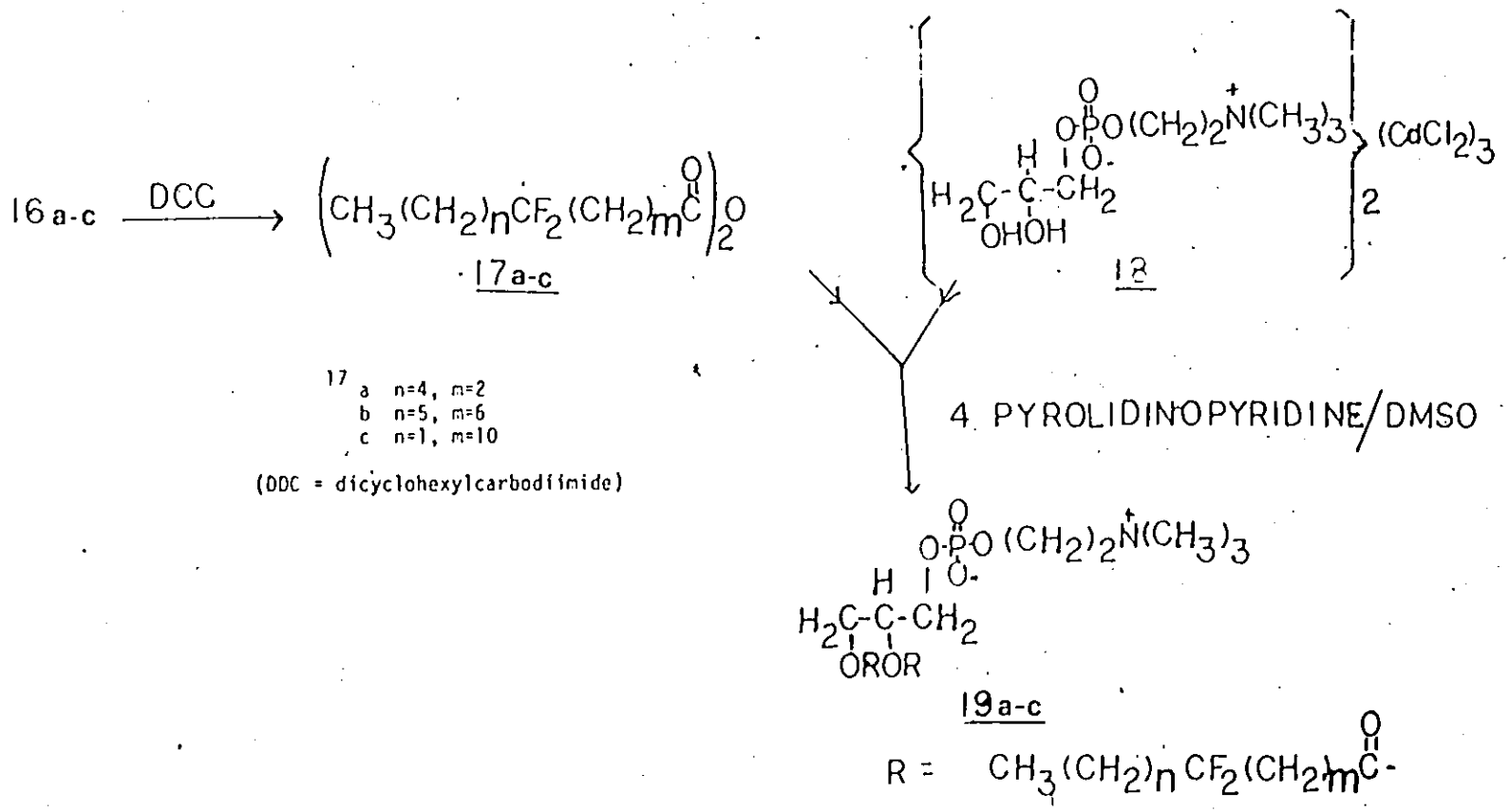

widths compared as a function of temperature and protein content of the mixture. Since all ^{19}F-nmr spectra were obtained at 235.36 MHz the time scale of the nmr experiment would be $\sim 10^{-4}$s (compared to 10^{-3}s for previous ^{2}H and ^{31}P NMR experiments, it was though possible that boundary lipid might exchange slowly enough to be observed.

CHAPTER THREE

RESULTS AND DISCUSSION

3.1 Synthesis of FEM and FEM-d_2

The synthesis of the maleimides 22a and 22b and their precursors proceeded in good yields (Figure 53). The only major difficulty encountered was the volatilization of either 2,2,2-trifluoroethylamine or 2,2,2-trifluoro-1,1-dideuteroethylamine during the work up of the $LiAlH_4$ or $LiAlD_4$/trifluoroacetamide mixtures with 5% NaOH (Section 4.2).

3.2 Kinetic Studies of the Reaction of FEM with Thiols, Oxygen and Nitrogen Nucleophiles

Solutions of 1mM FEM and either 26mM thiol or L-lysine, L-serineand L-histidine were mixed and their rates of reaction monitored by the stopped flow technique(Section 4.3.1-4.3.4). kobs and $t_{\frac{1}{2}}$ were determined for each reaction over a range of pH values and are given in Table 9a and 9b. A composite plot of log kobs vs. pH for the reaction of FEM with thiols and other nucleophiles (Figure 15) demonstrates that FEM reacts at least 10^5 fold faster with thiols than with the other nucleophiles, i.e., amines, alcohols and imidalazoles. A comparison of the kobs values for FEM hydrolysis with the rate constants of the reaction of the FEM reaction with L-lysine, L-histidine or L-serine the same pH values (Table 9b) shows that these values agree within the calculated statistical error (± 1

standard deviation). Thus, the hydrolysis of FEM proceeds at rates that equal or exceed the rate of any reaction with these amino acids. The only new product observed by the TLC analysis in any of these reactions was N-2,2,2-trifluoroethylmaleamic acid, 21a the product of FEM hydrolysis and L-lysine, L-serine or Lhistidine. A least squares analysis for the log kobs vs pH plot for FEM hydrolysis (Figure 15) gives a slope of 1.00 which indicated a 10-fold increase in rate for each 10-fold increase in OH^-.

Log kobs vs pH plots for the reaction of 1mM FEM and 26mM thiol solutions (Figure 15), also gave a consistant slope of 1.00 (± .03) for the least squares fit. A possible explanation for this might be in the form of kapp, the apparent second order rate constant, in the pH region (pH 5.00 - 7.00) in which the kinetic measurements were made. As stated previously in Chapter 2, Section 2.2, the expression of kapp was previously shown to be pH dependant. For the carboxy thiols reacted with FEM in the pH 5.0 - 7.0 region (i.e., N-acetyl-L-cysteine 4, L-cysteine 3 and glutathione 5) where $K_1 < H_3O^+ \leq K_2$, kapp is of the form given by Eqn. 3.

Eqn. 3 $$kapp = \frac{k_0 - K_1}{H_3O^+} + ko$$

If $ko << ko^- K_1 / H_3O$ and since kobs = kapp [Thiol], then

Eqn 12 $$\log kobs = \log ko^- + \log [Thiol] - pka + pH$$

Table 9a: $\bar{k}$obs and $\bar{t}_{\frac{1}{2}}$ values for the reaction of various thiols (26mM) with 1mM FEM at different pHs. T=30.0 ± 0.1°C.

β-mercaptoethanol pH	kobs ± 1 S.D. (s^{-1})	$t_{\frac{1}{2}}$ ± 1 S.D. (s)
5.11	(4.13 ± .07) x 10^{-1}	(1.68 ± .03)
5.70	1.49 ± .03	(4.65 ± .09) x 10^{-1}
6.17	4.60 ± .08	(1.51 ± .03) x 10^{-1}
6.66	(1.55 ± .06) x 10^{1}	(4.46 ± .18) x 10^{-2}
7.16	(4.35 ± .10) x 10^{1}	(1.59 ± .04) x 10^{-2}
7.66	(1.17 1 .05) x 10^{2}	(5.89 ± .25) x 10^{-3}

L-cysteine pH	kobs ± 1 S.D. (s^{-1})	$t_{\frac{1}{2}}$ ± 1 S.D. (s)
5.15	1.71 ± .07	(4.03 ± .16) x 10^{-1}
5.65	6.31 ± .23	(1.10 ± .04) x 10^{-1}
6.15	(1.82 ± .03) x 10^{1}	(3.81 ± .07) x 10^{-2}
6.65	(4.23 ± .11) x 10^{1}	(1.64 ± .04) x 10^{-2}

N-acetyl-L-cysteine pH	kobs ± 1 S.D. (s^{-1})	$t_{\frac{1}{2}}$ ± 1 S.D. (s)
5.16	(2.29 ± .07) x 10^{-1}	3.03 ± .09
5.65	(7.05 ± .10) x 10^{-1}	(9.82 ± .15) x 10^{-1}
6.15	2.18 ± .07	(3.18 ± .10) x 10^{-1}
6.65	5.42 ± .17	(1.28 ± .04) x 10^{-1}
7.15	(1.94 ± .06) x 10^{1}	(3.58 ± .11) x 10^{-2}

Glutathione pH	kobs ± 1 S.D. (s^{-1})	$t_{\frac{1}{2}}$ ± 1 S.D. (s)
5.16	(7.22 ± .23) x 10^{-1}	(9.61 ± .31) x 10^{-1}
5.68	2.59 ± .14	(2.68 ± .14) x 10^{-1}
6.16	7.08 ± .18	(9.78 ± .24) x 10^{-2}
6.67	(2.46 ± .06) x 10^{1}	(2.80 ± .07) x 10^{-2}
7.18	(7.10 ± .22) x 10^{1}	(9.76 ± .29) x 10^{-3}

Table 9b:

i: kobs and $t_{\frac{1}{2}}$ Values for FEM hydrolysis at 30.0 ± 1°C

pH	kobs ± 1 S.D. (s^{-1})	$t_{\frac{1}{2}}$ ± 1 S.D. (s)
9.04	$(5.61 \pm .20) \times 10^{-3}$	$(1.24 \pm .04) \times 10^{2}$
9.41	$(1.30 \pm .08) \times 10^{-2}$	$(5.34 \pm .06) \times 10^{1}$
9.80	$(3.22 \pm .06) \times 10^{-2}$	$(2.15 \pm .04) \times 10^{1}$
10.24	$(8.95 \pm .34) \times 10^{-2}$	$(7.74 \pm .29) \times 10^{0}$
11.25	$(8.84 \pm .27) \times 10^{-1}$	$(7.83 \pm .24) \times 10^{-1}$
11.63	$(2.24 \pm .08) \times 10^{0}$	$(3.09 \pm .11) \times 10^{-1}$

ii: kobs and $t_{\frac{1}{2}}$ values for the mixing of 30mM L-lysine HCl Solutions of varying pH with 1mM FEM at 30.0 ± 0.1°C

pH	kobs ± 1 S.D. (s^{-1})	$t_{\frac{1}{2}}$ ± 1 S.D. (s)
9.36	$(1.37 \pm .05) \times 10^{-2}$	$(5.06 \pm .18) \times 10^{1}$
9.76	$(3.32 \pm .07) \times 10^{-2}$	$(2.09 \pm .04) \times 10^{1}$
10.22	$(9.36 \pm .56) \times 10^{-2}$)	$(7.40 \pm .44) \times 10^{0}$
11.60	$(2.39 \pm .09) \times 10^{0}$	$(2.90 \pm .11) \times 10^{-1}$

iii: kobs and $t_{\frac{1}{2}}$ values for the mixing of 30mM L-Histidine HCl Solutions of varying pH with 1mM FEM at 30.0 ± 0.1°C

pH	kobs ± 1 S.D. (s^{-1})	$t_{\frac{1}{2}}$ ± 1 S.D. (s)
9.39	$(1.31 \pm .04) \times 10^{-2}$	$(5.29 \pm .16) \times 10^{1}$
9.77	$(3.26 \pm .10) \times 10^{-2}$	$(2.13 \pm .07) \times 10^{1}$
10.17	$(9.74 \pm .11) \times 10^{-2}$	$(8.72 \pm .12) \times 10^{0}$
11.63	$(2.37 \pm .12) \times 10^{0}$	$(2.97 \pm .15) \times 10^{-1}$

Table 9b: Cont.

iv: kobs and $t_{\frac{1}{2}}$ values for the mixing of 30mM L-serine HCl Solutions of varying pH with 1mM FEM at 30.0 ± 0.1°C

pH	kobs ± 1 S.D. (s^{-1})	$t_{\frac{1}{2}}$ ± 1 S.D. (s)
9.40	$(1.30 \pm .08) \times 10^{-2}$	$(5.30 \pm .18) \times 10^{1}$
9.80	$(3.29 \pm .11) \times 10^{-2}$	$(2.10 \pm .08) \times 10^{1}$
10.19	$(9.44 \pm .32) \times 10^{-2}$	$(7.00 \pm .50) \times 10^{0}$
11.61	$(2.41 \pm .15) \times 10^{0}$	$(2.81 \pm .15) \times 10^{-1}$

Figure 15

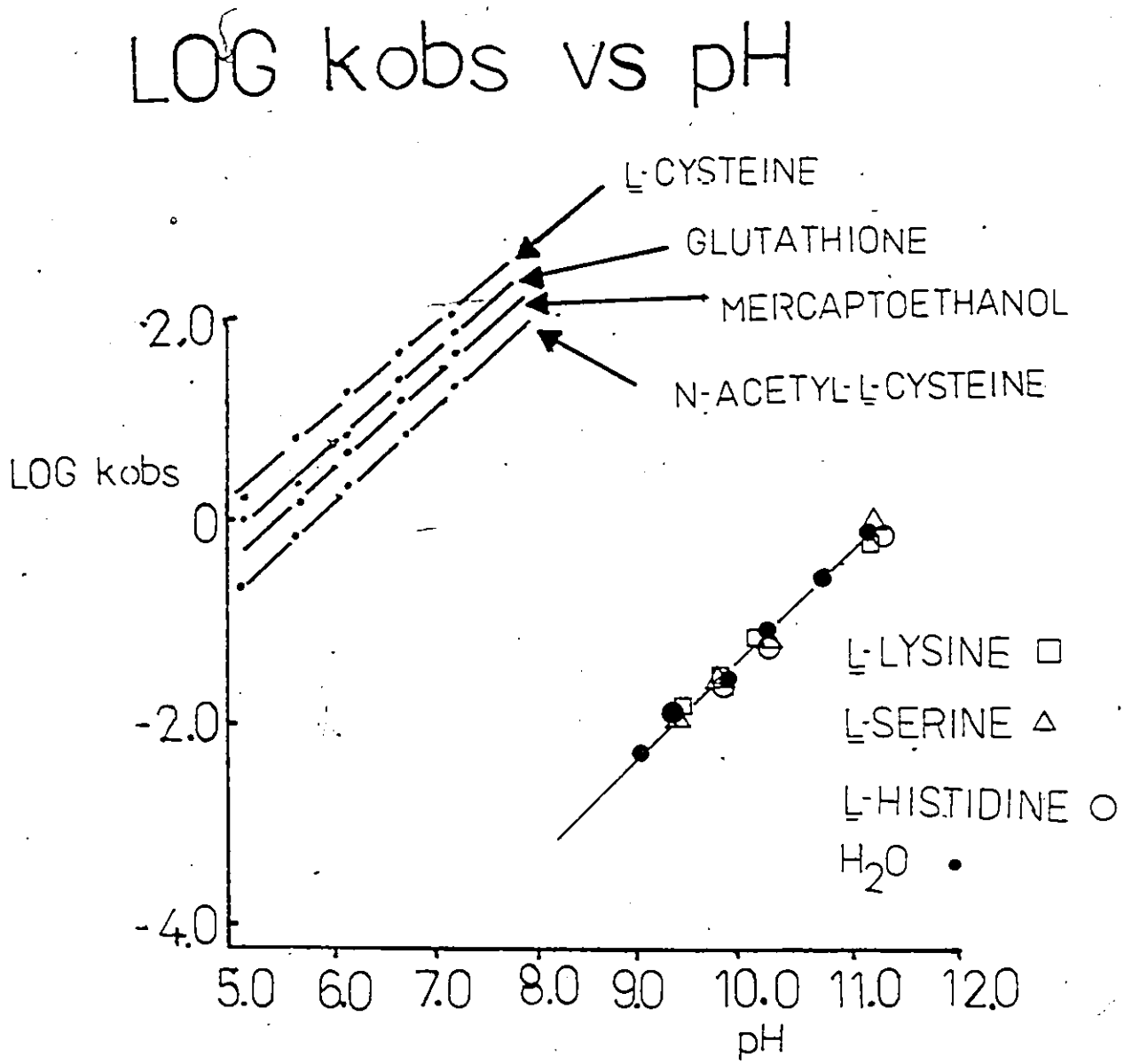

A composite plot of log kobs vs. pH for the reaction of FEM with thiols or other nucleophiles.

If a similar assumption is made for p-mercaptoethanol in the pH 5.0 - 7.0 range, i.e.,

$$k_1 << k_2 \, Ka/[H_3O]^+$$

then

Eqn. 13 $$\log kobs = \log[Thiol] + \log k_2 - pKa + pH$$

Consequently, a plot of log kobs vs pH would be expected to have a slope of 1.0. The ko^- and ko values determined by Sekine[63] for the reaction were in the order of 10^6 and $10^2 M^{-1} sec^{-1}$ respectively (with no reported error limits) which corresponded to $ko^- K_1/H_3O^+$ values no less than 100-fold greater than ko over the same pH range. Likewise Sekine's k_1 and k_2 values for mercaptoethanol were 4.35×10^7 and $5.0 \times 10^2 \, M^{-1} sec^{-1}$ giving values of $k_2 Ka/[H_3O^+]$ that were at least 10 - 1,000 fold greater than k_1 over the pH 5.0 to 7.0 range. Since we were dealing with a similar 1,4-addition process using the same carboxythiols as Sekine but a different maleimide, FEM, it was likely that we were dealing with a similar situation where $ko^- K_1/[H_3O^+] >> ko$ and $k_2 Ka/[H_3O^+] >> k_1$. Since the true second order rate constants, ko, ko^-, ko^-, k_1 and k_2 were not determined, a comparison with those calculated by Sekine[63] was not possible. The apparent second order rate constant, kapp, for the reaction of 1mM FEM thiols at pH 6.65 was determined from the slopes of kobs vs [Thiol] plots (Figure 16 and Table 10).

Figure 16

kobs vs [Thiol]

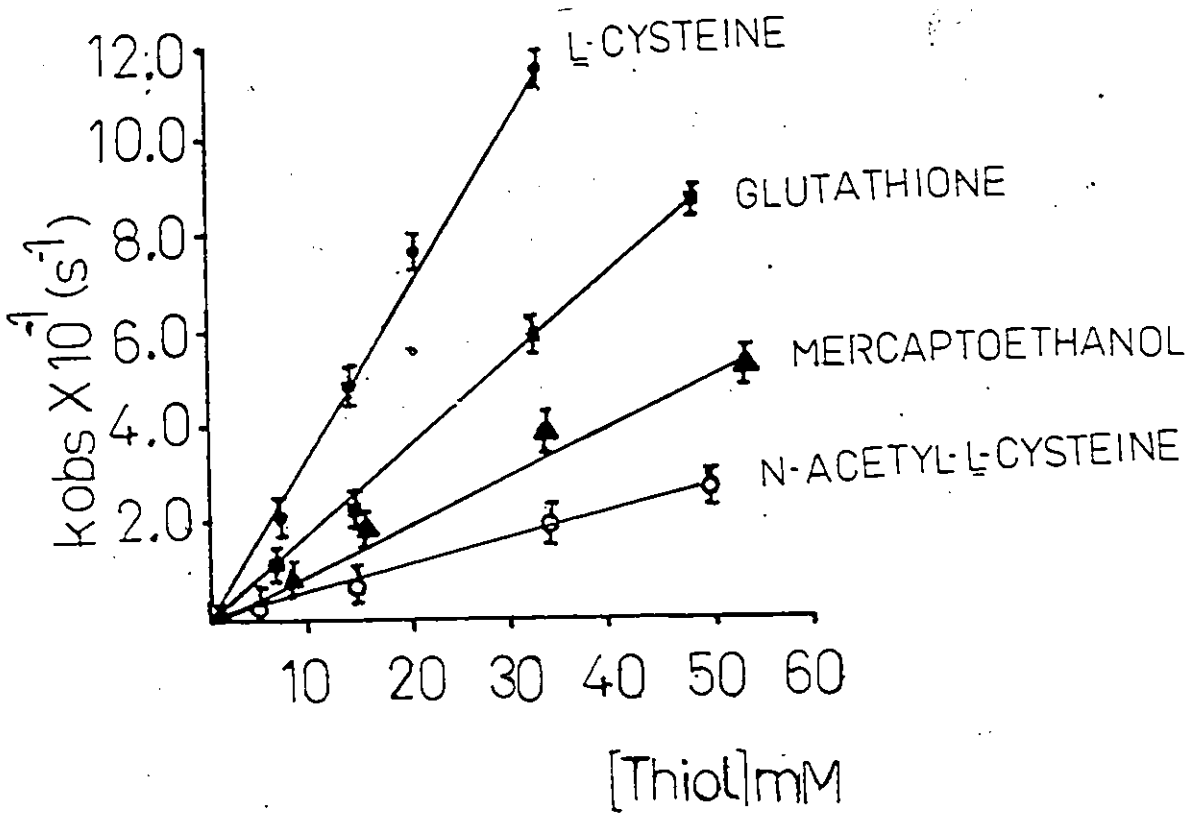

Table 10 kapp values at pH 6.65 and 30 ± 0.1 °C

Thiol	kapp. ($M^{-1}min^{-1}$)
L-cysteine	(2.46 ± .14) X 10^5
Glutathione	(1.07 ± .08) X 10^5
β-mercaptoethanol	(5.76 ± .46) X 10^4
N-acetyl-L-cysteine	(3.35 ± .18) X 10^4

A plot of log kapp vs pKa of the thiol (Figure 17) shows a very good linear correlation with a least squares slope -0.51 (± 0.08). If the previous assumptions about the form of kapp in the pH 5.0-7.0 range are indeed true and k_2 and ko^- values are of the same order of magnitude then

Eqn. 14 $\log kapp = \log ko^- - pK_1 + pH$ or

Eqn. 15 or $\log kapp = \log k_2 - pKa + pH$

Subsequently, a plot of log kapp vs pKa would be expected to be linear with a slope of -1.00 in contrast to the experimentally observed slope of -0.51. Since the true second-order rate constants were not determined, the reasons for this discrepancy are not known.

Arrhenius plots for the reactions of thiols with FEM as well as the apparent activation parameters at pH 6.65 are shown in Figure 18 and Table 11 respectively. In the determination of these apparent activation parameters, the relatively large errors in the least squares intercept (± 13) resulted in similar errors in $\Delta G^{\ddagger}app$ and $\Delta S^{\ddagger}app$, therefore there are no significant differences between the values for each thiol. The comparatively smaller error in the slope (~5%) of the same plots resulted in $\Delta H^{\ddagger}app$ and $\Delta E^{\ddagger}app$ values which were different for each thiol.

The most important result from all of the kinetic data is that FEM reacts much more quickly with thiols than other

Figure 17

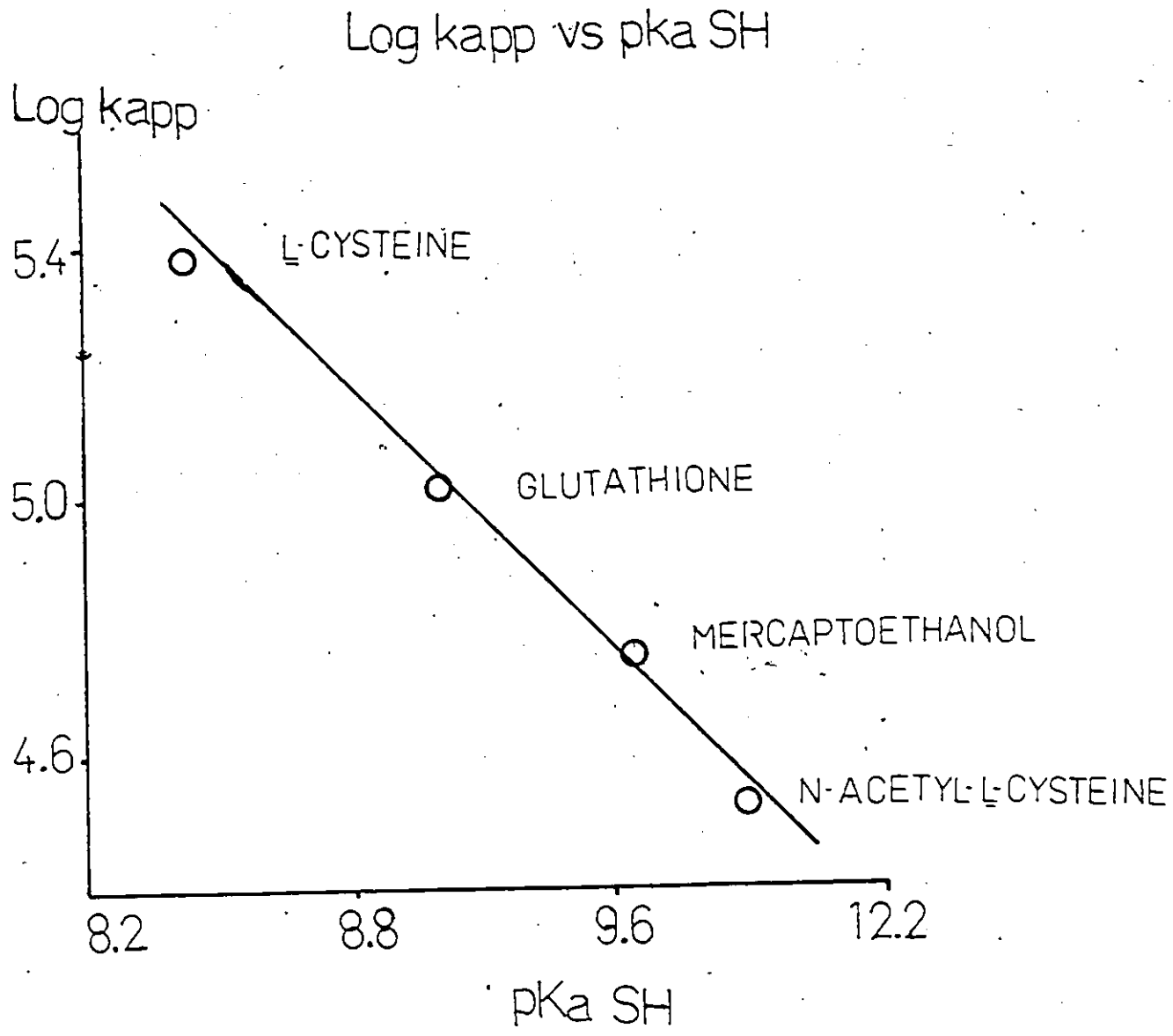

A plot of log kapp vs pKa SH at pH 6.65 for each thiol reacted with FEM.

Figure 18

Arrhenius plots for the reaction of various thiols (26mM) With FEM

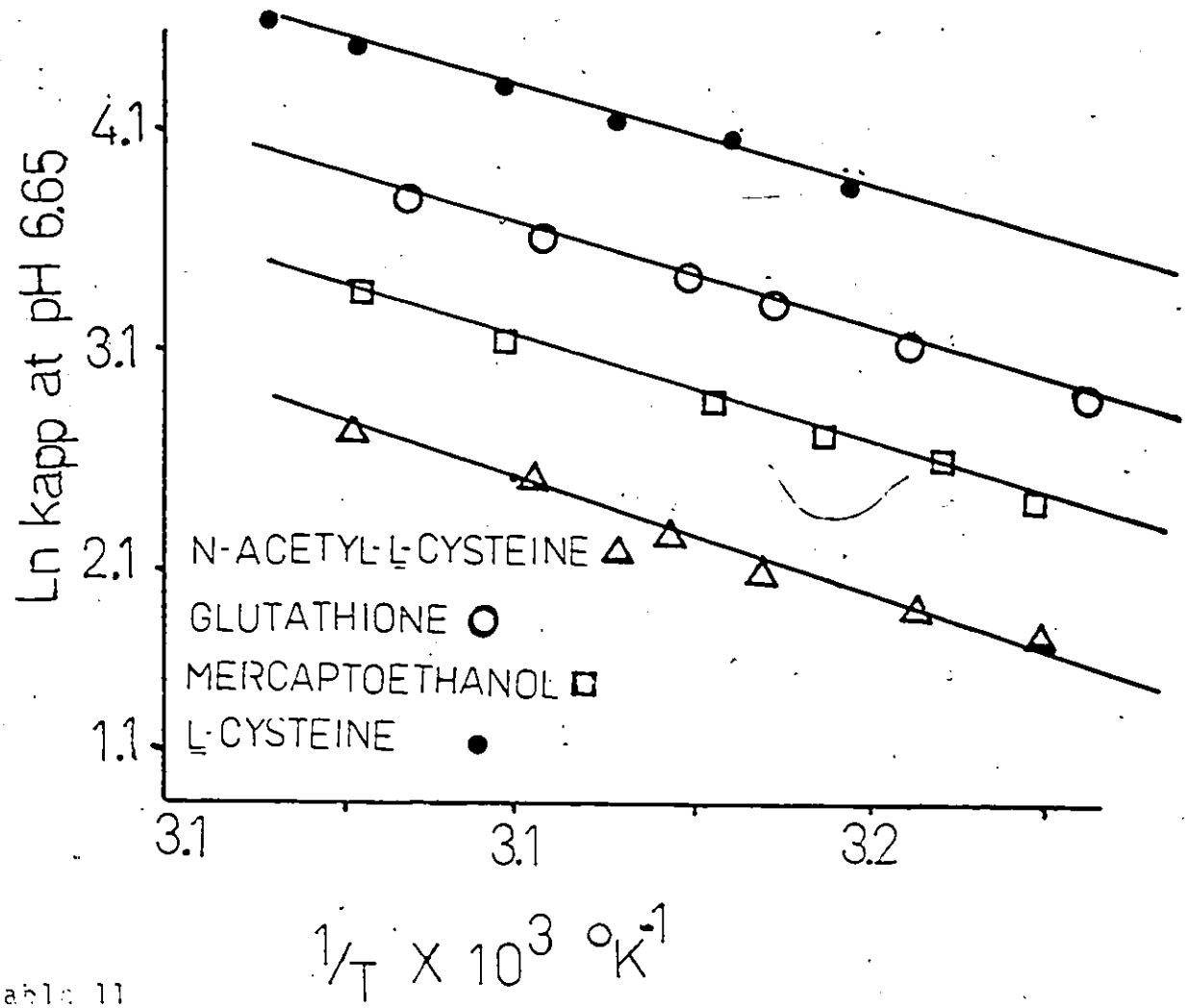

Table 11

Activation parameters for the reaction between various thiols and FEM at pH 6.65

Thiol	Happ($\frac{kcal}{mole}$)	Sapp($\frac{cal}{°K\ mole}$)	Gapp($\frac{kcal}{mole}$)	Eapp($\frac{kcal}{mole}$)
L-cysteine	8.66 ± .11	-13.2 ± 1.2	13.1 ± 1.5	12.1 ± .1
Glutathione	10.3 ± .2	-9.36 ± 1.78	13.2 ± 1.3	10.9 ± .2
N-acetyl-L-cysteine	11.5 ± .3	-8.14 ± 3.40	13.1 ± 1.5	9.18 ± .03
B-mercaptoethanol	9.36 ± .33	-13.6 ± 3.4	13.6 ± 1.1	9.67 ± .11

potentially nucleophilic residues found on proteins; therefore it would be expected that protein cysteine residues would react rapidly and specifically with FEM without interfering side reactions, except for hydrolysis which proceeds at least 10^5 to 10^6 times more slowly. In studies of proteins by chemical modification, it is often the case that the specificity of the reaction of a reagent with the target or other R groups, is not studied in detail. Consequently, unexpected side reactions occur on other sites.

3.2.1 Preliminary Kinetic Studies with Bovine Serum Albumin (BSA)

When commercial fraction V BSA (10^{-5}M) and FEM (10^{-3}M) were mixed, an absorbance decrease was observed at 276nm. Five kobs values were determined with an average value kobs ($\pm$ 1 standard deviation) of ($1.38 \pm .13$) x 10^{-2} sec^{-1} with an average half-life of $5.00 \pm .45$ sec at pH 6.64. Subsequent Sephadex G-25 chromatography of an aliquot of the protein solution and DTNB analysis (Sect. 4.5), of the protein fraction showed no remaining sulfhydryl residues compared to 0.68 SH/mole prior to FEM treatment. In comparison with the rate of reaction of FEM with low molecular weight thiols in which the thiol concentrations were 25 mM (as opposed to 6.8×10^{-6}M for the protein solution) the expected half-life of the reaction

of 1mM FEM with 26mM protein (1 SH/mole) solution at pH 6.65 would be in the order of 1×10^{-3} sec. which is ~ 10-fold faster than L-cysteine or any other thiol at 6.65. Consequently, the protein modification experiment could be designed such that FEM can be added to the protein solution, specific and rapid modification of the protein sulfhydryl residue occurs and the excess label can be removed immediately by Sephadex G-25 chromatography or dialysis. It was decided that FEM-d_2 would be used for the labelling and ^{19}F-nmr studies of BSA since the ^{19}F signal of FEM-d_2 (in H_2O) shows a single resonance at -70.63 ppm whereas the ^{19}F resonance of FEM is a triplet at -70.41 ppm. Consequently, the line broadening of ^{19}F resonance due to the slower rotational correlation of the modified protein would be more easily observed for the single resonance of FEM-d_2 as opposed to the broadening of each of the lines comprising the triplet ^{19}F signal of FEM.

3.3 Examination of the N-F Transition of BSA

3.3.1 Specificity of the FEM-d_2 and Bromotrifluoropropanone Labels

To investigate the specificity of FEM-d_2 for the cysteine sulfhydryl residue of BSA, a sample of purified mercaptalbumin monomer (Section 4.5) was prepared and treated with iodoacetamide under conditions where the sulfhydryl residue has been shown to be exclusively and quantitatively modified (as shown wint ^{14}C-iodoacetamide labelling followed by amino acid analysis). After the reaction of acetamide-BSA with FEM-d_2 at pH 6.65,

followed by dialysis, no ^{19}F-resonances were observed after 40,000 scans v_o = 84.66 MHz). This result indicates that any FEM reaction with non-sulfhydryl protein nucleophiles occurred to an extent less than 0.5 %. The value of 0.5% was determined from a comparison of signal to noise ratios of aqueous FEM-d_2 solutions of varying concentrations after 40,000 scans. In contrast to this result, ^{19}F-NMR spectra of mercaptalbumin monomer which had been treated with FEM-d_2(BSA-FEM-d_2),(Sect. 4.5.1) for 20 minutes at pH 6.50 after the excess label removed by dialysis showed resonances at approximately -68.2, -69.2 and -71.8 ppm whose relative magnitudes were pH dependant (Section 3.3.1, Figure 24). In order to ascertain whether or not non-covalent binding of FEM-d_2 to the protein occured, excess FEM-d_2 was added to either acetamide-BSA or BSA-FEM-d_2 and the linewidth and chemical shift of the excess label monitored as a function of protein or FEM-d_2 concentration. When excess FEM-d_2 was added to either BSA-FEM-d_2 or acetamide-BSA solutions, a single narrow ^{19}F resonance ($V_{\frac{1}{2}h}$ = 10hz) was observed at -70.31 ppm whose linewidth or chemical shift was invariant with protein or FEM-d_2 concentration. This suggested that strong non-covalent binding of FEM-d_2 by the protein did not occur since either protein bound FEM-d_2 or FEM-d_2 that exchanged between a bound and unbound state would result in larger ^{19}F-nmr linewidths and/or a different chemical shift that unbound FEM-d_2. ^{19}F-NMR spectra (v_o = 84.66 MHz) of mercaptalbumin monomer treated with 1-bromo-3,3,3-trifluoro-propane under conditions identical to those of Zurawski[120]

(i.e., pH 7.20 for 1 hr) showed, in addition to resonances at approximately -82.0 and -84.1 ppm (labelled A' and B' respectively) whose relative proportions were pH dependent and (Section 3.4.3.8) a peak at -83.6 ppm whose relative magntiude (~14%) (Figure 19) did not change with pH. Alternatively, BSA treated with Br-TFP at pH 6.50 for 20 min. (Sect. 4.5.3) showed no resonance at -83.6 ppm. However, after treatment of BSA-FEM-d_2 with Br-TFP in addition to the trifluoroacetate internal standard (-75.96 ppm) and BSA-FEM-d_2 resonances a -83.6 ppm peak which comprised 20% of the total areas (excluding trifluoroacetate) (Figure 20) was observed. Clearly the -83.6 ppm peak is due to non-sulfhydryl labelling - most likely the reaction of a lysine amino residue as previously observed.[119] Therefore, it is likely that some of the ^{19}F resonances observed by Zurawski[120] were the result reactions of Br-TFP at residues other than the sulfhydryl groups.

3.3.2 Circular dichroism (CD) and fluorescence profiles of BSA, BSA-FEM-d_2 and BSA-TFP

The perturbing nature of the FEM-d_2 and Br-TFP sulfhydryl labels on BSA was assessed by the examination of CD and fluorescence (Sect. 5.1, 5.2, 4.5.5 and 4.5.6) profiles of all three proteins. BSA-TFP was prepared by reacting Br-TFP with mercaptalbumin monomer at pH 6.65 for 20 min. (where non-sulfhydryl labelling did not occur (Section 3.2.1)), followed by removal of the excess label by dialysis. Circular dichroism (CD) profiles of BSA, BSA-FEM-d_2 and BSA-TFP were found to be essentially identical. Typical CD spectra are shown in Figure 21.

Figure 19

Typical 84.66 MHz ^{19}F-NMR Spectra of BSA-TFP in the in the pH 3.00 - 4.00 range.

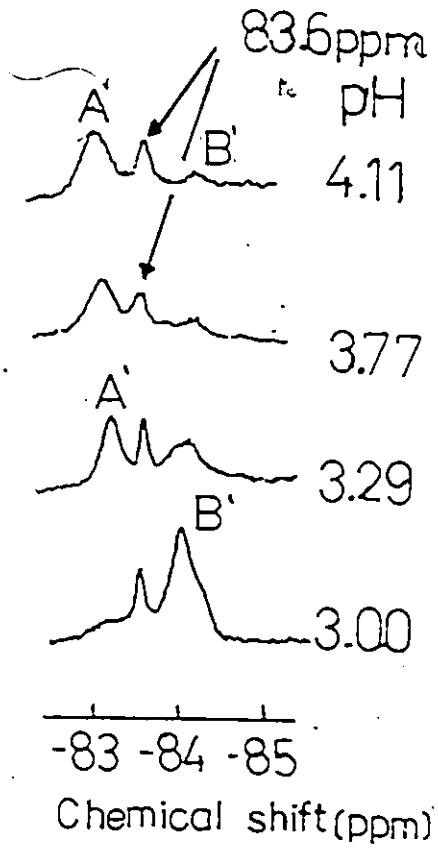

Figure 20

235.36 MHz ^{19}F-NMR Spectrum of BSA-FEM-d_2 treated with 3-Bromo-1,1,1-trifluoropropanone.

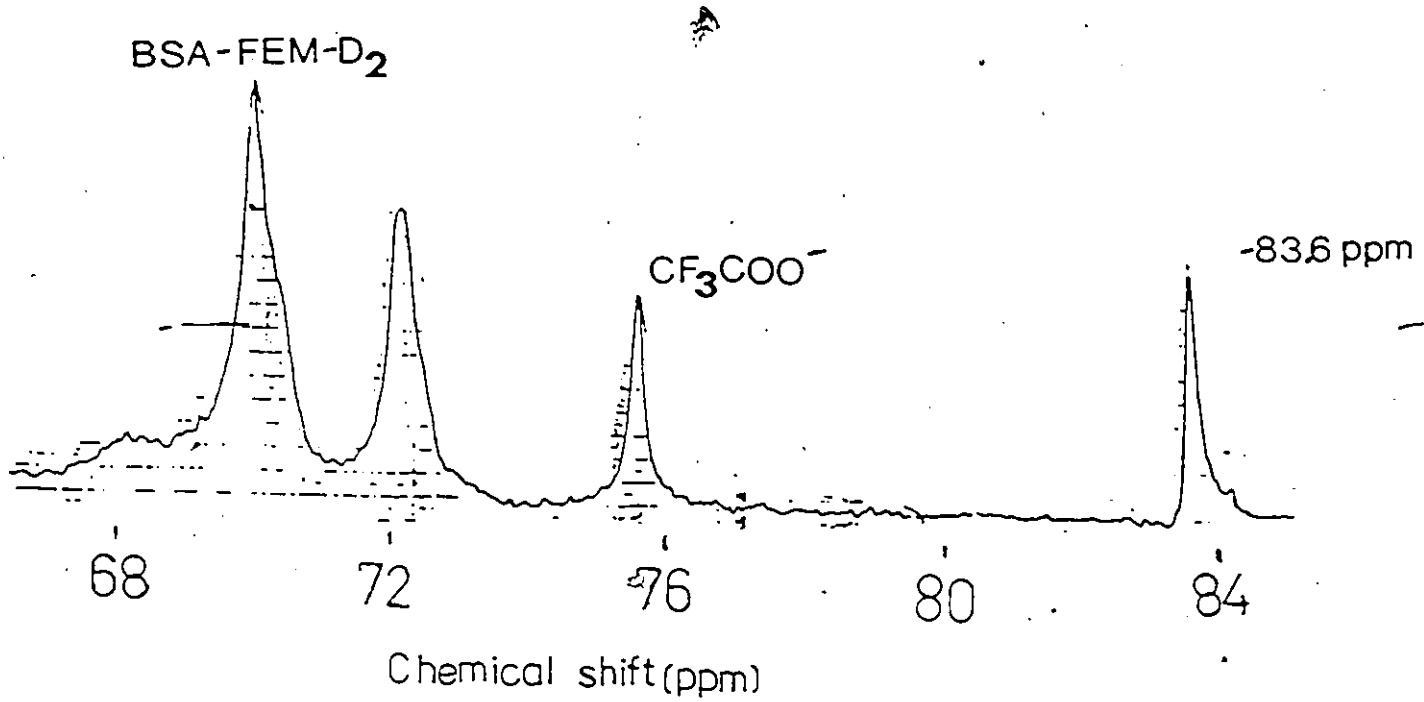

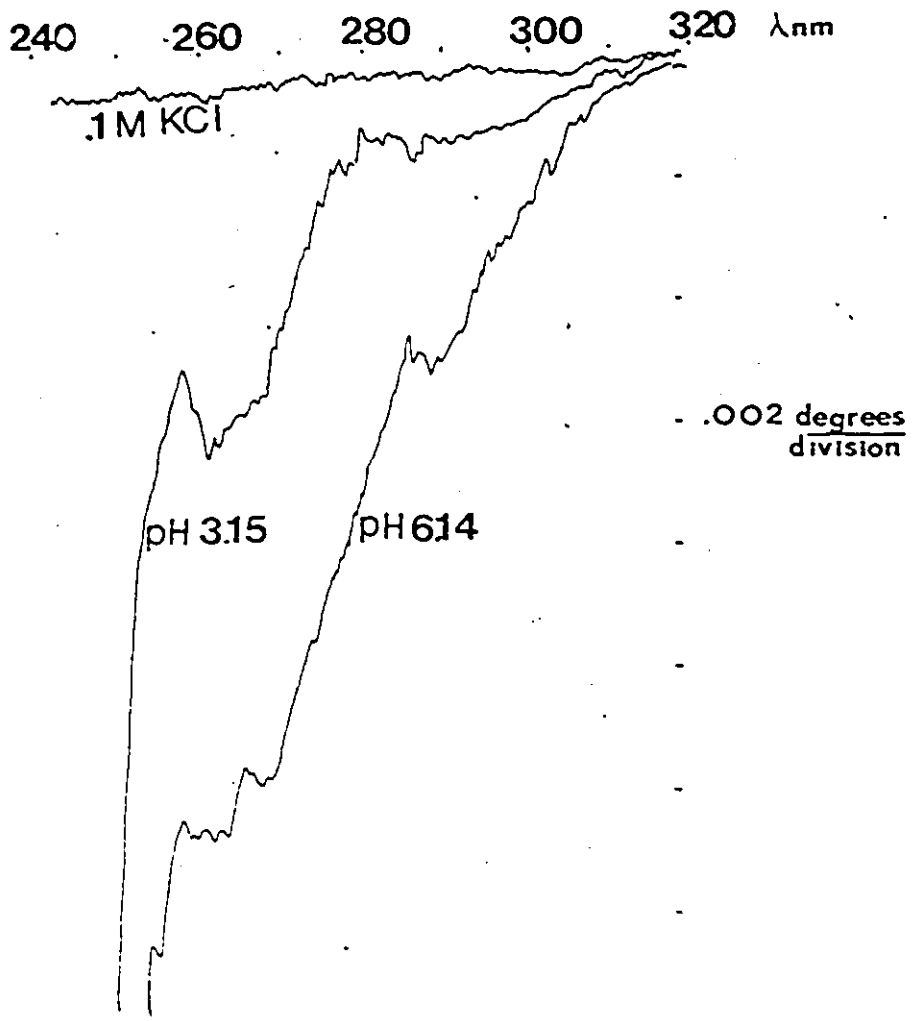

Figure 21

Plots of $[\theta]_{262}$ vs pH for both the modified and unmodified proteins (Figure 22) were identical within experimental error with those reported by Janatova.[141]

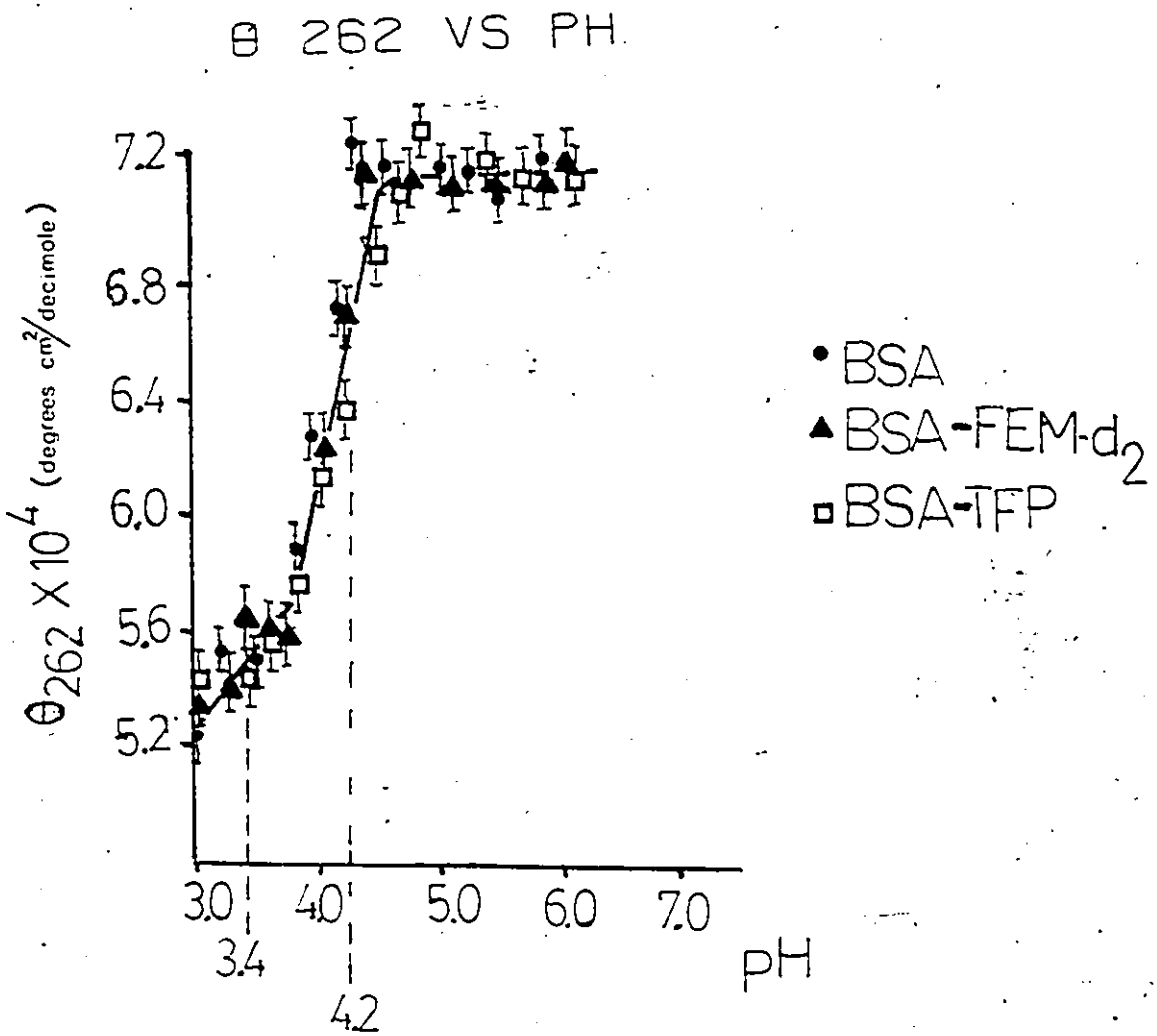

Figure 22

The observed midpoints at pH 4.2 and 3.4 agree closely with the reported[141] values of pH 4.10 and 3.40, respectively. Thus, the introduction of either the FEM-d_2 or TFP labels appears to have resulted in no noticeable perturbation on the orientation of the disulfide bonds in either the F or N states of the protein.

In their fluorescence spectra, BSA, BSA-FEM-d_2 and BSA-TFP showed identical behaviour with respect to the pH dependance of λ_{max} of emission and relative fluorescence intensity in the pH 3.0 to 6.0 region. As the pH was increased from 3.0 to 6.0, a 1.33 fold increase in fluorescence intensity at 343nm was observed, together with a shift of λ_{max} of emission from 323 to 343 nm (λ_{ex} = 280 nm) (Figure 23A) in agreement with the reported values for unmodified BSA.[141,142] In addition, the absolute fluorescence intensity at 343nm of solutions of all three proteins at the same concentration (10^{-5}M) and identical instrumental settings agreed to within ± 3%. The observed midpoint at pH 4.6 for all three proteins (Figure 23B) did not agree with the reported value of pH 4.20. The reason for this discrepancy is not known.

From the fluorescence studies presented it would appear that the tryptophan residue (try 54) undergoes the same "red shift" in both the modified and unmodified proteins. Together with the CD studies, the fluorescence data indicates the introduction of either sulfhydryl label caused no perturbation of the protein structure.

Figure 23

a/ Fluorescence spectra of either BSA, BSA -FEM-d_2 or BSA-TFP at various pHs (λexc = 280nm)

b/ Plots of relative fluorescence at 343nm vs. pH for the same three proteins.

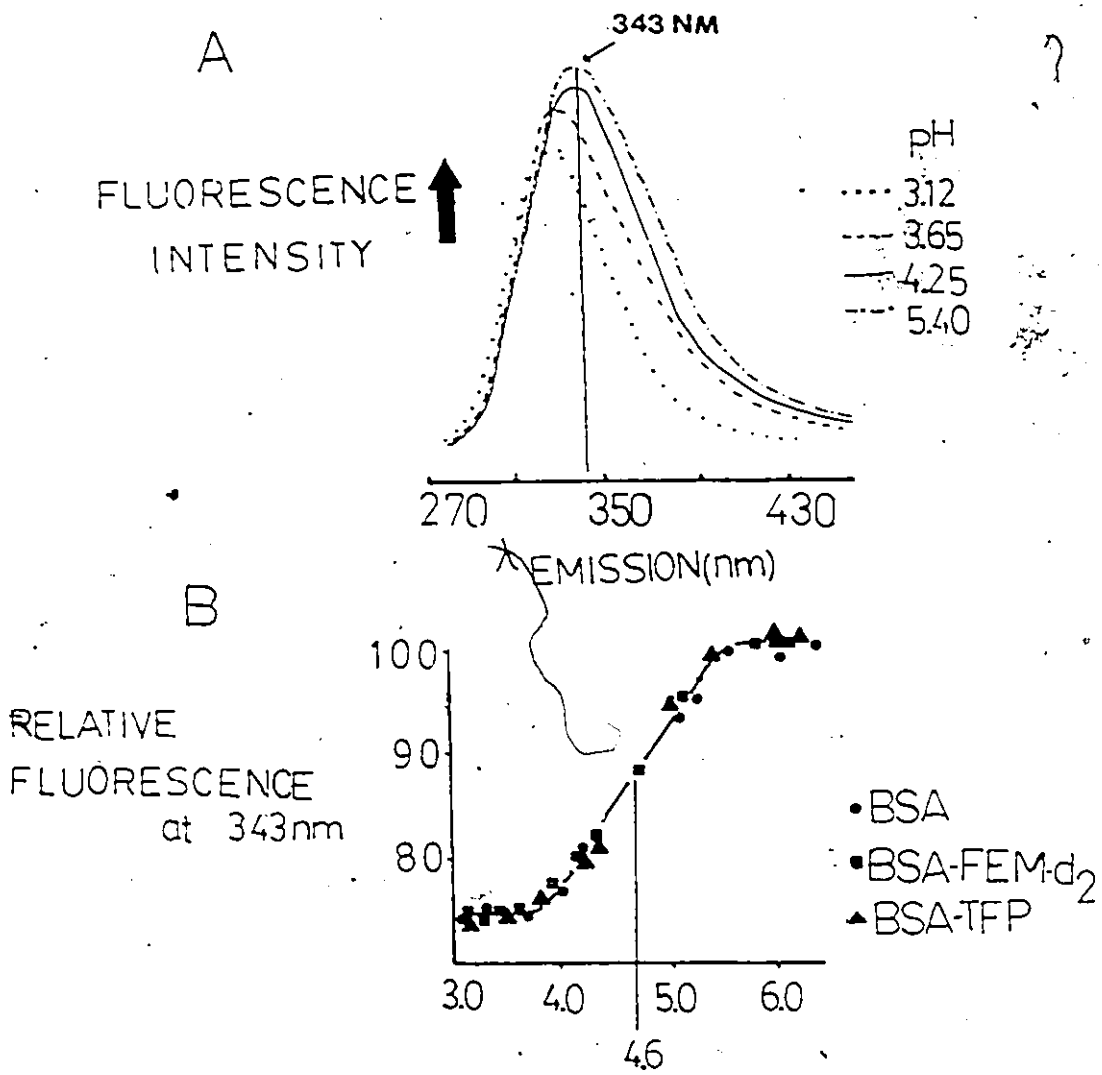

3.3.3 ^{19}F-NMR Studies of BSA-FEM-d_2

3.3.3.1 pH 3.0 - 6.0

Typical ^{19}F-nmr spectra of BSA-FEM-d_2 (νo = 84.66 MHz) over a pH range covering the N-F transition are shown in Figure 42. Linewidths of the ^{19}F-resonance of BSA-FEM-d_2 were approximately 40 Hz compared to 10 Hz for the free FEM-d_2 label. Generally, four resonances were observed at -68.2, 69.8, -70.2 and -72.2 ppm which are denoted as peaks A, B, C and D respectively in Figure 24. Except for the -72.2 ppm resonance, D, the relative areas under these signals varied with pH and were fully reversible over this pH range.

At 235.36 MHz, the ^{19}F-nmr resonances were generally broader ($V_{\frac{1}{2}}h$ = 100 Hz) compared to the 40 Hz half-widths at 83.66 MHz. The chemcial shift anisotropy contributions to the linebroadening were approximately linear with the applied field strength: in the worst case, this broadening may have increased as the square of the applied magnetic field (Appendix I, Sect. 5.4.2). Typical ^{19}F-nmr spectra are shown in Figure 25. Resonance C seen at 84.66 MHz (Figure 24), is comprised of two overlapping peaks (C^+ and C) at approximately -70.1 and -70.3 ppm in the pH 4.0 - 4.5 range. A comparison at pH 4.25 is shown in Figure 26.

Figure 24

84.66 MHz ^{19}F-NMR Spectra of BSA-FEM-d_2 at Various pHs of the N-F Transition. Trifluoroacetate (not shown) was used as an Internal Reference at -75.959 ppm.

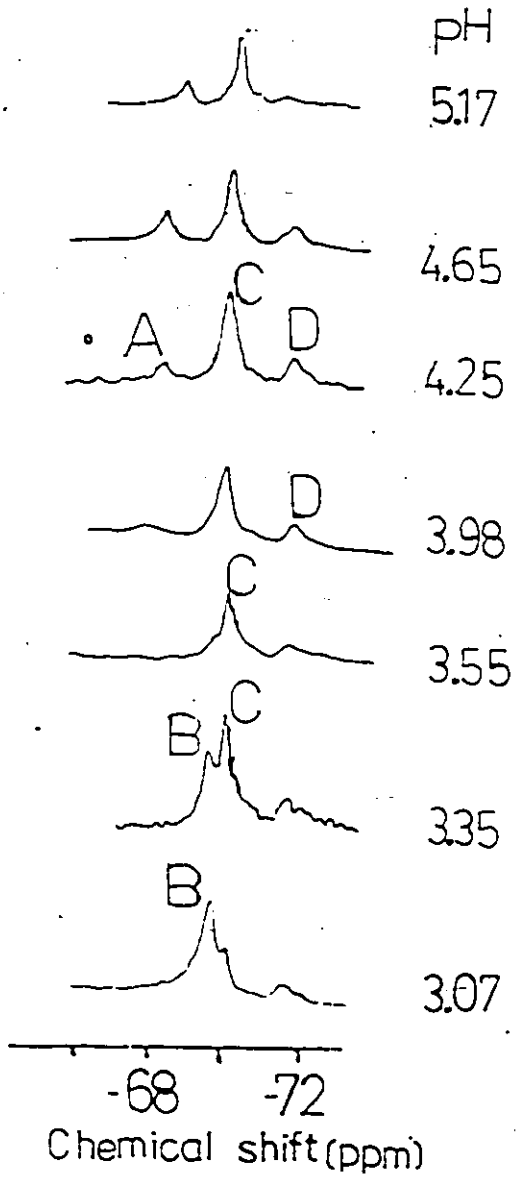

Figure 25

235.36 MHz ^{19}F-NMR Spectra of BSA-FEM-d_2 at Various pHs of the N-F Transition. Trifluoroacetate (not shown) was used an an Internal Standard at -75.05.95 ppm.

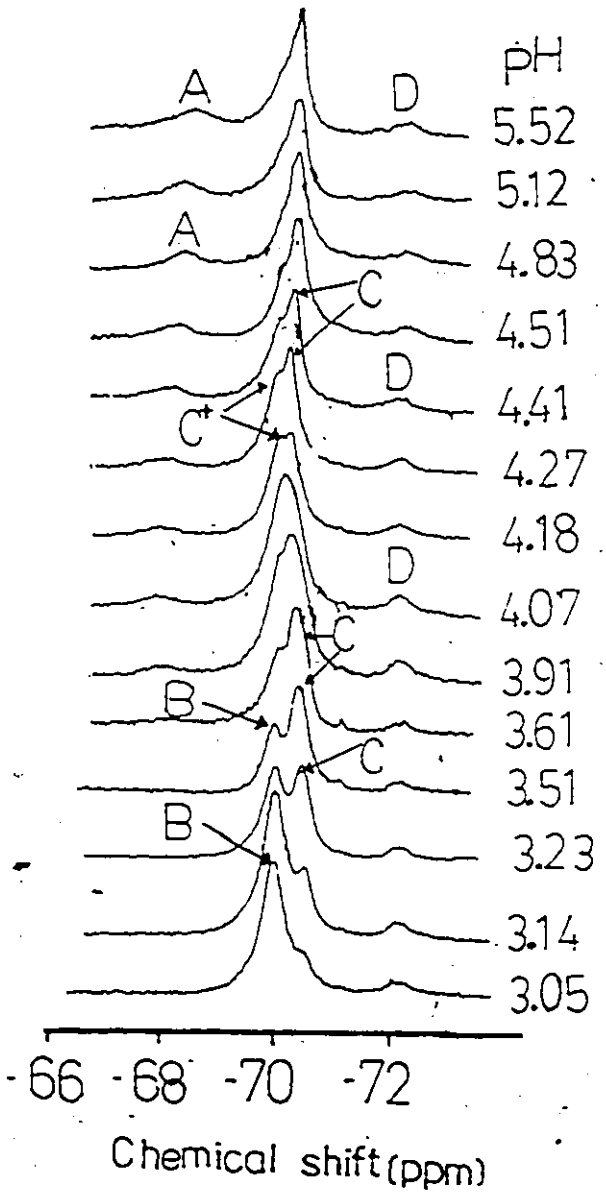

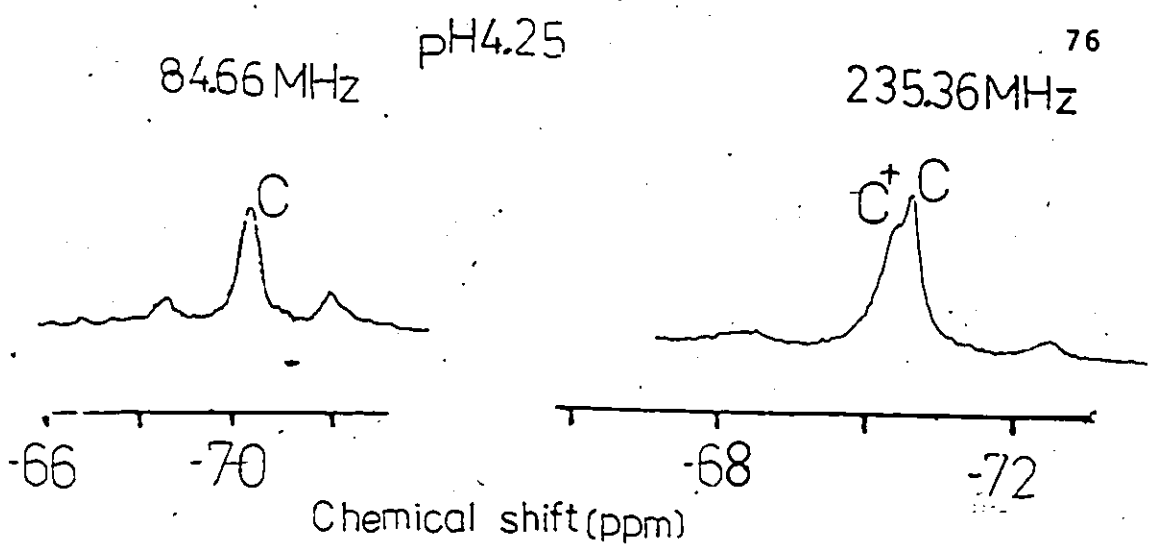

Figure 26

The explanation for this observed difference is the increased resolution at the higher applied field strength.

From even a cursory examination of Figures 24 and 25, it is clear that the relative areas of these resonances vary with pH. Clearly the FEM-d_2 label experiences a number of chemical environments in this narrow pH range. In Figue 27, the percentage of the total area of each pH dependant resonance (as determined by curve analysis, Sect. 4.1) is plotted as a function of pH over the range pH 3.0 to 6.0.

In addition to the correlation of percentage areas with pH, the variation of other parameters such as chemical shift and linewidth were also examined. In the case of overlapping spectra, chemical shifts and linewidths were determined for each resonance from peaks of the curve resolved spectra. Figures 28.1-28.4 illustrate these three parameters plotted against pH for the four resonances A, B, C^+ and C respectively. Resonance

Figure 27

Plots of % Area vs. pH for the Curve Resolved 235.36 MHz ^{19}F-nmr Resonances of BSA-FEM-d_2. All error limits shown are ± the Root Mean Square (RMS) Errors.

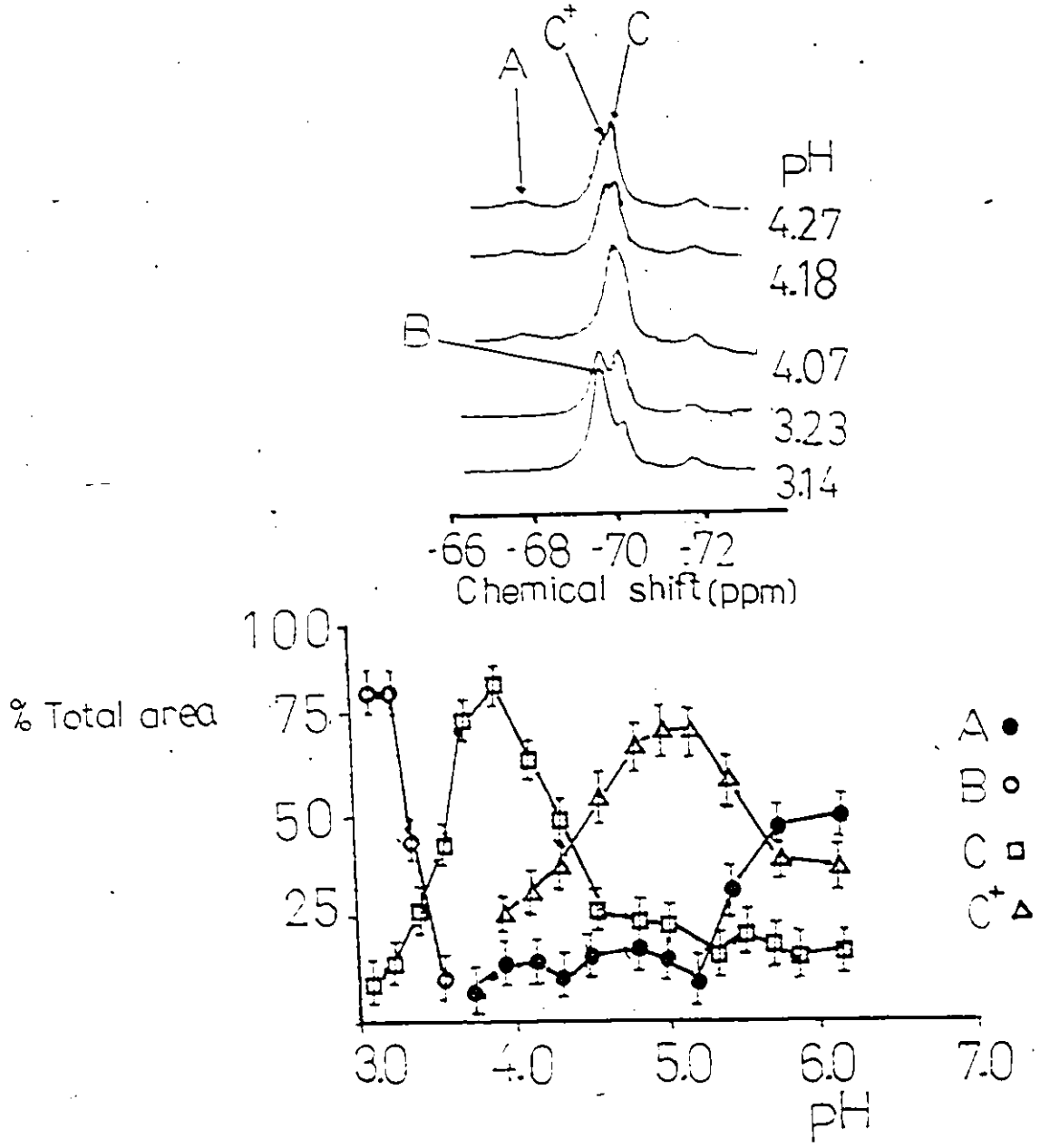

A (Figure 28.1) shows nearly parallel trends in chemical shift, percentage area and linewidth changes over the pH 4.0 - 6.0 range with a major increase in all three at pH 5.80. Resonance B (Figure 28.2) on the other hand shows a decrease in linewidth from approximately 100 to 60 Hz which parallels a decrease in percentage area from ~ 80 to 5% in the pH 3.0 to 3.6 region. The chemical shifts for this resonance were constant over the same pH range. Although resonance C^+ (Figure 28.3) shows no changes in either chemical shifts or linewidth (~80 Hz), the percentage area rises then falls reaching a maximum at pH 5.0. The midpoints of the rise and fall of peak C^+ are obvserved at pH 4.4 and 5.5 , respectively. Major changes in chemical shift, area and linewidth occur for resonance C (Figue 28.4) over the same pH region. The chemical shift changes from ~ -70.5 to -70.3 ppm with a minimum value at ~pH 4.20, before rising slightly. Both the linewidth and percentage area rise and then fall over this range, paralleling the chemical shift changes. The midpoints of all of these transitions are all very similar, pH 3.8 and pH 4.4. These midpoints agree closely with the CD midpoint at pH 4.2, (Figure 22).

How does this data relate to the N-F transition of BSA? The most interesting result from the ^{19}F-nmr experiments is that ther sulfhydryl label experiences more than one pH dependant

Figure 28.1

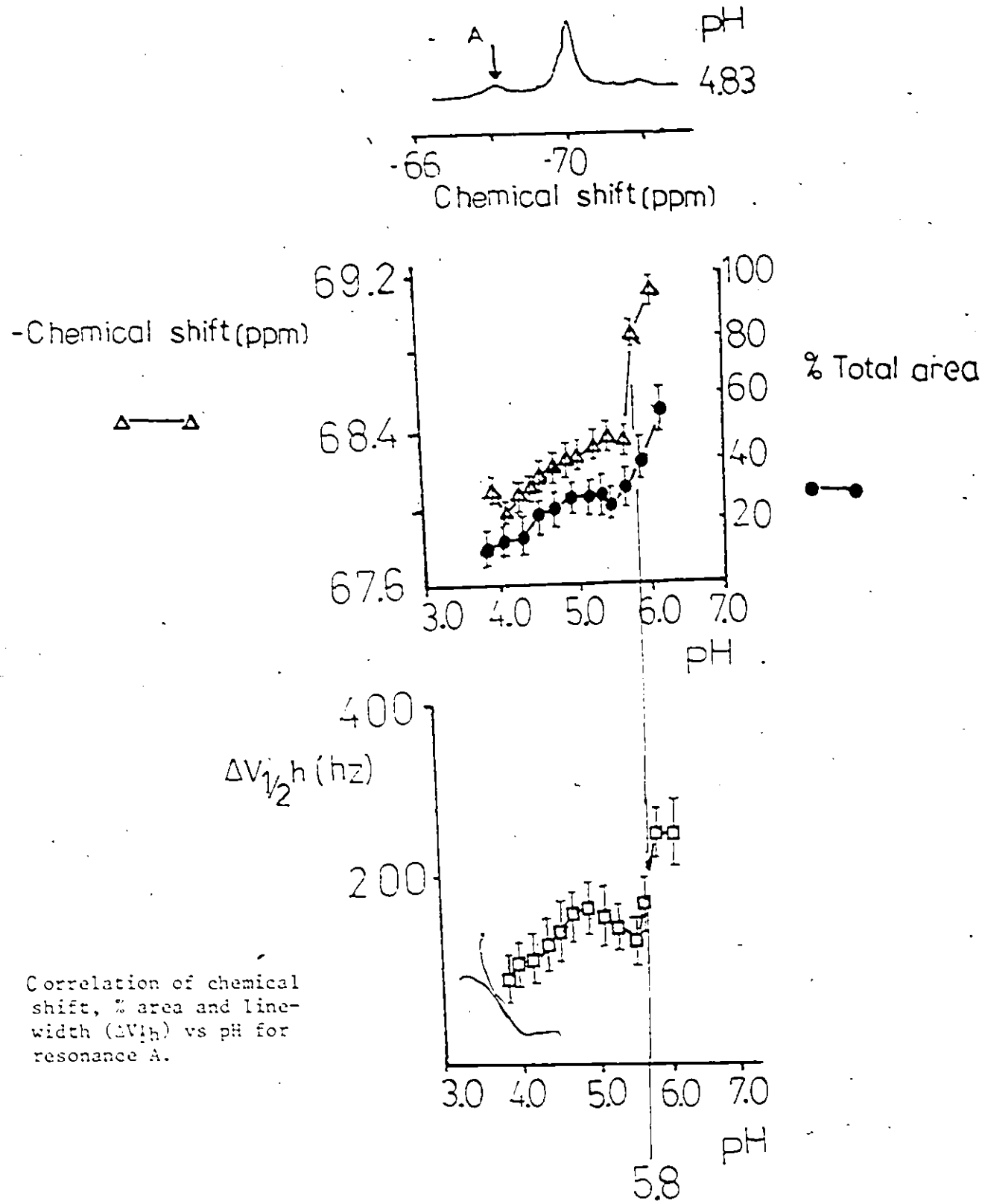

Correlation of chemical shift, % area and line-width ($\Delta V_{1/2}h$) vs pH for resonance A.

Figure 28.2

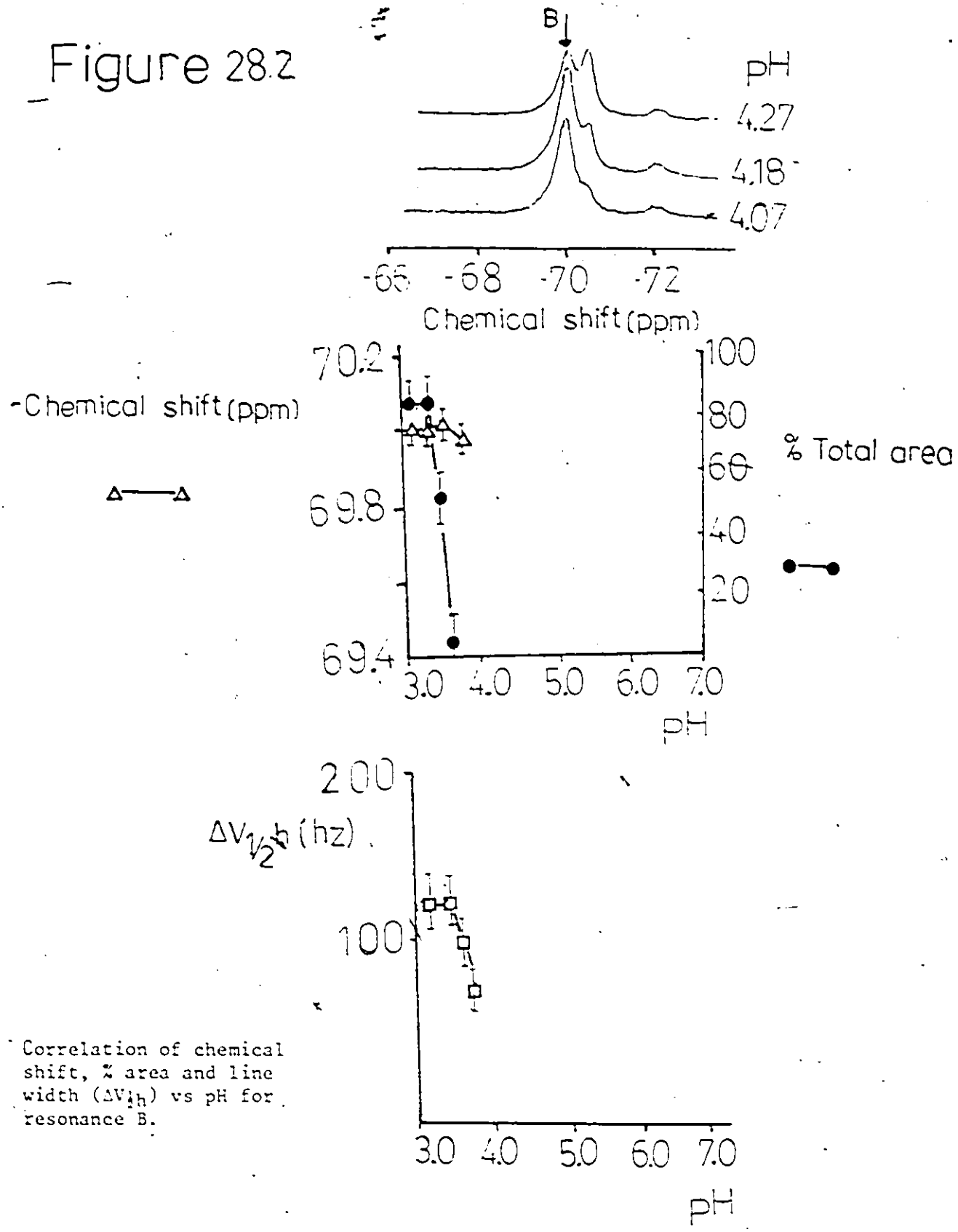

Correlation of chemical shift, % area and line width ($\Delta V_{1/2h}$) vs pH for resonance B.

Figure 28.3

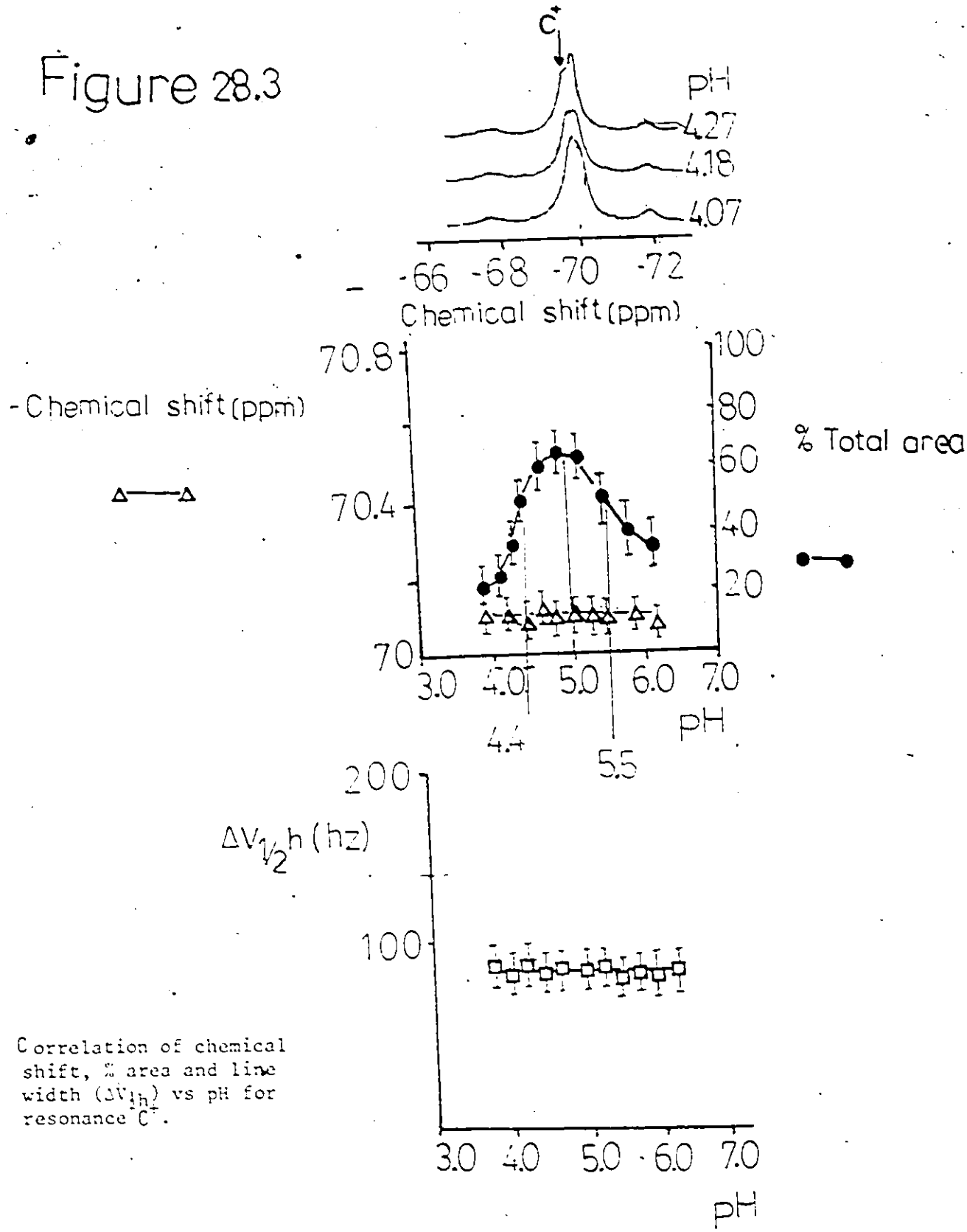

Correlation of chemical shift, % area and line width ($\Delta V_{1/2}h$) vs pH for resonance C^+.

Figure 28.4

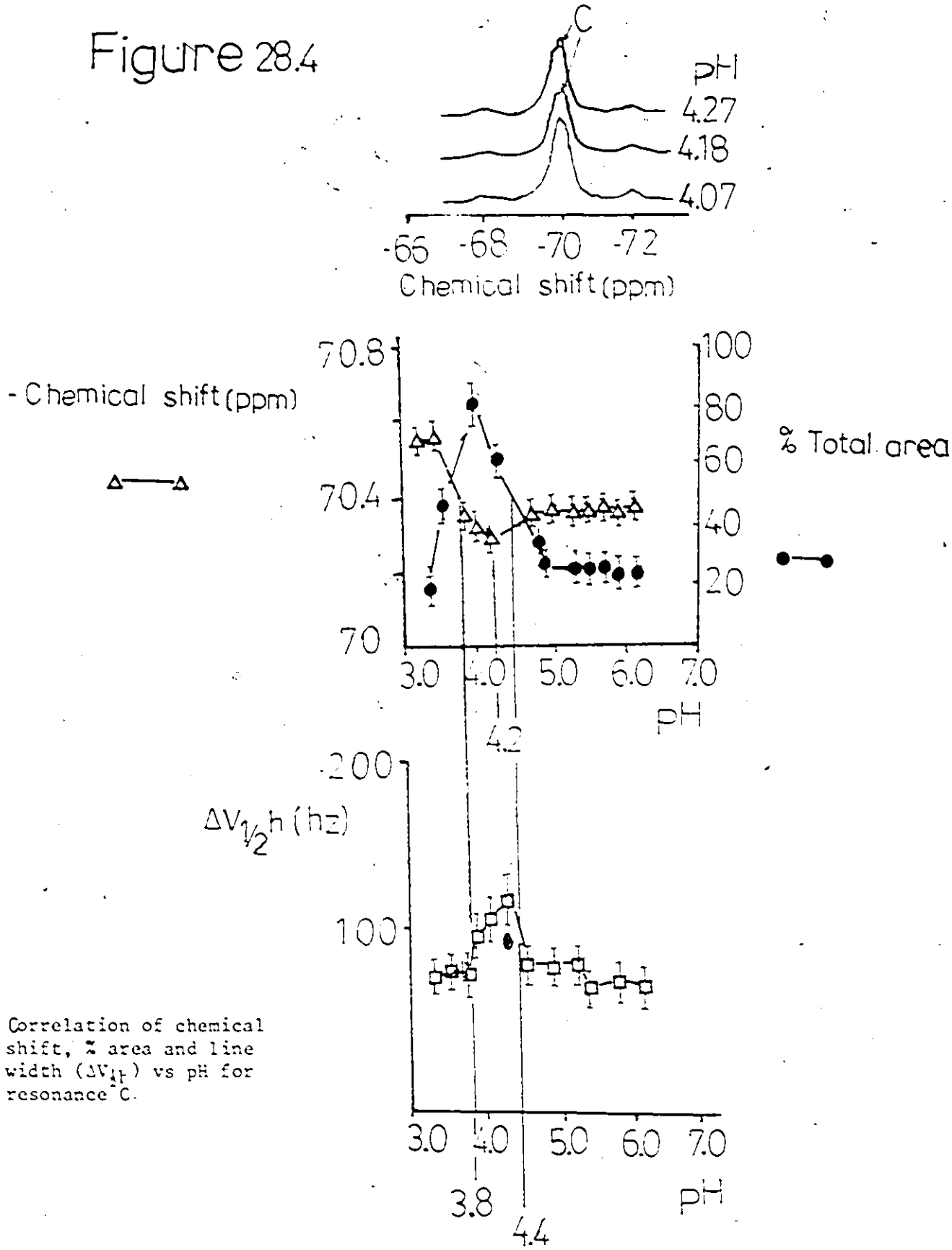

Correlation of chemical shift, % area and line width ($\Delta V_{1/2}$) vs pH for resonance C.

chemical environment in the pH range of the N-F transition. At pH values below the reported CD and fluorescence midpoints (pH 4.20) where the protein is the F state, two different ^{19}F environments were observed, resonances B and C (Figure 28.2 and 28.4). Above pH 4.20, the ^{19}F label was found to interconvert between three distinct chemical environments represented by resonances A, C^+, and C. In total, four different chemical environments are experienced by the FEM-d_2 label as a function of pH indicating the presence of more than one pH dependant ^{19}F environment about the sulfhydryl residue of the protein in the pH 3.0 to 6.0 region. The fluorescence studies which monitored changes about the single tryptophan residue provided no evidence for more than two protein states while the CD studies which monitored changes about the disulfide bonds showed two pH midpoints corresponding to three states of the protein. Previously reported esr data using spin-labelled maleimides[145-147] (Figure 11) that labelled the cysteine residue of BSA, provided no evidence for more than two environments about the sulfhydryl residue over this pH range.

3.3.3.2 <u>pH 7.0 - 10.0</u>

The weak resonance at -72.0 ppm resonance D showed no pH dependance in the pH 3.0 - 6.0 region; a totally different trend was observed above pH 7.00. ^{19}F-nmr spectra of BSA-FEM-d_2 at pHs above 6 (Figure 29A) show an irreversible increase in the

Figure 29

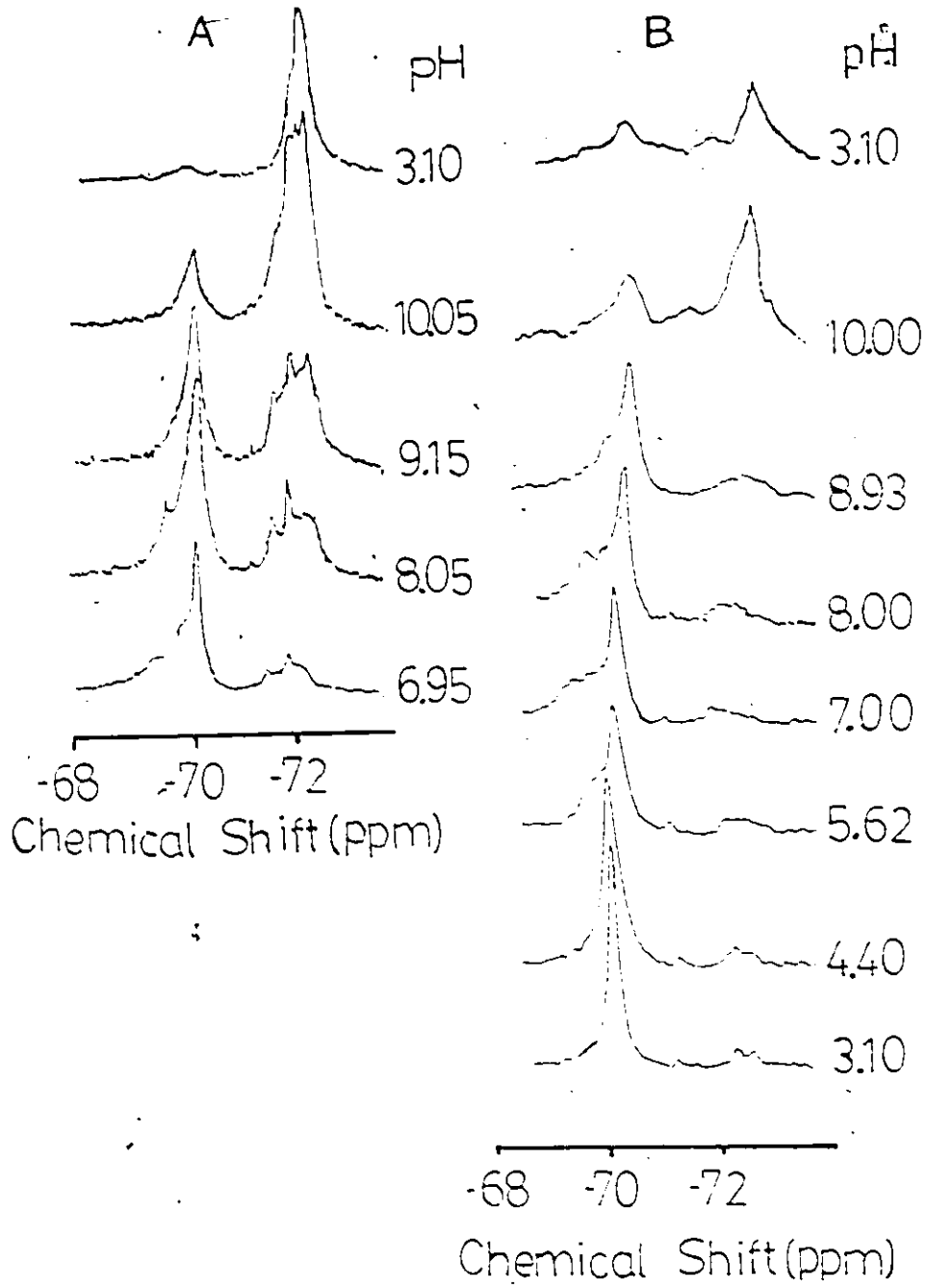

235.36 MHz ^{19}F-NMR Spectra of BSA-FEM-d_2 in the presence (B) and absence (A) of 8M urea. The pHs of the solutions were increased in the order shown and then adjusted to pH 3.10.

intensity of this resonance. In contrast, ^{19}F-nmr spectra of BSA-FEM-d_2 obtained under identical conditions, except for the addition of a protein denaturant (8M Urea, Figure 29B), differ from those in the absence of urea in two ways: first, the linewidths ($V_{1/2h}$) of the ^{19}F-nmr signals were generally narrower in the presence of urea, (eg, at pH 3.10, linewidths of 30 Hz and 130 Hz were observed in the presence and absence of urea) and second, the rate of increase in the percentage of -72 ppm peaks was much less slower over the same time period in 8M urea. Yarborough[204] has observed with BSA whose cysteine residue had been labelled with N-pyrenemaleimide underwent a facile intramolecular reaction which was non-existant under denaturing conditions. Our observations of BSA-FEM-d_2 using ^{19}F-nmr under basic conditions are consistant with an intramolecular reaction of the native protein (Shown in Figure 30) involving an N-terminal amino or lysine residue.

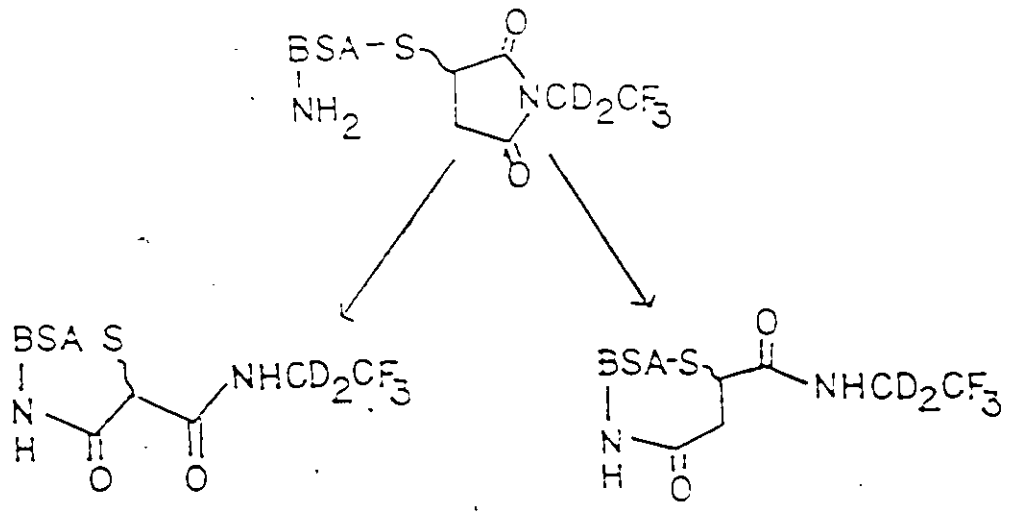

Figure 30

In the presence of denaturant, the "unfolding" of the protein may less the availability of amino groups for an intramolecular reaction and hydrolysis of the label may occur (Figure 31).

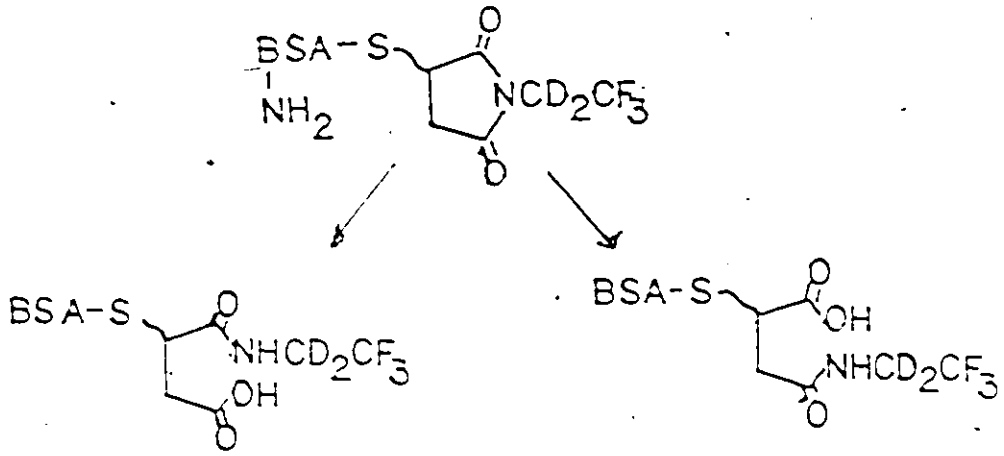

Figure 31

Ring opening involving an intramolecular attack by an amino group and subsequent ring opening of aminothiolmaleimide reaction products resulting in lactam formation are known reactions.[205] (Figure 32).

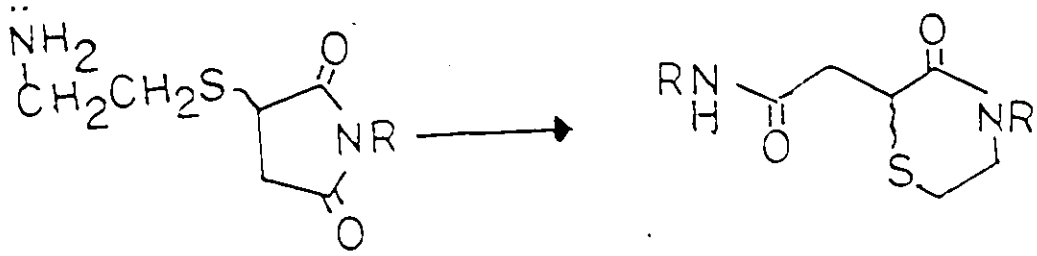

Figure 32

The pH dependance of the ^{19}F-nmr spectra of the FEM adducts of N-acetyl-L-.cysteine (25) and L-cysteine (23) were examined. The synthesis and purification of (25) and (23) is described in Section 4.4. An examination of the ^{19}F-nmr spectra of these adducts at pHs 7.0 and above (Figure 33) show a relatively slower build-up of a -72.1 ppm triplet at the expense of the triplet of -69.8 for the N-acetyl-L-cysteine adduct compared to the L-cysteine adduct.

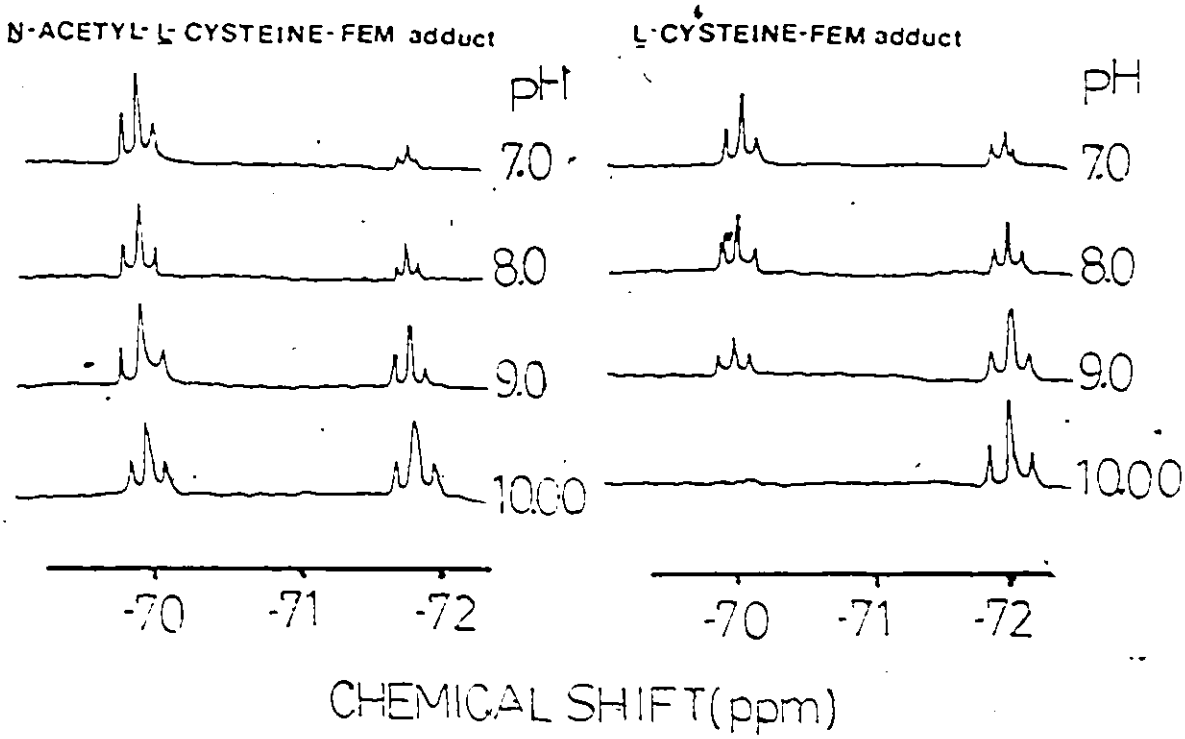

Figure 33

A TLC analysis of the solution of the L-cysteine adduct at pHs 7.0 and above showed the build-up of two new components (Rf = .50 and .22) in addition to the decrease of the adduct (Rf = .40) The Rf=.50 spot gave negative ninhydrin and nitroprusside tests indicating the absence of amino and thiol groups respectively. On the other hand the Rf = .22 spot showed a positive ninhydrin and negative nitroprusside tests indicating the presence of the amino group and absence of the

thiol group respectively. At pH 10.0, the relative amount of the Rf = .50 material in was judged to be approximately 90% of the total TLC spot intensity with only the Rf = .22 spot present. Similarly, the N-acetyl-L-cysteine adduct 25 showed, in addition to a spot due to the adduct at Rf = .65, a spot at Rf = 0.30 which corresponded to approximately 30% of the total spot intensity at pH 10.00. Both spots gave negative nitroprusside and ninhydrin tests showing the absence of thiol or amino groups respectively. Although the hydrolysis products were never isolated or characterized, it would appear that the L-cysteine adduct (23) in addition to the hydrolysis of the succinimide ring was undergoing an intramolecular reaction giving rise to the Rf - 0.5 spot, while the N-acetyl-L-cysteine adduct 25 undergoes simple hydrolysis of the succinimide ring (Rf = .30 spot) (Figure 34).

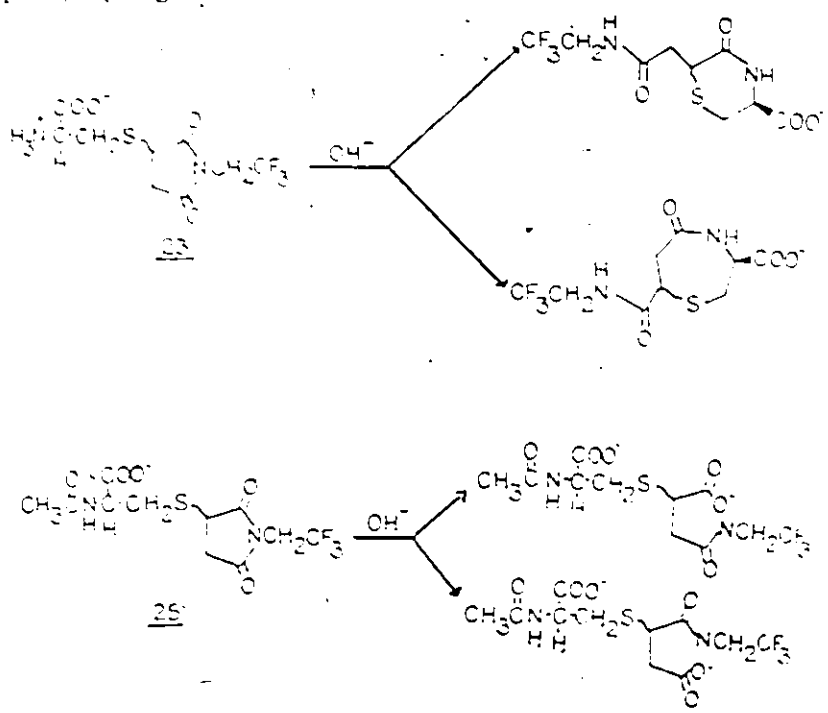

Figure 34

The combined TLC and ^{19}F-NMR -pH studies gave good qualitative evidence of the importance of a proximate amino group in the opening of the succinimide ring after FEM or FEM-d_2 has reacted with thiol gruop. By virtue of BSA's intact tertiary structure in the absence of a denaturant an amino group of a lysine or N-terminal aspartic residue may be near enough to the succinimide ring leading to a cross-linked protein at pHs above 7.0 (Figure 30).

This was not proven conclusively since quantitative analysis of the modified proteins amino groups were not performed either before or after the pH of BSA-FEM-d_2 solutions were adjusted to pH 7.0 and above. Due to these irreversible reactions above pH 7.0, ie, hydrolysis on intramolecular cyclization, the study of FEM-d_2 labelled proteins are limited to pHs below 8.0.

3.3.4 ^{19}F-NMR Studies of BSA-TFP

^{19}F-nmr spectra (ν_o = 235.36 MHz) of BSA which had been reacted wtih 3-bromo-1,1,1-trifluoropropanone (Br-TFP) for 20 min. at pH 6.65 are shown in Figure 35. Each resonance observed at ν_o = 84.66 MHz (peaks A' and B', Figure 19) appeared to be comprised of two closely overlapping peaks at ν_o = 235.36 MHz. These peaks are denoted as A', A" and B', B" in Figure 35. In contrast to the ^{19}F-nmr studies of BSA-FEM-d_2 (Section 3.2.3. a and b) the relative proportions of all observed ^{19}F resonances were both pH dependant and reversible above and below pH 7.0. A plot of the percentage of the total area vs. pH for the curve resolved resonances is shown in Figure 36.

Figure 35

235.36 MHz ^{19}F-NMR Spectra of BSA-TFP. Trifluoroacetate (not shown) was used as an Internal Reference at -75.595 ppm.

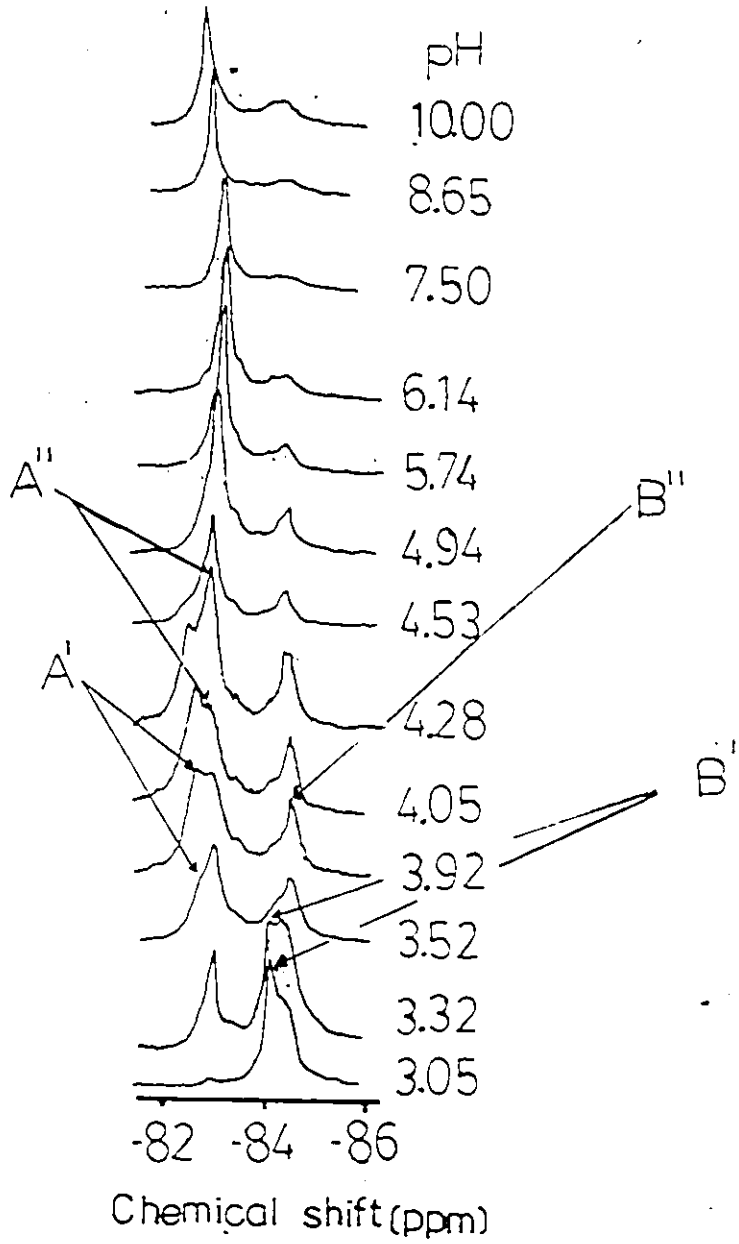

Figure 36

Plots of % Area vs. pH for the Various Curve Resolved 235.36 MHz. 19F-nmr Resonances of BSA-TFP in the pH 3.0-6.0 Range. Error limits are the ± Root Mean Square (RMS) Errors.

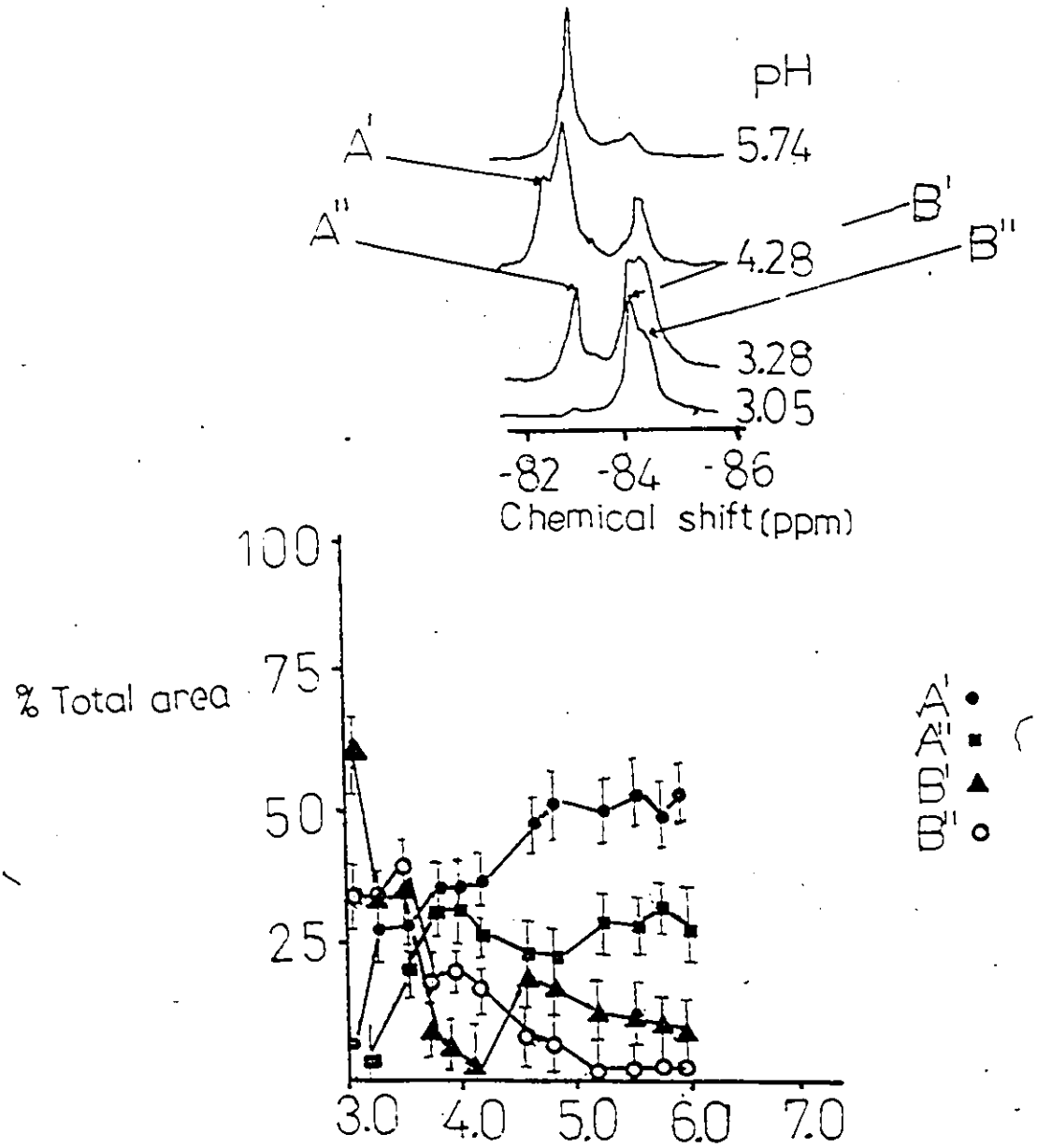

The percentage area, chemical shift and linewidth correlation with pH are shown in Figures 37.1-37.4. As was the case with BSA-FEM-d_2, chemical shifts and linewidths for overlapping spectra were determined from the curve resolved spectra. Along with a change of chemical shift in A' of approximately 0.3 ppm an increase in the percentage area from ~20 to 60% with a plateau at ~ pH 5.0 while the linewidth decreased from ~ 100 to 70 Hz (Figure 37.1). The changes in chemical shift and linewidth have a midpoint at ~ 5.0. Resonance A" (Figure 37.2) showed no other changes in either chemical shift (~ -83.1 ppm), or linewidth but a constant percentage area of ~ 30% after an initial increase from 2 to 30% from pH 3.30 to pH 3.50. Resonance B' (Figure 37.3) showed a drop in percentage area from 58 to 10% with a minimum of 5% at pH 4.2 and a corresponding increase in linewidth from 65 to 190 Hz with a maximum at ~ pH 4.2 and midpoints at 4.1 and 4.5 which agree with the CD studies (Figure 22) and reported fluorescence midpoint of pH 4.20. Resonance B" (Figure 37.4) shows nearly parallel behaviour in chemical shift, area and linewidth changes over the pH 3.0 to 6.0 region. An overall decrease in chemical shift, from ~ -84.5 to -84.3 ppm with a midpoint at pH 4.8 closely parallels a decrease in linewidth from ~ 71 to 20 Hz with the same midpoint at pH 4.8. This agrees closely with the fluorescence midpoint at pH 4.6 (Figure 23). A corresponding drop in percentage area from 30 to 7% was also observed.

Figure 37.1

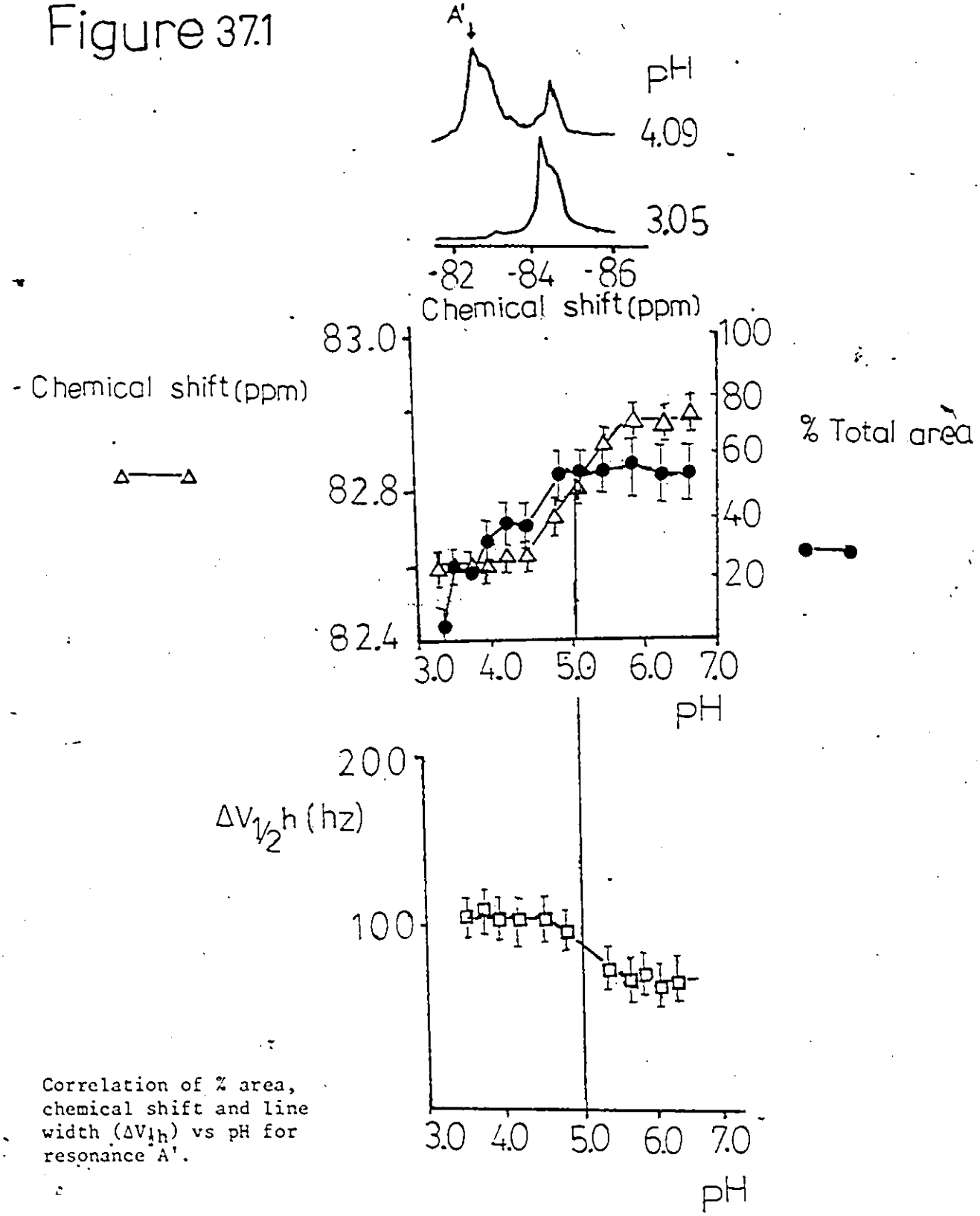

Correlation of % area, chemical shift and line width ($\Delta V_{\frac{1}{2}h}$) vs pH for resonance A'.

Figure 37.2

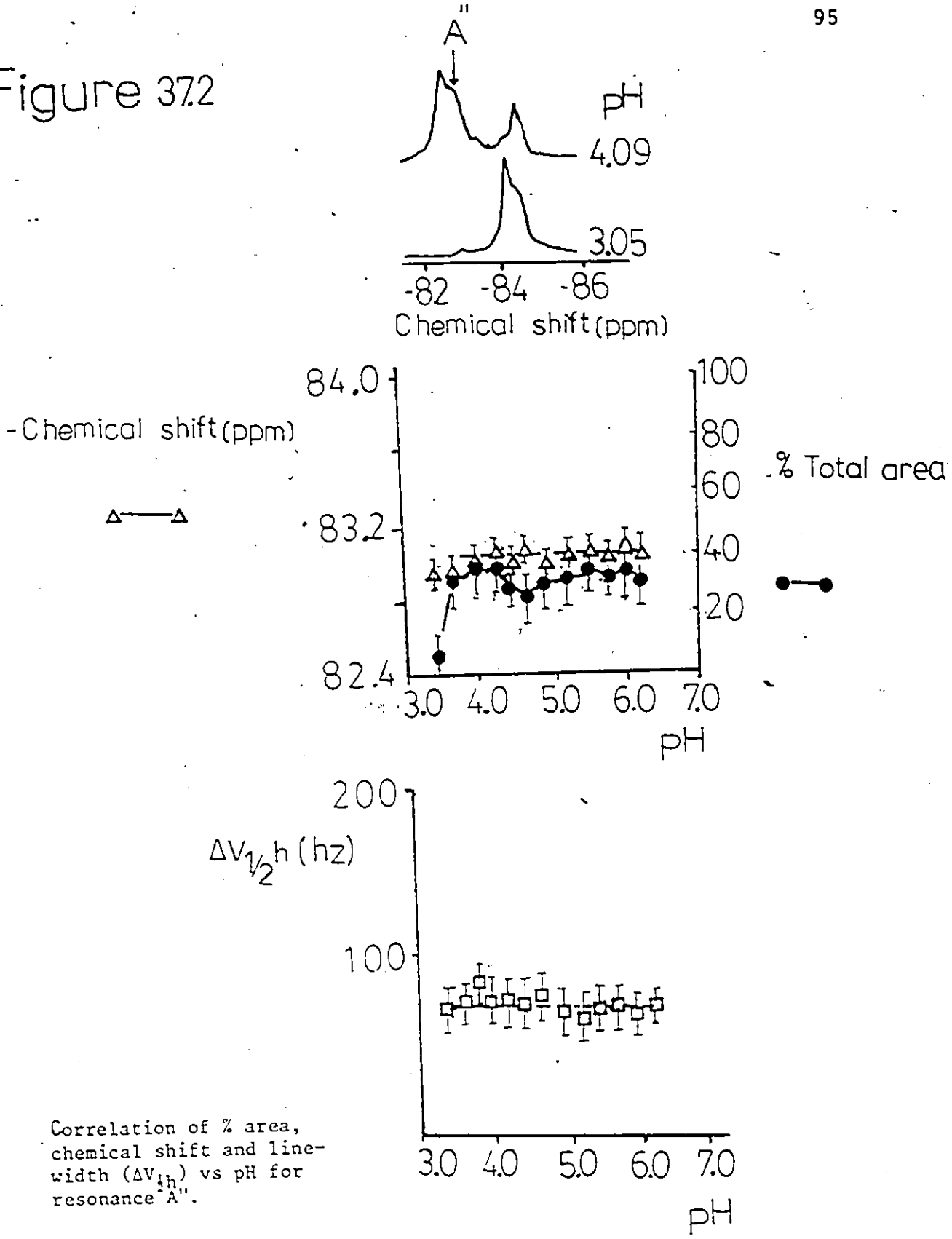

Correlation of % area, chemical shift and line-width ($\Delta V_{\frac{1}{2}h}$) vs pH for resonance "A".

Figure 37.3

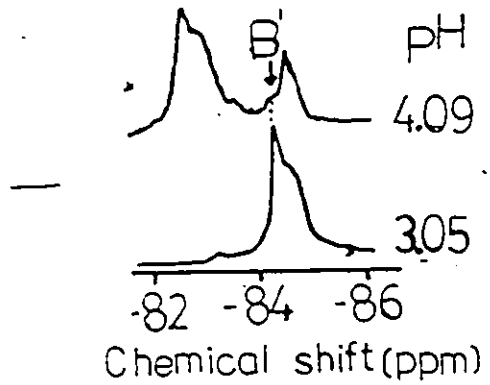

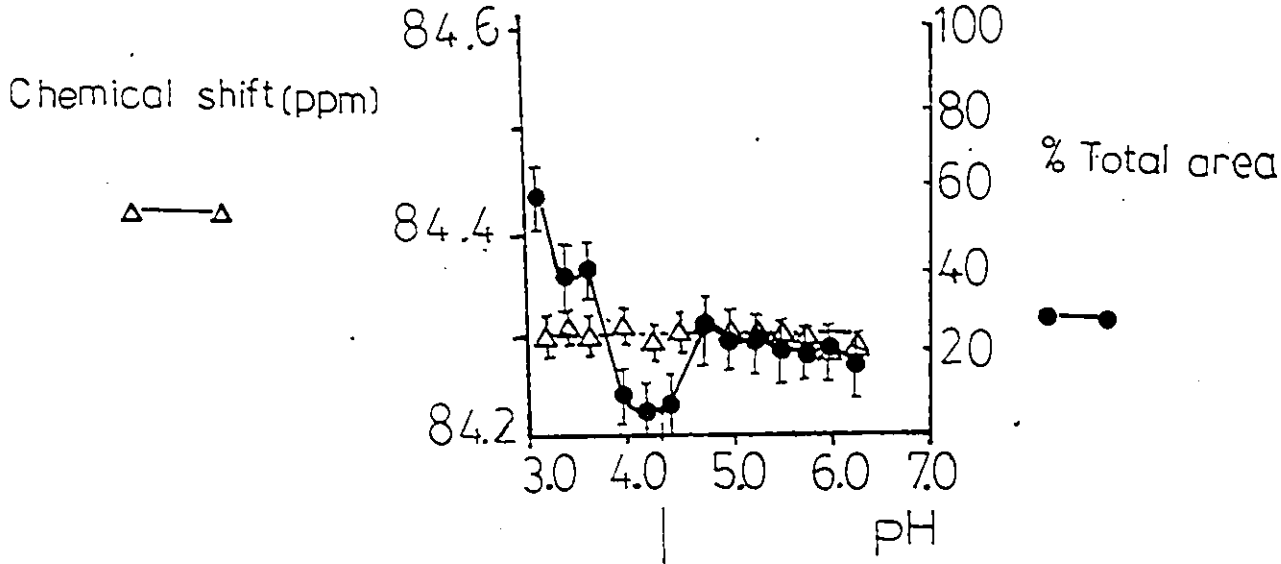

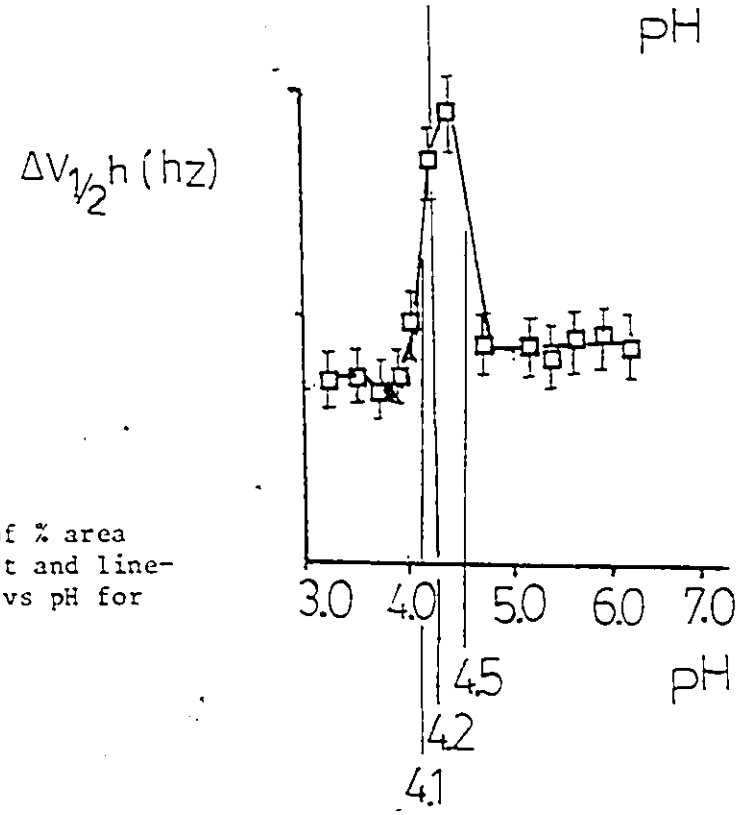

Correlation of % area chemical shift and line-width ($\Delta V_{\frac{1}{2}h}$) vs pH for resonance 'B'.

Figure 37.4

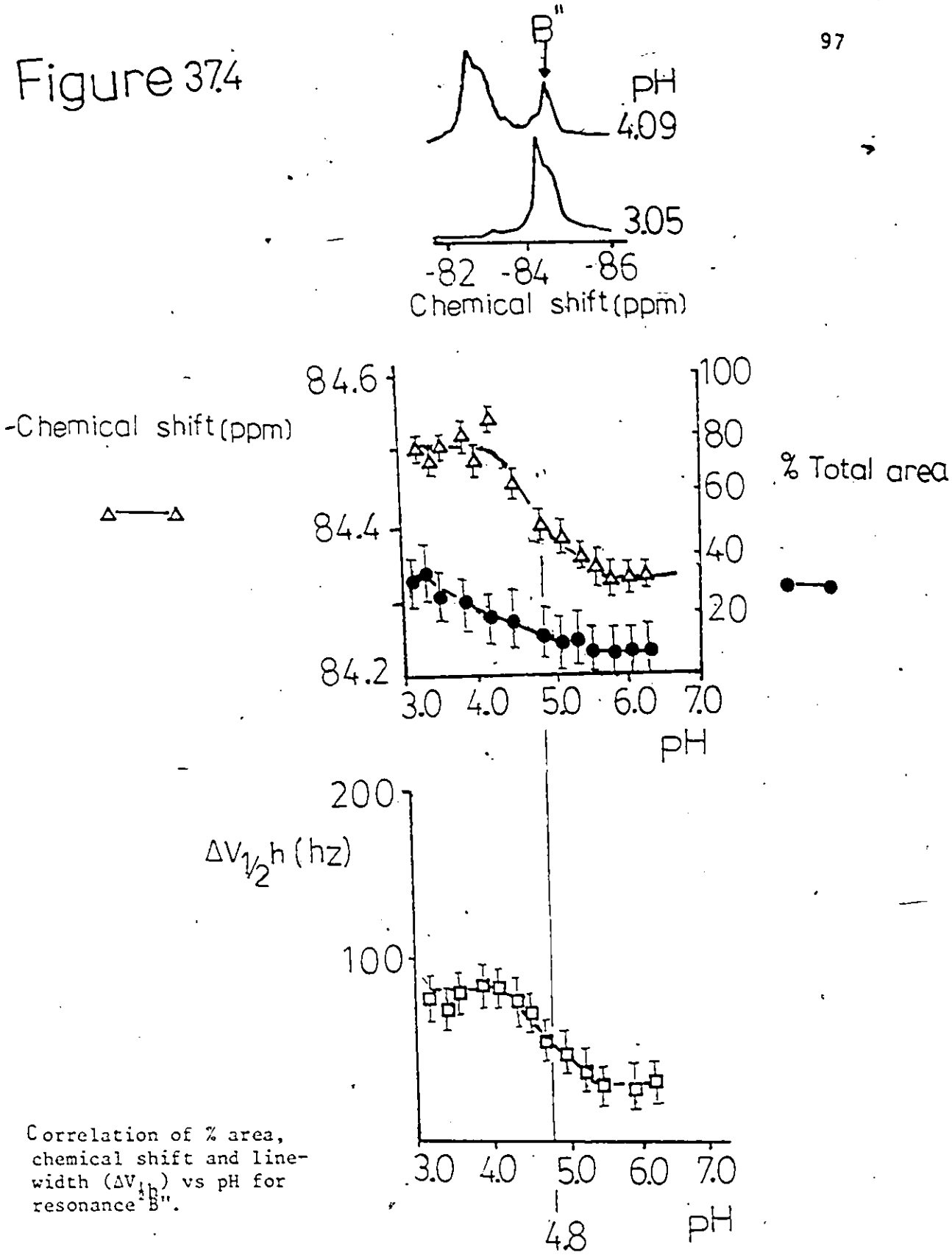

Correlation of % area, chemical shift and line-width ($\Delta V_{1/2}h$) vs pH for resonance "B".

In addition to these pH dependant trends a minor resonance at -83.6 ppm (Figure 38), previously shown to be due to non-sulfhydryl labelling (Section 3.3.1) made up approximately 0.7% of the total peak area.

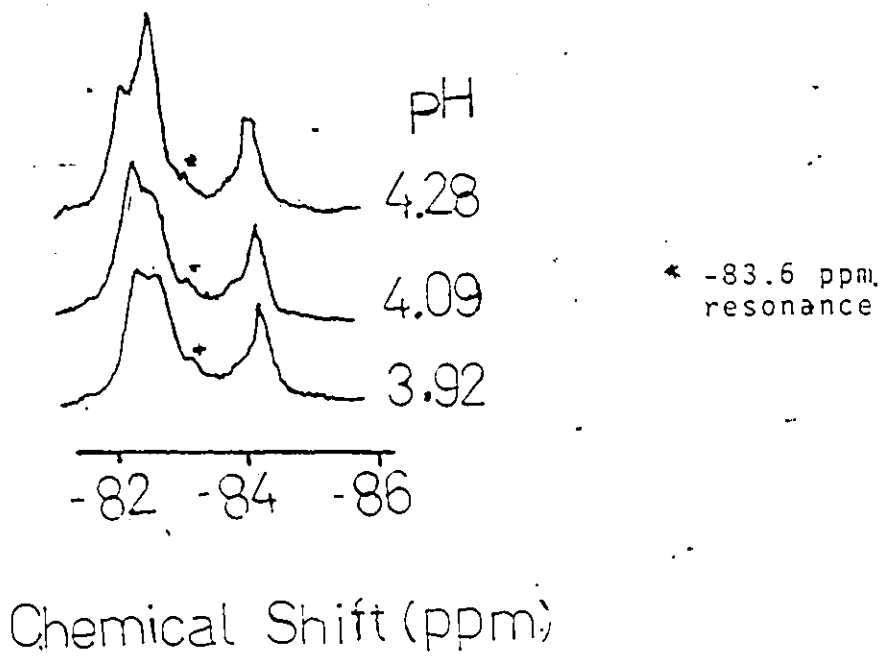

Figure 38

In addition, in the pH 6.0 - 10.00 region, the relative percentage area of peak A' decreases with a corresponding increase in the area of A" while B' remains constant (Figure 39). Chemical shifts, percentage area and linewidth correlations with pH are shown in Figures 40.1-.3 inclusive. While the percentage area of A' dropped from ~ 55% at pH 6.14 to 5% at pH 6.35, correspondingly smaller changes occurred in the chemical shift and linewidth of this resonance. Resonance A"

Figure 39

Plots of % Area vs. pH for the Curve Resolved 235.36 MHz ^{19}F-NMR Resonances of BSA-TFP in the Range of pH 7.0-10.00.

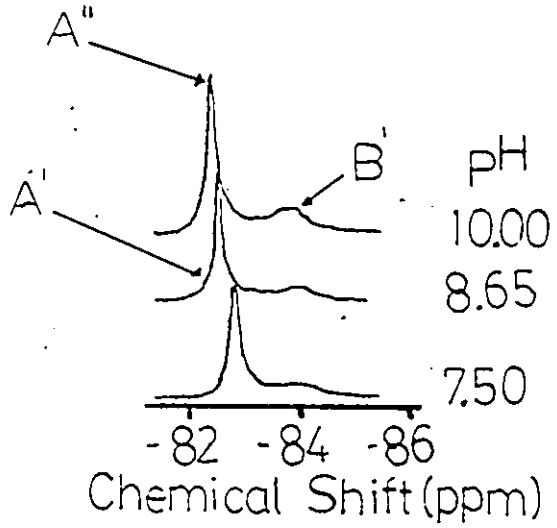

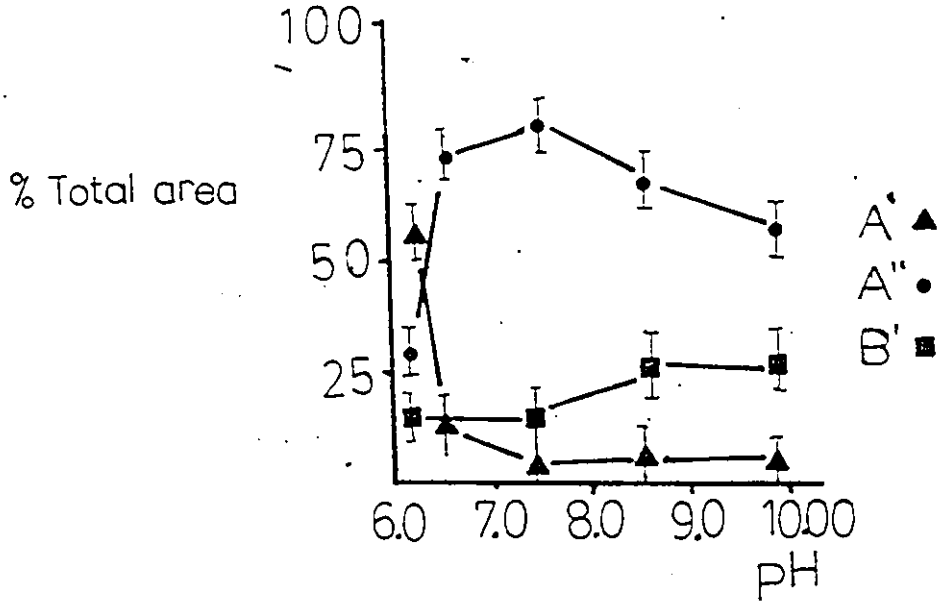

(Figure 40.2) on the other hand showed large increase in area (~ 20% to 6%) which plateaus by pH 6.35. A decrease in chemical shift from ~ -83.0 to -82.7 ppm also occurs in the pH 6.0 - 10.0 region with no change in linewidth. While no changes in chemical shift or area occur for resonance B' (Figure 40.3) a large increase in linewidth from ~ 75 to 140 Hz occurred with a maximum at pH 9.0. In contrast to Zurawski's observations that only a single ^{19}F resonance was present for BSA-TFP in the pH 6.0 - 10.0 region, two resonances were readily observed, A" and B"; the percentage of A' was determined from curve analysis. In addition, a chemical shift change from -77.1 to -78.0 ppm with a midpoint at pH 8.0 was reported by these authors[120] in contrast to the smaller chemical shift changes for resonances A' and B' in the pH 6.0 - 10.0 region. The reason for this discrepancy is not clear.

3.3.5 A Comparison of FEM-d_2 and Br-TFP Sulfhydryl Labels

Several differences and similarities were observed in the ^{19}F spectra of BSA labelled with either FEM-d_2 and Br-TFP. At pH values below 4.00, BSA-FEM-d_2 showed two resonances (B and C); above pH 4.00, three resonances A, C^+ and C, (Figure 26). BSA-TFP on the other hand, showed all four resonances. A', A", B', and B" above and below pH 4.20 (Figure 35). Above pH 4.0 the relative proportion of downfield resonance C increased as

Figure 40.1.

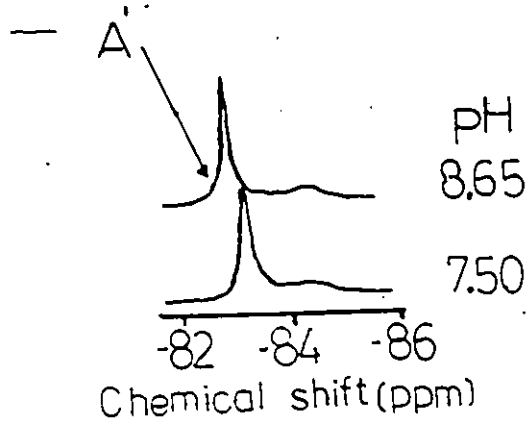

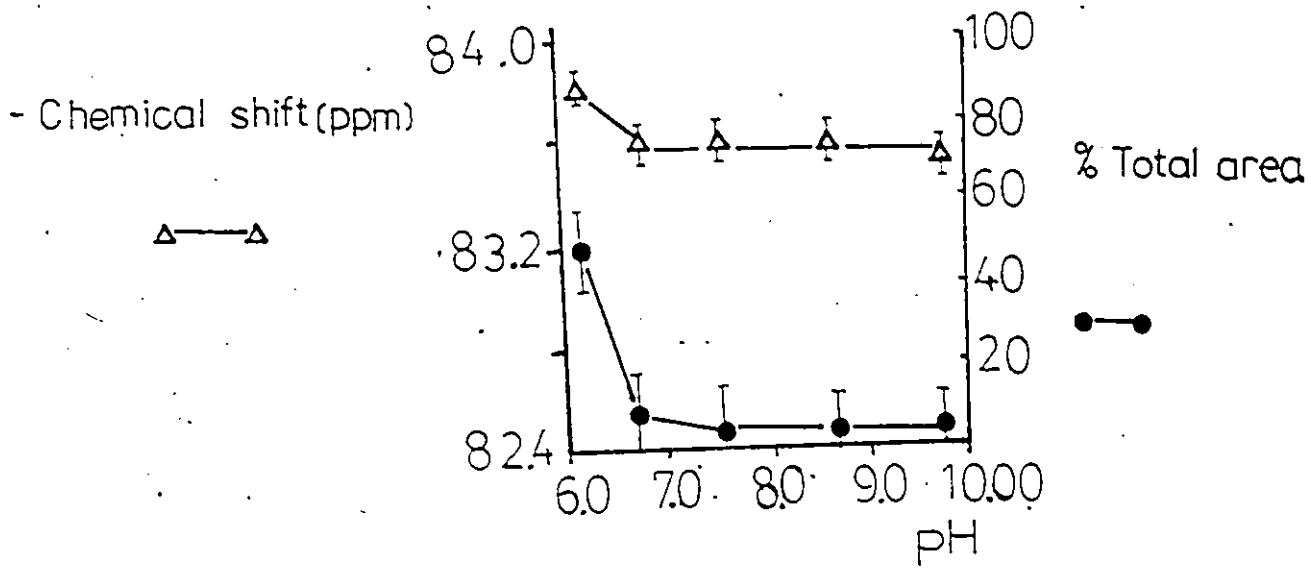

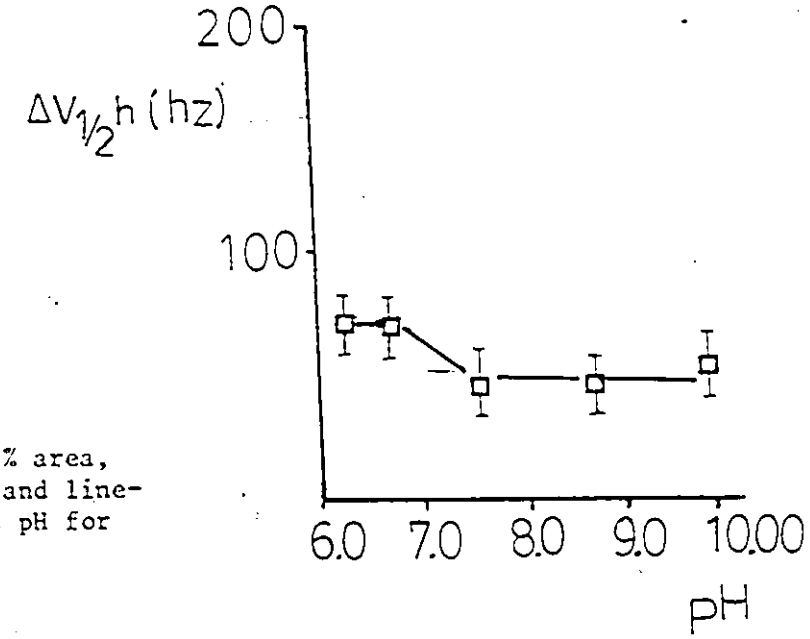

Correlation of % area, chemical shift and line-width ($\Delta V_{\frac{1}{2}h}$) vs pH for resonance 'A'.

Figure 40.2

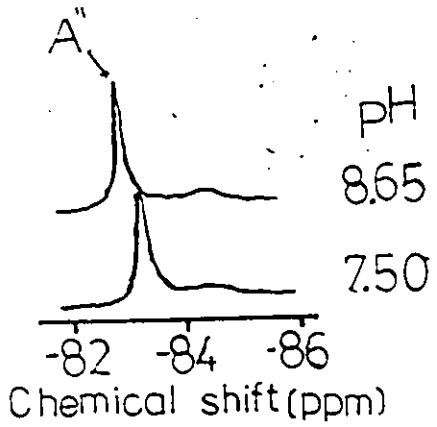

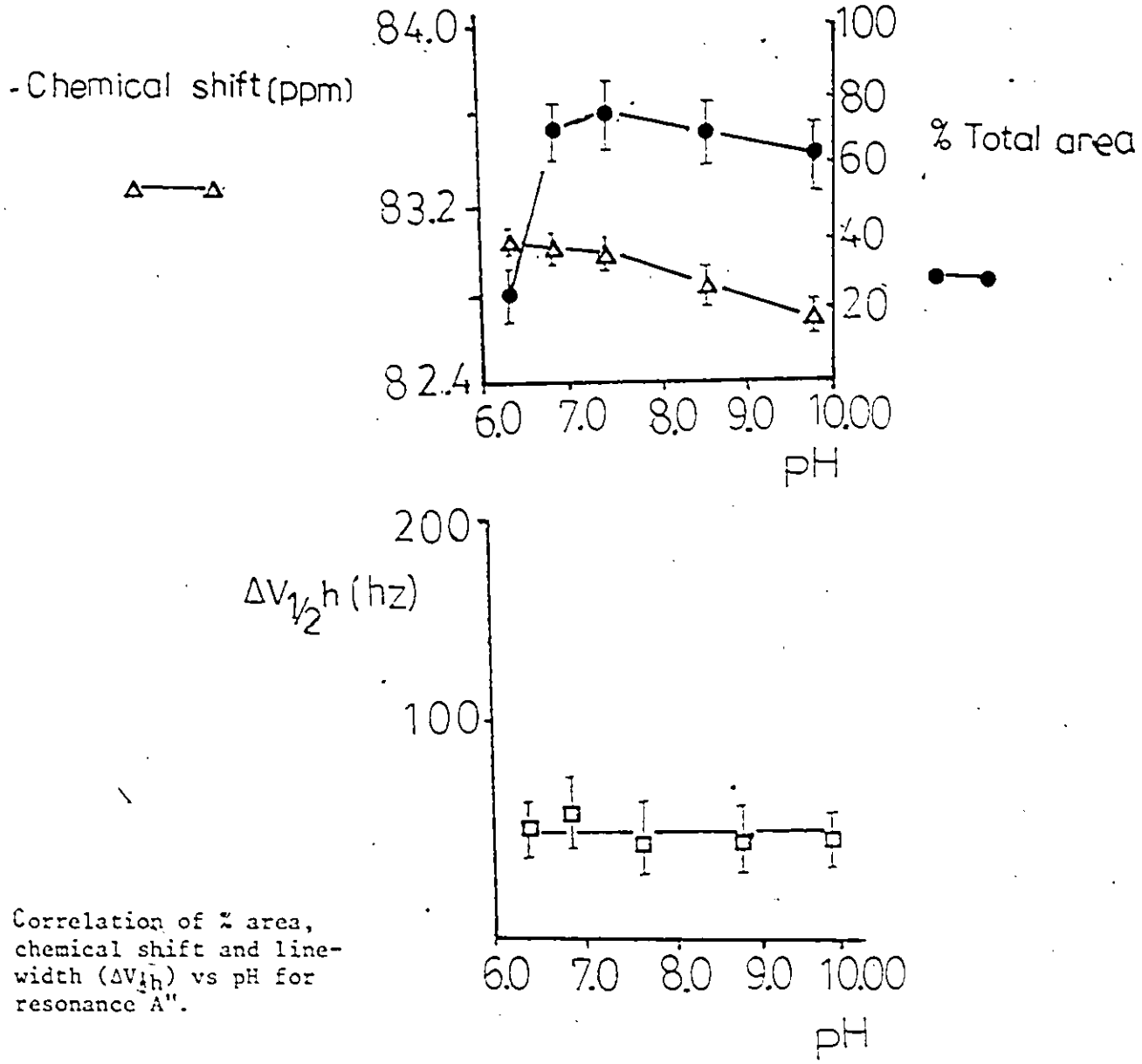

Correlation of % area, chemical shift and line-width ($\Delta V_{1/2}h$) vs pH for resonance A".

Figure 40.3

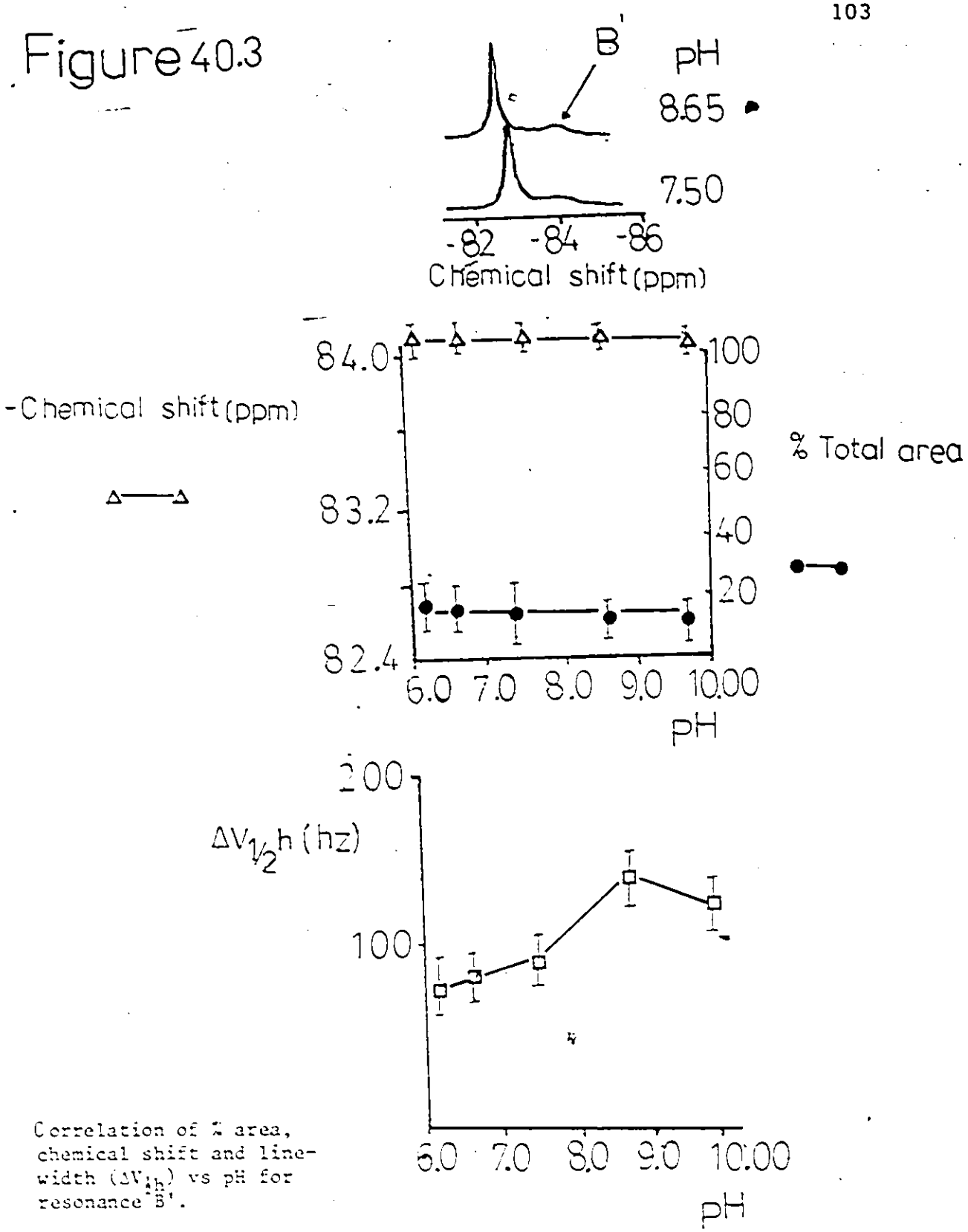

Correlation of % area, chemical shift and line-width ($\Delta V_{1/2}h$) vs pH for resonance 'B'.

the upfield resonance B decreased with an approximate chemical shift difference between B and C of 0.4 ppm. In contrast, the relative proportion of the upfield resonances A' and A" increase at the expense of the downfield resonances B' and B" with a chemical shift difference between these pairs of resonances of approximately 1 ppm. With respect to area changes of individual resonances, C, and B' (Figure 28.4 and 37.3) show correspond maximum and minimum respectively at pH 4.2. Resonances C and B" (Figure 28.4 and 37.4) show a change in chemical shift of approximately 0.2 ppm with C showing a minimum at pH 4.20 and B" a midpoint at pH 4.8. In addition, resonance C and B" show linewidth changes with maxima at pH 4.2 (Figure 28.4 and 37.4).

The differences in the area, chemical shift and linewidth vs pH trends for the ^{19}F-NMR spectra of BSA-FEM-d_2 or BSA-TFP might be attributed to the different sulfhydryl ^{19}F labels. the differences in these sulfhydryl labels are:

1. The fluorine atoms in the FEM-d_2 label are 6 atoms away from the sulfur atoms as opposed to 4 atoms for the TFP label (Figure 41).

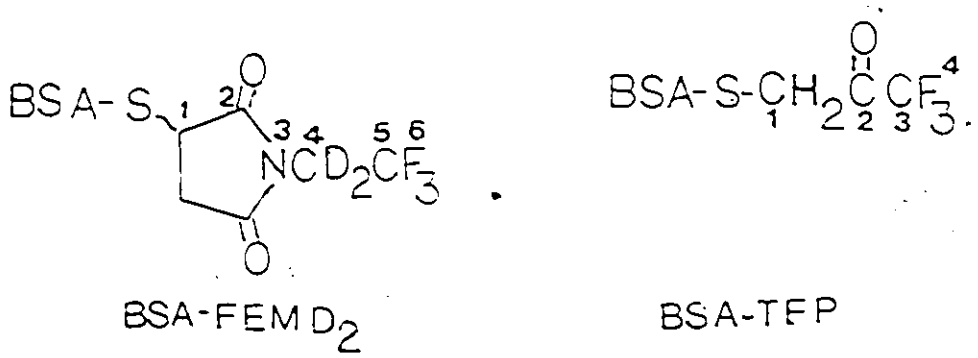

Figure 41

Consequently, the difference in chemical environments as reflected in the chemical shift differences between interconverting ^{19}F resonances is more pronounced in BSA-TFP (1.0 ppm) as compared to BSA-FEM-d_2 (0.4 ppm), and

2. In aqueous solution, the trifluoropropane label is known to exist as a gem-diol (Figure 42) which may lead to hydrogen bonding interactions between the hydorxyl hydrogens and suitable nearby sites. If this is the case, then what may actuallly be studied by ^{19}F-nmr may be various hydrogen bonded states of the ^{19}F-label having nothing to do with the proteins conformational state.

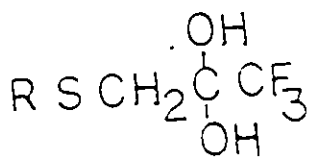

Figure 42

Irrespective of the differences between the two labels, it is evident that at least three different chemical environments are experienced by the ^{19}F nucleus at various pHs around the N-F transiton. The correlation between the states of the modified proteins detected by CD and fluorescence studies and the environments of the ^{19}F-labels observed through ^{19}F-nmr studies is summarized in Table 12.

Table 12: Correlation of Fluorescence and CD data with ^{19}F-nmr sutdies of BSA-FEM-d_2 and BSA-TFP in the pH 3.0-6.0 range.

Fluorescence Studies of BSA-FEM-d_2 and BSA-TFP	CD Studies of FSA-FEM-d_2 and BSA-TFP	^{19}F-NMR Data: BSA-FEM-d_2	^{19}F-NMR Data: BSA-TFP
F state-pH 3.80	F state-pH 3.80	2 ^{19}F chemical environments -peaks B and C	4 ^{19}F chemical environments are evident in both the N and F states
midpoint at pH 4.65	midpoint, pH 3.40		
	midpoint, pH 4.20		
N state-pH 4.80 (Figure 23)	N state-pH 4.40 (Figure 22)	3 ^{19}F chemical environments -peaks C,C' and A (Figures 26,27, 28.1-28.4)	-peaks A',A",B' and B". (Figures 35,36 37.1-37.4)

3.4 Synthesis of bis 8-fluoro, 8-deutero and 12-fluoro-12-deutero dimyrisotoylphosphatidylcholines (F-8, D-8 and F-12, D-12, DMPC respectively.)

In our repeated attempts to synthesize gem-difluoro-dimyrisotoylphosphatidylcholines 19a (Figure 14) (Section 4.6.5) none of the requisite gem-difluoromyristates 15 were ever isolated from the reaction of DAST with various oxomyristates. In our hands the synthesis of ethyl 4,8 and 12-oxo myristates (14a-14c) and their precursors proceeded in yields comparable to those reported in the literature.[206] An alternate synthesis of DMPC's with -CDF- instead of $-CF_2-$ units was undertaken (Figure 43, Scheme 2) since DSC studies by Sturtevant[39] showed that the gem difluoro DMPCs 19a-c (Figure 14) had substantially altered phase transition temperatures and enthalpies compared to their unfluorinated counterparts. The introduction of a deuterium atom at the same carbon bearing the fluorine label was used as an ^{2}H-nmr label to assess the perturbing effect of the ^{19}F-label from a comparison of the quadrupole splittings (ΔV_Q) with those obtained by Oldfield[202, 183-4] for the $-CD_2-$ labelled counterparts.

Alternatively, the synthesis of deuteroalcohols 27a and b, fluorodeuteroethylmyristates, 28a,b and 8-F, 8-D and 12-F, 12-D DMPC (32a and b) proceed in good yield and purity (Section 4.6.6 - 4.5.12, Tables 23 - 28 inclusive). Attempts to synthesize

ethyl-4-hydroxy, 4-deuteromyristate by the reduction of ethyl-4-oxomyristate 14a with sodium borodeuteride failed due to lactonization (Figure 43, Scheme 1). All attempts to get around this problem met with failure (Section 4.6.6) so in the interest of time, the synthesis of bis-4-fluoro, 4-deutero dimyristoyl-phosphatidylcholine (F-4, D-4 DMPC) was abandoned.

3.5 Calorimetric and ^{2}H-nmr Studies of F-8, D-8 and F-12, D-12 DMPC

Differential scanning calorimetry traces (Sect. 4.1) (courtesy of Dr. R.M. Epand) for synthetic DMPC, F-8, D-8 and F-12, D-12 DMPC provided the phase transition temperatures and the enthalpies of these transitions (Figure 44 and Table 13). The thermal behaviour of our synthetic DMPC is identical in all aspects to that reported in the literature[220] showing a minor "premelt" transition at 13.9° and a major transition at 23.9°C. This suggests that this synthetic lipid was of extremely high purity which gave us confidence that the methods used for synthesizing and purifying the fluorinated lipids were adequate (Sect. 5.3). F-12, D-12 DMPC 32b showed a single sharp transition at 24.9° with a temperature range at half-height ($T_{m_{1/2}}$) of 0.5°C; there was no visible "pre-melt" transition at lower temperatures. Generally, "pre-melt" have enthalpies on the order of 0.5 kcal/mole or less and as such may be unobservable. The relatively narrow melting

Figure 43

SCHEME 1

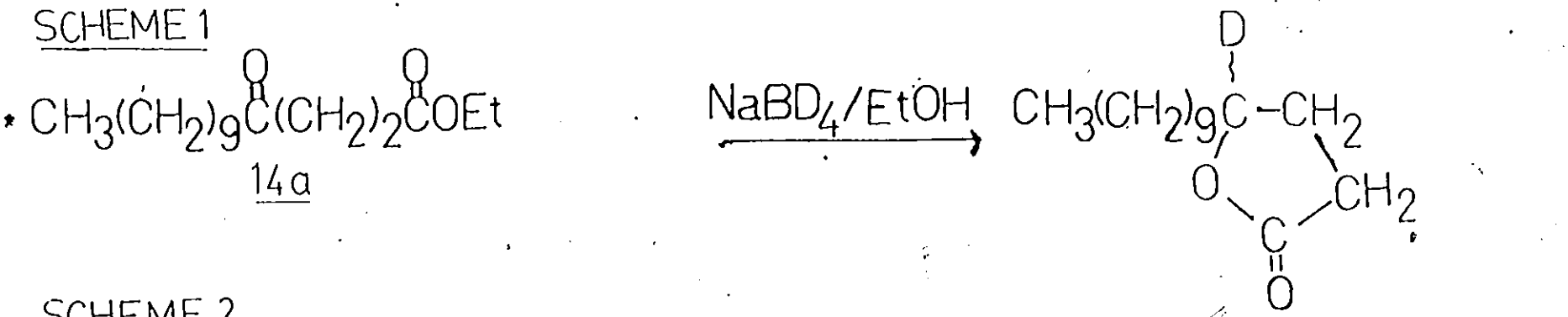

SCHEME 2

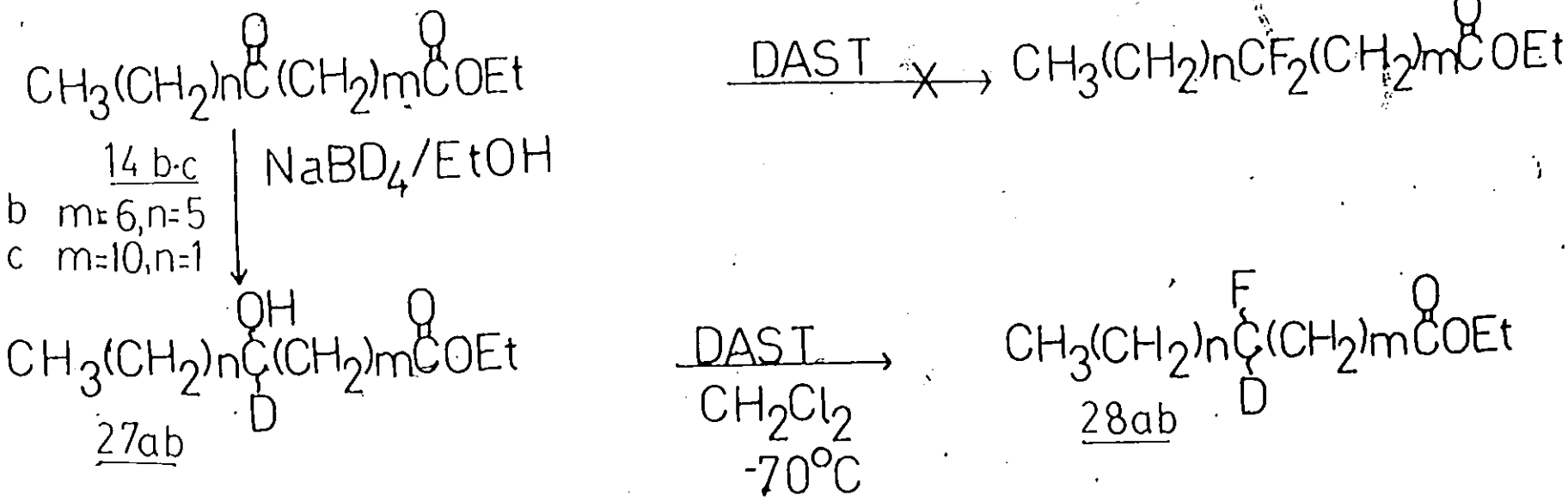

Figure 43(cont)

SCHEME 2 (cont)

For compounds 27-32

a m=6, n=5
b m=10, n=1

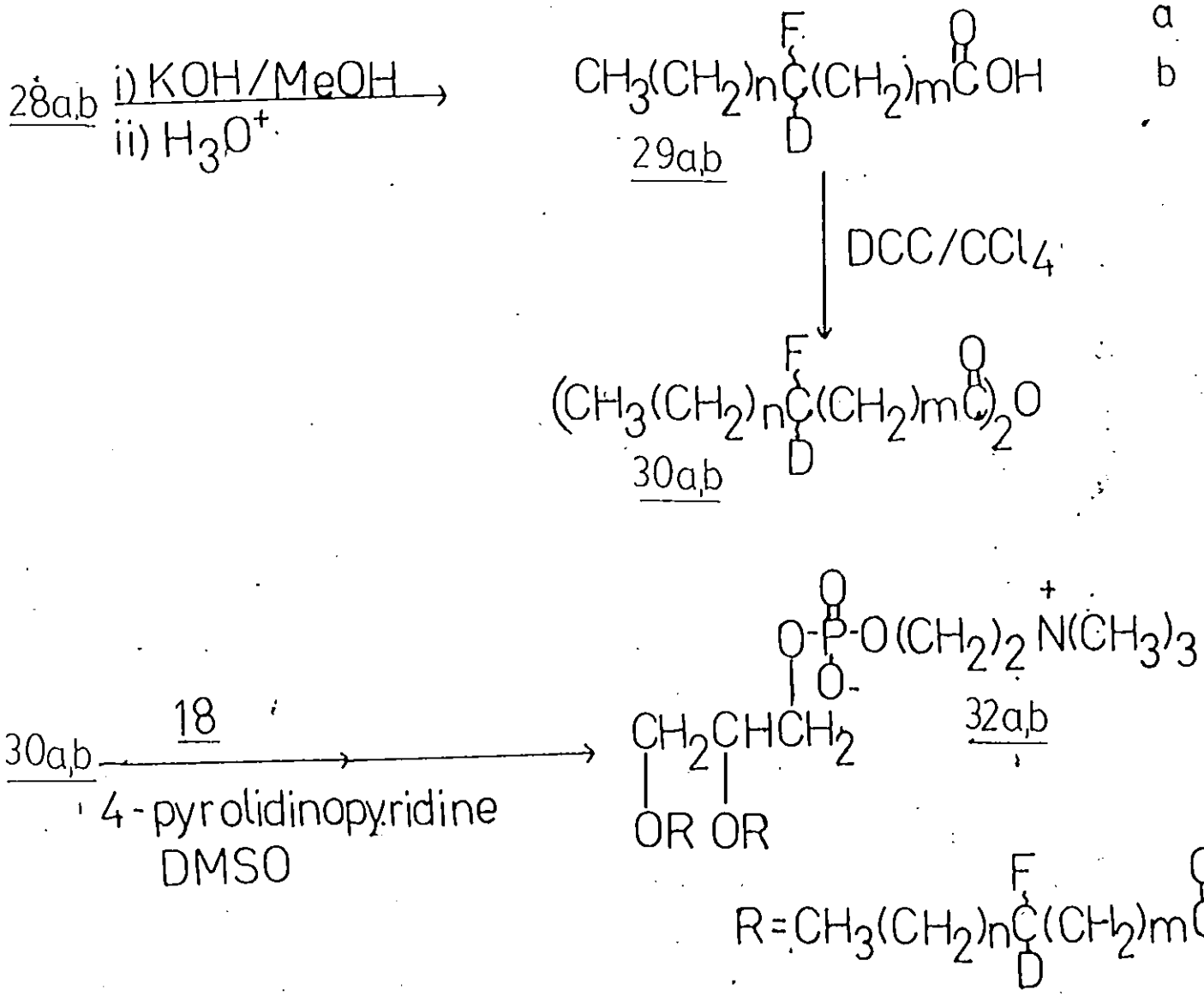

Figure 44

Differential Scanning Calorimetry Traces of Synthetic DMPC, F-8, D-8 and F-12, D-12 DMPC.

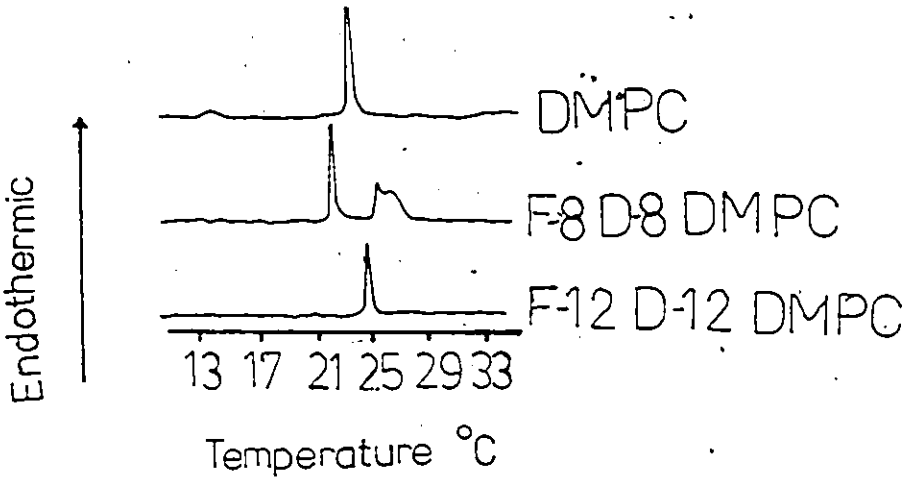

Table 13

Phospholipid	Transition Temp. (°C)	Tm (°C)	Enthalpy(kcal/mole)
DMPC	23.9 (lit. 24.0)	0.4	6.6 (lit. 6.65)
F-8, D-8 DMPC	22.5, 25.8 & 26.5	+0.5	*4.5
F-12, D-12 DMPC	24.9	0.5	5.6

* The sum of the enthalpies for all three transitions shown in Figure 44.

\+ For the transition at 22.5 °C only.

range of this fluorolipid is indicative of its high purity. No premelt transition was observed with F-8, D-8 DMPC 32a. In addition to a narrow transition at 22.5°C ($Tm_{\frac{1}{2}}$ ~ 0.5°C) an unusual pair or broader transitions were seen at 25.8 and 26.5°C. The addition of an equimolar amount of DMPC (Tm = 23.9°C) to F-12, D-12 DMPC 32b resulted in a Tm value lower than that of either of the two pure components (22.3°C) as well as a wider transition temperature range ($Tm_{\frac{1}{2}}$ = 1.5°C), (Figure 45).

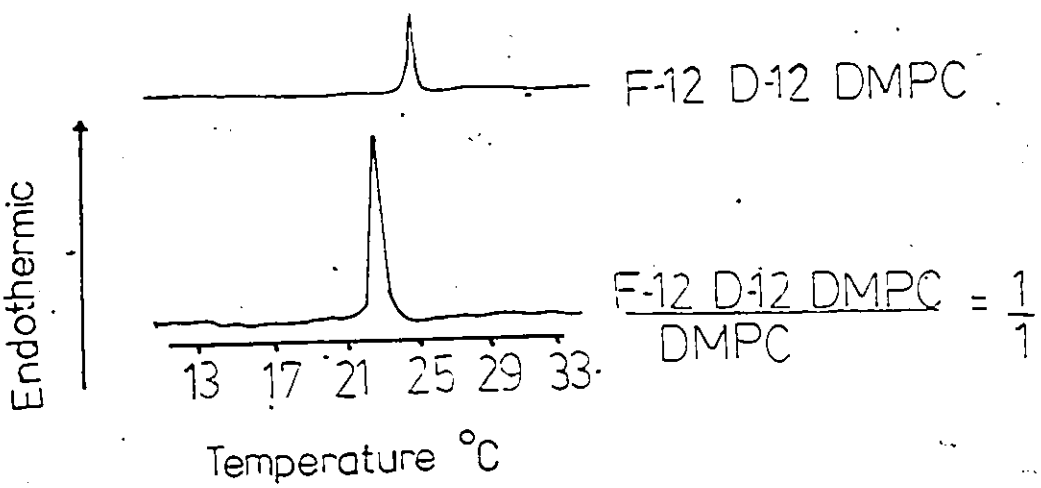

Figure 45

On the other hand, addition of increasing amounts of DMPC 31 with F-8, D-8 DMPC (Figure 46) resulted in the shift of the higher temperature transitions (25.8 and 26.5°C) of this fluorolipid to lower temperatures while the precentage contribution of these peaks to the total enthalpy of the phase transition decreased (Figure 47). In the case of F-8, D-8 DMPC 32a, the addition of DMPC resulted in the peak width of the main transition remaining relatively narrow (0.5°C). Although the Tm value of this transition decreased from 22.5 to 21.0°C on the addition of 1 mole equivalent of DMPC, the lack of peak broadening is unusual since it is often observed that DSC curves broaden on the addition of an impurity.

Previous DSC studies by sturtevant[40] have shown that gem-difluoro DMPCs have substantially altered phase transitions compared to their unfluorinated counterparts. In general, phase transition enthalpies on the order of 3 - 6 kcal/mole more exothermic than DMPC as well as phase transition temperatures at least 3 degrees higher or lower than DMPC. DSC studies by Sykes [108-109] on bis monofluorodipalmitoylphosphatidylcholines indicated that the DSC traces of these synthetic lipids have similar but broadened transitions relative to dipalmitoylphosphatidylcholine (DPPC). The phase transition temperatures of these fluorolipids were in a range of 0.2 to 5°C lower than DPPC

Figure 46

Differential Scanning Calorimetry (DSC) Scans of DMPC/F-8, D-8 DMPC Samples of Varying Mole Ratio.

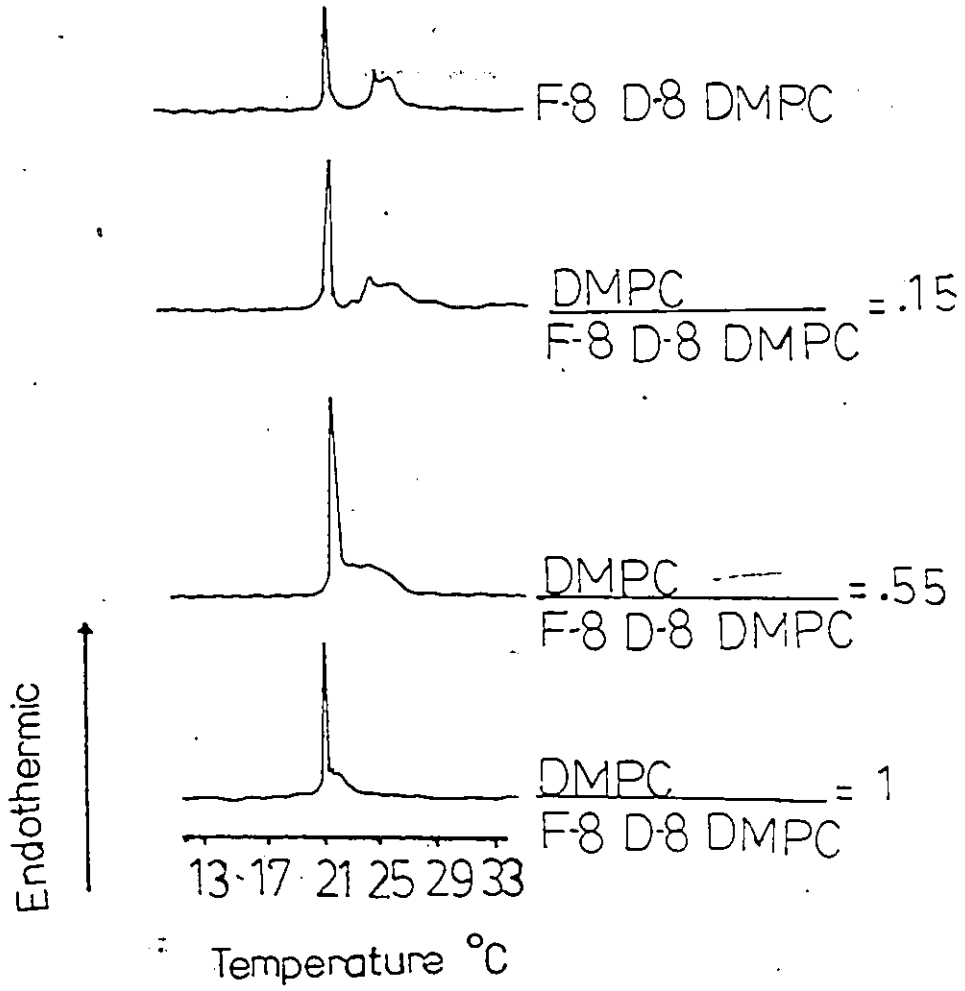

Figure 47

A plot of % Total enthalpy of the phase transition for the higher temperature transitions* of F-8, D-8 DMPC as a function of DMPC/F-8, D-8 DMPC molar ratio.

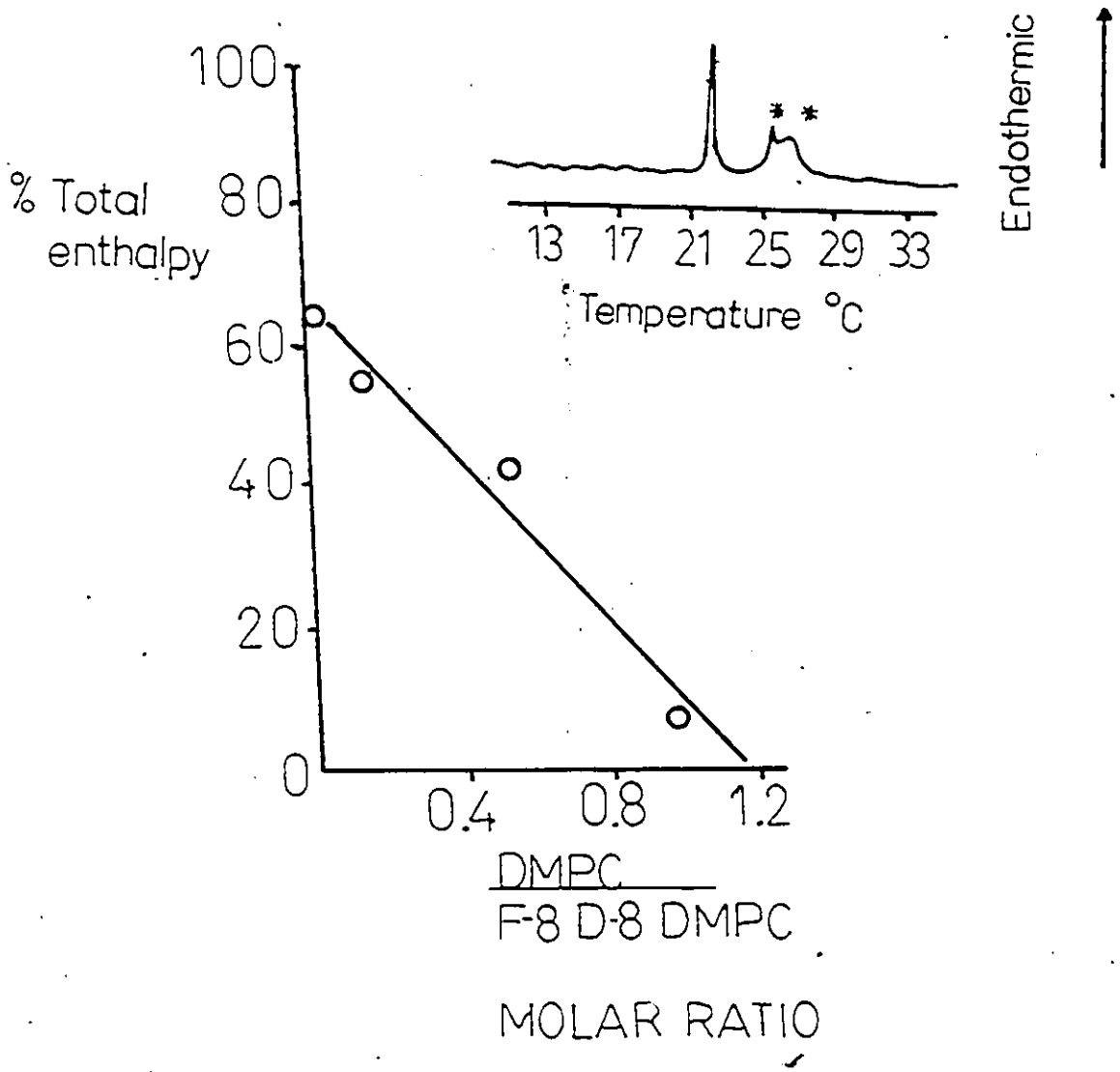

while the enthalpies were on the order of 3 kcal/mole less exothermic than DPPC. In terms of the phase transition enthalpies, F-8, D-8 and F-12, D-12 DMPC both closely mimic that of DMPC. The temperatures of the main phase transitions for F-8, D-8 and F-12, D-12 DMPC as well as DMPC are very close to one another (Table 13). The question now arises as to what the source of the higher temperature transitions at 25.8 and 26.5°C for F-8, D-8, DMPC. The observation that these higher temperatures transitions disappear on the addition of increasing amounts of DMPC indicate that these transitions are a result of the position of the fluorine label on the acyl chain since only a single transition is observed for F-12, D-12 DMPC (Figure 45). A possible explanation for these higher temperature transitions might be an alignment of C-F dipoles of the acyl chain that is disrupted on addition of DMPC.

^{2}H-nmr spectra of both fluoro, deutero DMPCs(32a and b) were kindly provided by Dr. James H. Davis, (University of Guelph) on a "home-build" instrument. Attempts to obtain ^{2}H-nmr spectra or ^{19}F-dipolar spectra on the Bruker CXP-200 solid state nmr Southwestern Ontario regional instrument, failed. Spectra of both fluorolipids above (35°C) and below (10°C) of both lipids are shown in Figure 48. At 10°C the broader unresolved spectra can be attributed to the smaller T_2 values of the deuterium atom resulting from the lower rotational correlation time in the gel state of the phospholipid. The quadrupolar splitting (ΔV_Q) for F-8, D-8, 32a and F-12, D-12 DMPC 32b are in good

Figure 48

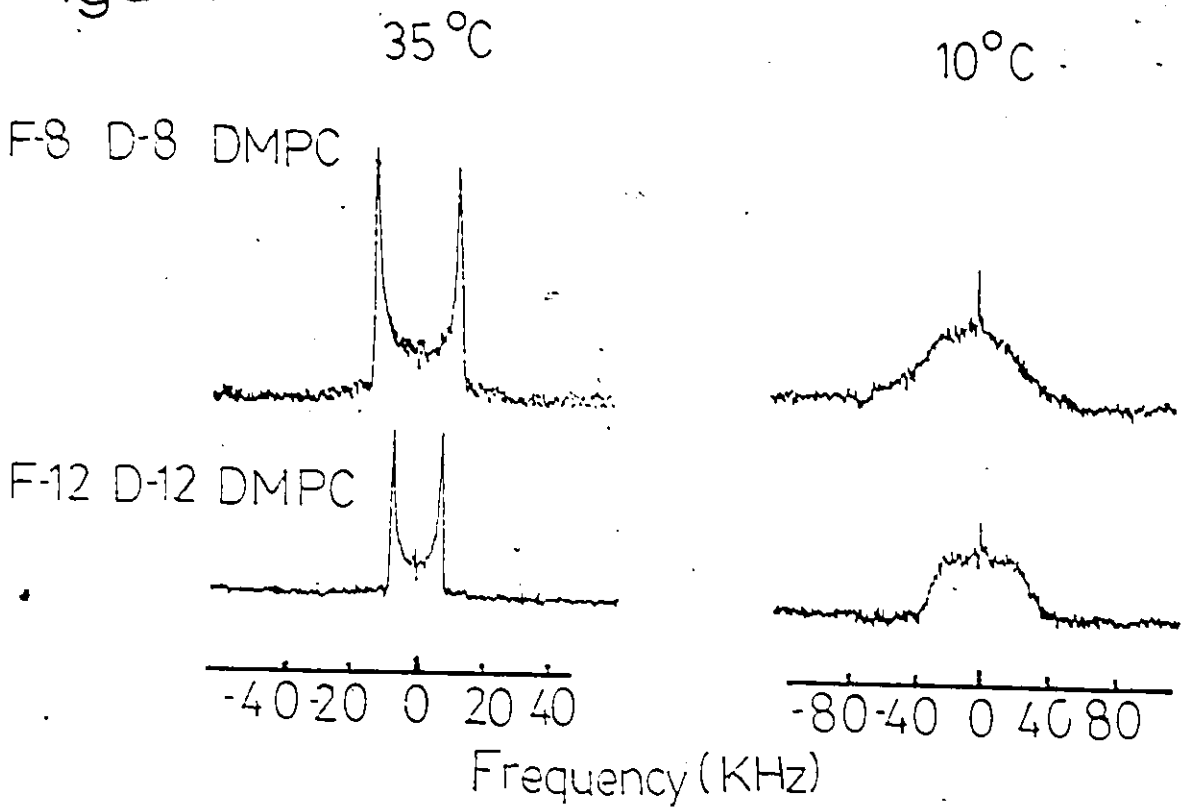

^{2}H-NMR spectra of F-8, D-8 and F-12, D-12 DMPC. Approximately 30mg of phospholipid was mixed with 100ul of H_2O. The natural abundance deuterium signal of HOD was used as a reference at 0. KHz. Note that the frequency scale of the 10°C spectra is twice that of the 35°C spectra.

Table 14

Lipid	$^*\Delta\nu_Q$ (± 1KHz)	$^*S_{C-D}$ (± .04)
F-8, D-8 DMPC	25	.15
sn-2, 8, 8-D_2 DMPC	27	.16
F-12, D-12 DMPC	15	.09
sn-2, 12, 12-D_2 DMPC	17	.10

$^*\Delta\nu_Q = 3/4\ e^2qQ/h\ \ S_{C-D}$ (Sect. 5.4.4)

agreement with those reported by Oldfield for Sn-2, -8,8 and Sn-2, 12, 12-dideutero DMPC's as shown in Table 14. ^{2}H-nmr spectra of both fluorinated lipids obtained at above and below their Tm values showed the identicial temperature dependance of S_{CD} as observed by Oldfield[220] for the $-CD_2$-lipids* as shown in Figure 49.

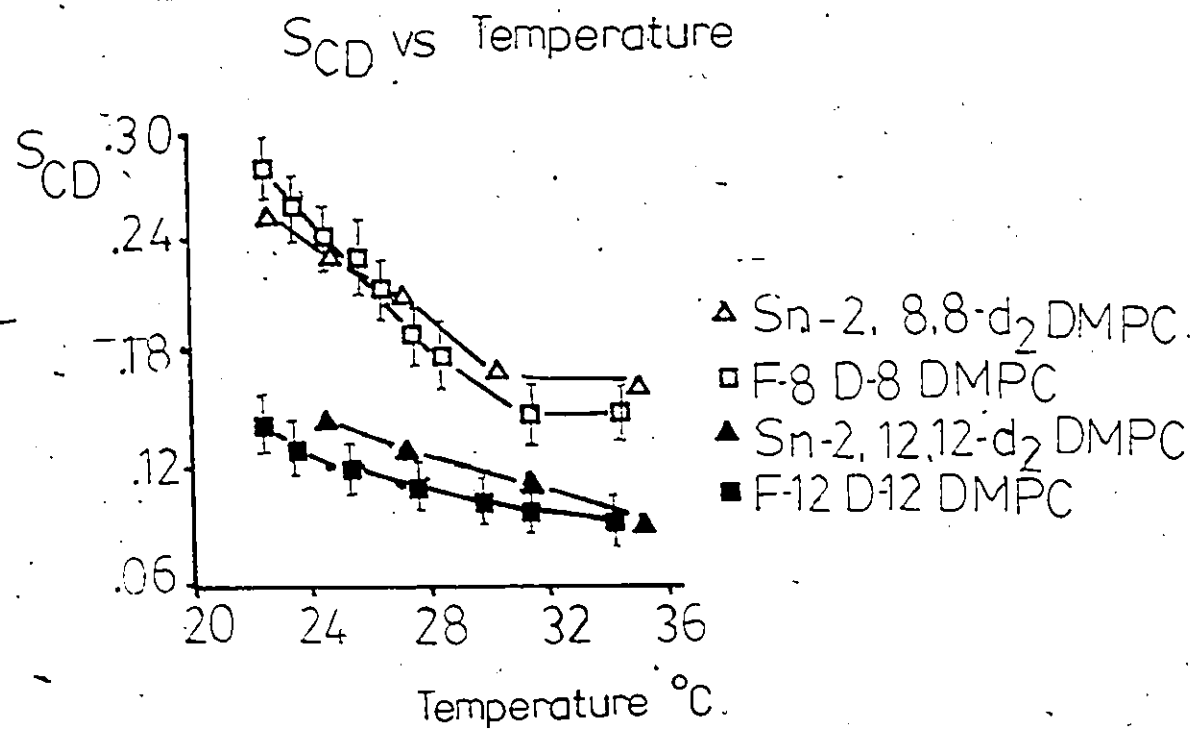

Figure 49

The DSC and ^{2}H-NMR data lead to two differing conclusions regarding the perturbation caused by the introduction of a fluorine atom. While ^{2}H-NMR spectra of both fluoro and deutero DMPC's are identical to their $-CD_2$- counterparts,[183-184] at the temperatures studies the DSC studies painted a different

picture. Both the phase transition temperatures and enthalpies of F-8,D-8 and F-12,D-12 DMPC (32a and b) were different then that of DMPC alone.

The extent of the perturbation as shown by the DSC traces is greatest for F-8,D-8 DMPC 32a when the fluorine atom is near the center of the acyl chain compared to F-12,D-12 DMPC where the fluorine label is near the end of the hydrocarbon chain. Although the reason for the higher temperature transitions at 25.8 and 26.5°C (Figure 44) for F-8,D-8 DMPC is not known, the disappearance of these peaks on addition increasing amount of pure DMPC (Figure 46) is of interest. The appearance of these DSC curves would suggest that the extent of the perturbation caused by the fluorine label is lessened with increasing amounts of DMPC present.

Recent studies by Sykes and McElhaney[108] on bis monofluoro DPPCs indicate that although the DSC traces of these synthetic lipids show similar but generally broader transitions relative to DPPC, order parameters (S_{CF}) calculated from ^{19}F-dipolar spectra[109] are approximately 20% lower from those calculated from ^{2}H-NMR spectra of $-CD_2-$ analogues (S_{CD}). The discrepancy is greatest towards the head group of the phospholipid where S_{CF} is approximately 50% than the reported S_{CD}.

Although it is not for certain whether or not the calculation of C-F order parameters based on their line-

fitting models is the source of this discrepancy, our C-D quardupole splittings (ΔV_Q) for deuterium labels at the same carbon atom bearing the fluorine atom for F-8,D-8 and F-12,D-12 DMPC(32a and b) show no difference (within experimental error) with those of Oldfield (Table 14). This suggests that the no perturbation of the motional properties at the 8 and 12 positions of the acyl chain occur on introduction of the fluorine label.

Perturbations caused by the introduction of CF_2 groups at varying positions along the acyl chain of phosphatidylcholines have been studied to a greater extent than the introduction of -CHF- units. ^{2}H-NMR studies by Seelig[136] on gem difluoro DMPCs with $-CD_2-$ groups at varying positions relative to the $-CF_2-$ group have shown an overall reduction in the observed ΔV_Q values compared to their unfluorinated counterparts. indicating an increased mobility about the deuterated positions. Sturtevant et al[39] have shown that DMPCs with $-CF_2-$ units at either the 4, 8, or 12 position of the acyl chain results in phase transition temperatures and enthalpies which are higher or lower than DMPC. Order parameters, S_{FF}, obtained from dipolar spectra of these same lipids show values which agree within 10% of the C-D order parameters determined from the ^{2}H-NMR spectra of the $-CD_2-$ containing counter parts.

In summary, the DSC studies on F-8,D-8 and F-12,D-12 DMPC show that the introduction of fluorine is not an innocuous

change contrary to what was shown by the ^{2}H-nmr studies presented. This must be kept in mind when using either fluorinated lipid for nmr studies. These results point out the need for caution when introducing a molecular probe into a biological system and the need to use more than one physical technique to study the perturbed and unperturbed system.

3.6 Modification of Lipophilin Cysteine Residues

The failure to observe a reaction between FEM and N-acetyl-L-cysteine methyl ester in various solvents (experimental, Section 4.7) in which lipophilin is soluble lead to the preparation of a water soluble form of the protein by the dialysis of lipophilin from 2-chloroethanol into water. The analysis of protein sulfhydryl groups using DTNB was undertaken before and after FEM-d_2 treatment of the protein using two different assay mixtures: 2-chloroethanol - 1% SDS and 2-chloroethanol (Section 4.7). These results were comparable to those obtained by Epand et al[176] (Table 15) using the same mixtures.

Table 15

Assay Mixture	Protein	# of determination	SH/mole	Reported SH/mole[176]
2-chloroethanol DTNB	lipophilin	3	1.01 ± .05	1.55 ± .05
	lip-FEM-d_2	4	0.30 ± .06	
	*lipophilin	3	1.03 ± .02	
2-chloroethanol ~1% SDS DTNB	lipophilin	3	1.75 ± .04	2.10 ± .05
	lip-FEM-d_2	3	1.03 ± .06	
	*lipophilin	4	1.69 ± .05	

* Lipophilin which had been dialyzed from 2-chloroethanol into water and freeze dried.

The sulfhydryl assays of lipophilin which had been dialyzed from 2-chloroethanol into water and freeze-dried (denoted by *) showed no observable differences from the same protein that had not undergone dialysis or freeze drying. A comparison of ^{19}F-nmr signal to noise ratios of a lip-FEM-d_2 solution in 2-chloroethanol with standard FEM-d_2/2-chloroethanol solution showed that ∿ 0.7 SH/mole of protein had been modified which was in good agreement with the DTNB assays (Table 15) Unfortunately, a comparison of the proteins by their CD spectra was not possible at the time of these experiments due to technical difficulties with Cary 81 instrument (Experimental, Section 4.1)

3.7 ^{19}F-NMR Studies of lipophilin and lip-FEM-d_2 incorporated into 8-F, 8-D and 12-F, 12-D DMPC.

A sample spectrum of lip-FEM-d_2 incorporated into F-8, D-8 (58% by weight protein at 35°C) is shown in Figure 50.

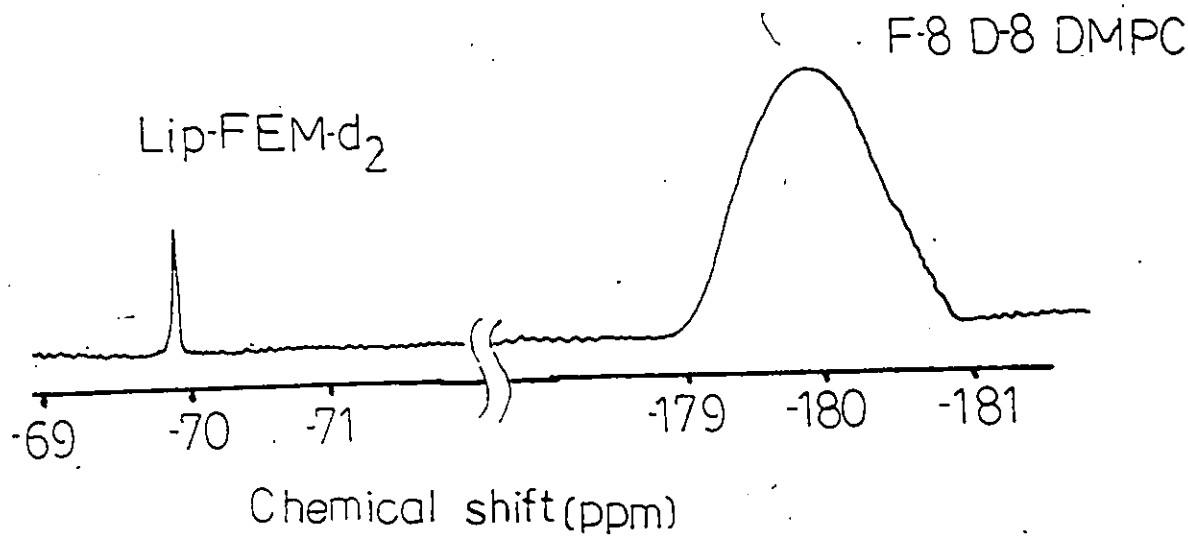

Figure 50

The ^{19}F-nmr resonance of lip-FEM-d_2 showed no variance in chemical shift (-69.81 ppm) or linewidth ($\Delta \nu_{1/2}$h = 40 Hz) over the temperatures and protein/lipid ratios studied. In comparison, ^{19}F-nmr spectra of aqueous FEM-d_2 using the same acquisition parameters showed a chemical shift of -70.12 ppm with a linewidth of 40 Hz. The relatively narrow linewidth of the protein label suggested that the ^{19}F nuclei were in an environment where the $-CF_3$ group of the protein label was relatively mobile but the exact nature of this environment is unknown.

Consequently, no further information with regards to the environment of the sulfhydryl residue(s) of lipophilin was gained from these ^{19}F-nmr studies. ^{19}F-NMR spectra of a few lipophilin or lip-FEM-d_2/fluorophospholipid mixtures of

varying weight ratios at V_o = 84.66 MHz, and at two temperatures showed fluorophospholipid linewidths that were approximately 1.6 (Table 16) fold narrower than V_o = 235.66 MHz which suggests CSA contributions increased by a factor of .56 as the applied field.

In contrast, ^{19}F-nmr studies by Gent[103,104] on gem-difluoro DMPCs have indicated that the linewidths of the observed ^{19}F resonances increased four fold for a corresponding two fold increase in applied field strength; indicating chemical shift anisotropy contributions varied as the square of the applied field strength (Sect. 5.11.2), and increased with decreasing temperature over the same temperature range.

Linewidth vs. Temperature plots (Figure 51 A & B) for various protein/phospholipid mixtures showed similar trends and no ^{19}F-signals were observed below the phase transition of the lipids. Phospholipid ^{19}F-chemical shifts were found to be invariant with temperature and protein concentrations. A plot of the lipid ^{19}F-nmr resonance linewidths vs. % weight of protein at 35°C (Figure 52 A & B) showed a similar trend for both the modified and unmodified proteins for F-12, D-12 DMPC. However, a totally different trand is observed for F-8, D-8 DMPC. The observed phosphilipid ^{19}F-nmr linewidths for the lip-FEM-d_2 mixtures show very little change in increasing protein in contrast to lipophilin. Repeated ^{19}F-nmr studies of the same or freshly prepared samples of

Table 16 A comparison of linewidths for lipophilin or lip-FEM-d_2/fluorophospholipid mixtures at ν_0=84.66 or 235.36 MHz at various temperatures.

Protein-lipid mixture	Protein-lipid weight ratio (%)	Temp. (°C)	$V_{\frac{1}{2}h}$ (235.36 MHz)	$V_{\frac{1}{2}h}$ (84.66 MHz)
lipophilin/ F-8,D-8 DMPC	58.6	24.0	1190 Hz	768 Hz
	38.1		675	417
	0.0		490	306
	58.6	32.	749	496
	38.1		501	307
	0.0		251	161
lipophilin/ F-12,D-12 DMPC	54.5	23.2	860	544
	31.0		670	413
	0.0		560	337
	54.5	32.0	520	325
	31.0		306	190
	0.0		250	160
lip-FEM-D_2/ F-8,D-8 DMPC	55.0	24.	960	600
	31.0		620	388
	0.0		440	270
	55.0	32.	410	250
	31.		300	185
	0.0		250	160
lip-FEM-D_2/ F-12,D-12 DMPC	54.5	23.2	1053	658
	32.4		831	500
	0.0		522	324
	54.5	32.	504	304
	32.4		304	189
	0.0		250	161

Figure 51A

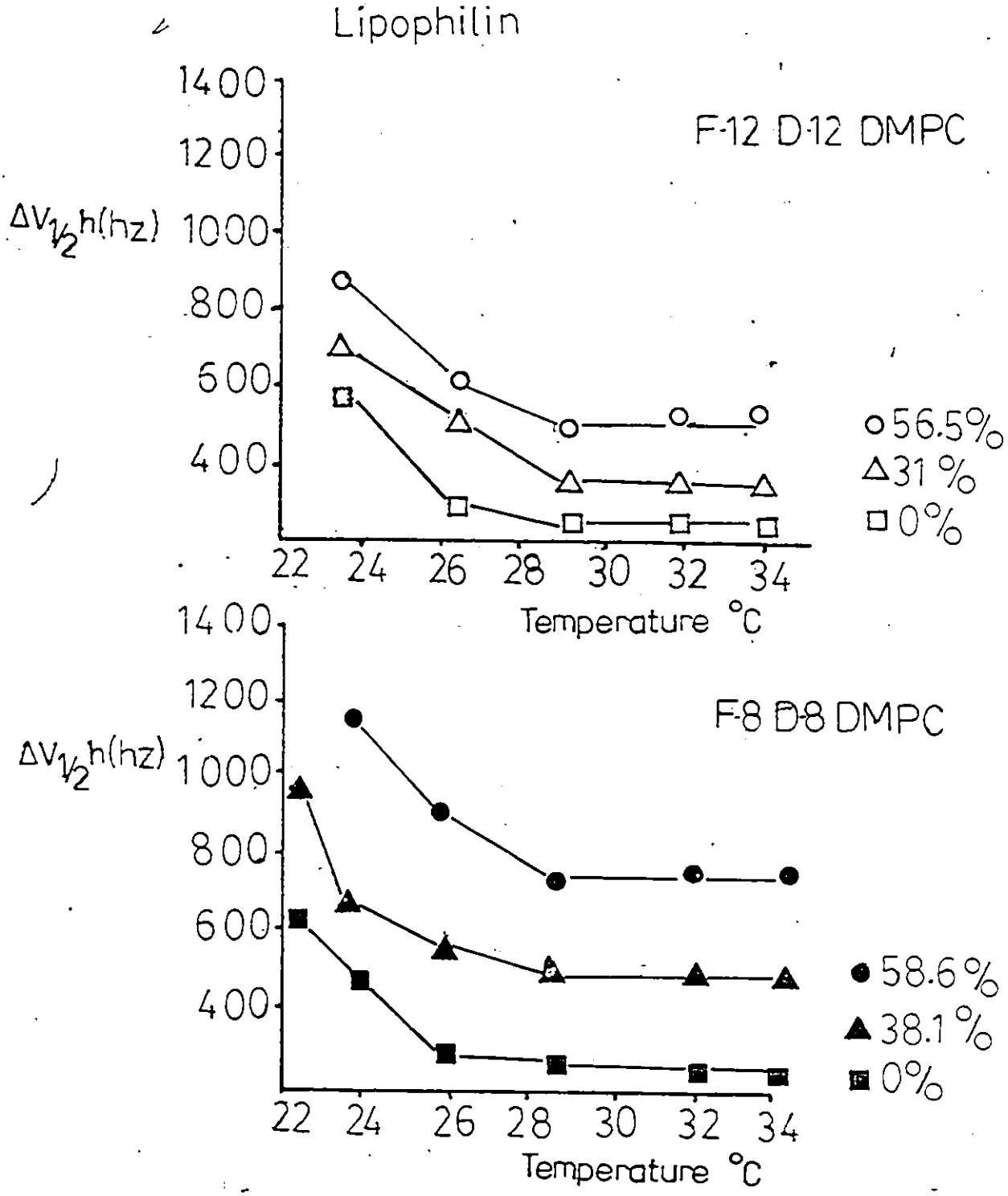

Plots of $V_{\frac{1}{2}}h$ vs. Temperature for Lipophilin-fluorophospholipid complexes of varying % weight protein (as indicated).

Figure 51B

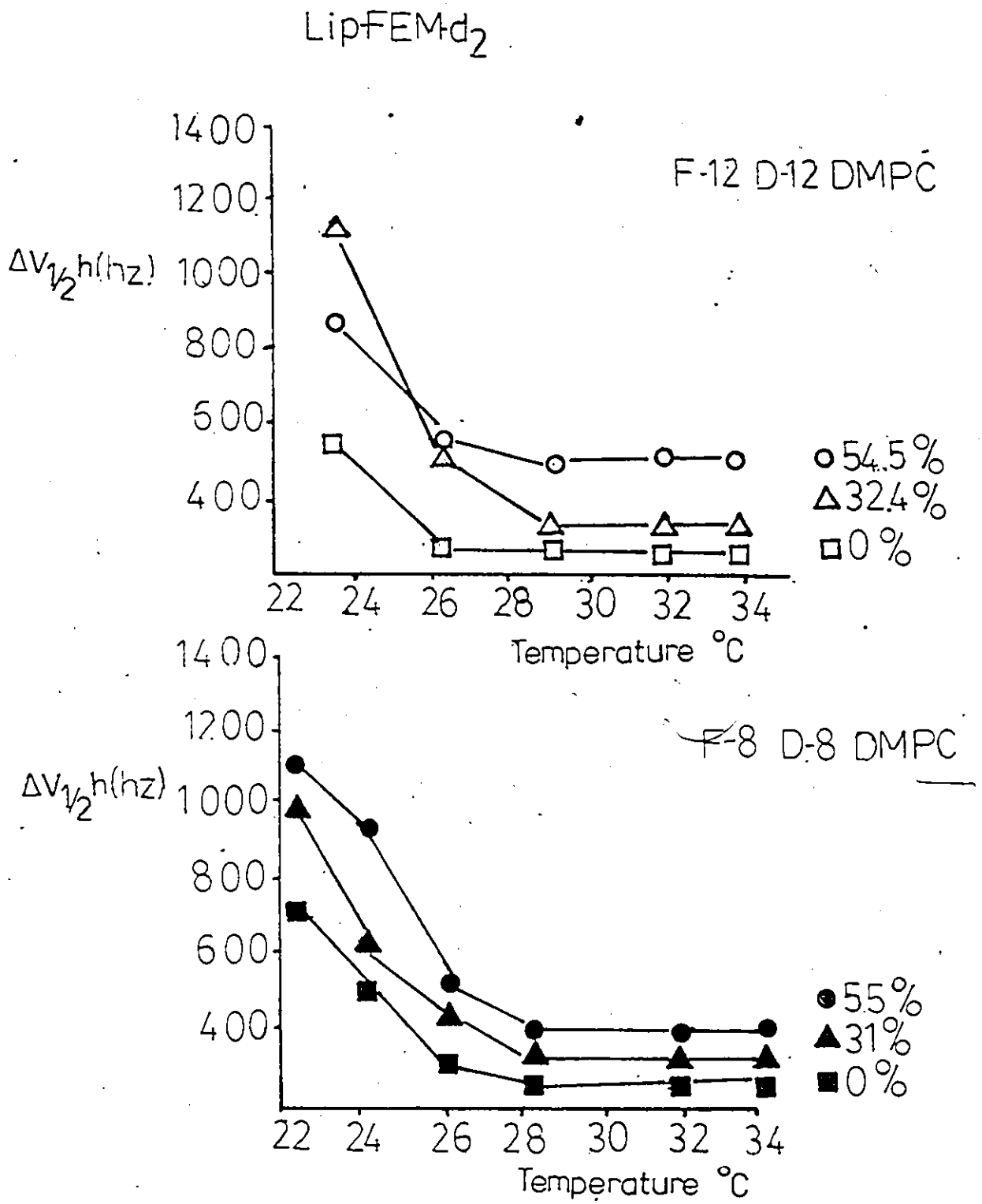

Plots of V½h vs. temperature for lip-FEM-d_2-fluorophospholipid complexes of varying % weight protein (as indicated).

Figure 52A

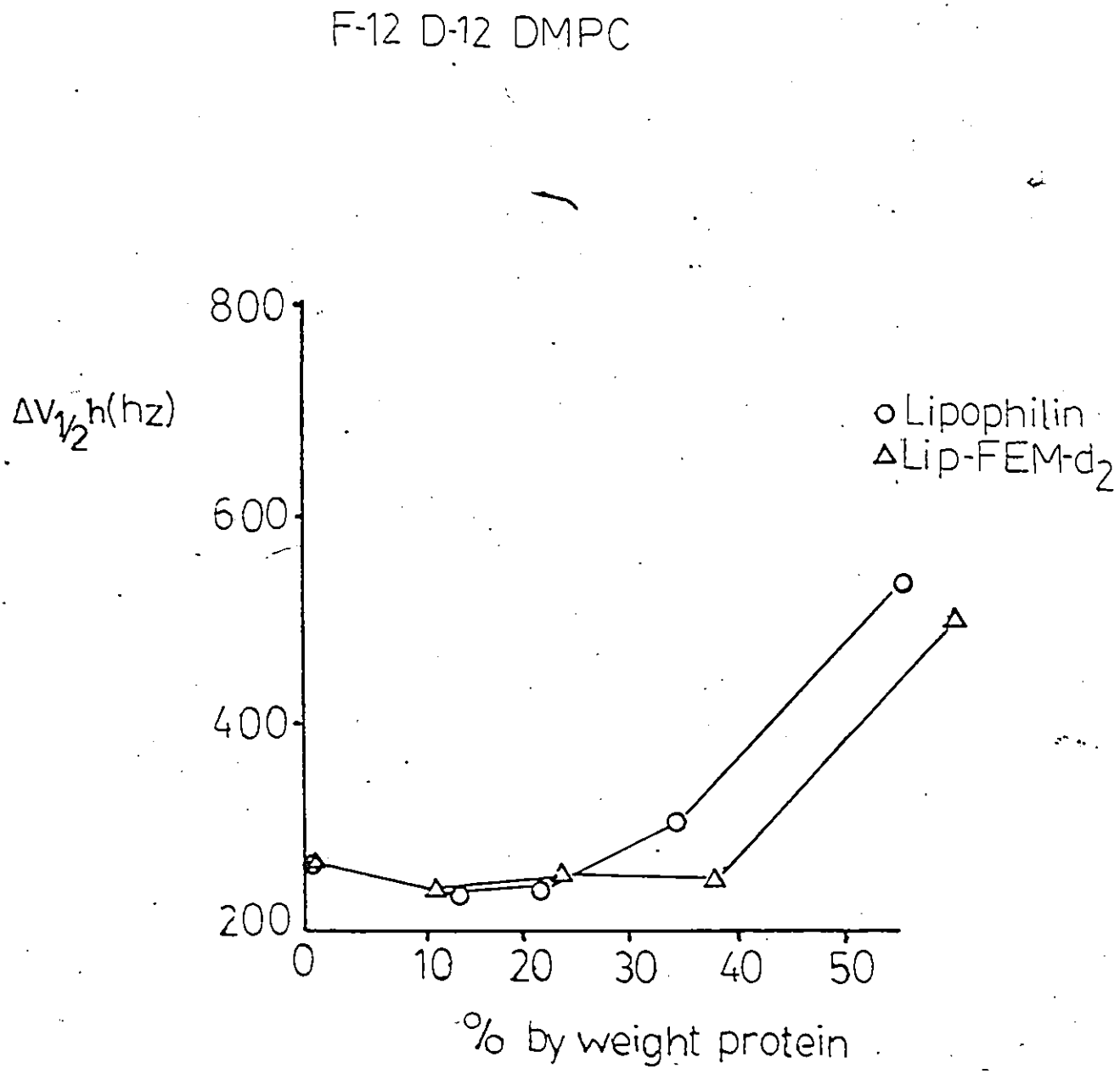

$V_{\frac{1}{2}}h$ vs. % weight protein for F-12, D-12 DMPC protein mixtures at 35°C.

Figure 52B

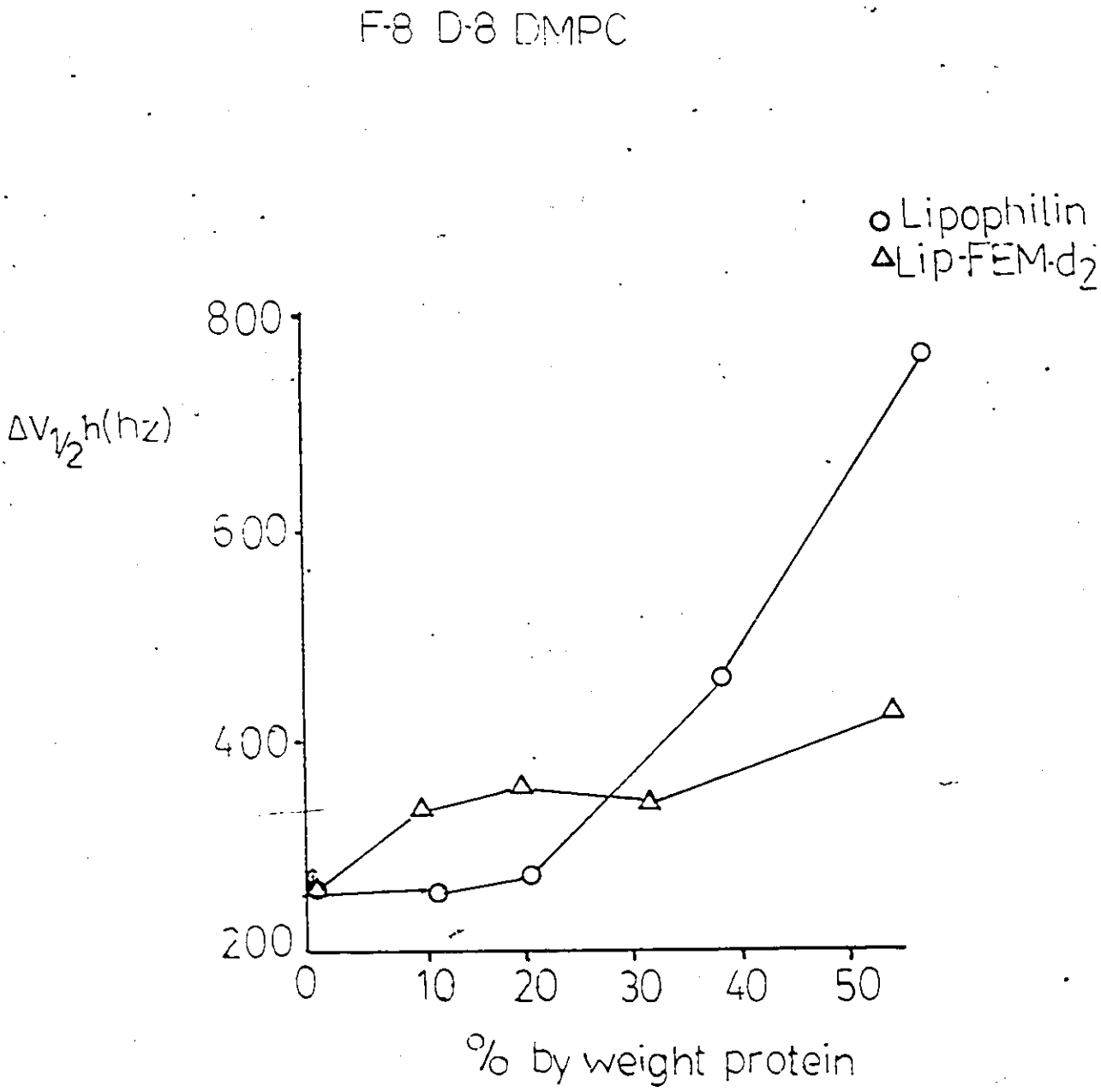

$V_{\frac{1}{2}}h$ vs. % weight protein for F-8,D-8 DMPC protein mixtures at 35°C

protein F-8,D-8 DMPc or F-12,D-12 DMPC mixtures gave the same results. It would appear that the modification of lipophilin by FEM-d_2 is the only cause for this discrepancy with F-8,D-8 DMPC (Figure 52B) and it is therefore unlikely that the modified protein is a good model for the behaviour of lipophilin in the same phospholipid mixture. The exact nature of this discrepancy was not explored using other methods usch as DSC on ^{2}H-nmr.

Generally, phospholipid ^{19}F resonances broadened with increasing amounts of protein which is consistant with the idea of increasing amount of "boundary" or immobile lipid with more protein present. However, no distinct ^{19}F-nmr signals corresponding to free of boundary lipid were observerd at V_0= 235.36 MHz. Significant changes in the ^{19}F-nmr line-widths of both fluorophospholipids do not occur below 30% by weight lipophilin (Figure 52A&B) in contrast to what has been previously observed by DSC and esr studies of the same protein in reconstituted protein/phospholipid mixtures.[195-201] Broadening of the DSC traces were observed with protein/lipid weight ratios as low as 5%. Likewise, esr studies[195-198] using spin labelled fatty acids as probes showed the presence of an "immobile" component of esr spectra at protein/lipid weight ratios of 20% or above. This may be attributed to both the greater sensitivity of the DSC and esr methods compared to

^{19}F-nmr and the time scale of the ^{19}F-nmr (~ 10^{-4}s) compared to the esr experiment (~ 10^{-6}s). Our results indicate that any boundary lipid present was likely exchanging with bulk lipid on a time scale faster than the nmr experiment, i.e., < 10^{-4}s. Since calorimetric or esr studies were not undertaken with lipophilin (lip-FEM-d_2) fluorophospholipid mixtures, the relative mole ratio of boundary lipid to protein is not known consequently a more extensive analysis of our ^{19}F-nmr results is not possible. In any case, these ^{19}F-nmr studies do not show "boundary lipid" as a distinct entity as seen in previous esr and DSC studies.[195-201]

3.8 Summary and Conclusions

In summary, the work covered in this thesis has dealt with the development of a fluorinated maleimide, FEM, and its deuterated counterpart, FEM-d_2 for protein ^{19}F-nmr studies. A detailed kinetic study has shown that FEM reacts quickly and specifically with thiols over other nuclophilic residues found in proteins and the only side reactions that occurs is hydrolysis to its maleamic acid. The ^{19}F-nmr studies of the N-F transition BSA-FEM-d_2 or BSA-TFP have shown that there is more than two "pH dependant" chemical environments about the cysteine residue of the protein BSA, in either the N or F states. Previous reports using spin-labelled maleimides (Section 2.3) to study the N-F transition showed no such "multi-environment"

phenomena. Neither CD or fluorescence studies presented in this work showed evidence for the existance of "substates" in the N or F states of the modified proteins. While it was shown that FEM-d_2 is specific for the cysteine sulfhydryl residue of BSA, Br-TFP in addition to sulfhydryl labelling, reacted elsewhere on the protein to the extent of 20%. A further interesting result was the observation of a "pH dependant" multi-environment phenomena at pH's during the N-F transition of BSA-TFP by ^{19}F-NMR previously unobserved by Zurawski[120] who studied the same modified protein by ^{19}F-nmr.

At pHs above 7.0 the succinimide ring of the BSA-FEM-d_2 was found to be unstable since it underwent hydrolysis and/or intramolecular ring opening. This limits the use of FEM(-d_2) as a protein label to pH 7.0 and below.

Two fluorinated and deuterated phosphatidylcholines, F-8 D-8, and F-12, D-12 DMPC (32a and b) were successfully synthesized and characterized by calorimetry and ^{2}H-NMR studies. Attempts to simultaneously monitor the environments of lipophilins cysteine residues after FEM-d_2 modification and F-8, D-8 or F-12, D1-12 DMPC by ^{19}F-nmr were unsuccessful. The ^{19}F-nmr resonance of lip-FEM-d_2 was invariant in chemical shift of linewidth with either temperature of protein/lipid content. As a consequence, little information concerning the labelled sulfhydryl residues of lipophilin was obtained. Although lipid ^{19}F-resonances were generally broader in the presence either

lipophilin or lip-FEM-d_2, no distinct resonances which could be attributed to "boundary lipid" were seen. Irrespective of these failures, F-8, D-8 and F-12, D-12 DMPC may prove to be interesting lipids for future ^{2}H, ^{31}P and ^{19}F-nmr and/or calorimetric studies.

CHAPTER FOUR

EXPERIMENTAL

4.1 General - Instruments and Standards

Melting points were obtained using a Hoover capillary apparatus and are uncorrected. Infrared (I.R.) spectra were obtained on a Perkin-Elmer Model 283 Spectrophotometer and all reported peaks are given in reciprocal wave numbers (cm^{-1}) with polystyrene as the reference signal at 1602 cm^{-1}. The following abbreviations were used to describe I.R. peaks:

s = strong	ms = medium sharp
b = broad	ss = strong sharp
m = medium	sb = strong broad
w = weak	

^{1}H-NMR spectra unless otherwise indicated were obtained at 90 MHz using a Varian Associates EM-390 CW instrument. 250MHz ^{1}H-NMR spectra were obtained using a Bruker WM-250 Fourier Transform spectrometer. All NMR absorbances are reported in parts per million (δ) ppm with the following abbreviations:

s = singlet	q = quartet
d = doublet	dd = doublet of doublets
t = triplet	m = multiplet

Coupling constants, J, are reported in Hz (sec^{-1}). Trimethylsilane (TMS) was used as an internal reference at-

0 ppm when ^{1}H-NMR spectra were obtained using $CDCl_3$ or acetone-d_6 as solvents. DOH (4.65 ppm) was used as an internal reference when D_2O was used as a solvent. ^{13}C and ^{2}H-NMR spectra were obtained at 62.9 and 38.4 MHz respectively on the Bruker WM 250 spectrometer. All ^{13}C-NMR spectra were proton broad-band decoupled and referenced to $CDCl_3$ (76.9 ppm) or acetone-d_6 (29.2 and 204.1 ppm). ^{19}F-NMR spectra were obtained either at 84.66 or 235.36 MHz on a Bruker WH-90 or Bruker WM 250 Multinuclear F.T. instruments respectively with trifluoroacetate (-75.96 ppm), or trifluoroacetamide (-76.26 ppm) used as internal or external standards.

For spectra obtained at 84.66 MHz a 10 mM ^{19}F-probe was used with a D_2O external lock. Typical spectral widths and memory sizes used were 6,000 Hz and 4K or 12,000 Hz and 8K respectively which resulted in an acquisition time of 0.679 sec. Other spectra parameters used were, offsets of either 1,000 or 2,000 Hz, pulse widths of 25μsec ($t_p = 90^o$) delay times of 200μsec, a line broadening of 1.0 and a resolution of 1.47 Hz/data point. ^{19}F-NMR spectra were stored on a Nashua O.D. 15-8 Cartridge disk were transferred to a Nicolet FT-IR disk using the RSTR 10 and 11 programs respectively. Once all spectra were transferred to the FT-IR disk, they were curve resolved using the Curve Analysis Program (CAP).

235.36 MHz ^{19}F-Spectra were obtained using the following spectral parameters; memory size 16K, offset and sweepwidth 20,000 Hz and 40,000 Hz respectively, line broadening of 1.00, delay time of 12 μs, pulse width of 30 μs (tp=90°), acquisition time of .410s and a resolution of 2.44 Hz/point. Spectra were stored on floppy disks and transferred to a Nicolet FT-IR disk for curve analysis using SPCNIC and SPECNIC transfer programs respectively. Errors for the calculated linewidths for the curve resolved resonances were assumed to be twice the root mean square (RMS) error while in percentage area were assumed to be ± the RMS error. Chemical shift errors were assumed to be ± 1 data point.

^{2}H-quadrupole spectra were kindly obtained for us by Dr. James H. Davis (University of Guelph, Physics Department) using a home built instrument with variable temperature capability. The pulse sequence used in acquiring these spectra was the "quad-echo" sequence[81,58] shown below:

$$(90° - \tau - 90°)\ n^{-}$$

Spectral parameters used were: a resonant frequency of 41.31 MHz, a phase time τ of 3.5 μs, recycle time of 130 μs and dwell time of 3.5 μs. Prior to the acquisition of spectra, fluorodeuterophospholipid samples (∿30mg) were suspended in 100 μl of H_2O. Typically, spectra were processed after 10,000 scans and the HOD deuterium signal

used at the zero reference.

High resolution (HRMS) or low resolution (LRMS) mass spectra were obtained using a VG 7070 spectrometer (V.G. micromass, Altricham U.K.) with a VG 2035 data system. All mass spectral data are reported as: mass (mass fragment, relative intensity). All HRMS data is assumed to be accurate to 5 millimass (.005 mass) units. Elemental analysis were performed at Guelph Chemical Laboratories, Guelph, Ontario. For compounds not previously reported in the literature HRMS data or elemental analysis as well as ^{13}C-NMR data are included.

Kinetic studies were performed using a Durrum D-IIV Stopped-Flow Spectrophotometer equipped with a deuterium lamp, power supply and Nicolet Model 1170 Signal Averager. The temperature of the stopped flow system was controlled using with a Hotpack Model 320 water bath and variable speed water pump. All reactions were monitored by observing an absorbance decrease at 276 nm.

pH values of solutions were determined using a Radiometer Copenhagen Model 26 pH meter. The pH meter was standardized with pH 4.00, 7.00 and 10.00 buffers from the same manufacturer.

Optical density (O.D.) measurements were performed using a Gilson Model 240 Spectrophotometer using 1 cm pathlength cells.

All fluorimetric work was performed on an Aminco-Bowman fluorimeter equipped with a meter multiplier and Hewlett-Packard Model 8 x-y recorder.

Circular Dichroism Spectra were obtained on a Cary Model 61 instrument. The molar ellipicity [θ] at a desired wavelength was determined from the relationship:

Eqn. 16 $$[\theta] = \frac{\theta M}{10 \ell c}$$

where θ = the ellipicity in degrees as measured by the C.D. instrument

M = the gram molecular weight of the sample

ℓ = the cell pathlength in cm.

c = the protein concentration in gm/cm^3

Differential Scanning Calorimetery (DSC) scans were kindly obtained by Dr. Richard M. Epand (Department of Biochemistry) using a Microcal MC-2 Differential Scanning Calorimeter. Samples typically contained 1-2 mg of vacuum dried lipid and suspended in ∿1ml distilled deionized water prior to calorimetric studies. Scan rates of 0.5°C/min. along with timed calibration pulses of 3.62 mcal/min. were used for area analysis and subsequent enthalpy measurements. All samples were scanned from 8-40°C at least twice to ensure that the appearance of the DSC scan did not change over time.

Thin layer chromatography was preformed using silica

gel 60 F_{254} 0.2 mm thick plastic backed plates. Compounds on the plates were revealed by their UV absorption using a mineralight UVSL-25 UV lamp unless otherwise indicated. Silica gel or Saphadex G-25 chromatography were monitored using a Biorad Model 1300 U.V. monitor and sensor (unless otherwise noted) and fractions collected using a Gilson microfractionator.

Gas chromatographic (G.C.) analysis were performed using a Varian 6,000 G.C. equipped with Vista 402 computer and printer. Samples (~2μl) were injected into an O.V. 18 (8 ft X 2 mm I.D.) using nitrogen as a carrier gas (25 ml/min.). Temperature gradient runs from 100-310°C over 30 minutes as well as isothermal runs at 170°C were performed. Protein solutions were concentrated using Amicon ultra filtration apparatus (50 ml or 1l, with the permission of L. Berry or M. Hatton, Department of Pathology) equipped with UM-10 membranes.

4.2 The Synthesis of FEM and FEM-d_2

The general scheme for the synthesis of FEM and FEM-d_2 is shown in Figure 53. All relevant data for both maleimides including the intermediate maleamic acids is given in Table 17.

4.2.1 N-2,2,2-Trifluoromaleamic Acid, 21a

Lithium aluminum hydirde (LAH, Aldrich, 2 gm, 47.5mMoles) was placed in an oven dried 500 ml 3 neck round bottom flask equipped with condenser, magnetic stirrer bar and drying tube. Anhydrous diethylether (150 ml) was slowly added to the stirring LAH powder while keeping the solution at 0°C with an ice-water bath. An etheral solution of trifluoroacetamide (Aldrich, 5.37 gm, 47.5mMoles) in 50 ml ether was added dropwise to the stirring LAH/ether mixture with the aid of a dropping funnel at a rate of approximately 1 drop/second. After all of the trifluoroacetamide solution had been added, the mixture was allowed to warm up to room temperature and was stirred overnight. The water condenser was then replaced by a dry-ice acetone condenser, the reaction mixture cooled to 0°C with an ice water bath and a 5% NaOH solution was added to the reaction mixture dropwise with a syringe until no further effervescence occurred and a white granular precipitate remained. The resultant slurry was then poured into a 500 ml round bottom flask and the volatiles removed by vacuum transfer to a clean vessel. The distillate

Figure 53

Synthesis of FEM and FEM-d2

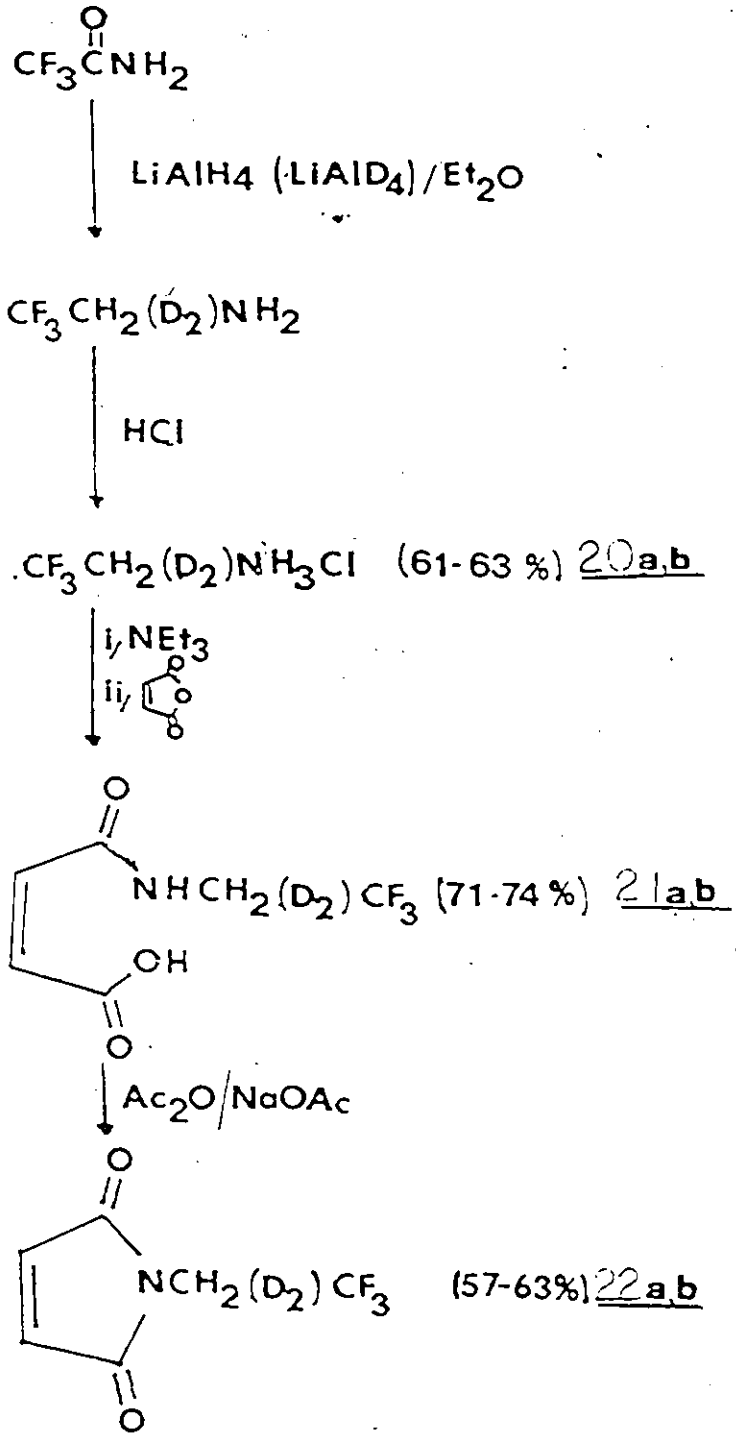

Table 17 Data for FEM, FEM-d_2 and Their Precursors

Compound	Yield	m.p. °C	b.p.	^{1}H-nmr(δ) (acetone d_6)(ppm)	^{19}F-nmr(δ) ($CDCl_3$)(ppm)	^{13}C-nmr (δ) (acetone d_6)(ppm)
21a 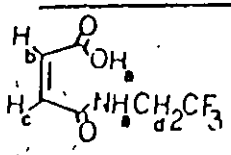	4.23gm 74%	107-108		6.10(dd, $^3J_{HH}$=11.2Hz,b,c) 4.21(q, $^3J_{HF}$=8.8Hz,d) 10.2(broad s, 2H)	-71.42 t, $^3J_{H-F}$=8.02Hz	174.3.(COOH), 168.4 (CONH) 154 (CH adjacent to COOH) 148.2 (CH adjacent to CONH) 122.2 (q, CF_3, $^1J_{C-F}$=-289.24Hz) 38.7 (q, CH_2 $^2J_{C-F}$= 23.6Hz)
22a 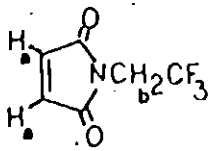	2.35gm 62.6%	59-61		($CDCl_3$) 7.10(s,2Ha) 4.12(q, $^3J_{HF}$=8.82Hz,b)	($CDCl_3$) -70.69 t, $^3J_{HF}$=8.81Hz	($CDCl_3$) 168.7 (C=O) 134.3 (C=C) 122.8 (q, CF_3, $^1J_{CF}$ = -276.5Hz) 38.4 (q, CH_2, $^2J_{CF}$ = 24.7Hz)
20b $CF_3CD_2NH_3Cl$	2.05gm 76%	209-210			(D_2O) -71.821	123.1 (q, $^1J_{CF}$ = -287Hz) 37.5 (CD_2)
21b 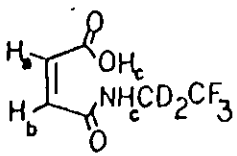	4.10gm 71.1%	108-109		(acetone d_6) 6.1 (dd, $^3J_{HH}$=11.0Hz,a,b) 10.10(broads, 2H, c)	($CDCl_3$) -71.41	174.3 (COOH), 168.2 (CONH) 154.1 (CH adjacent to COOH) 149.2 (CH adjacent to CONH) 122.4 (q, CF_3, $^1J_{CF}$ = -289.2Hz) 38.4 (CD_2)
22b 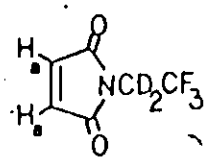	2 gm 57.2%	58-59		($CDCl_3$) 7.12 (s,a)	($CDCl_3$) -70.82	168.73 (C=O) 134.3 (C=C) 122.8 (q, CF_3, $^1J_{C-F}$ = -279.3) 39.0 (CD_2)

Table 17 Continued

Compound	^{1}H-nmr (δ)ppm	I.R. (KBr pellet)	LRMS	HRMS
21a 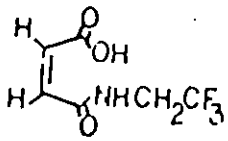		3000 (sf -OH str.) 1770 & 1720 (ss-Amide I and II bands) 1690 (ms, C=O str, COOH) 1440 (ss, C=C, stretch) 1340 1263 (ms, C-F, str.)	m/z (rel. intensity) 197 (M^+, 8.5) 153 (197-CO_2, 29) 128 (197-CF_3, 27) 99 (197-$NHCH_2CF_3$,100)	Calc. for M^+ = 197.0278 Obs. 197.0297
22a 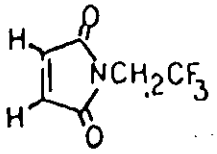		1745(w) & 1729(ss) (Imide I and II bands) 1402 (ms, C=C str.) 1340 & 1263 (ms, C-F, str)	179 (M^+, 15) 110 (179-CF_3,100)	Calc. for M^+, 179.0279 Obs. 179.0270
20b $CF_3CD_2NH_3Cl$	1.21	2421 (N-H str.) 1340 1263 (ms, C-F str.)		
21b 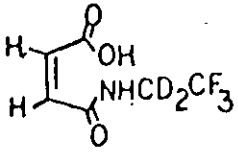	Acetone d_6	3000 (sb, OH str.) 1770 1720 (ss, amide I and II) 1690 (ss, C=O str, COOH) 1443 (ss, C=C, str.) 1340 1263 (ms, CF, str.)	199 (M^+, 9) 182 (199-OH, 35) 155 (199-CO_2, 30) 99 (199-$NHCD_2CF_3$,100)	Calc. for M^+, 199.1342 Obs. 199.1307
22b 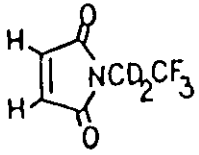	($CDCl_3$) 4.08	1745( ) (Imide I and 1732(ss) II bonds) 1404 (ms, C=C, str.) 1342 1262 (ms, C-F, str.)	181 (M^+, 18) 112 (181-CF_3, 100)	Calc. for M^+ 181.0336 Obs. 181.0367

was allowed to warm to ∿ 5°C, dried over Na_2SO_4, and saturated with HCl gas until no further precipitation occurred. N-2,2,2-trifluoroethylamine hydrochloride 20 was filtered and dried over P_2O_5 *in vacuo* until no decrease in weight was observed. The hydrochloride salt 20a was then sublimed onto an ice-water cold-finger at 0.1 mm using a 100°C oil bath, to yield 4.05gm (30mMoles, 62.1%) of white crystals m.p. 218-220°C, lit. 220-222°C); 90MHz ^{1}H-NMR (D_2O) δ 4.20 (q, J^3_{H-F} = 8.80 Hz). 2,2,2-trifluoroethylammoniumchloride (20a) (4.00gm, 29.5mMoles) was placed in a dry 300ml round bottom flask equipped with magnetic stirrer bar, condenser and drying tube. $CHCl_3$ (75ml) was added and the stirring mixture cooled to 0°C in an ice-water bath. Triethylamine (4.1ml, 1equiv.) which had previously been dried over $LiAlH_4$ was added slowly to the stirring mixture and the solution allowed to warm up to room temperature and stirred for a further half hour. The mixture was then poured into a clean dry 250ml round bottom flask and the volatiles collected by vacuum transfer. A 60 MHz ^{1}H-NMR spectrum (D_2O) of the remaining solid residue showed that it was indeed triethylammonium hydrochloride (δ 1.31t, 3.22q with a rel. ratio of 3:2). The distillate was allowed to warm up to ∿ 5°C, dried over Na_2SO_4 and transferred to a 250ml 3-neck round bottom flask equipped with condenser, magnetic stirrer bar and

drying tube and the solution colled to ∿ $0^{o}C$ in an ice-water bath. A solution of maleic anhydride (2.8gm, 28.6 mMoles, 0.98 equiv.) was added dropwise to the stirred amine solution via the dropping funnel. A white, floculant precipitate formed immediately; after all of the maleic anhydride had been added, the mixture was allowed to stir for a further three hours at room temperature. The precipitate was then filtered, washed with a minimal volume of cold ether (∿2ml) and dried in vacuo over P_2O_5. The N-2,2,2-trifluoromaleamic acid 21a was then sublimed onto an ice-water cold finger at $80^{o}C$ at 0.2mm affording 4.23gm of a white solid. (Yield = 74%).

4.2.2 N-2,2,2-Trifluoroethylmaleimide (FEM), 22a

A dry 50ml 3-neck round bottom flask equipped with condenser, drying tube and magnetic stirrer bar was charged with the above maleamic acid (21a). After the addition of flame-dried sodium acetate (1.88gm, 1 equiv.) and acetic anhydride the mixture was heated in an $85^{o}C$ oil bath for 45 minutes with stirring and then allowed to cool to room temperature. After the addition of the pale brown reaction mixture to an ice cold 100mM sodium phosphate buffer (pH 7.4, 180ml) the mixture was stirred vigorously for 10 minutes, resulting in the separation of a pale brown solid. The aqueous mixture was then extracted with chloroform (3 X 180ml)

and the combined chloroform extracts washed with saturated brine (2 X 200 ml). The chloroform layer was then dried over Na_2SO_4, and evaporated under reduced pressure to afford a light brown crystalline solid. The crude material was sublimed twice at 55°C onto an ice-water cold finger condenser at 0.1mm to yield FEM 22a as a white crystalline solid (2.35gm, 62.6% yield).

4.2.3 FEM-d_2,22b

The synthesis of FEM-d_2 was carried out in the same way as that of FEM except that lithium aluminum deuteride (LAD, Merck, Sharp and Dohme 1.9 gm) was used to reduce trifluoro acetamide (5.2 gm, mMoles) to 2,2,2-trifluoro-1,1-dideuteroethylamine. The yields and physical data for 2,2,2-trifluoro-1,1-dideuteroethylammonium chloride(20b) N-2,2,2-trifluoro-1,1-dideuteroethylmaleiamic acid (21b) and N-2,2,2-trifluoro-1,1-dideuteroethylmaleimide (FEM-d_2) (22b) are given in Table 17.

4.3 Kinetics of the Reaction of Low Molecular Weight Thiols with FEM

Kinetic studies were performed under pseudo-first order conditions where the thiol concentrations were usually 25-fold greater than FEM. The thiols reacted with FEM were β-mercaptoethanol, L-cysteine, N-acetyl-L-cysteine and glutathione.

4.3.1 pH Dependance of k_{obs} at 30.0°C

The general procedure for the preparation of the thiol solutions was as follows: Dibasic sodium phosphate, NaH_2PO_4 and thiol stock solutions were prepared by dissolving the appropriate amount of each so that phosphate and thiol concentrations, after aliquots were withdrawn and adjusted to the appropriate pH and volume, were 100 and 26mM, respectively. FEM solutions (~ 1mM) were prepared by dissolving ~ 9 mg of the maleimide in 50ml distilled water. The concentrations of FEM solutions were determined exactly by taking absorbance readings at 276nm (ε=476$M^{-1}cm^{-1}$). In order to determine the pH of the actual reaction mixture being observed by the stopped flow technique, the pH of solutions containing an equivalent volume thiol solution and/or an equivalent volume of borate buffer or H_2O were monitored. It was found that pHs of these mixtures did not differ nor did they change on going from room temperature

($25^{o}C$) to $30^{o}C$. Prior to beginning the stopped flow experiments FEM and thiol solutions were degassed both by stirring under reduced pressure using a water aspirator and bubbling thoroughly with nitrogen gas. This ensured that oxidation of the sulfhydryl groups to disulfides was much less likely. No fewer than 10 k_{obs} values were determined per pH value studied. The average values of k_{obs} ($\bar{k}_{obs}$) and $t_{\frac{1}{2}}$ ($\bar{t}_{\frac{1}{2}}$) $\pm$ 1 standard deviation (S.D.) for each thiol/pH studied were calculated.

4.3.2 Determination of kapp at pH 6.65

The general procedure for the preparation of thiol solutions was as follows: varying amounts of thiol and a constant amount of NaH_2PO_4 were dissolved in 20ml H_2O and adjusted to pH 6.50. The final volume was then adjusted to 25ml to afford a final phosphate concentration for 100mM. When aliquots (1ml) of thiol solutions at pH 6.50 and FEM solutions (1mM) were mixed with the phosphate buffer or 1ml H_2O, the pH of both mixtures were found to be 6.65 ($\pm$.02). Thus all determinations are reported for pH 6.65. All thiol and FEM solutions were degassed as described in part 4.3.1. No fewer than 10 k_{obs} values were determined for each set of conditions.

4.3.3 Determination of Apparent Activation Parameters for the Reaction of FEM with Thiols at pH 6.65

Stock solutions of 100mM NaH_2PO_4 and 26mM thiol were prepared and degassed as described above. The pH of the thiol stock solutions when diluted by a half with water or with 1mM FEM were found to independent of temperature over the temperature range used in these experiments. Temperatures were controlled to $\pm$ 0.1^{o}C. The errors were determined using a propagation of errors analysis.[221]

4.3.4 Kinetic Study of FEM Hydrolysis at 30.0^{o}

To ensure that FEM hydrolysis was being observed in the pH range studied, approximately 7mg of FEM was dissolved in 5ml 100mM pH 10.0 borate buffer and allowed to stir for 20 minutes. The solution was then acidified to pH 2.0 with 10% HCl and an aliquot chromatographed on a silica gel thin layer chromatography plate along with authentic samples of FEM 22a and N-2,2,2-trifluoroethylmaleamic acid 21a (TLC solvent: 30% MeOH/$CHCl_3$ containing 1.5 drops/ml of acetic acid). The TLC plate showed one spot by U.V. corresponding to N-2,2,2-trifluoroethylmaleamic acid. The kinetic studies were performed as follows: Boric acid (4.37gm, 70.6mMoles) was dissolved in H_2O (120ml) and six 20ml aliquots withdrawn. Each aliquot was adjusted to the desired pH with NaOH and the final volume adjusted to 25ml

with H_2O. The pHs of these solutions were checked after standardization of the pH meter with a standard pH 10.00 ($\pm$ .01) buffer. The final concentration of the borate buffers was 500mM. FEM solutions (1mM) were prepared by dissolving ~ 9mg of the maleimide in 50ml distilled water. The concentrations of the FEM solutions were determined exactly by taking absorbance readings at 276mm (ε = 476 $M^{-1}cm^{-1}$). The pH of solutions containing i/ an equivalent volume of borate buffer and FEM and ii/ an equivalent volume of borate buffer of H_2O were monitored. It was found that the pHs of these mixtures did not differ nor did they change on going from room temperature (25°C) to 30°C. Both the FEM and borate buffer solutions were degassed under reduced pressure with the aid of a water aspirator prior to loading into the syringes of the stopped-flow instrument. No fewer than five (k_{obs}) determinations were carried out per pH value studied. Average k_{obs} and half-life $t_{\frac{1}{2}}$ values $\pm$ 1 S.D. were calculated for each pH studied.

4.3.5 Kinetic Study of the Reaction of FEM with L-Lysine. L-Histidine and L-Serine

L-Lysine

Boric acid (4.367gm, 70.2mMoles) and L-lysine·HCL (0.822gm, 4.51mMoles) were dissolved in 120ml H_2O. Aliquots (4 X 20ml) were withdrawn and adjusted to the desired pH using

1M NaOH. The borate-lysine solutions were adjusted to a final concentration of borate and L-lysine were 500 and 30mM respectively. The actual pH determination of mixture observed by the stopped-flow technique as well as the preparation of FEM solutions and subsequent degassing were performed as described in 4.2.1.

L-Histidine and L-Serine

The procedure used was identical to that described for L-lysine only that 0.86gm, (4.50mMoles) L-histidine·HCl or .62gm (4.50mMoles) L-serine·HCl were used.

4.4 Characterization of FEM-Thiol Adducts

The adducts of glutathione, L-cysteine and N-acetyl-L-cysteineconsist of mixtures of diasteriomers whereas the β-mercaptethanol adduct is racemic. No attempts were made to separate the diastereomeric products. Due to the complexity of the ^{1}H-NMR spectra of these adducts, all ^{1}H-NMR data is presented separately in Table 18. For all FEM-thiol adducts, 2-D J-correlated (COSY) spectra were obtained at 250MHz in order to aid in the spectral assignments. The following parameters were used in the 2D NMR spectra: 4K data points in the t_2 dimension, 200 acquisitions in the t_1 dimension with a resolution of 4 Hz/data point and 16 Hz/data point for the observed transform of a 2K X 512 matrix. Spectra were subsequently simulated using an ITRCAL and

Spectral addition (SA) program on a Nicolet 1180 FTIR instrument with RMS errors no greater than 0.26%. It is important to note that the resonances are not assigned to a specific stereoisomer but are designated as a,b,c... or a', b',c'... to denote different sets of coupled nuclei. Preparations and characterizations of FEM-thiol adducts are given in the following subsections. All other data for each adduct is reported in Table 19.

L-cysteine-FEM Adduct , 23

L-cysteine (13.5mg, 0.11mMoles) was dissolved in distilled, deionized and degassed water resulting in a pH 3.0 solution. A constant stream of N_2 bubbles was maintained through the thiol solution and a solution of FEM (20mg, equiv) in 0.5ml acetone added. The solution was stirred for 5 hours during which small aliquots were spotted on a TLC plate (along with L-cysteine and FEM) and chromatographed using n-butanol/acetic acid/H_2O = 80/20/20 (v/v/v); the TLC plates were visualized using either I_2 vapor or nitroprusside spray. When there appeared to be no evidence for starting materials, the aqueous solvent of the reaction mixture was removed under vacuum. The resulting white solid was recrystallized in a minimal volume of acetone/H_2O = 1/1 (v/v) to yield 23.4mg of a white crystalline solid, m.p. 192 dec. 90MHz ^{1}H-NMR of recrystallized and crude material appeared identical to that

Table 18: ^{1}H-nmr data for FEM-thiol adducts (D_2O)

L-cysteine adduct 23

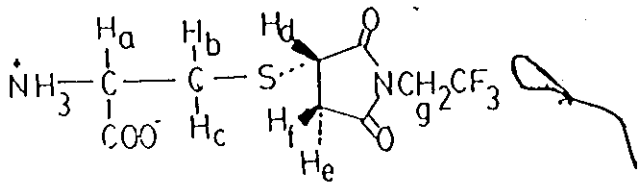

Proton	Chemical Shift(ppm)	Coupling Constant(Hz)
Ha	4.24	$J_{a,b} = J_{a,c} = 5.78$
Hb, Hc	3.53	
Hd	4.16	$J_{d,e} = 7.84$
Hc	3.63	$J_{e,f} = 14.66$
		$J_{e',d} = 7.84$
Hf	3.35	$J_{e,f} = 14.66$
		$J_{d,f} = 4.31$
Hg	4.48	$^3J_{H-F} = 8.85$

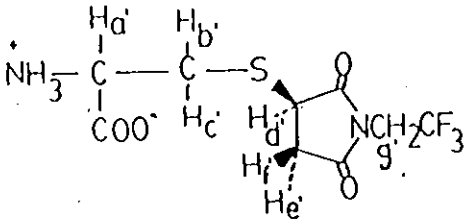

Ha'	4.24	$J_{a',b'} = J_{a',c'} = 5.78$
Hb', Hc'	3.53	
Hd'	3.57	$J_{d',e'} = 4.20$
		$J_{d',f'} = 8.09$
He'	3.57	$J_{d',e'} = 4.20$
		$J_{e',f'} = 19.05$
Hf'	2.98	
		$J_{f',d'} = 8.04$
Hg'	4.15	$^3J_{H-F} = 8.85$

N-acetyl-L-cysteine adduct 25

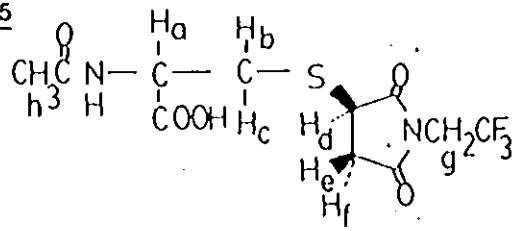

Proton	Chemical Shift(ppm)	Coupling Constant(Hz)
Ha	4.72	$J_{a,b} = 5.51$
		$J_{a,c} = 6.38$
Hb	3.27	$J_{b,c} = 14.16$
Hc	3.31	
Hd	4.24	$J_{d,e} = 3.93$
		$J_{d,f} = 8.55$
He	3.43	$J_{e,f} = 18.47$
Hf	2.67	
Hg	4.18	$^3J_{H-F} = 8.02$
Hh	2.07	

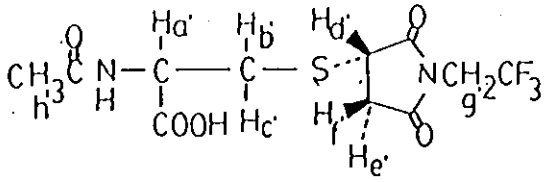

Ha'	4.72	$J_{a',b'} = 4.36$
		$J_{a',c'} = 8.43$
Hb'	3.03	$J_{b',c'} = 13.9$
Hc'	3.53	
Hd'	4.24	$J_{d',e'} = 4.12$
		$J_{d',f'} = 8.74$
He',	2.61	$J_{e',f'} = 18.48$
Hf'	3.38	
Hg'	4.31(t)	$^3J_{HF} = 8.86$Hz
Hh'	2.07(s)	

Table 18: Continued

Glutathione-FEM Adduct 24

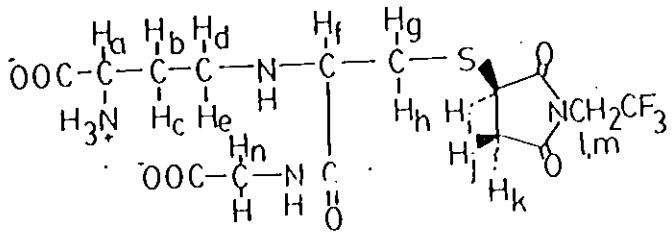

Proton	Chemical Shift(ppm)	Coupling Constant(Hz)
Ha	3.61	$J_{a,b}$ = 7.25 $J_{a,c}$ = 7.25
Hb	2.01	$J_{b,d}=J_{c,d}$=7.12Hz=$J_{b,c}$
Hc	1.99	
Hd	2.38	
He	2.37	
Hf	4.53	$J_{f,g}$ = 5.18 $J_{f,h}$ = 8.30
Hg	3.11	$J_{g,h}$ = 14.08
Hh	3.02	
Hi	4.66	$J_{i,k}$ = 7.79 $J_{i,j}$ = 10.19
Hj	2.61	$H_{j,k}$ = 19.08
Hk	3.23	
Hl, Hm	4.23(q)	$^3J_{H-F}$ = 8.87
Hn	3.63	$J_{n,o}$ = 17.00
Ho	3.59	

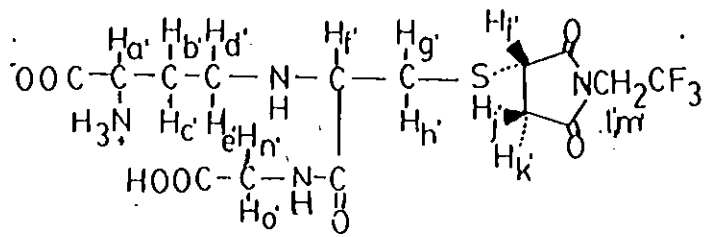

Proton	Chemical Shift(ppm)	Coupling Constant(Hz)
Ha'	3.61	$J_{a',b'}$=$J_{a',c'}$=7.25Hz
Hb'	2.01	$J_{b',d'}$=$J_{b',e'}$ =$J_{c',e'}$=$J_{c',d'}$=7.12Hz
Hc'	1.99	
Hd'	2.38	
He'	2.37	
Hf'	4.53	$J_{f',g'}$ = 9.07 $J_{f',h'}$ = 4.89
Hg'	2.86	$J_{g',h'}$ = 14.10
Hh'	3.24	
Hi'	4.67	$J_{i',k'}$ = 7.79
Hj'	2.61	$J_{i',j'}$ = 10.19 $J_{j',k'}$ = 19.08
Hl', Hm'	4.23(t)	$^3J_{Hf}$ = 8.86
Hn'	3.62	$J_{n',o'}$ = 17.27
Ho'	3.59	

Table 18: Continued

β- Mercaptoethanol adduct 26

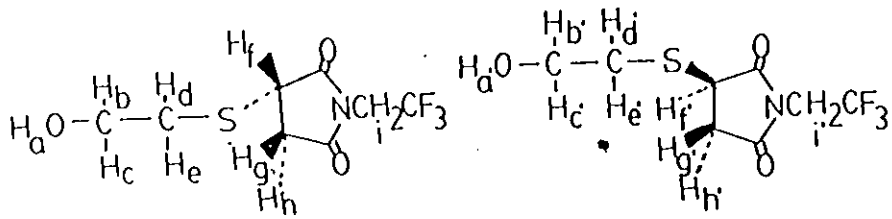

Proton	Chemical Shift(ppm)	Coupling Constant(Hz)
Ha, Ha'	2.36 (broad,s)	
Hb, Hc Hb', Hc'	3.65 3.65	$J_{b,d}=J_{b',d'}=5.02$ $J_{b,c}=J_{b',c'}=5.97$ $J_{c,e}=J_{c',e'}=6.10$ $J_{c,d}=J_{c',d'}=5.15$
Hd, Hd'	2.91	
He, He'	2.64	$J_{e,d}=J_{e',d'}=14.58$
Hf, Hf'	3.74	$J_{f,g}=J_{f',g'}=3.92$ $J_{f,h}=J_{f',h'}=39.37$
Hg, Hg'	3.02	
Hi, Hi'	4.21(t)	$^3J_{H,F}=8.87$

Table 19: Data for FEM-thiol Adducts

Compound	Yield	m.p.	b.p.	^{1}H-nmr	^{19}F-nmr (δ) (D_2O) (ppm)	^{13}C-nmr (δ) (D_2O) (ppm)
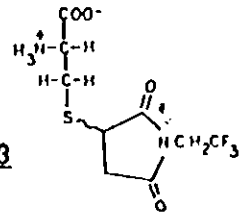 **23**	23.4 mg (70.1%)	192 dec.			-69.71 (t, $^3J_{HF}$=8.82Hz)	183.6, 183.0, 123 (q, CH_3, $^1J_{CF}$=-279.3Hz) 63.86, 59.44, 43.62, 41.43, 40.91, 38.28 (q, CH_2-CF_3), $^2J_{C-F}$=24.6Hz, 37.25, 32.03, 29.16
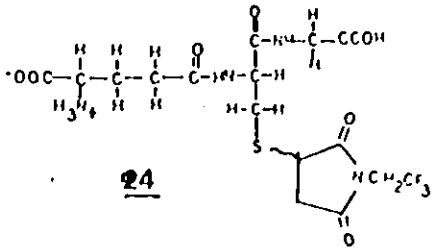 **24**	31.6mg (68%)	190 dec.			-69.71 (t, $^3J_{HF}$=8.87Hz)	174.07, 173.81, 171.70, 169.17, 168.87, 168.71, 123.21 (q, CF_3, $^1J_{CF}$=285.21Hz) 52.71, 52.57, 50.63, 50.01, 49.92, 38.73, 38.06, (q, CH_2CF_3, $^3J_{CF}$=25.2Hz), 37.62, 37.56, 34.41, 34.31, 34.02, 33.40, 26.34, 22.05
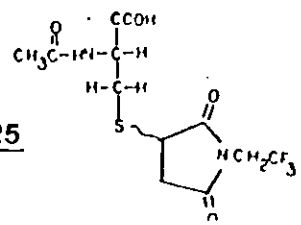 **25**	35.8mg (65%)	220 dec.			-69.69 (t, $^3J_{HF}$=8.85Hz)	166.21, 165.11, 164.01, 161.88, 161.55, 122.3 (q, CF_3, $^1J_{CF}$=282.3Hz) 44.48, 43.79, 43.41, 42.98, 38.26, (q, CH_2-CF_3, $^3J_{CF}$=26.2Hz), 28.97, 23.06, 22.89, 22.53, 21.71.
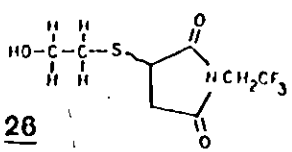 **26**	23 mg (61.2%)	62-63			-69.70 (t, $^3J_{HF}$=8.81Hz)	175.6 172.71 123.11 (q, CF_3, $^1J_{CF}$=279.11Hz), 61.65 (H-OH-CH_2) 40.40 (q, CH_2-CF_3, $^3J_{CF}$=26.6Hz) 39.41, 39.31, 36.04, 35.04.

Table 19 : Continued

Compound	I.R. (cm^{-1})	LRMS	HRMS	Elemental Analysis
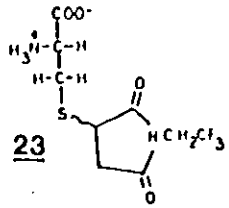 **23**	(KBr pellet) 3,000 (sb, OH str) 1792(vs) (lmide I and II 1720(s) (bands) 1602 (s, C=O str, acid) 1260 (ms, CF str.) 1130	300 (M^+, 8) 282 (300-NH_4^+, 28) 255 (300-CO_2H, 12.5) 213 (282-CF_3, 53.2) 110 (300-$(NH_3)^+CH(COO^-)$ CH_2) (100)	Calc. for M^+ 300.0415 Obs. 300.0392 Calc. for M^+-NH_4^+ 282.0042 Obs. 282.0055	
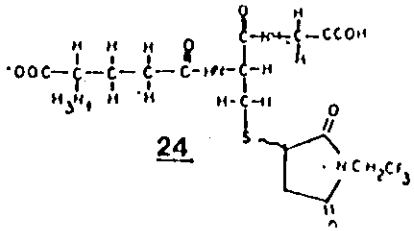 **24**	(KBr pellet) 3003 (sb, OH str.) 2960 (w, NH str.) 1792(vs) (lmide I and II) 1718(s) 1760(ms) (CF str.) 1130			Calculated for $C_{16}H_{21}N_4O_8SF_3$ C=39.57, H=4.32, N=11.52 Found: C=39.71, H=4.54,
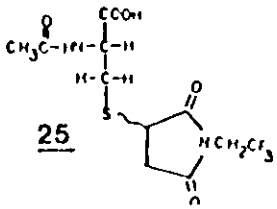 **25**	(KBr pellet) 3000 (s.b, OH str.) 1792(S) lmide I and II 1718(s) 1680 (ms, C str, amide) 1621 (ms, C str. acid) 1260 (m, CF, str.) 1130	3421 (M^+, 5) 298 (341-$C(=O)CH_3$, 25.2) 272 (341-CF_3, 60.1)	Calc. for M^+ 341.2143 Obs. 341.2097 Calc. for M^+-$C(=O)CH_3$, 298.3841 Obs. 298.3800	
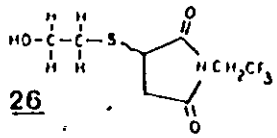 **26**	($CDCl_3$) 1790 (w) (lmide I and II, 1729 (s) bonds, C-O str.) 1260 (m.s, CF, str.) 1130	257 (M^+, 5.2) 239 (257-H_2O, 68.2) 237 (257-CH_2O-H, 21.2) 161 (227-CH_2S, 100)	Calc for M^+, 257.0333, M^+-H_2O 239.0228 Obs. 257.0345, 239.0220	

of the crude product.

Glutathione(24) and N-acetyl-L-cysteine FEM (25) adducts were prepared and purified in the same way except in the case of N-acetyl-L-cysteine where $CHCl_3$/MeOH = (1/1. v/v) was used as the recrystallization solvent.

β-Mercaptoethanol-FEM Adduct 26

A pH 6.65 1.28mM solution of β-ME (100ml) was reacted with FEM for 10 min. under N_2 atmosphere. The solution was then extracted with $CHCl_3$ (10ml, 3X) and the combined chloroform extracts dried over anhydrous Na_2SO_4 (∿ 1gm). The organic solvent was then removed under reduced pressure and resultant colourless oil chromatographed on a Merck Size B silica gel column using 5% MeOH/$CHCl_3$ as the eluting solvent. The progress of the chromatography was monitored using a Biorad Model 1300 U.V. monitor and sensor and fractions collected using a Gilson microfractionator. Fractions containing the desired adduct were combined and the organic solvent removed under reduced pressure. The oil crystallized to a white solid on cooling. Yield 23mg (61.2%) m.p. 62-63°C ^{1}H-NMR - see Table 18.

4.5 Purification of Defatted Mercaptalbumin Monomer

Fraction V BSA (6gm, Sigma Lot #1276-064) was charcoal defatted according to the procedure of Chen.[207] The protein (6gm) was dissolved in 60ml distilled deionized and degassed

water and with 6gm of activated charcoal. The pH of the solution was lowered to 3.0 with 0.1M HCl and the mixture stirred in an ice water bath for 1 hour under N_2 atmosphere. The solution was quickly filtered through a celite bed under N_2 pressure, made 50mM in sodium phosphate and adjusted to pH 7.0 with 1N NaOH. The protein solution was then filtered and loaded onto a DEAE-Sephadex A-50 solumn (48 X 3.31cm) containing gel which had been previously equilibrated in pH 7.0, 50mM sodium phosphate buffer for 24 hours at $4^{o}C$ prior to packing of the column. A linear phosphate gradient elution was performed according to the procedure of Janatova.[141]

Two sodium phosphate solutions (1570ml 50mM and 1570ml 125mM phosphate) were used to generate the desired linear gradient (2.5×10^{-5}M/ml). Fractions (8ml) were collected using a Gilson microfractionator and a constant flow rate of $\approx$ 30ml/hour was maintained using a column head height of $\approx$ 2.5ft. Optical density (O.D.) measurements at 279nm were performed on every fifth fraction. A typical plot of $O.D._{280}$ vs. Tube # is shown in Figure 54 Sulfhydryl assays on the fractions were performed using Ellman's reagent,5,5'-Dithiobis(2-nitrobenzoic acid)(DTNB).[208] To 0.5ml of protein solution and 0.5ml 4mM DTNB - 3.0ml pH 8.00, 500mM sodium phosphate - 2M Urea buffer and taking $O.D._{412}$ measurements of the above mixture subsequent to using the appropriate

Figure 54

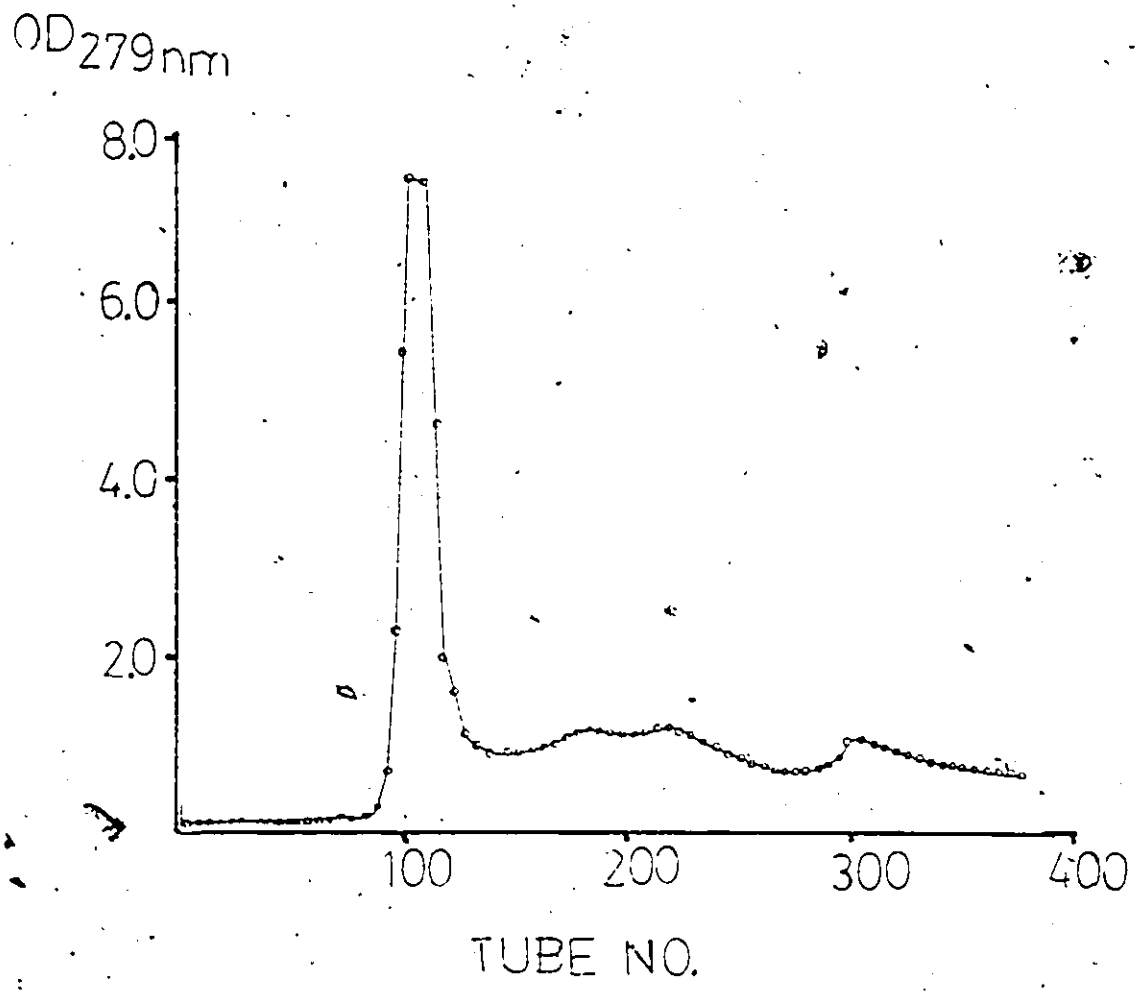

Chromatogram of purification of defatted fraction I BSA on DEAE-Sephadex A-50 (48cm long, 3.31cm diameter). Column eluted with sodium phosphate gradient 2.5×10^{-5}M/ml. Fraction volume, 8ml

reference solution(0.5ml 4mM DTNB + 3.5ml pH 8.00, 500mM sodium phosphate-2M Urea buffer). An extinction coefficient of 13,600 $M^{-1}cm^{-1}$ was used for the TNB anion. These measurements were performed in triplicate and SH assays were reproducible within an error of ± 1%. Fractions corresponding to high sulfhydryl content (~80%)(Fig 57 Tube #95-125) were pooled, made 50mM in sodium thioglycolate and adjusted to pH 5.60. After 24 hours, 3ml of the BSA/thioglycolate and chromatographed on a 20 X 1.7cm Sephadex G-25 column using a degassed pH 6.5 50mM sodium phosphate. The progress of the chromatography was monitored using a Bio-Rad 1300 model flow cell and a U.V. sensor. Protein concentrations in protein-containing fractions were detemined at 279nm (1cm pathlength cell, $\varepsilon = 4.37 \times 10^{-4} M^{-1} cm^{-1}$); thiol concentrations were determined using the method of Ellman. The thioglycolate-reduced protein fractions were found to have 0.98 (± 0.01)mole SH per mole protein. Prior to labelling the BSA sulfhydryl group, the BSA/thioglycolate solutions were concentrated to approximately 10ml using both a 1ℓ and 50ml Amicon Ultrafiltration apparatus fitted with UM-10 membranes as a final protein concentration of about 64 mg/ml.

4.5.1 Preparation of BSA-FEM-d_2

The BSA-thioglycolate concentrate above was chromatographed on a 81 X 2.55cm Sephadex G-25 column using a pH 6.5, 50mM sodium phosphate buffer and column head height

of ∿ 1 meter. A constant stream of N_2 bubbles was maintained in the main solvent reservoir to ensure that no oxidation of mercaptalbumin took place on the column. SH analyses were performed in duplicate on every third fraction collected and the SH contents found to be 98(± 1%). FEM-d_2 (20mg, 0.11mmoles) was dissolved in the mercaptalbunin solution and the mixture stirred in an N_2 atmosphere for approximately 20 minutes. The pH of the solution was brought-down to 3.30 by the dropwise addition of 0.1M HCl and a 5ml aliquot chromatographed on a Sephadex G-25 column (20 X 1.5cm). Sulfhydryl assays on the isolated protein fractions showed the absence of any protein sulfhydryl group. The remaining BSA/FEM-d_2 solution was dialyzed against 2ℓ of pH 3.00 50mM sodium phosphate 0.1M KCl buffer for 48hr. at 2°C. After dialysis, the BSA-FEM-d_2 solution was concentrated by ultrafiltration to ∿ 10ml where an $O.D._{279}$ reading of a 100-fold diluted sample of the modified protein gave a concentration of 1.17 mM. It was found that BSA-FEM-d_2 could not be concentrated beyond 1.17mM at pH 3.00 without gelation and/or precipitation of the protein.

4.5.2 Preparation of Acetamide-BSA

A sample of mercaptalbumin prepared by the method described in Section 4.5 was treated with a 10-fold excess of iodoacetamide a pH 7.00 for 1 hour under the conditions

where the SH group is modified exclusively. A 3ml sample of this solution was chromatographed on a small Sephadex G-25 column (25 X 1.7cm) and the isolated protein fractions assayed for sulfhydryl content using DTNB. No remaining free sulfhydryl groups were found. The remaining BSA-Iodoacetamide sample was dialyzed against 2? pH 3.65 50mM sodium phosphate-0.1M KCl buffer for 48hr. at 2°C. The protein solution was then concentrated to ∿ 1.1mM by ultrafiltration.

4.5.3 Preparation of BSA-TFP

Mercaptalbumin monomer was prepared as described previously (4.3). On isolation of the thioglycolate reduced BSA monomer, the protein solution (.15mM) was adjusted to pH 7.00 and treated with 1-bromo-3,3,3-trifluoropropanone (Br-TFP, Aldrich) (100ul, 3x excess) for 1hr. as described by the method of Zurawski.[120] A 5ml aliquot of the reaction mixture was chromatographed on a Sephadex G-25 column (20 X 1.5cm); sulfhydryl assays of the protein fractions revealed the absence of protein sulfhydryl groups. A second sample of BSA-TFP was prepared using different conditions for the reaction between BSA and Br-TFP; 20 min at pH 6.50. Again, sulfhydryl assays on a chromatographed aliquot of the reaction mixture revealed the absence of sulfhydryl groups. Both BSA/Br-TFP solutions were dialyzed against 2? pH 3.00 50mM Sodium phosphate -0.1M KCl buffer for 48 hours at 2°C. The protein

solutions were then concentrated by ultrafiltration to a final concentration of $\approx$ 1mM.

4.5.4 Treatment of BSA-FEM-d_2 with trifluoropropanone

A 10ml 1mM BSA-FEM-d_2 solution was treated with a 3-fold excess of Br-TFP (150ul) at pH 7.00 for 1 hr. The pH of the solution was adjusted to 3.00 using 0.1M HCl and subsequently dialyzed against 2ℓ pH 3.00 50mM sodium phosphate -0.1M KCl for 48hr. The protein solution was then concentrated to $\approx$ 1mM by ultrafiltration.

4.5.5 Fluorescence Measurements

Protein solutions were prepared by taking 100ul of either ~1.0mM BSA-FEM-d_2, BSA-TFP or freshly prepared mercaptalbumin to 4.0ml of 50mM -0.1M KCl solutions of varying pH. The pH of the protein solutions were noted and the solutions degassed by gently blowing N_2 over the solution surface. All fluorimetric work was performed within 2 hours of the preparation of the protein samples. BSA, BSA-FEM-d_2 and BSA-TFP solutions with an $O.D._{279}$ value of 0.128 at pH 6.0 were found to have the same absolute fluorescence ($\pm$ 2%) at 343mm for the same instrumental sensitivity settings. Also, the absolute fluorescence at 343mm of these same protein solutions diluted by 1/2 and 1/3 were 1/2 and 1/3 respectively at pH 6.0 indicating that fluorescence varied.

linearly with concentration over this concentration range studied. The meter multiplier response at λ emmission = 343 nm was monitored for each protein solution of varying pH and the relative fluorescence 343nm plotted as a function of pH (Figure 28b). The final readings at pHs 5.90, 6.00 and 6.11 were set at 100% and all other readings expressed relative to them. Contributions from the tyrosine fluorescence appear to be neglibible since the measured widths at half-height for all fluorescence spectra at various pHs remain the same. No corrections were made for light scattering.

4.5.6 Circular Dichroism Spectra

BSA, BSA-FEM-d_2 and BSA-FTP (1mM) solutions were prepared as described in parts 4.3, 4.3.1, and 4.3.3. 100ul of protein solution was added to 4ml of 0.1M KCl solutions of varying pH and the protein concentrations determined by $O.D._{279}$ measurements. $[\theta]_{269}$ values were obtained from the difference of the measured ellipicity θ from plots of θ_{269} vs wavelength (λ) from 320 to 230nm for 0.1M KCl and protein solutions and converted to $[\theta]_{262}$ values. 1cm pathlength cells were used. The errors in these measurements are assumed to be + the pen deflection (noise) in θ vs λ plots. Measurements below 230nm were not possible due to the inherent baseline instability of the instrument.

4.5.7 84.66 and 235.36 MHz ^{19}F-NMR Spectra

BSA-FEM-d_2 or BSA-TFP solutions (~2ml) were placed in a 10mm O.D. NMR tube and the pH of the protein solution adjusted as desired by adding 1M NaOH or 1M HCl dropwise. ^{19}F-NMR spectra were processed and recorded after approximately 8,000 acquisitions. Signal-to-noise ratios of the largest peaks in the spectra varied between 16:1 and 23:1.

4.6 Synthesis of Monofluoro, Monodeutero DMPC's

4.6.1. Monoethyl Acid Esters (10a-c)

All monoethyl acid esters were synthesized according to the procedure of Jones et al.[206] The synthesis of monoethylsuccinate, 10a, is typical and is described below. All spectral data for the monoacid esters 10a-c is given in Table 20.

Monoethylsuccinate 10a

Succinic acid (Aldrich, 40gm, 0.34moles), diethyl succinate (Aldrich, 34.4gm, 0.17moles), di-n-butyl ether (16ml) and concentrated HCl (8.4ml) were refluxed for 0.5hr. in a 250ml round bottom flask fitted with condenser and drying tube. Ethanol (95%, 8.4ml) was added through the top of the condenser and the mixture refluxed for a further 2hr. After a second addition of 95% ethanol (6.8ml) the mixture was refluxed for 15 hrs, then allowed to cool to room temperature. The reaction mixture was then placed in a 65°C oil bath and a vacuum distillation performed using aspirator pressure to remove dibutylether, ethanol and water. On cooling to room temperature the mixture was poured into 300ml of diethyl ether and allowed to stand for 1hr. The precipitated succinic acid (~7gm) was removed by filtration, the ethereal solution extracted with sodium bicarbonate (0.4M, 400ml, 3x) and the washings combined and acidified with HCl.

Table 20: Data for monoethyl acid esters

Compound	Yield	m.p.	b.p.°C	^{1}H-nmr (δ) (ppm)	I.R. (cm^{-1}) ($CHCl_3$)	m/z (rel. intensity)
$CH_3CH_2O\overset{O}{\overset{\|\|}{C}}(CH_2)_2\overset{O}{\overset{\|\|}{C}}OH$ (d, c, b, a) **10a**	26.7gm 55%		87-90°C at 0.5mm litt. pb. corrected +00.5mm=94°C	10.1 (s, 1H, a) 4.10(q, $^3J_{HH}$=8.9Hz, 2H,c) 2.60(s, 4H, b) 1.31(t, $^3J_{HH}$=8.9Hz, 3H,d)	3000(sb,OH str. acid) 1742(ss, C=O str. ester) 1729(ss, C=O str. acid) 1240 (ms, C-O str)	129(M^+-OH, 12) 101(129-CO_2H,100) 73 (129-$COCH_2CH_3$, 19.1)
$CH_3CH_2O\overset{O}{\overset{\|\|}{C}}CH_2(CH_2)_4CH_2\overset{O}{\overset{\|\|}{C}}OH$ (e, d, b, c, b, a) **10b**	32.5gm 56.2%		125-128°C at 0.2mm litt. bp. corrected to .2mm=121°C	11.6(s,1H,a) 4.05(q, $^3J_{HH}$=8.5Hz, 2H,d) 2.32, 2.08 (t, $^3J_{HH}$=7.8Hz, 4H,b) 1.1-2(m,8H,c) 1.23(t, $^3J_{HH}$=8.9Hz, 3H,c)	3000(sb,OH str. acid) 2942(s, CH str) 1742(ss, C=O str. ester) 1712(s, C=O str. acid) 1241(m, C-O str)	185(M^+-OH,2.1) 157(M^+-OCH_2CH_3 or CO_2H, 69) 88($[CH_3COCH_2CH_3]^+$, (McClafferty, 100)
$CH_3CH_2O\overset{O}{\overset{\|\|}{C}}CH_2(CH_2)_8CH_2\overset{O}{\overset{\|\|}{C}}OH$ (e, d, b, c, b, a) **10c**	42gm 50.1%	39-41 litt. 42-43°C	147-151°C at 0.1mm	11.0(s,1H,a) 4.10(q, $^3J_{HH}$=8.7Hz, 2H,d) 2.39, 2.10 (t, $^3J_{HH}$=7.9Hz, 4H,b) 1.20-2.00(m,16H,C) 1.23(t, $^3J_{HH}$=3.7Hz, 3H,e)	3000(sb,OH str. acid) 2940(s, C-H str.) 1245(ss, C=O str. ester) 1712(ss, C=O str. acid) 1242(s, C-O str.)	241(M^+-OH, 7.9) 213(M^+-OCH_2CH_3 or CO_2H, 67) 88($[CH_3COCH_2CH_3]^+$, (McClafferty, 100)

The acidic solution was then extracted with diethyl ether (600ml, 3X) and the combined ether extracts dried over Na_2SO_4 and the ether subsequently removed under reduced pressure. Monoethyl succinate was then purified by fractional distillation in vacuo to yield a single component that distilled at 87-90°C at 0.5mm Hg. Yield = 26.7gm (55%).

Both monoethyl suberate 10b and monoethyl 1,12-didodecanoate 10c were synthesized by the same procedure used to obtain monoethyl succinate with the following modifications: the reaction mixtures were refluxed for 2hr. after the second addition of 95% ethanol. Suberic acid (57.9gm, .33 moles) or 1,12-didodecanoic acid (81.7gm, .35 moles) along with 0.5 equivalents of their corresponding diethyl esters were used in the synthesis of 10b and 10c respectively. The molar ratios of 95% ethanol HCl and di-n-butylether used were the same as for the synthesis of 10a.

4.6.2 Monoethylester Acid Chlorides, 11a-c

Monoethyl esters 10a-c were converted into their corresponding acid chlorides by the same general procedure.[209] These esters 10a-c were each placed in a dry 100ml 3-neck round bottom flask equipped with a condenser. The amounts used were 112gm (.082moles), 17gm (.084moles) and 16.0gm (.062moles) of 10a, b and c respectively. Thionyl chloride (1.2 equiv.) was added and the mixture warmed in a 72°C oil bath for ~ 1 hour. The progress of the reaction was monitored by removing an aliquot (1ml) of the reaction mixture and running a 90 MHz ^{1}H-NMR spectrum. The reaction was judged to be complete when the intensity of the COOH resonance(~11ppm) was constant. Excess thionyl chloride as well as SO_2 and HCl biproducts were removed under reduced pressure using a rotaryevaporator. Acid chlorides 11a-c were purified by fractional distillation *in vacuo*. Data for acid chloride 11a-c is given in Table 21.

Table 21: Data for Monoethyl Ester Acid Chlorides

Compound	Yield	m.p. °C	b.p.	^{1}H-nmr (δ) (Hzeet) (ppm)	I.R. (cm^{-1}) ($CHCl_3$)	LRMS m/z (rel. intensity)
$CH_3CH_2OC(=O)CH_2CH_2C(=O)Cl$ (d, a, c, b) **IIa**	10.2gm 81%		37-40°C litt. bp. corrected to 0.5mm 36°C	4.13(q, $^3J_{HH}$=8.8Hz,2H,a) 3.21(t, $^3J_{HH}$=7.62Hz,2H,b) 2.66(t, $^3J_{HH}$=7.62Hz,2H,c) 1.23(t, $^3J_{HH}$=8.8Hz,3H,d)	2941 (m, C-H str) 1795 (ss, C=O str. acid chloride) 1745 (s, C=O str. ester) 1241 (ms, C-O str)	129 (M^+-Cl, 35.1) 84 (129-OCH_2CH_3, 55.2)
$CH_3CH_2OC(=O)CH_2(CH_2)_4CH_2C(=O)Cl$ (e, a, c, d, b) **IIb**	17gm 84%		68-73°C at 0.07mm litt. bp. corrected to 0.77mm = 62°C	4.10(q, $^3J_{HH}$=8.7Hz,2H,a) 3.00(t, $^3J_{HH}$=7.6Hz,2H,b) 2.27(t, $^3J_{HH}$=7.6Hz,c) 1.22(t, $^3J_{HH}$=8.7Hz,3H,e) 1.0-2.0(m,8H,d)	2920 (s, CH str.) 1795 (ss, C=O str. acid chloride) 1740 (ss, C=O str. ester) 1243 (s, C-O str.)	185 (M^+-Cl, 21.1) 140 (185-OCH_2CH_3, 11.2) 88($[CH_3CH_2OCCH_3]^+$, (McClafferty)
$CH_3CH_2OC(=O)CH_2(CH_2)_8CH_2C(=O)Cl$ (e, a, c, d, b) **IIc**	14gm 85%		108-112 at 0.1mm litt. bp. corrected to 0.1mm =105°C	4.08(q, $^3J_{HH}$=8.7Hz,2H,a) 2.90(t, $^3J_{HH}$=7.6Hz,2H,b) 2.28(t, $^3J_{HH}$=7.6Hz,2H,c) 1.10-2.(m,lett, d) 1.23(t, $^3J_{HH}$=8.5Hz,3H,e)	2921 (s, CH str.) 1800 (ss, C=O str, acid chloride) 1740 (ss, C=O str. ester) 1244 (s, C-O str.)	241 (M^+-Cl, 11.2) 196 (241-OCH_2CH_3, 21.2) 88 ($[CH_3CH_2OCCH_3]^+$, (McClafferty, 100)

4.6.3 Preparation of Alkyl Grignards, 12a-c

Decyl (12a); hexyl (12b) and ethyl (12c) magnesium bromides (Figure 14) were prepared by the same general method.[209] A typical preparation is described for ethylmagnesium bromide. Magnesium turnings (3.69 gm, .152mol) and 50 ml of dry ether and were placed in a 500 ml 3-neck round bottom flask and equipped with condenser and a dry nitrogen flushing system. To this stirred mixture was added a solution of ethyl bromide (11.1 ml, .17mole) in 250 ml dry ether dropwise with the aid of a dropping funnel. When no further reaction was evident, the ethereal solution was quickly decanted into a 250ml graduated cyclinder for volume measurement (190 ml), poured into a clean dry reagent bottle and the bottle sealed with a rubber septum after flowing N_2 gas over the Grignard solution.

The molarity of the Grignard solution was determined using the procedure of Watson.[210] Tetrahydrofuran (5ml) was placed in a 50 ml 3-neck round bottom flask along with a small crystal of 1, 10 phenanthrolines H_2O. Two necks of the round bottom flask were sealed with rubber septa and the third (middle) neck fitted with a septum which itself was fitted with 5ml biuret. The biuret was filled with 0.502M sec-butanol in xylene. Approximately 2ml of the ethyl Grignard solution was injected into the stirring THF solution resulting in a "wine red" solution. The THF solution was subsequently titrated with the sec-butanol/xylene mixture to a

pale yellow end-point and 1.00ml aliquots of the Grignard solution were injected and titrated until titration volumes were reproducible to 0.01 ml. The concentration of ethylmagnesium bromide was found to be 0.546M (75% yield). The yields of hexyl (12b) and decyl (12a) Grignards were found to be 66 and 69% respectively.

4.6.4 Ethyl-oxo-myristates, 14a-c

Ethyl 4-oxo, 8-oxo or 12-oxo-myristates (14a-14c, respectively, Figure 14), were prepared by the same general method.[206] A typical procedure is described for ethyl 12-oxo-myristate. Freshly fused and powdered zinc chloride (12.6gm, mole) was placed in a dry 3-neck 500ml round bottom flask equipped with condenser, stirrer bar and stopper. While keeping the powder stirring under dry N_2 atmosphere, 140ml of a 0.396M (1 equiv.) ethyl Grignard 12c solution was added dropwise with the aid of a dropping funnel. After the initial vigorous reaction, the mixture was refluxed for 2 hr. during which time the solution became milky white colour. The magnetic stirring apparatus was then replaced with a mechanical stirrer and a solution of 14gm (1 equiv.) of monoethyl-1, 12-didodecanoate acid chloride (11c) made up to 40ml with dry benzene, was added dropwise to the stirring ethyl zinc chloride solution. The mixture was refluxed for 3 hr. during which time the solution became increasingly viscous and difficult to stir. After allowing the mixture to cool to room

temperature, it was poured into a solution of 0.4M sodium bicarbonate and stirred vigorously for 1/2 hr. The zinc and magnesium salts were removed by filtration and washed with diethyl ether (100ml, 2x). The combined ether washings dried over anhydrous sodium sulfate, and the ether removed under reduced pressure. The resultant clear colourless oil subjected to fractional distillation in vacuo. A fraction which distiled at 129-134°C at 0.02 mm was collected and became a white crystalline solid on cooling.

In a similar manner n-decyl (12a) and n-hexyl (12b) Grignard solutions were converted to their corresponding alkyl zinc chlorides (13a and b respectively, Figure 14) where upon they were treated with 1 equivalent of the requisite monoester acid chloride. Reaction of the decyl reagent 13a with monoethyl succinic acid chloride 11a gave the 4-oxo-myristate (14a) whereas the hexyl reagent (13b) on reaction with 11b gave the 8-oxo-myristate. Data for ketoesters 14a-c is given in Table 22.

4.6.5 Attempted Synthesis of Gem-Difluoroethyl-Myristates 19a-c

Contrary to reports by Cross,[211] the attempts to fluorinate ketoesters 14a-c, (Figure 14) using diethylaminosulfur trifluoride (DAST, Aldrich) afforded none of the desired gem-difluoroesters 15a-c (Figure 14). For example, ethyl 12-oxo-myristate (0.5 gm, 1.83 mMole) was mixed with DAST (.223 ml, 1 equiv.) in a variety

of solvents (CCl_4, $CHCl_3$, $CHCl_2$, benzene and toluene) under dry N_2 atmosphere and allowed to stir for 5hr. The reaction was monitored by taking an aliquot of the mixture (0.2 ml) and quenching with 0.4M sodium bicarbonate. The solution was extracted with $CHCl_3$ (1ml, 3X) and the combined organic washings dried with Na_2SO_4. The chloroform was removed under reduced pressure and the resultant pale yellow solid taken up in 0.5ml $CDCl_3$. A ^{1}H-NMR spectrum was identical to ethyl, 12-oxomyristate (14c). The same $CDCl_3$

Table 22: Data For Ethyl Oxo-Myristates

Compound	Yield	m.p.	b.p.	^{1}H-nmr (δ) (ppm) ($CDCl_3$)	I.R. (cm^{-1}) ($CHCl_3$)	EIMS
$CH_3CH_2OC(=O)CH_2CH_2C(=O)CH_2(CH_2)_8CH_3$ (a, b, c, d, e) **14a**	9.9gm 48%		116-120°C at 0.15mm lit bp. corrected to 0.15mm = 112°C	4.12 (q, $^3J_{HH}$=8.75Hz, 2H, a) 2.42, 2.36 (t, $^3J_{HH}$=7.5Hz, 4H, b) 2.30 (t, $^3J_{HH}$=7.6Hz, 2H, c) 0.9-1.55 (m, 19H, e) 1.22 (t, $^3J_{HH}$=8.7Hz, 3H, d)	2921 (s, CH, str.) 1722 (ss, C=O str. ketone) 1741 (ss, C=O, str. ester) 1242 (s, C=O, str.)	225 (M^+-OCH_2CH_3, 7) 144 ($[CH_3CH_2OC(=O)(CH_2)_2C(=O)CH_3]^+$, (McClafferty, 41) 129 (144-CH_3, 80) 101 (144-$C(=O)CH_3$, 100)
$CH_3CH_2OC(=O)CH_2(CH_2)_4CH_2C(=O)CH_2(CH_2)_4CH_3$ (a, e, c, d, b, b, d, d) **14b**	19.7gm 73.8%		108-114°C at 0.1mm lit bp. corrected to 0.1mm = 112°C	4.09 (q, $^3J_{HH}$=8.7Hz, 2H, e) 2.31 (t, $^3J_{HH}$=7.7Hz, 4H, b) 2.26 (t, $^3J_{HH}$=7.5Hz, 2H, c) 1.0-1.9 (m, 19H, d) 1.20 (t, $^3J_{HH}$=8.7Hz, 3H, e)	2920 (s, CH, str.) 1732 (s, C=O str. ester) 1721 (ss, C=O str. ketone) 1242 (s, C-O str.)	270 (M^+, 8) 225 (270-OCH_2CH_3, 24) 185 ($[CH_3CH_2OC(=O)(CH_2)_6C(=O)CH_3]^+$ (McClafferty, 15) 170 (185-CH_3, 52) 143 (185-$C(=O)CH_3$, 100)
$CH_3CH_2OC(=O)CH_2(CH_2)_8CH_2C(=O)CH_2CH_3$ (a, c, b, d, b, b, d) **14c**	12.5gm 75%	53-54 lit 55°C	129-134°C at 0.2mm lit bp corrected to 0.2mm = 133°C	4.10 (q, $^3J_{HH}$=8.7Hz, 2H, a) 2.48, 2.29 (t, $^3J_{HH}$=8.7Hz, 6H, b) 0.45-1.9 (m, 19H, d) 1.21 (t, $^3J_{HH}$=8.7Hz)*	2920 (s, CH, str.) 1732 (s, C=O str. ester) 1720 (ss, C=O str. ketone) 1241 (s, C-O str.)	270 (M^+, 6) 241 (270-CH_2CH_3, 37) 225 (270-OCH_2CH_3, 50) 199 (M^+-$CH_3CH_2OC(=O)$-CH_3, 100)

solution was spotted on a silica gel TLC plate along with 11c and chromatographed using 3.5% ethyl acetate/hexane as the solvent. The plate when developed with 0.4M Ce^{4+}/H_2SO_4 spray followed by charring showed no new products.

The temperature of the reaction mixture was elevated by 10°C increments every 2hr. while monitoring the reaction by ^{1}H-NMR and TLC as previously described. No new products were evident. The reaction mixtures were heated eventually to the solvent boiling points each time resulting in black, tar-like products. After quenching the reaction mixture with 10ml of 0.4M bicarbonate followed by extraction with $CHCl_3$ (10ml, 3x), drying the organic extracts over Na_2SO_4 and removal of $CHCl_3$ under reduced pressure, mass recoveries of organic materials never exceeded 5%. Again, none of the desired gem-difluoro-esters were evident by either TLC or ^{1}H-NMR.

To ensure that the DAST reagent was of good quality, the fluorination of benzaldehyde to α, α-difluorotoluene under conditions described by Middleton[212] was attempted. Crude benzaldehyde was purified by washing with 0.4M sodium bicarbonate, drying over Na_2SO_4 and distillation <u>in vacuo</u> over sodium carbonate. Benzaldehyde (1.73gm, 16.3mmole) was

added dropwise with the aid of a dropping funnel to a stirred solution of DAST (2ml, 1 equiv.) in 10ml of dry CH_2Cl_2 in a 50ml round bottom flask fitted with condenser and N_2 flush. After 1 1/2 hr. a 0.5ml aliquot of the reaction mixture was quenched with ~1 ml 0.1M sodium carbonate and washed with $CHCl_3$ (1ml, 2x). After drying over Na_2SO_4, $CHCl_3$ was removed under reduced pressure and the resultant pale brown oil taken up in ~1ml $CDCl_3$, a comparison of the integral ratios of the CHO resonance to the aromatic protons showed that the reaction had gone to ~75% completion. An ^{1}H-NMR analysis of an aliquot taken 2 1/2 hr. later showed that the reaction had not gone beyond 75% completion.

The mixture was then washed into 0.4M sodium carbonate and extracted with $CHCl_3$ (30ml, 3x). The $CHCl_3$ extracts were dried over Na_2SO_4 and the organic solvent removed under reduced pressure resulting in 1.60gm of a pale brown oil or 90% mass recovery. Although the oil was never purified, a 84.66MHz ^{19}F-NMR spectrum showed only a doublet at -110 ppm ($^2J_{H-F}$ = 44Hz) indicating the presence of the difluoro functionality. Analysis of the crude product by silica gel TLC using 10% ethyl acetate/hexane followed by H_2SO_4 spray and charring showed a major new component (Rf = 0.62) and starting material (Rf = 0.22) in an estimated ratio of 3 to 1.

4.6.6 Ethyl, hydroxy,deutero Myristates, 27a,b

Sodium borodeuteride (MSD, 2.5gm, 44mMoles) and 10ml of absolute ethanol were placed in a clean dry 50ml 3-neck round bottom flask fitted with condenser and drying tube. The solution was cooled in an ice-water bath and a solution of ethyl 8-oxomyristate (14b) (12gm, 44mMole) in 20ml absolute ethanol added dropwise with the aid of a dropping funnel. The progress of the reduction was monitored by taking aliquots (∿ 0.1ml), quenching with 10% HCl and washing with ∿1ml $CHCl_3$. The $CHCl_3$ wash was then spotted on a silica gel TLC plate along with starting material, chromatographed using 30% ether/hexane and the TLC plate was developed by charring. After 1hr, only a single new component with an Rf = 0.38 was observed compared to ethyl 8-oxomyristate 14b with an Rf=0.68. The reduction mixture was then quenched by the addition of 10% HCl until no further effervescence occurred. A further 20ml of H_2O was added and a clear colorless oil separated. The solution was then extracted with $CHCl_3$ (50ml, 3x) and the organic washings dried with Na_2SO_4. Chloroform was then removed under reduced pressure and the resultant oil subjected to fractional distillation to yield ethyl 8-hydroxy-8-deutero-myristate 27a as a clear colourless oil which distilled at 145-149°C at .009mm.

Similarily, ethyl 12-oxomyristate 14c (10gm, 36.6 mMole) was treated with 1 equiv. of sodium borodeuteride with the following modification; the reaction was carried out at room tempertature because of the inherent insolubility of the ketoester in ethanol at 0°C. Ethyl 12-hydroxy-12-deutero-myristate 27b distilled as a clear colourless oil at 144-145°C and 0.1mm which solidified on cooling (m.p. 33-34). Data for deutero alcohols 27a and b are given in Table 23.

In the reduction of ethyl 4-oxomyristate 14a, rapid lactone formation could not be avoided whether using 10% HCl, 0.1M sodium acetate (pH 6.50) or 0.1M sodium borate (pH 9.50) in the work-up procedure (Figure 43, Scheme 1). All three procedures resulted in the formation of a product whose ^{1}H-NMR spectra showed a multiplet between 0.7 and 1.7 ppm (23H) and multiplet at 2.20 (2H). The I.R. spectrum showed a single carbonyl stretch at 1772cm^{-1} indicating lactone formation.

Alternatively, attempts to hydrolyze the lactone in NaOEt/HOEt or KOH/MeOH or hydrolysis of 14a (Figure 43, Scheme 1), to the corresponding acid prior to the reduction afforded tar-like mixtures which showed no less than six spots by TLC (using 30% Et_2O/hexane as the mobile phase).

Table 23: Data for Ethyl hydroxy, deuteromyristates

Compound	Yield	m.p.	b.p.	^{1}H-nmr (δ)(ppm) ($CDCl_3$)	^{13}C-nmr (δ)(ppm) ($CDCl_3$)
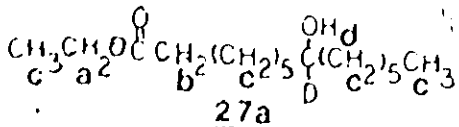 **27a**	10.1gm 83%		145-149°C at .009m	4.08 (s, 1H, d) 4.13 (q, $^3J_{HH}$=8.7Hz, 2H, a) 2.26 (t, $^3J_{HH}$=7.8Hz, 2H, b) 0.8-1.8(m, 23H, c)	173.04 (C=O), 70.68 (t, $^1J_{CD}$=38Hz), 59.54 (CH_2-O-C), 37.07, 36.93, 33.87, 31.44, 28.99, 29.82, 28.70, 28.30, 25.18, 25.03, 24.50, 22.15, 13.75, 13.50
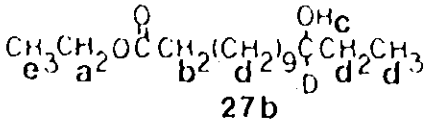 **27b**	8.12gm 81.3%	33-34	144-151°C at 0.1m	4.10 (q, $^3J_{HH}$=8.7Hz, 2H, a) 2.27 (t, $^3J_{HH}$=7.5Hz, 2H, b) 1.70 (broad, 3H, c) 1.0-1.7 (m, 23H, d) 1.22 (t, $^3J_{HH}$=8.7Hz, 3H, e)	173.54 (C=O), 72.71 (t, $^1J_{CD}$=38.1Hz, C-OH), 59.98 (CH_2-O-C), 36.88, 34.36, 30.05, 29.68, 29.51, 29.44, 29.36, 29.16, 29.12, 25.59, 24.97, 14.19, 9.67.

Compound	^{2}H-nmr (δ)(ppm)($CDCl_3$)	I.R. (cm^{-1}) ($CHCl_3$)	LRMS m/z(rel. intensity)	HRMS
27a	3.52	3620(w, free OH str.) 1740(s, C=O str. ester) 1240(s, C-O str.)	255(M^+-H_2O, 6) 210(255-OCH_2CH_3,22) 185(255-CH_2-$COCH_2(CH_2)_2CH_3$, 62) 88($(CH_3COCH_2CH_3)^+$ (McClafferty, 62) 55($C_4H_7^+$, 100)	Calc. for M^+-H_2O, 225.2308, Obs. 225.2295 Calc M^+-CH_2-CO-$(CH_2)_2CH_3$ = 185.154 Obs 185.154
27b	3.51	3622(w, free OH str.) 1740(s, C=O str. ester) 1241(s, C-O str.)	255(M^+-H_2O, 6) 210(255-OCH_2CH_3, 7) 198(255-CH_2-CO-CH_2CH_3,35) 88($(CH_3COCH_2CH_3)^+$, (McClafferty, 83) 55($C_4H_7^+$, 100)	Calc. for M^+-H_2O, 225.2308, Obs. 255.2290, Calc , 255-CH_2-$COCH_2CH_3$ = 198.1621 Obs 198.1603

4.6.7 Ethyl fluorodeuteromyristates, 28a,b

A solution of DAST (4.6ml, 36.6mMole) was added to 20ml of CH_2Cl_2 (distilled over P_2O_5) in a clean dry 50ml, 3-neck round bottom flask fitted with a magnetic stirrer bar and stoppers. This operation was carried out in a dry N_2 glove bag to avoid atmospheric moisture. The solution was quickly removed from the glove bag and fitted with a condenser equipped with a dry N_2 flush. The CH_2Cl_2 solution was then cooled to -78°C in a dry-ice acetone bath and a solution of 10gm (1 equiv.) of ethyl 8-hydroxy-8-deutero myristate 27a made up to 50ml in CH_2Cl_2 added dropwise (with the aid of a dropping funnel) to the stirred DAST solution. The mixture was allowed to cool to room temperature and a 1ml aliquot quenched with 1ml 0.1M sodium carbonate. The organic layer was spotted on a silica gel TLC plate along with 27a and chromatographed in 3.5% ethyl acetate/hexane (v/v). Visualization of the TLC plate by charring showed nearly no starting material, (Rf = .08) and two spots of equal intensity (Rf = .41 and .32). The reaction mixture was then quenched by the slow addition to 100ml of 0.1M sodium carbonate while stirring until no further bubbling occurred. The mixture was then extracted with $CHCl_3$ (100ml, 3x) and the combined organic washings dried over Na_2SO_4. The organic solvent was removed under reduced pressure and the resultant pale yellow oil

purified by passing it down a silica gel column (30 X 4.5 cm, 200-400 mesh) using 0.5% ethyl acetate/hexane as the eluting solvent. Fractions at 650 drops/fraction were collected using a Gilson microfractionator and the progress of the chromatography monitored by spotting every 5th fraction on a silica TLC plate along with a sample of unchromatographed material and running the plate in 3.5% ethyl acetate/hexane followed by visualization by charring. All fractions showing spots with the Rf values of .32 and .41 were pooled separately and the organic solvents removed under reduced pressure. Fractions containing both materials were pooled, rechromatographed, and pooled with the previous fractions showing either Rf = .32 or .41 material. An ^{2}H-NMR of undistilled material which had a single spot at Rf = .32 snowed a doublet at 4.42ppm ($^{2}J_{DF}$ = 7.73Hz). An ^{19}F-NMR spectrum (84.66MHz) showed a single resonance at -181.23ppm with $V_{1/2h}$ = 80Hz. In contrast, the ^{2}H-NMR spectrum of Rf = .41 material showed a single resonance at 5.35ppm and ^{19}F-NMR spectrum showed no ^{19}F-NMR signal, suggesting that it was an unsaturated biproduct of the reaction of DAST with 27a. ^{13}C-NMR spectra of this latter material showed signals at ~120ppm. The Rf = .32 material was purified further by fractional distillation <u>in vacuo</u> to give Ethyl 8-fluoro,8-deuteromyristate <u>28a</u> as a clear, colourless oil which distilled at 115-119°C at 0.1mm.

The same procedure was used in the synthesis and purification of ethyl 12-fluoro-12-deuteromyristate 28b using 27b (8gm, 29.3 mole) and 1 equivalent of DAST. Again, analysis of the reaction mixture by TLC (using 3.5% ethyl acetate/hexane) showed 2 major products - one with Rf - .32, the desired product, the other, Rf = .41 material, the unsaturated bi-product(s). Data for fluorodeuteromyristates 28a and 28b is given in Table 24.

4.6.8 Gas Chromatographic Analyses of 28a and 28b

Gas chromatographic analyses were performed as described in Section 4.1. Samples of either 28a or 28b (5mg) or the unsaturated biproducts from the synthesis 28a or b (4.6.7) were dissolved in ~200µl $CHCl_3$. Area analyses of the peaks of the chromatograms of the isothermal runs showed that 28a or 28b were no less than 96.8% pure (ret. time = 10.2 min.) with the only impurities being the unsaturated ethyl myristates (ret. time = 7.0 min.)

4.6.9 Fluorodeutero Fatty Acids, 29a and 29b

Ethyl 8-fluoro-8-deuteromyristate (4.40gm, 16mMole) 28a or 12-fluoro-12-deutero myristate 28b (2.55gm, 93mmoles) were disolved in 50ml of a methanolic KOH solution (2gm in 50ml) and refluxed over a steam bath under N_2 atmosphere for ~1 1/2 hrs. The reaction mixture was acidified with 10% HCl and extracted with $CHCl_3$

Table 24: Data for Ethylfluorodeuteromyristates

Compound	Yield	m.p.	b.p.	^{1}H-nmr (δ)(ppm)($CDCl_3$)*	^{19}F-nmr (δ)(ppm)	^{13}C-nmr (δ)(ppm)
$CH_3CH_2O\overset{O}{\overset{\|\|}{C}}CH_2(CH_2)_5\overset{F}{\overset{\|}{C}}(CH_2)_5CH_3$ (a, b, c, c, D, c, c, d) **28a**	4.45gm 45%		115-119°C at 0.1mm	4.12 (q, $^3J_{HH}$=8.8Hz, 2H, a) 2.30 (t, $^3J_{HH}$=7.6Hz, 2H, b) 0.9-2.0 (m, 23H, c) 1.21 (t, $^3J_{HH}$=8.8Hz, 3H, d)	($CDCl_3$) -181.23 $\nu_{1/2}$ = 80 Hz	($CDCl_3$) 178.93 (C=O), 58.27 (C-OCH_2), 35.12, 35.03, 34.79, 34.69, 31.64, 29.01, 28.85, 24.90, 24.82, 24.76, 24.45, 18.15, 13.69 (terminal-CH_3)
$CH_3CH_2O\overset{O}{\overset{\|\|}{C}}CH_2(CH_2)_9\overset{F}{\overset{\|}{C}}CH_2CH_3$ (e, a, b, c, D, c, d) **28b**	2.60gm 35%		117-124°C at .005mm	4.11 (q, $^3J_{HH}$=8.7Hz, 2H, a) 2.25 (t, $^3J_{HH}$=7.6Hz, 2H, b) 0.9-1.2 (m, 20H, c) 0.95 (t, $^3J_{HH}$=7.2Hz, 3H, d) 1.22 (t, $^3J_{HH}$=8.7Hz, 3H, e)	($CDCl_3$) -180.93 $\nu_{1/2}$ = 80 Hz	($CDCl_3$) 178.85 (C=O), 58.27, (CH_2-OC), 34.61, 34.28, 33.88, 29.36, 29.26, 29.09, 28.95, 28.00, 27.66, 24.99, 24.93, 24.62, 18.17, 9.18 (d, $^3J_{HH}$=5.1Hz, terminal CH_3 β to F)

Compound	^{2}H-nmr (δ)(ppm) ($CDCl_3$)	I.R. (cm^{-1}) ($CHCl_3$)	LRMS m/z (rel. intensity)	HRMS
28a	4.42 d, $^2J_{DF}$ = 43Hz	2920(s, CH, str.) 1740(s, C=O str.) 1240(w, CF, str.) 1240(s, C-O, str.)	255(M^+-HF, 3) 210(255-OCH_2CH_3, 5) 209(210-H; 11) 88($[CH_3CH_2\overset{O}{\overset{\|\|}{C}}OCH_3]^+$, (McClafferty, 100))	Calc. for M^+-HF 255.2308, Obs. 255.2336 Calc. 255-OCH_2CH_3 = 210.1970 Obs 210.1997
28b	4.43 d, $^2J_{DF}$ = 7.33Hz	2921(s, CH, str.) 1740(s, C=O, str.) 1238(w, CF, str.) 1241(s, C-O, str.)	255(M^+-HF, 4.1) 210(255-OCH_2CH_3, 10) 209(210-H; 12) 88($[CH_3CH_2\overset{O}{\overset{\|\|}{C}}OCH_3]^+$, (McClafferty, 100))	Calc. for M^+-HF 255.2308, Obs. 255.2351 Calc 255-OCH_2CH_3 = 210.1996 Obs 210.1987

(50ml, 3X). The combined chloroform extracts were dried over Na_2SO_4 and chloroform removed under reduced pressure to yield white crystalline solids. The solids were recrystallized from a minimal volume of acetone/water - 1/1 = (v/v), filtered and dried in vacuo over P_2O_5. The mother liquor was concentrated and subjected to further recrystallization. Data for the fluoro-deutero fatty acids 29a and 29b is given in Table 25.

4.6.10 Fluorodeuteromyristic anhydrides,30a,b

S-F,S-D (3.55gm, 1.4mMole) 29a or 12-F,12-D myristic acids(2.10gm, 8.50mMole)29b were dissolved in dry CCl_4 (25ml) and place in a dry 50ml 3-neck round bottom flask equipped with condenser and N_2 flush. To this stirred mixture, a solution of dicyclohexylcarbodiimide (DCC, ½ equiv.) in 10ml CCl_4 was added and a white precipitate formed almost immediately. The solution was allowed to stir for 15hr. and the dicyclo-hexylurea precipitate filtered with the aid of aspirator pressure. The filtered CCl_4 solution was concentrated in vacuo and the resultant white solid residue recrystallized from a minimal volume of dry acetone. The mother liquor was concent-rated and recrystallized two more times and the white crystalline precipiates pooled. Data for both anhydrides 30a and 30b are given in Table 26.

Table 25 Data for Fluoro, deuteromyristic Acids

Compound	Yield	m.p.	b.p.	^{1}H-nmr (δ) (ppm) ($CDCl_3$)	^{19}F-nmr (δ) (ppm) ($CDCl_3$)	^{13}C-nmr (δ) (ppm) ($CDCl_3$)
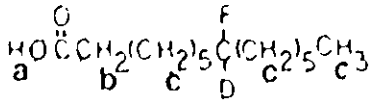 **29a**	3.59gm 92%	62-64°C		10.5 (s, 1H, a) 2.25 (t, $^3J_{HH}$=7.6Hz, 2H, b) 0.8-1.9 (m, 23H, c)	-180.23 J_{FH} = 80 Hz	179.62 (C=O), 35.16, 35.07, 33.84, 34.73, 33.89, 31.64, 29.06, 29.00, 28.85, 24.99, 24.99, 24.93, 24.85, 24.79, 24.53, 22.44, 13.82 (terminal CH_3)
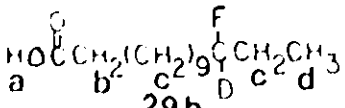 **29b**	2.12gm 91%	59-60°C		10.8 (s, 1H, a) 2.25 (t, $^3J_{HH}$=7.5Hz, b) 1.1-1.9 (m, 20H, c) 0.92 (t, $^3J_{HH}$=7.5Hz, 3H, d)	-180.55 J_{FH} = 80 Hz	179.63 (C=O), 34.71, 34.36, 33.92, 29.30, 29.11, 29.01, 25.10, 25.00, 24.66, 9.13 (d, $^3J_{HH}$=5.3Hz, terminal CH_3)

Compound	^{2}H-nmr (δ) (ppm) ($CDCl_3$)	I.R. (cm^{-1}) (CCl_4)	LRMS	HRMS
29a	4.33 d, $^2J_{DF}$=7.35Hz	3001(wb, OH, str. acid) 2921(s, CH, str.) 1718(ss, C=O, str. acid) 1240(w, CF, str.)	227(M^+-HF, 7) 210(227-OH, 5) 209(210-H, 22) 60($[CH_3\overset{O}{C}\text{-}OH]^+$ McClafferty, 32) 69($C_4H_9^+$, 100)	Calc. for M^+-HF 227.1995, Obs. 227.1989 Calc 227-OH = 210.1967 Obs 210.1957
29b	4.35 d, $^2J_{DF}$=7.40Hz	3000(wb, OH, str. acid) 2922(s, CH, str.) 1720(ss, C=O str. acid) 1241(w, CF, str.)	227(M^+-HF, 3) 210(227-OH, 32) 209(210-H, 18) 60($[CH_3\overset{O}{C}OH]^+$ (McClafferty, 30)	Calc. for M^+-HF 227.1995; Obs. 227.1980 Calc 227-OH = 210.1963 Obs 210.1947

Table 26: Data for Fluoro, deuteromyristic Anhydrides

Compound	Yield	m.p.	b.p.	^{1}H-nmr (δ) (ppm) ($CDCl_3$)	^{19}F-nmr (δ) (ppm) ($CDCl_3$)	^{13}C-nmr (δ) (ppm) ($CDCl_3$)
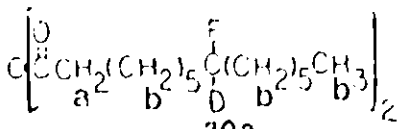 **30a**	2.2gm 63%	58-59 °C		2.40 (t, $^3J_{HH}$=7.7Hz, 4H, a) 0.9-2.0 (m, 46H, b)	-180.33 J_{FH} = 80 Hz	169.28 (C=O), 35.03, 34.96 34.76, 34.63, 31.59, 29.02 28.60, 24.87, 23.59, 22.41 13.86 (terminal CH_3)
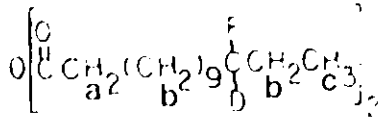 **30b**	1.20gm 61%	55-56.5 °C		2.42 (t, $^3J_{HH}$=7.7Hz, 4H, a) 1.1-2.0 (m, 40H, b) 0.91 (t, $^3J_{HH}$=8.2Hz, 6H, c)	-180.24 J_{FH} = 81 Hz	169.23 (C=O), 34.49, 34.38, 34.04, 29.12, 28.99, 28.80, 28.51, 27.77, 27.44, 24.76, 24.69, 24.61, 23.90, 8.91 (d, $^3J_{C-F}$=5.3Hz, terminal CH_3)

Compound	^{2}H-nmr (δ) (ppm)	I.R. ($CHCl_3$)	LRMS	HRMS
30a	4.32 d, $^2J_{CF}$=7.33Hz	2921(s, CH, str.) 1825(s), 1757(s) (C=O, str. anhydride) 1240(w, CF, str.)	230([C(=O)(CH$_2$)$_6$CFO(CH$_2$)$_5$CH$_3$]$^+$, 10) 210(230-HF, 25) 209(210-H, 15) 84(210-CH$_2$CH=CO$_2$,(CH$_2$)$_5$CH$_3$, 47) 55($C_4H_7^+$, 100)	Calc. for C(=O)(CH$_2$)$_6$CFO(CH$_2$)$_5$CH$_3$, 230.2031 Obs. 230.2056 Calc. for 230-HF 210.1964 Obs. 210.1973
30b	4.35	2920(s, CH, str.) 1826(s), 1757(s) (C=O, str. anhydride) 1241(w, CF, str.)	230([C(=O)(CH$_2$)$_{10}$CFCH$_2$CH$_3$]$^+$, 8) 210(230-HF, 8) 209(210-H, 10) 55($C_4H_7^+$, 100)	Calc. for (C(=O)(CH$_2$)$_{10}$CFCH$_2$CH$_3$)$^+$ 230.2031 Obs. 230.2051 Calc. for 230-HF 210.1964 Obs. 210.1973

4.6.11 Cadmium Chloride Complex of L-α Glycerophosphoryl choline, 18

Phosphatidylcholines were isolated from crude egg yolk lecithins using the procedure of Singleton[213] Egg yolk lecithins (25mg, Sigma Type XE, Lot #89C-7560) were dissolved in 500ml of $CHCl_3$. The yellow solution was loaded onto an alumina column (20-80 mesh, 89 x 4.3cm) previously equilibrated with $CHCl_3$. A further 400ml of $CHCl_3$ was passed down the column while adjusting the flow rate to ~10ml/min. Two solvent systems were used in the chromatographic separation, $CHCl_3$/MeOH = 9/1 (v/v) and $CHCl_3$/EtOH/H_2O = 2/5/2 (v/v/v). The fractions collected are described in Table 27. Fractions were spotted in triplicate on three silica gel plates along with dimyristoylphosphatidylcholine and its corresponding lysophospholipid. TLC plates were run in triplicate in $CHCl_3$/MeOH/H_2O = 65/25/4 (v/v/v) and visualized with either I_2, ninhydrin spray for the detection of phosphatidylethanolamines or molybdate apray,[214] for the detection of phosphates. Fractions 6-12 inclusive which contained the desired lipids were pooled and the solvent removed under reduced pressure to yield 14gm of crude phosphatidylcholine.

L-α-glycerophosphorylcholine (GPC) was prepared by the method of Brockeroff.[215] The crude cholines were suspended in

Table 27 Description of Fractions Collected in the Elution of Phosphalidylcholines.

Fr#	Volume (ml)	Colour	Solvent
1	250	Clear	$CHCl_3$/MeOH=9/1 (v/v)
2	250	Pale yellow	
3	125	Clear	
4	200	Pale yellow	
5	300	Pale yellow	
6	250	Cloudy	
7	250	Cloudy	
8	250	Clear	
9	260	Clear	
10	300	Clear	
11	410	Clear	
12	400	Clear	$CHCl_3$/EtOH/H_2O =2/5/2 (v/v/v)
13	400	Pale yellow	
14	400	Dark yellow	
15	400	Dark yellow	
16	300	Pale yellow	

100ml of diethyl ether and stirred vigorously while 13ml of 25% tetrabutylammonium hydroxide in methanol added. Immediately, a clear brown solution formed and a grey gelatinous precipitate settled to the bottom of the flask. The solution was stirred for a further 1hr., the ether layer decanted and the precipitate washed with ether (10ml, 2x). After dissolving the precipiate in ∿3ml methanol, the crude glycerophosphorylcholine was reprecipitated by addition of 100ml of ether. The procedure was repeated twice more and the precipitate dried in vacuo over P_2O_5 resulting in 3.91gm of L-α-glycero-phosphorylcholine·H_2O (α_D = 54.3° lit, 54.5°).

GPC(3.10gm) as dissolved in 20ml of 90% ethanol and added dropwise to a stirring solution of 5gm $CdCl_2$ in 5ml 90% EtOH. $(GPC)_2(CdCl_2)_3$ 18 (Figure 14) formed as a white precipitate instantaneously and the solution was placed in a 4°C fridge overnight for further crystallization. The precipitate was filtered, washed with 95% EtOH and dried *in vacuo* over P_2O_5 to a constant weight. Yield, 6.02gm (91%); m.p. 165-166° lit. 168°C.

4.6.12 Synthesis of DMPC 31, F-8-D 8-DMPC and F-12 D-12 DMPC (32a and b)

$(GPC)_2(CdCl_2)_3$ 18 was dried extensively *in vacuo* in a drying pistol at 65°C then dissolved in dry DMSO (.612gm in .5ml)

a 50ml round bottom flask equipped with condenser and N_2 flush. The solution was warmed to 50°C in an oil bath and a solution of myristic anhydride (2.02gm, 4.60mMole) and 4-pyrrollidinopyridine (0.654gm, 1 equiv.) in 2ml of dry benzene added to the DMSO solution and allowed to stir.[216] Periodically (∿1hr.) an aliquot was spotted on a TLC plate along with authentic DMPC and starting materials, the plate run in $CHCl_3/MeOH/H_2O$ = 65/25/4 (v/v/v) and the plate visualized with Mo spray followed by charring. When the reaction was judged complete after ∿5 hr. the mixture was poured into ∿20ml $H_2O/MeOH$ = 1/1 (v/v) and stirred for ∿1hr. under a stream of nitrogen. When the solvent had nearly evaporated, the mixture was redissolved in a minimal amount of $CHCl_3/MeOH$ = 5/3 (v/v) and loaded onto a silica gel column (200-400 mesh, 32 X 3.7cm) previously equilibrated with $CHCl_3/MeOH$ = 9/v/(v/v). Three solvent elution systems were used in the order: $CHCl_3/MeOH$ = 9/1, $CHCl_3/MeOH$ = 7/3 and $CHCl_3/MeOH/H_2O$ = 65/25/4. Fractions (650 drops/fraction) were collected using a Gilson microfractionator and the eluting solvent changed every 80 fractions. Myristic acid and $CdCl_2$ were collected in the first 80 fractions and 4-pyrrollidinopyridine in the second. DMPC was collected in the third set of 80 fractions using $CHCl_3/MeOH/H_2O$ = 65/25/4 as the eluting solvent. Fractions containing DMPC 31 were removed and concentrated under reduced pressure. The crude DMPC was

Table 28 Data for DMPC, F-8, D-8 and F-12, D-12 DMPC

Compound	Yield	m.p.	b.p.	^{1}H-nmr (δ) (ppm)	^{19}F-nmr (δ) (ppm)	^{13}C-nmr (δ) (ppm)
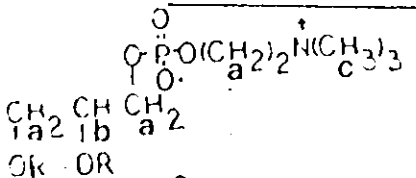	0.68gm 87.4 %			($CDCl_3$) 5.21 (m, 1H, b) 3.7-4.5 (m, 8H, a) 3.48 (s, 9H, c) 2.28 (t, $^3J_{HH}$=7.5Hz, 6H, d) 0.7-1.8 (m, 50H, e)		
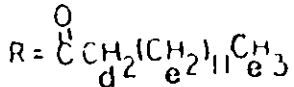 **31**				($CDCl_3$) 5.25 (m, 1H, b) 3.7-4.6 (m, 8H, a) 3.47 (s, 9H, c) 2.32 (t, $^3J_{HH}$=7.8Hz, 4H, d) 1.2-1.9 (m, 40H, e)	($CDCl_3$) -180.62 A_{AB} = 80 Hz	($CDCl_3$) 173.51 (CH2-CH) OR O O-C* 172.91 (CH2-CH-) O OR O-C* 70.52 (-CH-CH2-O-P) OR 66.62 (P-O-CH2CH2N(CH3)3) O 63.39 (CH2-CH) OR OR 63.03 (CH2N(CH3)3 59.22 *CH2-CH- OR OR 54.59 N(CH3)3 35.55, 34.49, 35.21, 34.29, 31.95, 29.40, 25.26, 25.08, 22.72, 14.03 (terminal CH_3)
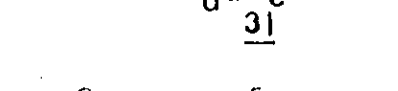 **32a**	0.70gm 76.2 %					
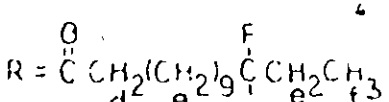 **32b**	.34gm 76.2 %			($CDCl_3$) 5.25 (m, 1H, b) 3.7-4.6 (m, 8H, a) 3.45 (s, 9H, c) 2.32 (t, $^3J_{HH}$=7.8Hz, 4H, d) 1.2-1.9 (m, 40H, e) 1.00 (t, $^3J_{HH}$=8.2Hz, f)		($CDCl_3$) 173.51 (CH2-CH) OR O O-C* 172.91 (CH2-CH-) O OR O-C* 70.52 (-CH-CH2-O-P) OR 66.62 (P-O-CH2CH2N(CH3)3) O 63.39 (CH2-CH) OR OR 63.03 (CH2N(CH3)3 59.22 *CH2-CH- OR OR 54.59 N(CH3)3 34.70, 34.56, 34.32, 28.08, 27.72, 24.92, 9.22 (terminal CH_3)

Table 28: Continued

Compound	^{2}H-nmr (δ)(ppm) ($CDCl_3$)	I.R. (cm^{-1}) ($CHCl_3$)	Elemental Analysis
31		2921(s, CH, str.) 1733(ss, C=O, str.) 1458(w, P=O, str.)	
32a	4.32 d, $^2J_{DF}$=7.7Hz	2920(s, CH, str.) 1735(s, C=O, str. ester) 1460(w, P=O, str.) 1240(w, CF, str.)	Calc. for $C_{36}H_{48}O_2F_2NO_8P$ C = 60.33, H = 10.06, N = 1.96 Found: C = 60.26, H = 10.20, N = 1.87
32b	4.35 d, $^2J_{DF}$=7.51Hz	2921(s, CH, str.) 1733(s, C=O, str. ester) 1462(w, P=O, str.) 1240(w, CF, str.)	Calc. for $C_{36}H_{48}O_2F_2NO_8P$ C = 60.33, H = 10.06, N = 1.96 Found: C = 60.33, H = 10.35, N = 1.89

dissolved in 26ml $CHCl_3$ and filtered H_2O 17ml and 200ml of hexane added in that order and the solution allowed to stand for 48hrs. at 0°C and the DMPC collected by filtration. After a second recrystallization DMPC was dried extensively over P_2O_5 *in vacuo*.

Similarily, F-8-D-8 and F-12-D-12 DMPC (32a,b) were prepared from F-8-F-8-(2.20gm) and F-12-D-12-myristic anhydride (1.20gm) respectively, using the same molar ratios of $(GPC)_2$ $(CdCl_2)_3$ and 4-pyrrollidinopyridine as in the synthesis of DMPC. F-8,D-8- and F-12-D-12-myristic acid (29a and b) were recovered in the silic gel purification of the fluorodeutero DMPC's. Data for DMPC, F-8-D-8- and F-12-D-12- DMPC is given in Table 28.

All DMPC's were assayed for purity by G.C. analysis after hydrolysis. F-8, D-8-, F-12,D-12 DMPC or DMPC (30mg) were dissolved in ~50ml 1M methanolic NaOH and refluxed under N_2 atmosphere over a steam bath for 1hr. The solution was acidified and extracted with $CHCl_3$ (50ml, 3x). The chloroform extracts were then dried over Na_2SO_4 and the solvent removed under reduced pressure. The resultant white solids (~20mg) myristic acid, and 29a and b were placed in separate reactivials and treated with ~200ml of Ethyl-8 (Pierce). Approximately 2µl of these solutions were injected and analyzed by G.C. in exactly the same way as described in Section 4.1. DMF

solutions of unsaturated fatty acid ester biproducts from the synthesis of ethyl fluorodeuteromyristates (Section 4.6.7) were also injected as standards. Repeated injections and analysis showed that both 8-F,8-D and 12-F 12-D-DMPC hydrolysates had greater than 98.7% fluorodeutero fatty acids with the only impurities being the unsaturated fatty acids. Likewise, the hydrolysate of synthetic DMPC showed a single component (ret. time = 9.1 min.) which corresponded to ethyl myristate and a purity of 99.5%. Differential scanning calorimetry (DSC) scans and ^2H "quad echo" spectra were obtained for each phospholipid as described in Section 4.1

4.7 Preparation of Lipophilin-FEM-d_2

The following solvents were investigated as candidates for the reaction media for the modification of lipophilin with FEM-d_2: $CHCl_3$, 2-chloroethanol, and CH_2Cl_2. In each case N-acetyl-L-cysteine methyl ester (~10mg) was dissolved in each solvent (~20ml), mixed with FEM-d_2 (10mg, 1 equiv.) and stirred under N_2 atmosphere at room temperature. Every hour, aliquots of the reaction mixture were spotted on a silica gel TLC plate along with starting materials and chromatographed using 5% MeOH/$CHCl_3$. No new products were apparent after visualization of the plate by I_2, nitroprusside spray or charring. Catalytic amounts of triethylamine (0.1 -1 equiv.) were added to the

reaction mixtures and still no reactions were apparent on examination of the TLC plates. The failure to observe modification of thiol group in any of these solvents in which lipophilin is readily soluble, prompted us to prepare the water solubilized form of the protein and subsequently modify thiol groups under these conditions. From our previous kinetic investigations (Section 3.2) it was shown that in aqueous media, thiol modification was rapid and specific.

Lipophilin(300mg) was a kind of gift from Dr. M.A. Moscarello (University of Toronto, Sick Children's Hospital). The protein (230mg) was dissolved in 200ml of freshly distilled and degassed 2-chloroethanol. The solution was sonicated, filtered through glass wool and then dialyzed against .4ℓ of distilled-deionized water for 24hr. while maintaining a continous stream of N_2 bubbles through the dialysis medium. During this time, the dialysis medium was changed twice. Samples of undialyzed lipophilin, 2.5mg, were dissolved in either 5ml of 2-chloroethanol or 2-chloroethanol -1% SDS for subsequent SH analysis[176] $O.D._{279}$ measurements of each solution were used to determine protein concentration. 0.9ml aliquots of the protein solution were treated with 0.1ml of 10mM DTNB and then 0.1ml of 2M triethylamine, both in 2-chloroethanol. Absorbance readings at 412 nm were followed over a period of 1hr. during which a maximum

was reached followed by a slow linear decrease. The true reading was obtained by extrapolation to zero time. An extinction coefficient of 14,500 $M^{-1}cm^{-1}$ was used for the TNB anion in 2-chloroethanol. The aqueous protein solution was subsequently treated with 30mg FEM-d_2 and stirred for 1hr. The solution was subsequently dialyzed against water (4ℓ) for 24hr. at 4°C while maintaining a constant flow of nitrogen in the dialysis medium. The FEM-d_2 treated protein solution was then freeze-dried and 225mg (93%) of the protein recovered. Sulfhydryl assays on the freeze dried protein pre-treated with FEM-d_2, and a protein sample which had not been treated with FEM-d_2 but dialyzed and freeze dried in the same manner were performed in 2-chloroethanol and 2-chloroethanol 1%SDS as described previously.

A small aliquot of the lyophilized sample (15mg) was dissolved in a minimal amount of 2-chloroethanol and chromatographed down a Sephadex LH-20 column (23 X 2.2cm) using $CHCl_3$/MeOH = 1/1 (v/v) as the eluting solvent. A single fraction was observed and the solvent was removed <u>in vacuo</u> resulting in 13.8mg (94% recovery) of protein. ^{19}F-nmr spectra of 10mg of chromatographed or unchromatographed protein (in 1 ml of 2-chloroethanol) after 50,000 scans showed a single ^{19}F-resonance at -69.21 ppm with a singal to noise ratio of 7.5/1 (± .2). In contrast, ^{19}F-nmr spectra of varying

amounts of FEM-d_2 in either 2-chloroethanol or 2-chloroethanol containing FEM-d_2 modified protein showed FEM-d_2 a single narrow resonance at -70.21 ppm. This indicated that it was unlikely that FEM-d_2 was non-covalently bound to the protein.

4.8 Preparation of protein/fluorophosphilipid mixtures

Lipophilin or lipophilin-FEM-d_2 fluorophospholipid complexes were prepared by the procedure of Gagnon.[167] The desired amount of protein was dissolved in ∿ 3ml of 2-chloroethanol along with a constant amount of fluoro lipid 32a or b and dialyzed into distilled deionized degassed water at 4°C for 24hrs.

Three changes of the dialysis medium were performed during this time. The aqueous suspensions were then freeze-dried in tared 10mm NMR tubes and total mass recoveries were never less than 93%. The amount of phospholipid present in the protein/lipid complex was determined by the procedure of Bartlett,[217] for determining phosphates (Appendix II). Analysis of lipophilin or lip-FEM-d_2 alone showed no phsophate. Protein concentrations were determined by $O.D._{279}$ measurements of a ∿1mg sample of protein/phospholipid dissolved in 1ml of 2-chloroethanol (ε=4.31 x $10^4 M^{-1} cm^{-1}$), and corrected for any residual absorbance of the fluoro lipid which never exceeded 2% of that of the protein. Prior to ^{19}F-NMR studies, the

freeze-dried protein - phospholipid mixtures were suspended in 2ml of pH 7.4.5mM NaCl, 2mM Hepes Buffer.

4.8.1 ^{19}F-NMR Studies

^{19}F-NMR spectra were obtained at 235.36MHz and various temperatures using the following spectral parameters: Sweep Width = 62,500Hz, Offset = 70,000Hz, Pulse width = 25μs (tip angle = 90°), delay time = 10μs, line broadening = 1.00, aquisitiontime = 0.2s and resolution of 3.95 Hz/pt. Trifluoroacetate (-75.959ppm) was used as an external reference and all measured chemical shifts were reproducible to within ± 1 data point. The probe temperature was measured using a Gilson 28a thermocouple with digital readout.

Appendix I

5.1 Plane vs. Circularily Polarized Light

An electromagnetic wave is characterized by the orientation of its component electric and magnetic fields. Plane polarized radiation shown in Figure 55 below has its electric and magnetic field vectors (denoted by E and H respectively) perpendicular to one another in the z and y

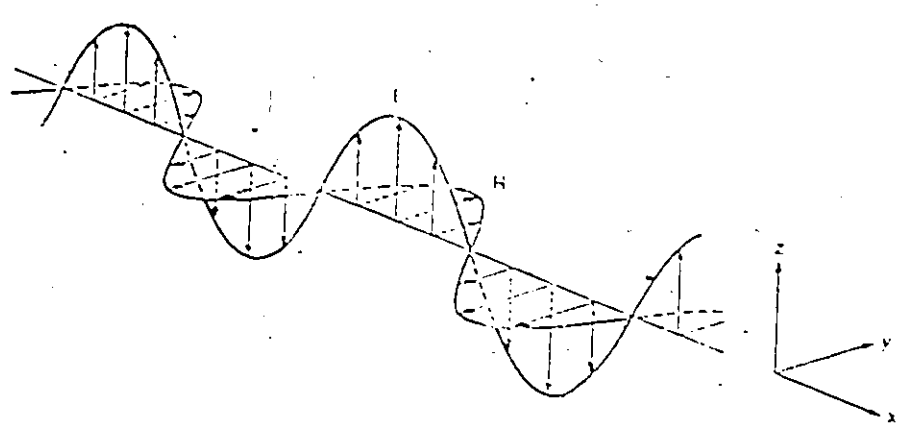

Figure 55 (Taken from Ref. 10)

direction and to the direction of propogation, the x axis. However, circularily polarized light has rotating electric and magnetic fields (perpendicular to one another). This is represented in Figure 56 below (only E is shown)[10]

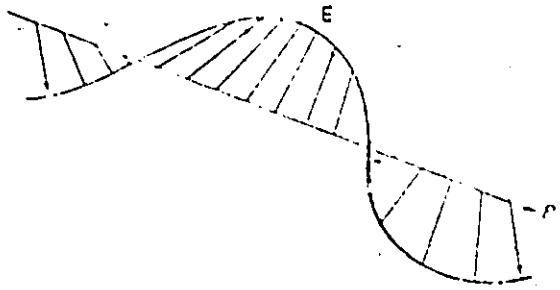

Figure 56 (Taken from Ref. 10)

An observed at point P would see a field rotating in a clockwise direction with respect to the direction of propogation. CPL can be either right handed or left handed depending on the sense of rotation with respect to the direction of propogation. If left and right circularily polarized waves of equal amplitude are combined the vector addition of the fields will result in plane polarized light as shown below in Figure 57.

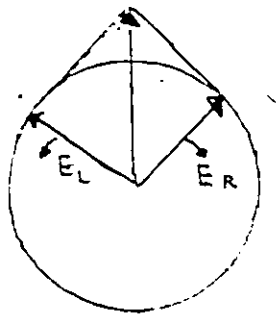

E_L and E_R denote the electric field components of left handed and right handed circularity polarized light respectively.

Figure 57

If the two circularily polarized components are of unequal amplitude, which is the case for optically active compounds, the result is elliptically polarized light shown below in Figure 58.

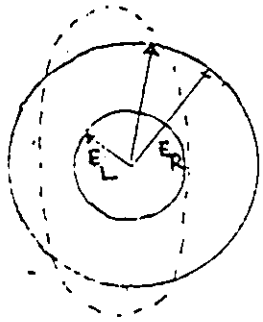

Figure 58

This leads to the observed phenomenon of circular dichroism (CD). At a given wavelength, the CD is dedined as $\Delta\epsilon = \epsilon_L - \epsilon_R$, the difference in the exitinction coefficients for left and right circularily polarized light respectively (LCL and RCL).

Similarly, optically active compounds display a phenomenon called optical rotation, in which the plane of polarized light when passed through the optically active sample has its plane of polarization rotated as shown in Figure 59 below.

(taken from. Ref. 10)

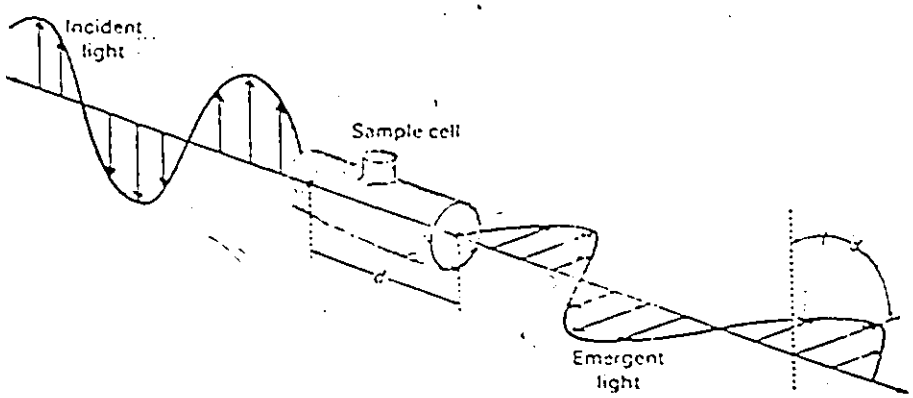

Figure 59

The variation of α with changing wavelength is called Optical Rotary Dispersion (ORD).

To obtain a CD spectrum, elipticities are measured and plotted over a range of wavelengths, (200-350nm). The measured ellipticities are related to the sample concentration. The dependence of the shape of the CD curve on conformation is illustrated by Figure 60 shown various CD curves for α, β and random coil conformations for polylysine.

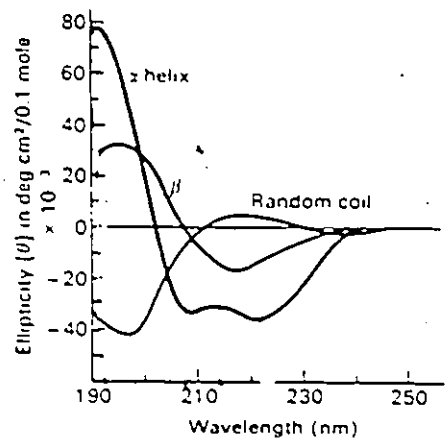

(Taken from Ref. 10)

Figure 60

Optical rotary dispersions can be used to estimate the relative percentages of α, β or random coil structure in a polypeptide. The molar rotation m' is defined as:

Eqn. 17 $$m' = (\alpha) \frac{3}{(n^2+2)} \frac{M}{100}$$

where α = observed angle of rotation

n = refractive index of the medium

M = solute molecular weight

The wavelength and conformational dependance of m' is given by the Moffit equation

Eqn. 18 $$(m') = \frac{a_o \lambda_o^2}{\lambda^2 \lambda_o^2} + \frac{b_o \lambda_o}{(\lambda^2 \lambda_o^2)} + \ldots\ldots$$

a_o and b_o are constants referred to as Moffit parameters

λ_o = band center wavelength

λ = a particular wavelength

A plot of $(m^1)(\lambda^2-\lambda^2)$ versus $(\lambda^2-\lambda_o^2)-1$ gives a straight line with slope as λ_o^2 and intercept $b_o\lambda_o^4$. The constants a_o and b_o can be used to estimate the percentages of α, β or random coil structure since these parameters are different for each conformation (Table 29).

Table 29 (Taken from Ref. 10)

	CD Extrema		ORD Extrema		Moffitt Parameters	
Structure	λ (nm)	$[\theta] \times 10^{-3}$ (deg·cm²/decimole)	λ (nm)	$[m]$ (deg·cm²/decimole)	a_0*	b_0
Random coil	237	−0.2	205	−15,000	~ −600	0
	217	+5	190	+17,000		
	197	−42				
α helix	222	−36	233	−15,000	+650	−630
	208	−33	198	+70,000		
	191	+77				
Antiparallel β	217	−18	230	−6,000	400–700	0
	195	+32	205	+26,000		

* Depends very much on solvent and amino acid composition. All values are approximate and subject to change.

5.2 Fluorescence Spectroscopy

Possible decay mechanisms from electronically excited states are shown in Figure 61.[218]

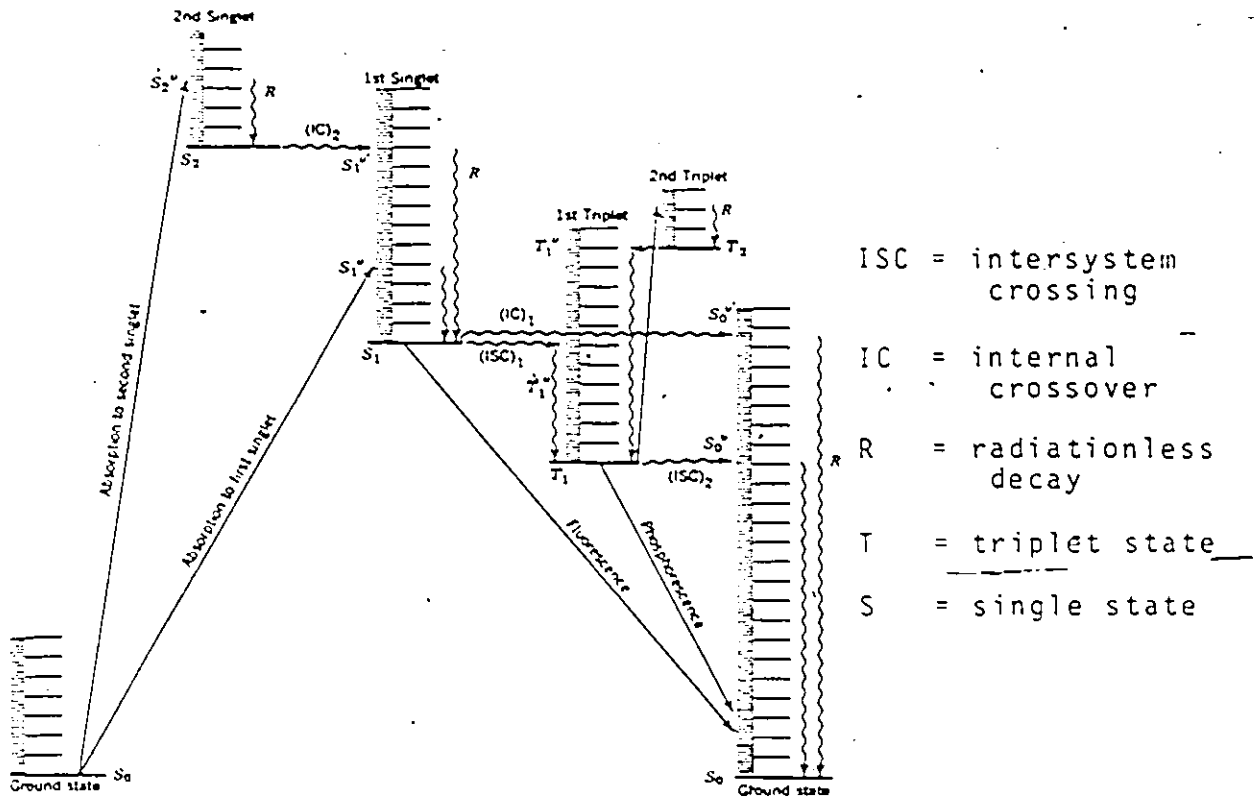

Figure 61

(Taken from Ref. 218)

Values of radiative lifetimes τ can be calculated from

Eqn. 19 $$\frac{1}{\tau} = 2.9 \times 10^{-9} n^2 v_{max} \int_0^\infty \epsilon \, d\bar{v}$$

where n = refractive index of the medium

$\bar{v}$ max = value in cm^{-1} at the band maximum

ϵ = molar absorptivity

The $\int_0^\infty \epsilon \cdot d\bar{v}$ term represents the integration under absorption curve. Fluroescence is defined as emission from a singlet excited state (S_1) to a ground state S_o.

5.3 Differential Scanning Calorimetry (DSC)

DSC allows the direct measurement of phase transition enthalpies and temperatues of phospholipids. Small amounts of lipid, typically on the milligram scale are required. The calorimeters used have two containers - one for the solvent (blank) and the other for the solvent and phospholipid. the electrical energy that has to be put in for each cell to maintain a constant temperature is measured for a range temperatures and a typical DSC curve will appear as so:

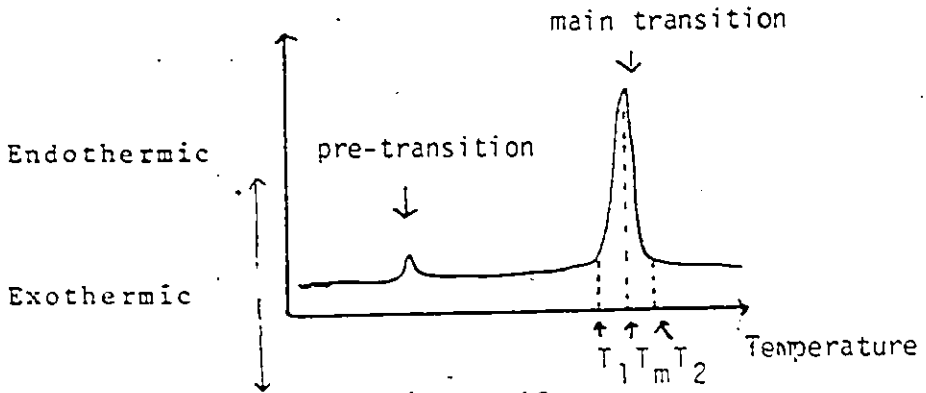

Figure 62

The Van't Hoff enthalpy H_{VH}, is expressed as

Eqn. 20 $$H_{VH} = \frac{4RT_m^2}{T_2 - T_1}$$

Where T_m is the main transition temperature.[219] The area under the peak of the DSC thermogram may be integrated and the enghalpy H_{calc} obtained which is related to the Van't Hoff enthalpy by Eqn. 48.

Eqn. 21 $$\frac{H_{calc.}}{H_{VH}} = \ell$$

Where ℓ is the co-operativity unit for the phase transition.

5.4 NMR

The angular momentum of a nucleus, α, is related to the spin quantum number I by the relation

Eqn. 22 $$\rho = I\hbar = \frac{Ih}{2\pi}$$

where h = Planck's constant

The angular momentum vector can be expressed as

Eqn. 23 $$\mu = \gamma \rho = \frac{Ih}{2\pi}$$

where γ = gyromagnetic ratio of the nucleus

In the nmr experiment, only nuclei with non-zero I values are of interest. If a nucleus is placed in a magnetic field of strength H_o, the nuclear magnetic moment μ is inclined at an angle θ relative to the direction of H_o (Figure 63).[69]

Figure 63

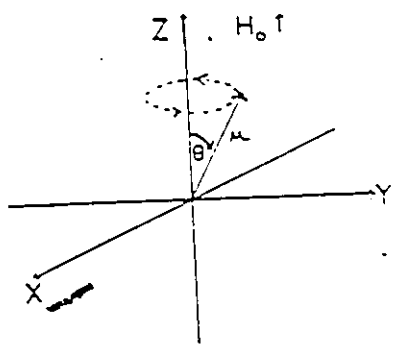

The interaction of μ and H_o creates a torque, L, which acts perpendicular to the plane containing H_o and μ and is determined by the change in angular momentum L, i.e.,

Eqn. 24 $$L = \frac{dp}{dt} = \mu x H_o$$

and $$\frac{du}{dt} = \gamma\mu \, x H_o$$

The net result is that μ precesses about H_o at an angular velocity $\bar{\omega}_o$ so

Eqn. 25 $$\frac{du}{dt} = \omega_o \times \mu; \qquad \omega_o = \gamma H_o$$

The larmour precession frequency ν_o is simply

$$\frac{\gamma H_o}{2\pi}$$

A total of 2I _ 1 energy states are possible but for the sake of simplicity the I = 1/2 case will be dealt wiht. Two possible orientations with respect to the applied field are possible as shown in Figure 64.

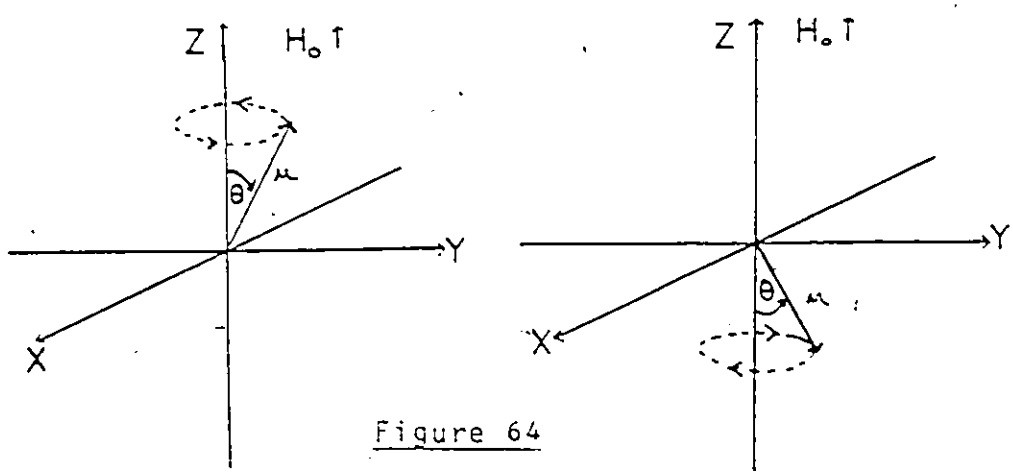

Figure 64

In dealing with an ensemble of nuclei in a magnetic field some will be oriented with or against the field (Figure 65.)

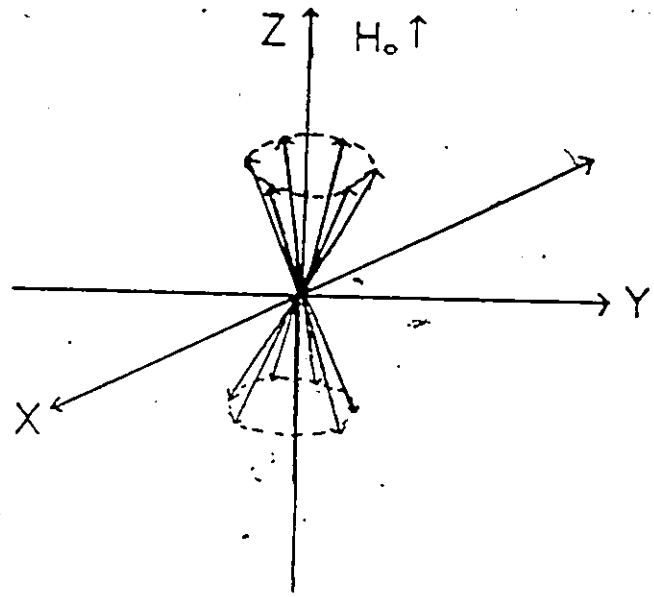

Figure 65

The NMR experiment causes a change in the orientation of some moments μ from the lower to higher energy state i.e, a spin flip which causes changes in the orientation of μ's. The relative number of spins in the low and high energy states is given by the familiar Boltzman distributions:

Eqn. 26 $$\frac{\text{No. in lower state}}{\text{No. in higher state}} = \exp(-\Delta E/kT)$$

where k is the Boltzman constant and T the temperature. For the NMR experiment ΔE is small. For example, for an $H_o = 10^4$ Gauss (ν_o = 40 MHz) there are 1 in 10^5 nuclei more in the lower energy spin state, therefore NMR is a relatively insensitive technique due to this small population difference. The energy of any particular spin state is given by $Em = \frac{\gamma hm}{2\pi} H_o$ where m = -I, -I + 1, ...I. (Figure 66).

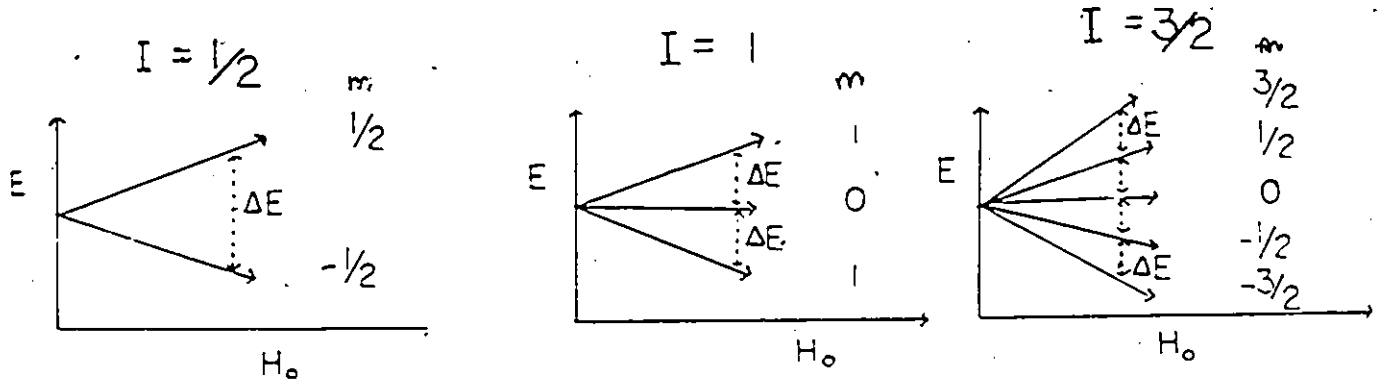

Figure 66

The energy difference ΔE between allowed transitions (where $\Delta m = \pm 1$) increases with inceasing the applied field strength H_o. To induce transitions from low to high energy spin states, a weak field H_1 which precessses at ν_o along with μ is applied in the x-y plane (Figure 67).

Figure 67

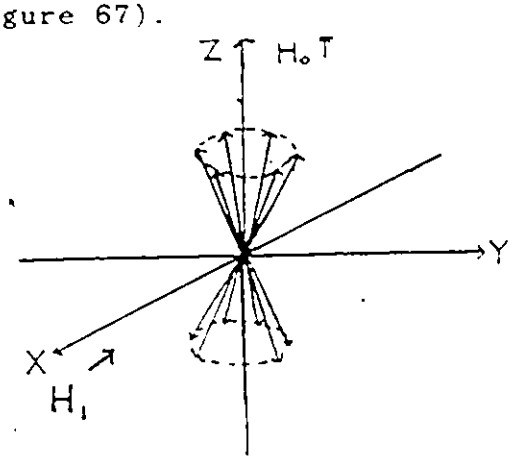

Typically, H_o (and ν_o) is kept constant while the frequency of the H_1 field is varied. This is known as the FREQUENCY SWEEP mode and the experiment is known as CONTINUOUS WAVE nmr. When $\nu = \nu_o$ the condition for transitions between energy spin states is met and NMR signals are observed.

The magnetic field experienced by a particular nucleus can be expressed as $H = H_o (1-\sigma)$ where σ is the shielding factor which when rewritten, the Larmour Frequency can be expressed as $\nu_o = \frac{\gamma}{2\pi} H_o (1-\sigma)$. the shielding factor σ for various nuclei depends on the electronic structure of the molecule and influenced by factors such as electron density, ring currents etc. whch is covered in detail elsewhere. Spin coupling interactions between neighboring nuclei lead to multiple nmr signals due to modulation of the energies of the spin states. The chemical shift scale, which is dimensionless is given by $\delta = \frac{\nu sample - \nu reference}{\nu reference} \times 10^6$. A detailed review of spin coupling (J) coupling is given elsewhere.[92] A sample spectrum of ethylchloride is shown below.

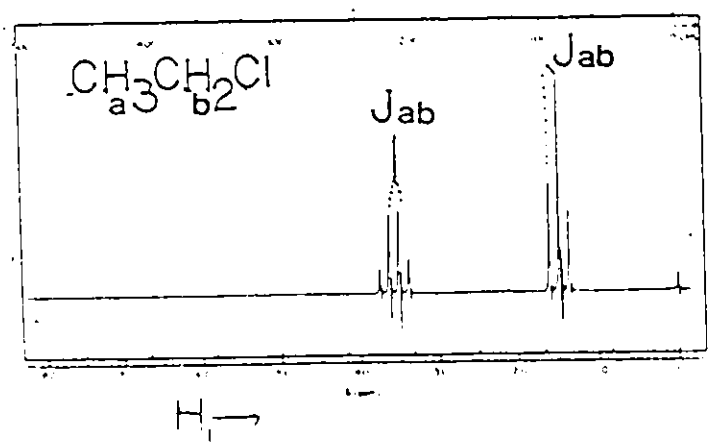

Multiplicity of a or b is 2nI + 1; n=number of neighboring nuclei and I=½ for ^1H.

(Taken from Ref. 92)

Figure 68

In pulsed NMR experiments all magnetic moments μ are treated in a rotating frame of reference (rotation at ν_o) so they appear stationary and algaebraeically added to give a net magnetization along the $z(H_o)$ axis, to give a net magnetization M_o along the z axis. (Figure 69).

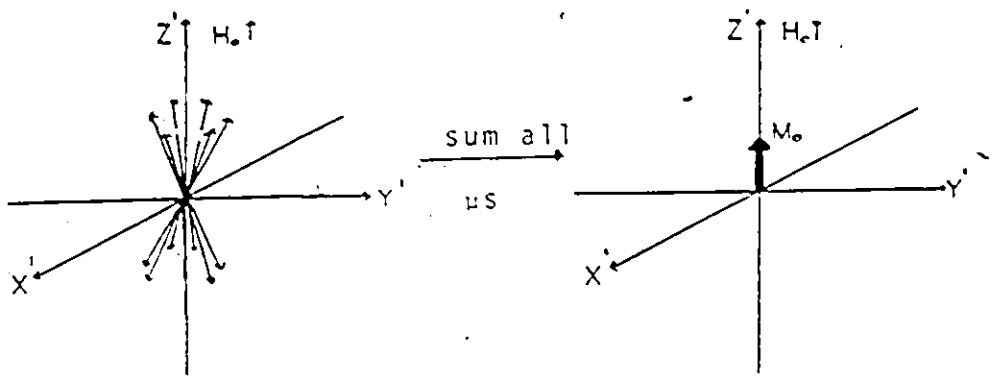

Figure 69

Keep in mind throughout the course of the discussion that M_x + M_y + M_z, the components of magnetization along each axis are important. In the FT NMR experiment, the equillibrium is disrupted with a burst of radio frequency B_1 causing M_o to "tip" away from the z axis and then return to its equillibrium state when B_1 is shut off. (Figure 70).

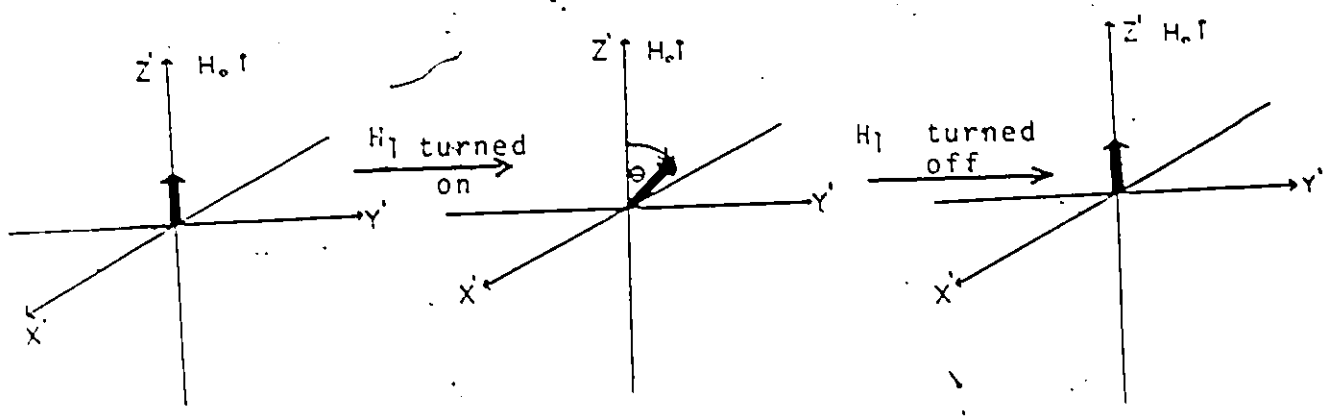

Figure 70

Where $\theta = \gamma H_1 t_p$; t_p = time of the applied pulse

The relaxation of the components of M_o to its equillibrium value can be viewed from the z axis as shown above and the x', y' plane, as shown below (Figure 71).

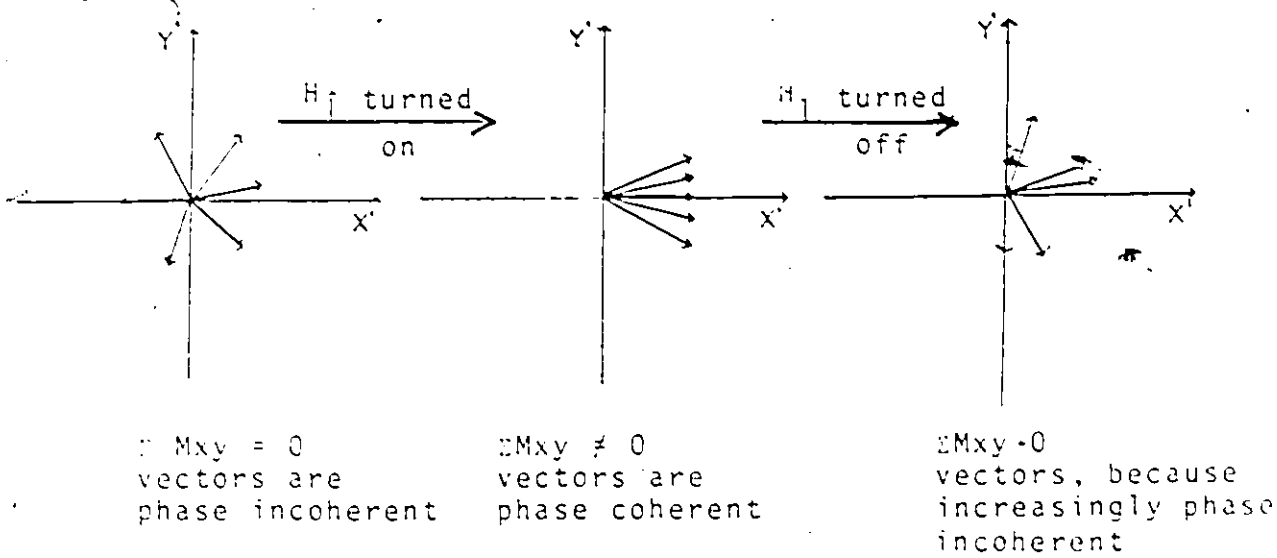

Figure 71

The return of the M_x, M_y, M_z to their equillibrium positions before the application of an H_1 field is given by the Bloch postulates:

Eqn. 27 $$\frac{dM_x}{dt} = \gamma(M_y H_o + M_z H_1 \sin\omega t) - \frac{M_x}{T_2}$$

Eqn. 28. $$\frac{dM}{dt} = \gamma(M_z H_z \cos\omega t - M_x H_o) - \frac{M_y}{T_2}$$

Eqn. 29 $$\frac{dM}{dt} = \gamma(M_z H_1 \sin\omega t + M_y H_1 \cos\omega t) - \frac{(M_z - M_o)}{T_1}$$

The solution of these equations predicts the observed line shape of the NMR signal which is either the normal Lorentzian absorption signal or the dispersion signal.

During the return to equillibrium, the induced voltage in the x^1-y^1 plane is monitored by a radio frequency coil and the resultant signal is known as the free induction decay (FID). A subsequent Fourier transformation of the FID which is in the time domain to the desired frequency domain gives the desired NMR spectrum (Figure 72).

Pulse applied off resonance ($v-v_o$)

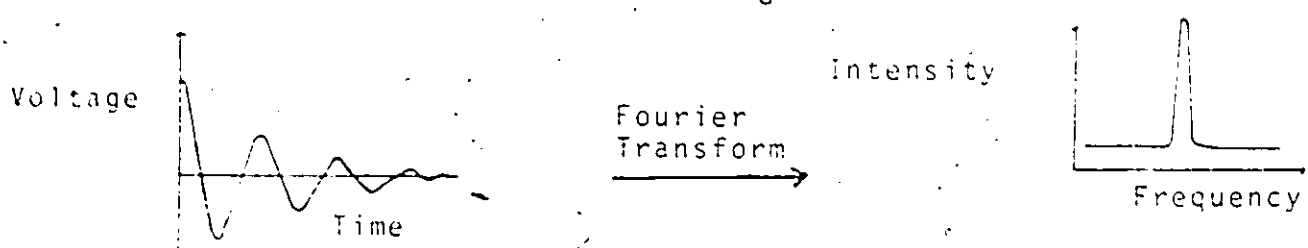

Figure 72

The linewidth at half-height of the nmr signal (V 1/2h) is $1/\pi T^*_2$ which equals

$$\frac{1}{\pi T_{2a}} + \frac{1}{\pi T_{2b}}$$

T_{2a} = natural T_2 value, T_{2b} is due to inhomogeneities from field The free induction decay is sampled at various times not continuously during the decay (as shown below).

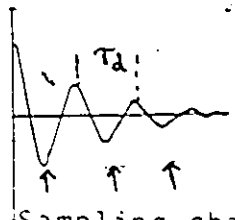

Sampling channels

Where τ_d = dwell time and for N channels $2\tau_{acqu}N = \tau_d$, τ_{acqu} is the acquisition time

The spectral resolution R is defined as sweep width/memory size for example 6000Hz in 4K memory has a resolution of 1.5 Hz/point. The acquisition time τ_{acqu} is 1/R which for the FT experiment should be $\geq 3T_2$*.

There are several advantages in using FT cmopared to CW nmr.

a) improvement of signal/noise by repetition of pulses and addition of FID's before Fourier transformation - especially in the case of less sensitive nuclei.

b) optimum field homogeneity can be maintained during the shorter pulse experiment

c) spectra of short-lived species can be obtained

d) measurement of the decaying magnetization of the individual spectral lines to yield T_1 and T_2 values which are useful for chemical shift assignments and provide information about molecular motion

5.4.1 Dipolar Interactions

A spinning nucleus with a magnetic moment μ will generate local magnetic fields which other nuclei may interact with through space (Figure 73).

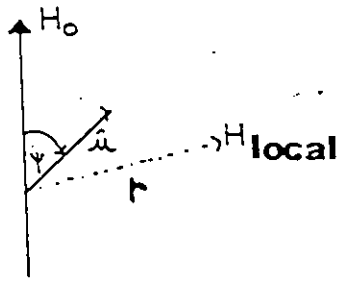

$$H_{local} = \frac{\mu_o 2\hat{\mu}\cos\psi}{4_r 3}$$

r = internuclear distance

μ_o = permeability constant

Figure 73

These local field are on the order of 0.2m Tesla where coupling constants or chemical shifts expressed in field units are on the order of μTelsa.[92]

Such interactions are called dipolar and affect nuclear relaxation times. Under the condition of isotropic tumbling, dipolar interactions will average out to zero which is not the case for solids or liquid crystalline solutions. When free tumbling does not occur and dipolar relaxation mechanisms because very effective leading to broad nmr lines. It is important to note that dipolar interactions are "through space" whereas spin coupling occurs through bonds. Dipolar relaxation will be maximal for nuclei which are directly bonded.

Dipolar interactions constitute the basis of the nuclear Overhauser effect (NOE). Consider a AX spin system with the following spin states:

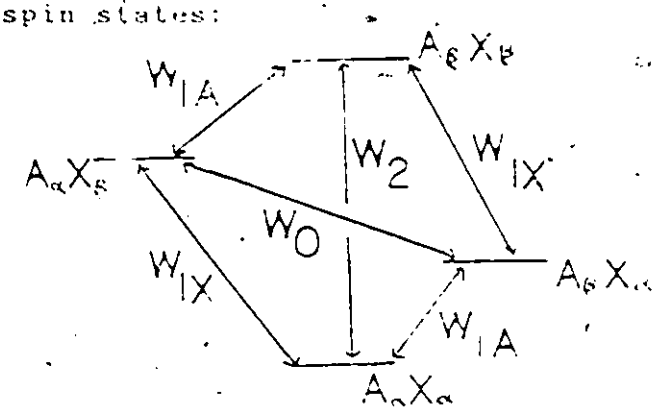

Figure 74

w's indicate the possible transition rates between spin states. the total nmr signal inensity for nucleus A or x will be proportional difference as given by the quantities N_A and N_x.

Eqn. 30 $\quad N_A = (n\alpha\alpha - n\beta\alpha) + (n\alpha\beta - n\beta\beta)$

Eqn. 31. $\quad N_x = (n\alpha\alpha - n\alpha\beta) + (n\beta\alpha - n\beta\beta)$

On saturation of the x magnetization so that $n\alpha\alpha = n\beta\beta + n\beta\alpha$ $n\beta\beta$.

Eqn. 32 $$\frac{N_A^*}{N_A^o} = 1 + \frac{N_x^o \quad (W_2 - W_o)}{N_A^o \quad (W_2 + 2W_{1A} + W_o)}$$

where * and o superscripts denote saturation and presaturation of x respecitvely. Skipping the mathematical details the ratio of signal intensities

Eqn. 33 $$\frac{S_A}{S_A^o} = 1 + \frac{y_x}{y_A} \frac{(W_2 - W_o)}{(W_2 + 2W_{1A} + W_o)}$$

which is the observed NOE. For a heteronuclear dipolar interaction, the NOE can be written as

$$\sigma_{AX}/R_x$$

where $\sigma_{AX} = \frac{h^2}{8\pi^2} \frac{y_A^2 y_B}{r_{AX}^6} \tau_r$

and $R_x = 1/T_{1x}$

τ_r = isotropic correlation time.

The maximal NOE is simply $1 + \frac{\gamma_x}{2\gamma_A}$.

The NOE experiment is useful in a number of ways. One use is in providing additional sensitivity for ^{13}C-H nmr experiments; by irradiating all proton frequencies simultaneously (Broad Band decoupling) the increase in ^{13}C signals is 1.99 for carbons bound directly to protons, and since the effect is $1/r^6$ dependant, conformational information can be obtained.[51]

5.4:2 Chemical Shift Anisootropy

The magnetic field experience at a nucleus is given by:

$$H(\text{nucleus}) = Ho - \sigma Ho$$

Anisotropies in σ may lead to a mechanism for relaxation, since as the nucleus tumbles in solution, the field at the nucleus is continuallly changing in magnitude.[69] The components of this random tumbling motion at the Larmour frequency can lead to spin lattice relatation. If σ is axially symmetric:

Eqn. 34 $$\frac{1}{T_1} = \frac{2}{15} \gamma^2 H^2 (\sigma'' - \sigma^{\perp}) \tau_c$$

where σ'' and $\sigma^{\perp}$ refer to the components ofthe shielding tensor parallel and perpendicular to the axis of symmetry. This predicts that T_1 decreases quadrádically with increasing magnetic field. For most molecules this relaxation mechanism if particularly importnat for ^{19}F.[67]

5.4.3 ^{19}F-dipolar NMR Spectra

the dipolar coupling constant Δ between two nuclei labelled as 1 and 2 is given by:

Eqn. 35 $$\Delta = \frac{\gamma_1 \gamma_2 \mu_o h}{4\pi r^3 2\pi}$$

where r = distance between the two nuclei

μ_o = permeability constant

which is on the order of mTesla. In the case of lipids with $-CF_2-$ units along acyl chains, Post et al.,[107] have shown that the well known Carr-Purcell-Meibloom-Gill (CPMG) pulse sequence i.e., $90°-(180-)_n$ allows the sampling of F .. F dipolar interactions while neglecting all other interactions such as heteronuclear dipolar coupling and chemical shift anisotropy. The obsered dipolar splitting can be related to the order parameter S_{FF} by

Eqn. 36 $$\Delta = |S_{FF}| \Delta_o$$

where Δ is the observed splitting and Δ_o the rigid lattice value (15.4 KHz). S_{FF} in turn is defined as 1/2 (3Cos θ-1) where θ is the average angle between the F-F vector and the bilayer normal.

For lipids containing -CFH- units in the acryl chains, the dipolar interactions cntributing to ^{19}F-NMR linewidths, can be separated into orientation-independant interchain contributions Δ_o and orientation-dependant interchain contributions Δ_1 s that

Eqn. 37 $$\Delta = \Delta_o + \Delta_1 \frac{(3\mathrm{Cos}^2\theta-1)}{2} S$$

where θ is the angle between C-F bond and the direction of the applied field, S the order parameter, and $\Delta = v_{1/2h}/2.36$. CSA contributions to the lineshape were estimated as -82.2ppm (from Teflon) and Δ_1 from samples run at varying aplied field strengths. Trial values of Δ_o and S were incorporated into computer line-fitting programs in order to obtain the best fit to the observed dipolar spectra.[10]

5.4.4 ^{2}H-quadrupole Echo Spectra

For C-^{2}H tyupe of bonds, the dipolar and chemical shift interactions are much smaller than the quadrupolar interaction. This in turn dependant on the motion abut the C-^{2}H bond (Figure 75)[54] and is dealt with thoroughly by a review by Davis.[81]

The effect of motion on the electric field gradient and the appearance of the ^{2}H nmr spectra is demonstrated in Figure 30 where the observed splitting constant ΔVQ can be related by:

Eqn.38 $$\Delta V_Q = \frac{3}{4} \frac{e^2qQ}{h} S_{C-D}$$

Figure 75

Origins of deuterium
Quadrupolar Spectra

Zeeman Interaction

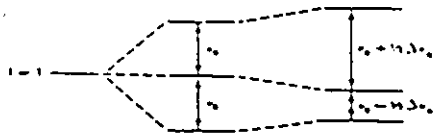

Deuterium is a quadrupolar nucleus with I=1. Interaction of the quadurpole moment with the electric field gradient leads to a perturbution of the Zeeman levels.

Effect of Quadrupolar Interaction

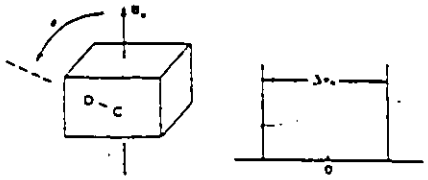

Energy level diagram indicates that NMR spectrum of an isolated C-D bond in a single crystal would have two lines. ΔV_Q is related to the angle θ that the C-D bond makes with the applied magnetic field, B_o.

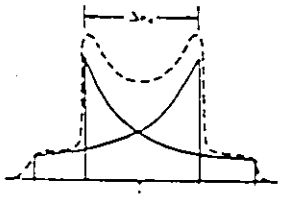

A typical quadrupolar powder pattern which arises because of random orientations of C-D bonds in a sample.

Static

Free Diffusion

Effect of molecular motion on lineshape.

(Taken from Ref. 54)

where S_{CD} is the order parameter and $\frac{3}{4}\frac{e^2qQ}{h}$ the static splitting constant which is ~ 167 Hz for hydrocarbon chains. S_{CD} in turn is given by the relation $1/2(3\cos^2\theta-1)$ where θ is the angle between the bilayer normal and the C-D bond.

The quadruopole echo sequence was developed essentially to overcome the limitations of receiver dead time in trying to observe a rapidly decaying free induction decay. For an ^{2}H-nmr spectrum with a 250KHz width, the receiver dead time must be on the order of 0.6μs which is difficult to obtain. The solution to this problem is to translate this dead time beyond the recovery time with a pair of 90° pulses separated by a time τ, i.e.,

$$(\pi/2 - \tau - \pi/2)_n$$

Typically, H_1 fields on the order of 1.5×10^{-2} Tesla for solid state nmr and subsequently high transmitter powers are required.

5.4.5 <u>2-Dimensional NMR</u>

In general, there are two classes of 2D-nmr spectra (a) Correlated spectra which are essentially correlation diagrams between two spectra and (b) Resolved spectra which spread out the peaks of a single spectrum in 2-Dimensions characterized by different nmr parameters.[53,92,55]

All two dimensional nmr experiments involve pulse sequences in which there are preparation, evolution and detection periods. A general schematic for a 2-D correlated spectrum (COSY is given in Figure 76).

Figure 76

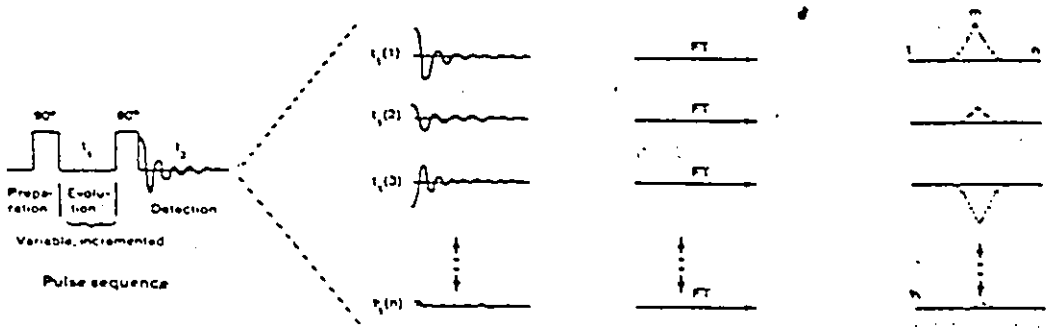

n free induction decays are obtained which differ from one another by equally spaced increments of t_1 and are Fourier Transformed.

A transpose is performed by composing an FID of the first point (column) of each of the n spectra. The FIDs for the first, m-1, m and m+1 and nth points are shown.

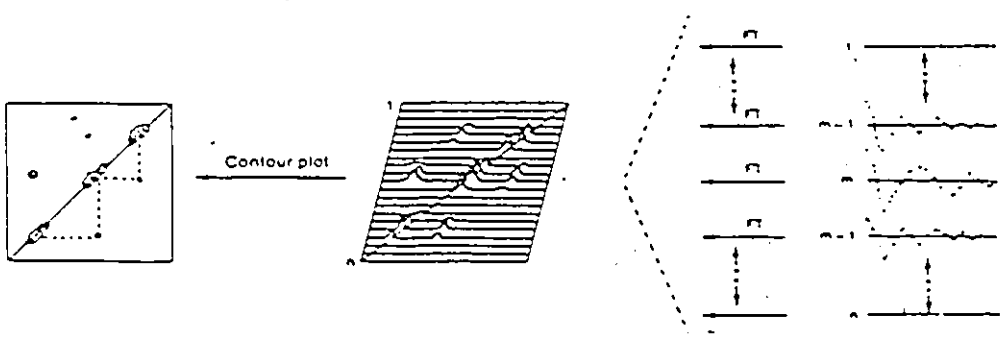

Construct a contour plot. The one dimensional spectrum appears through the diagonal and the off-diagonal peaks indicate J coupling between the diagonal peaks.

Scheme for performing a 2-D correlated spectrum (COSY)

(Taken from Ref. 54)

Appendix II

Phosphate Analysis

Dimyristoylphosphatidylcholine (DMPC) was dried over P_2O_5 in vacuo prior to the preparation of standard samples. A stock solution of DMPC (10 mg in 10 ml $CHCl_3$) was prepared and aliquots (.025, .050, .075 and 0.1ml) placed in separate volume calibrated test tubes and dried under a stream of N_2 gas. Similarily, solutions of 1 mg/ml of lipophilin or lip-FEM-d_2 fluorophospholipid mixtures in 2-chloroethanol were prepared and three 0.1ml aliquots transferred to separate test-tubes and dried extensively in vacuo. A solution of 10N H_2SO_4 (0.5ml) was added to each sample and the mixtures subsequently incubated in a 150°C oven overnight. The next day, 3 drops of 30% H_2O_2 was added to each test tube and returned to the oven for a further 1.5 hours. If any of the samples were not clear at this point, 3 more drops of 30% H_2O_2 was added and the samples returned to the oven for a further 1.5 hours. A finely ground reducing mixture of 15gm Sodium Bisulfite, 0.5 gm sodium sulfite and 0.25 gm 1-amino-2-naphthol-sulfonic acid was prepared and stored in the dark. A solution of 1.6 gm of the above reducer in 10ml distilled deionized water (DDW) was prepared just prior to the analysis. The volume of each sample (and standard) was brought to 4.0 ml using DDW and 0.5ml of 10N H_2SO_4 added to

each tube. A solution of 5% ammonium molybdate (0.2ml) was added to each tube followed by vortexing and addition of 0.2ml of reducing solution. The solutions were then incubated at 100°C for 10 min and on cooling the volume of each test-tube made up to 5.0ml with DDW. The test-tubes were then collected and absorbance readings taken at 830nm. A plot of OD_{830} vs μmoles phosphate (lipid) was constructed for the standard DMPC samples. From this plot, the lipid contents of the protein/phospholipid mixtures were determined.

REFERENCES:

1. Lehninger, A.L., Biochemistry, 2nd Edition, Worth Publishers Inc., (1976).

2. Dickerson, R.E., and Geis, I., Hemoglobin, Benjamin/Cummings Publishing Co. Inc., (1983).

3. Richardson, J., Adv. Protein Chem., 34, 167 (1981).

4. Cullis, A.F., Muirhead, H., North, A.C.T., Perutz, M.F., and Rossmann, M.G., Proc. Royal Soc. Lond., A265, 161, (1962).

5. Barker, R.E., Chemistry of Biological Compounds, Prentice-Hall Inc., (1971).

6. Recent Advances in the Chemical Modification and Covalent Structural Analysis of Proteins, Program in Bio-organic Chem., Vol. 3, p. 142 (1983).

7. Walsh, C., Tetrahedron, 38(7), 871 (1982).

8. Walsh, C., Enzymatic Reaction Mechanisms, U.H., Freeman and Co., p. 86-92.

9. Lippert, B., Metcalf, B.W., Jang, M.J., and Casara, P., Eur. J. Biochem., 74, 441, (1977).

10. Van-Holde, K.E., Physical Biochemistry, Prentice-Hall Inc., p. 180-220 (1971).

11. Hirs, C.H.W., Timasheff, S.N. and Wycoff, H., Methods in Enzymology, Vol. 114, Part A & B, (1985).

12. Chramback, A., and Robard, D., Science, 172, 440 (1971).

13. Brewer, J.M., and Ashworth, R.B., J. Chem. Ed., 46, 41, (1969).

14. Neville, D.M., J. Biol. Chem., 246, 6328 (1971).

15. Siegal, L.M., and Monty, K.J., Biochim. Biophys. Acta., 112, 346, (1966).

16. Greenfield, N., and Fasman, G.D., Biochem, 8, 4108 (1969)

17. Urness, P., and Doty, P., Advan.Protein.Chem., 16, 401, (1961)

18. Tanford, C., Advan.Protein.Chem., 23,121, (1968).

19. Doty, P., and Bunce, B., J.Am,Chem,Soc., 74, 5029 (1952)

20. Zimm, B.H., J.Chem.Phys., 16, 1099, (1948)

21. Belamy, R.A., The Infrared Spectra of Complex Molecules, J.R. Book, V.1, 3rd Edition, (1978)

22. Tsuboi, M., J.Polymer Sci., 59, 139, (1962)

23. Guibault, G.C., Fluorescence - Theory Instrumentation and Practice, Marcel Dekker Inc., N.Y., 443 (1967)

24. Wehry, E.L., Modern Fluorescence Spectroscopy, Academic Press, (1975)

25. Styer, L., Science, 162, 526, (1968)

26. Van Duren, B.L., J.Org.Chem., 26, 2949 (1961)

27. Weber G., Biochem.J., 51, 145, 155 (1952)

28. Martin, R.G., and Ames, B.N., J.Biol.Chem., 236, 1372 (1961)

29. Yang, J.T., Adv.Protein.Chem., 16, 323, (1961)

30. Cerf, R., and Scheraga,H.A., Chem.Rev., 51, 185 (1952)

31. Cohen, J.S., Magnetic Resonance in Biology, Wiley Inter-Science, (1983)

32. Shepler, K.L., Dunhame, R.H., Fec., J.A., and Abeles, R.H., Biochem.Biophys.Acta., 397, 510 (1975)

33. Swartz, H.M., Boultan, J.R., and Borg J.C., Biological Applications of Electron Spin Resonance, Wiley-Inter-science, Ch, 7, (1971)

34. Singer, S.J., and Nicolson, G.L., Science, 175, 720-731, (1972)

35. Eibl, H., Chem.Phys.Lip, 26, 405-429 (1980)

36. Boggs, J.M., Can.J.Biochem., 58, 755, (1980)

37. Zaccui, G., J.Mol.Biol., 134, 693 (1979)

38. Chapman, D., The Structure of Lipids by Spectroscopy and X-ray Techniques, Methnen, London, (1965)

39. Sturtevant, J.M., Ho, C., and Reiman, A., Biochem., Biophys.Acta., 76, 2239, (1979)

40. Albion, N., and Sturtevant, J.M. Proc. Nat. Acad. Sci. 75, 225 (1978).

41. Wa, K., Jacobson, K., and Papahodjopoulos, D., Biochem. 16, 3936, (1977)

42. Axelrod, G., PNAS, 73, 4594, (1977)

43. Yellin, P., and Levin, R., Biochem., 16, 642, (1977)

44. Verma, S.P., and Wallach, D.F.H. Proc. Nat. Acad. Sci. 73, 3358 (1976).

45. Hsia, J., Schneider, H., and Smith, I., Biochem.Biophys. Acta., 219, 514 (1970)

46. Pullman, B., Nuclear Magnetic Resonance Spectroscopy in Molecular Biology, D. Reidle Publishing Co., (1977)

47. Shulman, R.G., Biological Applications of Magnetic Resonance, Academic Press, (1979)

48. Becker, E.D.; High Resolution NMR - Theory and Chemical Applications, Academic Press, (1969)

49. Bloembergen, N., Purcell, E.M., and Pound, R.V., Phys. Rev, 73, 679 (1948)

50. Gutowsky, H.S. and Woessner, D.E., Phys.Rev., 104, 843 (1956)

51. Hosur R.V., and Govil G., Conformation of Biological Molecules - New Results from NMR, Springer-Verlag (1982)

52. Maciel, G.E., Science, 226, 282 (1984)

53. Benn, R., Bunther, H., Agnew.Chem.Int.Ed.Engl., 22, 350, (1983)

54. Jelinski, L.W., Chem and Eng. News, Nov. 5, 1984, 26-47

55. Bax, A., J.Mag.Res., 223, 101, (1981)

56. Turner, D.L., Prog. in nmr spectroscopy, 17(4) 281 (1985).

57. Doddrrell, G., and Pegg, S., J.Am.Chem.Soc., 102, 6388 (1980)

58. Davis, J.H., Bloom, M., Jeffrey, K.R., and Valic, M.I., Chem.Phys.Lett., 42, 390, (1979)

59. Levy, G.C., and Lichter, R.L., Nitrogen-15 Nuclear Magnetic Resonance Spectroscopy, Wiley-Interscience Publication, (1979)

60. Urry, D.W., Mitchell, L.W., Ohnishi, T., PNAS, 71, 3265 (1974)

61. Cohen, M., and Hu, A., J.Am.Chem.Soc., 102, 6594 (1980)

62. Morishmia, I., Inubushi, T., FEBS, LeH., 81, 57 (1977)

63. Jelinski, L.W., J.Mol.Biol., 138, 255, (1980)

64. Oldfield, E., Biochemistry, 23, 6138, (1984)

65. Hosur, R.V., Saran, A., and Govil, G., Chem.Phys.Lip., 21, 77, (1978)

66. Birdsal, N.V.M., J.Chem.Soc. Perk II, 1441, (1972)

67. Hauser, H., Biochem.Biophys.Acta, 508, 450 (1978)

68. Levine, Y.K., Biochem., 11, 1416, (1972)

69. Barker, R.W., Biochem.Biophys.Acta, 260, 161 (1972)

70. Yeagle, P.L., Hutton, W.C., Ching-Lsien, H., and Martin, R.B., Biochem., 16, 4344, (1977)

71. Yeagle, P.L. Proc. Nat. Acadm Sci. 72, 3477, (1975).

72. Seelig, J., Gally, H.N., Woglemoth, R., Biochem., 3647 (1975)

73. Seelig, A. and Seelig, J., Biochem. 16, 45, (1977)

74. Kholar, S.W., Klein, M.P., Biochem. 15, 967, (1976)

75. Dafoureq, J., Lussan, C., FEBS LeH. 26, 35, (1972)

76. Lee, A.G., Birdsall, N.V.M., Metcalfe, J.C., Biochim. Biophys.Acta., 260, 161, (1972)

77. Arvidson, G., Lindblom, G., Drakenberg, T., FEBS LeH. 59, p249, (1975)

78. Griffith, R.G., Powers, L., Pershan, P.S., Biochem., 17, p2718, (1978)

79. Urbina, J., Waugh, J.S., PNAS, 71, 5062 (1974)

80. Griffith, R.G., J.Am.Chem.Soc., 98, 851, (1976)

81. Davis, J.H., Biochim.Biophys.Acta., 737, 117, (1983)

82. Tulloch, A.P., Chem.Phys.Lip., 24, 391 (1979)

83. Das Gupta, S.K., Rice, D.M. Griffin, R.G., J.Lipid.Res., 23, 197, (1982)

84. Seelig, A., and Seelig, J., Biochem., 13, 4839, (1974)

85. Westerman, P.W. and Ghrayelo, W., Chem.Phys.Lipids., 29, 351 (1981)

86. Seelig, J. and Seelig, A., Biochim.Biophys.Acta., 406, 7, (1975)

87. Oldfield, E. and Rice, D., Biochem., 18, 3272 (1979)

88. Taylor, M.G.. Akiyama, T., and Smith, I.C.P., Chem.Phys. Lipids, 29, 327, (1981)

89. Rice, D., Hshung, J.C., King, T.E., and Oldfield, E., Biochem., 18, 5885, (1979)

90. Engle, A.K., and Cowburn, D., FEBS Lett. 126, 169 (1981)

91. Gerig, J.T., Biological Magnetic Resonance ed. by L.J. Berliner and J. Reuben, vol 1, (1978)

92. Harris, R., and Mann, B., ed. NMR and The Periodic Table, Academic Press, (1978)

93. Hull, W.E., and Sykes, B.D., Biochem., 15, 1535 (1976)

94. Schlosser, M., Tetrahedron, 34, 3, (1978)

95. Smallcombe, S.H., Gammon, K.L., and Richards, J.H., J.Am.Chem.Soc., 94, 4585, (1972)

96. Gerig, J.T., and Roe, D.C., J.Am.Chem.Soc., 96, 223, (1974)

97. Bendall, M.R., and Lowe, G., Eur.J.Biochem., 65, 493, (1976)

98. Johnson, T.W., and Muller, W., Biochem., 9, 1943, (1970)

99. Gerig, J.T., and Reinheimer, J.D., Biochem.Biophys.Acta, 178, 197 (1977)

100. Martinez-Carrion, M., and Tiemeier, D., Biochem., 6, 1715, (1967)

101. Birdsal, N.V.M., Tetrahedron Lett. 2675, (1971).

102. Birdsal, N.V.M., Lee, A.G., Levine, Y.K., and Metcalfe, J.C., Biochem.Biophys.Acta., 241, 693, (1971)

103. Gent, M.P.N., Cottam, P.F., and Ho, C., PNAS, 75, 630 (1978)

104. Gent, M.P.N., and Ho.C., Biochem., 17, 3023 (1978)

105. Post, J.F.M., James, E., and Beredensen, H.J.C., J.Magn. Res., 47, 251, (1982)

106. Post, J.F.M., James, E., and Beredensen, H.J.C., J.Magn. Res., 47, 264 (1982)

107. Post, J.F.M., Reuiter, E.E.J., and Bevedenson, H.J.C., J.Magn.Res., 47, 251, (1982)

108. McDonough, B., MacDonald, P.M., Sykes, B.D., and McElheny, R.N., Biochem., 22, ~5097, (1983)

109. MacDonald, P.M., MacDonough, B., Sykes, B.D., and McElheny, R.N., Biochem., 22, 5103, (1983)

110. MacDonald, P.M., Sykes, B.D., and McElheney, R.N., Biochem., 23, 4496, (1984)

111. Smith, D.G., Atsuo, N., Fruton, J.S., J.Am.Chem.Soc., 82, 4600, (1960)

112. Brewer, C.F., and Reim, J.P., Anal.Biochem., 18, 248 (1967)

113. Huestis, W.H., and Raftery, M.A., Biochem., 10, 1181 (1971)

114. Huestis, W.H., and Raftery, M.A., PNAS, 69, 1887 (1972)

115. Huestis, W.H., and Raftery, M.A., Biochem., 11, 1648 (1972)

116. Huestis, W.H., and Raftery, M.A., Biochem.Biophys.Res. Commun., 48, 678, (1972)

117. Huestis, W.H., and Raftery, M.A., Biochem., 12, 2531, (1973)

118. Huestis, W.H., and Raftery, M.A., Biochem., 14, 1886 (1975)

119. Huestis, W.H., and Raftery, M.A., Biochem., 15, 1992, (1976)

120. Zurawski, V.R., and Foster, J.F., Biochem., 13, 3465 (1974)

121. Kenney, W.C., J.Biol.Chem., 250, p3089, (1975)

122. Feldberg, N.T., and Hollacher, T.C., J.Biol.Chem., 247, 4539, (1972)

123. Heitz, J.R., Anderson, C.D., and Anderson, B.M., J. Biol. Chem., 127, 627, (1968).

124. Seizen, R.J., Coendens, F., and Hoenderz, J.H., Biochem. Biophys. Acta., 537, 456, (1976)

125. Lee, N., Scandella, N., and Inouge, M., Proc. Nat. Acad. Sci. 75, 127, (1978).

126. Benga, G., and Starch, S., Biochem. Biophys. Acta, 400, 70, (1975)

127. Johnson, M.E., Biochem., 17, 1223 (1978)

128. Henkin, J., J. Biol. Chem., 252, 4293, (1977)

129. Sekine, T., Ando, K., and Machida, M., Anal. Biochem., 48, 557, (1972)

130. Sekine, T., Ando, K., Minora, M., Kamoaka, Y., and Takamori, K., Biochim. Biophys. Acta., 354, 139 (1974)

131. Friedman, M., The Chemistry and Biochemistry of the Sulfhydryl Group in Amino Acids, Peptides and Proteins, Pergamon Press (1971)

132. Fleck, G.M., Chemical Reaction Mechanisms, Holt, Rinehart and Winston Publ. (1971)

133. Lowry, T.H., and Richardson, K.S., Mechanism and Theory in Organic Chemistry, Harper and Row Publishers (1971)

134. Skinner, E.L., Introduction to Chemical Kinetics, Academic Press (1976)

135. Peters, T., Adv. Protein Chem. 37, 161 (1985).

136. Feeny, R.E. and Whitaker, J.R., Modification of Proteins-Food, nutritional, and pharmacolbyical aspects, Advances in protein Chem. Series (J.Am.Chem.Soc.), (1982)

137. Sandor, G., Serum Proteins in Health and Disease, Williams and Wilkins Co., (1966)

138. Steiner, R.F., Roth, J. and Robbins, J., J.Biol.Chem. 241, 560, (1966)

139. Tabachnick, M., Downs, F.J., and Giorgio, N.A., Arch. Biochim.Biophys., 136, 467, (1970)

140. Ohkubo, A., J.Biol.Chem., 69, 803, (1971)

141. Janatova, J., Fulkr, J.K., and Hunter, M.J., J.Biol.Chem. 247, 7391, (1972)

142. Chen, R.F., J.Biol.Chem., 242, 173 (1967)

143. Coleman, D.L., and Blout, E.R., J.Am.Chem.Soc., 90, 2405, (1968)

144. Teal, F.W.J., and Kaplan, L.J., Biochem., 17, 1750, (1978)

145. Hull, H.H., Chany, R., and Kaplan, L.J., Biochim.Biophys. Acta., 400, 132, (1975)

146. Cormell, C.N. and Kaplan, L.J., Biochem., 17, 1755 (1978)

147. Cormell, C.N., and Kaplan, L.J., Biochem., 17, 1750, (1978)

148. Cuzner, M.L., and Davison, A.N., Molecular Aspects of Medicine, ed. by Baum, H A. Gergely, Pergamon Press (1979)

149. Cuzner, M.L., Davison, A.N., and Genegon, N.A., J.Neurochem., 12, 469, (1965)

150. Norton, W.T., Myelin , ed. by Morell, P. Pleunen Press (1977)

151. Hughes, R.A., Gray, J.A., Gregson, N.A. and Metcalfe, R. A., Acta.Neurol.Scand., 65, 161, (1982)

152. Bauer, H.K., McFarlin, D.E., Stadlan, E.M., and Waksman, B.H., Ann. Neurol., 2, 207 (1982)

153. Runtianienen, J., Arnadoltir, T., Molinar, G. and Salmi, H., Acta.Neur.Scand., 4, 196, (1981)

154. Eggers, A.E., Tarmin, L., Plank, C.R., and Gamboa, E.T., J.Neurol.Sci., 52, 385, (1981)

155. Rastogi, S.C. and Clausen, J., J.Neur.Sci., 51, 161, (1981)

156. Check, W.A., J.Amer.Med.Ass., 242, 315, (179)

157. Poser, C.M., J.Neur.Sci., 42, 173, (1979)

158. Brady, G.W., Feim, D.B., Wood, D.D. and Moscarello, M.A., FEBS LeH, 125, 159, (1981)

159. Robertson, M., Nature, 290, 357 (1981)

160. Mastaglia, F.L., Cala, L.A., Lancet, 1, 850, (1982)

161. Schlesinger, M.J., Ann.Rev.Biochem., 193, (1981)

162. Haskin, G.A., Wood, P.D., and Moscarello, M.A., Prog. Clin.Biol.Res., 39, 21, (1980)

163. Folch, J., Lees, M., and Stoffyn, P.N., J.Biol.Chem., 191, 807, (1951)

164. Folch, J., Lees, M., J.Biol.Chem., 26, 497, (1957)

165. Autilio, L.A., and Norton, W.T., J.Neurochem., 11, 17 (1964)

166. Gonzales-Saster, F., J.Neurochem., 17, 1049 (1970)

167. Gagnon, J., Finch, P.R., Wood, D.D. and Moscarello, M.A., Biochem., 10, 4756 (1971)

168. Miyamoto, E., and Kikiuchi, J., J.Biol.Chem., 249, 2769 (1974)

169. Folch, P.J., and Stoffyn, P.J., Anal., New York Acad. Sci., 107, 86 (1972)

170 Nussbaum J.L., Rouayreny, J.F., Mandel, P., Jolles, J., and Jolles, P., Biochem.Biophys.Res.Commun., 57, 1240 (1974)

171. Boggs, J.M., Vail, W.J., and Moscarello, M.A., Biochem. Biophys.Acta., 448, 517 (1976)

172. Boggs, J.M., and Moscarello, M.A., Biochem, 17, 5734, (1978)

173. Wood, D.D., Gagnon, J., and Moscarello, M.A., Am.Soc. Neurchem.Trans., 2, 117, (1971)

174. Wood, D.D., Vail, W.J. and Moscarello, M.A., Brain.Res., 93, 463, (1975)

175. Moscarello, M.A., Gagnon, J., Wood, D.D., Anthony, J., and Epand, R.M., Biochem., 12, 3402, (1973)

176. Cockle, S.A., Epand, R.M., Stollery, J.G. and Moscarello, M.A., J.Biol.Chem., 255, 9182, (1980)

177. Helenius, A., and Simons, K., Biochem.Biophys.Acta, 415, 29, (1978)

178. Sanderman, Jr., H., Biochem.Biophys.Acta., 515, 209 (1978)

179. Cherry, R.J., Biochem.Biophys.Acta, 559, 289 (1979)

180. Jost, P., Griffith, O.H., Capaldi, R.A. and Vanderkooi, G., PNAS, 70, 480, (1973)

181. Dahlquist, F.W., Muchmore, D.C., Davis, J.H., and Bloom, M., PNAS, 74, 5435, (1977)

182. Paddy, M.R., Dalquist, F.W., Davis, J.H., and Bloom, M., Biochem., 20, 3152 (1981)

183. Oldfield, E., Gilmore, R., Glaser, M., Gutowsky, H.S., Hshung, J.C., Kang, S.J., King, S.Y., Meadows, T.M. and Rice, D., PNAS, 75, 4657 (1978)

184. Rice, D., Hsung, J.C., King, T.E., and Oldfield, E., Biochem., 18, 5885 (1979)

185. Wieslander, A., and Rilfors, L., Biochem.Biophys.Acta., 466, 336 (1977)

186. Seelig, J., Tamm, L., Hymel, L. and Fleischer, S., Biochem., 20, 3922, (1981)

187. Brown, M.F., and Davis, J.H., Chem.Phys.Lett., 79, 431, (1981)

188. Yeagle, P.L., Biophys.J., 37, 227, (1982)

189. Kimelman, D., Tecana, E., Wolber, P.K., Hudson, B.S., Wickner, W.T., and Simmari, R.D., Biochem., 18, 5874 (1979)

190. Sklar, L.A., Hudson, B.S., and Simmari R.D., Biochem., 16, 813, (1977)

191. Sklar, L.A., Hudson, B.S. and Simmari, R.D., Biochem., 16, 819, (1977)

192. Tecana, E., Hudson, B.S., Sklar, L.A. and Simmari, R.D., Biochem., 16, 829 (1977)

193. Sklar, L.A., Hudson, B.S., and Simmari, R.D., Proc. Nat. Acad. Sci. 72, 1649, (1975).

194. Pink, D.A. Chapman, D., Laidlaw, D.J. and Wiedner, T., Biochem., 23, 4051, (1984)

195. Hemminger, M.A. and Pest, J.F.M., Biochem.Biophys.Acta., 436, 222, (1976)

196. Chapman, D., Gomez-Fernandez, H., and Goni, F.M., FEBS LeH, 98, p211, (1979)

197. Hubbell, W.M., and McConnel, W.L., J.Am.Chem.Soc., 96, 385, 1974.

198. Brophy, P.J., Horvath, L.J., and Marsh, D., Biochem. 23, 866, (1984)

199. Papahadjopolous, D., and Moscarello, M., J.Memb.Biol., 22, 143, (1975)

200. Boggs, J.M., Wood, D., Moscarello, M., and Papahadjopolous, D., Biochem., 16, 2325, (1977)

201. Boggs, J., Clement, I.R. and Moscarello, M.A., Biochem. Biophys.Acta., 601, 134, (1980)

202. Rice, D.M., Meadows, M.D., Scheinman, A.O., Goni, F.M., Gomez - Fernandez, J.C., Chapman, D., and Oldfield, E., Biochem., 18, 5893 (1979)

203. Post, J.F., deRuiter, E.E., and Beredensen, H.J., FEBS LeH. 132, 256 (1981)

204. Yarbrough, L.R., Chen-Wen, W., and Ying-Asieuh Wu, P., Biochem., 15 (13), 2863-2868, (1976)

205. James, L.H., Biochim.Biophys.Acta., 178, 111, (1968)

206. Jones, S.A., J. Amer. Chem. Soc. 44, 3091, (1945).

207. Chen, R.F., J.Biol.Chem., 242, 173, (1967)

208. Ellman, G.L., Arch.Biochem.Biophys., 82, 70, (1959)

209. Feiser, L., and Feiser, M., Organic Synthesis, Vol 7, (1968)

210. Watson, S.C. and Eastham, J.F., J.Organometal.Chem., 9, 165, (1967)

211. Boulton, K., and Cross, B.C., J.Chem.Soc.Perkin I, p1354, (1972)

212. Middleton, W.J., J.Org.Chem. 40(5), 574, (1975)

213. Singleton, W., Gray, M., Brown, M., and White, J., J.Am. Oil Chemists.Soc., 42, 53, (1965)

214. Thin Layer Chromatography - ed., by E.Stahl, Springer-Verlag Publishers, 1967

215. Brockeroff, H., and Yurkowski, M., Can.J.Biochem., 43, 1777 (1965)

216. Patel, K., Morrisett, J. and Sparrow, J.T., J.Lipid.Res., 20, 674, (1979)

217. Bartlett, G.R., J.Biol.Chem., 234, 466, (1959)

218. Truro, N.J., Modern Molecular Photochem, Benjamin/Cummings Publishing Co., 1978.

219. Beezer, A.E., Biological Microcalorimetry, Academic Press, 1980.

220. Oldfield, E., Meadows, M., Rice, D. and Jacobs, R., Biochem. 17, 2727 (1978).

221. Bevington, P.R., Data Reduction and Error Analysis for The Physical Sciences, McGraw-Hill, 1975.